ISSN 2409–4951(Online)
ISSN 2310–1008 (Print)

Ukrainian Journal of Food Science

Volume 13, Issue 2
2025

Kyiv 2025

Ukrainian Journal of Food Science publishes original research articles, short communications, review papers, news, and literature reviews.

Topics coverage:

Food engineering	Food nanotechnologies
Food chemistry	Food processes
Biotechnology, microbiology	Economics and management
Physical property of food	Automation of food processes
Food quality and safety	Food packaging

Publication frequency – 2 issues per year (June, December).

The research must be original, have a clear revelance to food science, and appeal to the broader international scientific community.

Editors are committed to ensuring a prompt and fair peer-review process, enabling the timely publication of accepted manuscripts.

Ukrainian Journal of Food Science is abstracted and indexed in the following databases:

Directory of Open Access Journals (DOAJ) (2023)
EBSCO (2013)
Google Scholar (2013)
Index Copernicus (2014)
Directory of Open Access scholarly Resources (ROAD) (2014)
CAS Source Index (CASSI) (2016)
FSTA (Food Science and Technology Abstracts) (2018)

Reviewing a manuscript for publication. All scientific articles submitted for publication in the Ukrainian Journal of Food Science undergo double-blind peer review by at least two reviewers appointed by the Editorial Board: one member of the Editorial Board and one reviewer who is not affiliated with either the Board or the Publisher.

Copyright. Authors submitting articles for publication are required to provide an electronic statement confirming that their work does not infringe any existing copyright and complies with all relevant legislation and international standards in academic publishing. For ease of dissemination and to ensure proper enforcement of usage rights, papers and contributions become the legal copyright of the publisher unless otherwise agreed.

For a Complete Guide for Authors please visit our website:
http://ukrfoodscience.nuft.edu.ua

Editorial office address:
National University of Food Technologies
Volodymyrska str., 68
Kyiv 01601
Ukraine

E-mail:
Ukrfoodscience@meta.ua

ISSN: 2409-4951 (Online), 2310-1008(Print)

ISSN: 2409-4951 (Online), 2310-1008(Print)

Contents

ISSN: 2409-4951 (Online), 2310-1008(Print)

Effect of Macgel functional mixture on whey protein denaturation

Alla Tymchuk[1], Nikita Solovyov[1], Volodymyr Lisnyuk[1], Olena Grek[1], Artem Bogachuk[2]

1 – National University of Food Technologies, Kyiv, Ukraine
2 – St. Lawrence College, Kingston, Canada

Keywords:

Macgel mixture
Whey
Proteins
Thermoacid denaturation

Article history:

Received 29.08.2025
Received in revised form 30.09.2025
Accepted 31.12.2025

Corresponding author:

Alla Tymchuk
E-mail: 589112@ukr.net

DOI: 10.24263/2310-1008-2025-13-2-3

Abstract

Introduction. The aim of the study was to investigate the effect of the functional mixture Macgel MT 100 on the thermoacid denaturation of whey proteins.

Materials and methods. Rennet whey and the functional mixture Macgel MT 100 were used in this study. The yield of protein concentrates, sensory attributes, moisture content, moisture evaporation dynamics determined by thermogravimetric analysis, and the water-holding capacity of the protein concentrates were evaluated.

Results and discussion. The use of the functional mixture Macgel MT 100 intensified the production of protein concentrate. Addition of 0.5% Macgel MT 100 to native whey reduced coagulation time by 20±1 min compared with the control under identical processing conditions and increased protein concentrate yield by an average of 16.4±0.2%. The shortened duration of whey protein denaturation was associated with reduced energy consumption and promoted faster and more efficient unfolding of polypeptide chains, as well as the formation of new intermolecular cross-links. These effects resulted in the development of a denser and more stable protein matrix. The protein concentrate obtained with the addition of the functional mixture Macgel MT 100 exhibited greater structural homogeneity and a slightly spreadable consistency, along with lower moisture content, higher water-holding capacity (52.1±1.3%), and an increased proportion of bound water compared with the control. The moisture evaporation dynamics of model protein concentrate samples were investigated. In the control sample, most of the moisture was removed within 7.0–8.0 min, whereas in the sample containing Macgel MT this process occurred within 9.0–10.0 min. The delayed moisture evaporation observed for the Macgel MT–enriched sample indicates an increased water-holding capacity and the formation of a more stable protein matrix with a higher proportion of bound water. The use of Macgel MT 100 to accelerate the process of thermoacid coagulation contributes to solving technological and raw material problems associated with the need for complete recovery of valuable whey proteins. The obtained protein concentrate is recommended for use as a milk-protein component of thermized multicomponent albumin products, semi-finished products, etc.

Conclusions. The effectiveness of the functional mixture Macgel MT 100 in intensifying the thermoacid denaturation process of whey proteins was confirmed.

ISSN: 2409-4951 (Online), 2310-1008(Print)

Introduction

For dairy processing enterprises, the problem of rational utilization of whey remains relevant. Standard processing approaches, including drying and membrane technologies, cannot be implemented at enterprises, including craft and artisanal ones, due to the lack of appropriate production capacities or insignificant volumes of raw material (Mirzakulova et al., 2025; Puryhin et al., 2025).

In Ukraine, due to insufficient implementation of economically feasible, low-cost, and technologically simple solutions that do not require the installation of additional equipment, whey at some enterprises is still not considered a full-fledged dairy raw material. Most often, after pasteurization, it is sent to bakery and confectionery enterprises or used for feed purposes in animal husbandry (Besediuk et al., 2024; Kochubei-Lytvynenko et al., 2022; Sychevskyi et al., 2019).

The average chemical composition of whey is (%): total solids – 4.5–7.2; proteins – 0.5–1.1; lactose – 3.9–4.9; milk fat – 0.3–0.5; minerals – 0.3–0.8 (Czarniecka-Skubina et al., 2025; Mirzakulova et al., 2025). At the same time, whey proteins are characterized by a uniquely balanced amino acid composition and are a valuable raw material for food production (Kochubei-Lytvynenko et al., 2023; Shevchenko et al., 2022; Yiğit et al., 2023). Their biological value is 104%, which exceeds the corresponding values of egg protein and casein (Escobedo-Monge et al., 2025).

Whey proteins do not form micelles, do not coagulate under the action of enzymes, and do not precipitate when acidified to pH 4.7. Conventionally, whey proteins are divided into thermolabile and thermostable fractions. Thermolabile fractions precipitate in an acidic environment during boiling for 28–32 min, whereas thermostable proteins remain in solution but undergo denaturation under the influence of acids (Minj et al., 2020).

Improvement of methods for recovering concentrates from whey and their use in various product technologies, including semi-finished products, as a base or fortifier is relevant. Thermoacid denaturation, as a classical processing method, involves treating whey at temperatures above 90–95 °C for about 88–92 min at pH 4.4–4.6, which results in high energy intensity of the process. Under such conditions, the degree of protein fraction recovery is approximately 40% (Sukmana et al., 2025).

Incomplete protein recovery is explained by the protective effect of electrolytes present in whey, as well as the dominance of the electrical charge of protein particles as a factor of their colloidal stability (Freire et al., 2022). To intensify the process of thermal denaturation, coagulant reagents are added to rennet whey, in particular whey with an acidity of 145–155 °T. The optimal pH range for the process is 4.4–4.6, which corresponds to a titratable acidity of 30–35 °T and the isoelectric point of thermolabile whey proteins, in particular the lactoalbumin fraction (Chen J. et al., 2023).

Tsygankov et al. (2018) have shown that the use of the food additive “Collagen pro 4402” in the production of albumin mass from liquid whey protein concentrate and rennet whey increases product yield and improves quality characteristics. Improvement of the thermoacid coagulation process of whey proteins requires additional scientific research to reduce denaturation time and increase protein recovery efficiency. In this context, the possibility of using the functional mixture Macgel MT 100 to intensify the denaturation process of whey proteins was considered.

Macgel MT 100 is used in the food industry to regulate consistency and increase product yield. It allows control of viscosity, texture, water retention, and product stability. In meat systems, such technological ingredients contribute to compaction of consistency, formation of gel structures, and reduction of syneresis, which increases product quality and yield (Bao

ISSN: 2409-4951 (Online), 2310-1008(Print)

et al., 2025). In dairy products, it provides a smooth surface, increased yogurt viscosity and cheese yield, and improved textural and rheological properties of fermented dairy products (Alam et al., 2025). According to the manufacturer FOODTECH, the recommended addition level of Macgel MT 100 is 0.5–0.7 g/kg of mixture. The functional additive consists of maltodextrin and the enzyme transglutaminase, which determine its functional properties and affect the rheological characteristics and stability of food systems.

Recent scientific studies confirm that the use of transglutaminase in cheese production significantly increases overall cheese yield (El Kiyat et al., 2021; Ivanov et al., 2021). The application of transglutaminase in combination with ultrasonic treatment in the production of soft cheeses from camel milk increased product yield while maintaining appropriate physicochemical and sensory characteristics (El-Sayed et al., 2025). In addition, transglutaminase contributes to an increase in the degree of protein and milk solids utilization in soft cheese production, which reduces protein losses in whey and increases the efficiency of the technological process (Velazquez-Dominguez et al., 2023). Thus, Macgel MT 100 can be an effective technological ingredient for increasing cheese yield, improving consistency, rheological characteristics, and the nutritional value of cheese products. The aim of the present study was to investigate the effect of the functional mixture Macgel MT 100 on the process of thermoacid denaturation of whey proteins.

Materials and methods

Materials

The raw material used for protein concentrate production was rennet whey with the following physicochemical characteristics: total solids content of 6.1±0.3%, including protein 1.0±0.05%, fat 0.1±0.01%, milk sugar (lactose) 4.5±0.2%, and minerals 0.5±0.02%. The whey had a titratable acidity of 18±2 °T and a density of 1018 kg/m³. The technological ingredient, the functional mixture Macgel MT 100, was a powder ranging in colour from white to light beige, with a taste and odour characteristic of the product, and a moisture content not exceeding 14%.

Method for obtaining whey protein concentrate

The study of the duration of the thermoacid coagulation process of native rennet whey was carried out as follows. From 4 l of milk whey, after reaching the optimal pH of 4.4–4.6 and a temperature of 90–95 °C, the process was conducted until protein flocs were formed. Every 10 min, the protein concentrate was removed using the same method. The duration of thermal treatment was 90±2 min.

The technological ingredient (functional mixture) Macgel MT 100 was added to the milk whey at the initial stage of thermal treatment in the form of a hydromodule (additive and milk whey in a ratio of 1:12) with holding for 30±2 min. Compliance with the above conditions is necessary for uniform distribution of the ingredient throughout the entire volume of whey. For research purposes, the application range of Macgel was expanded from 0.2% to 0.6%.

Methods for determining the quality parameters of protein concentrates

The yield of protein concentrates was determined by the formula:

ISSN: 2409-4951 (Online), 2310-1008(Print)

$$B = \frac{M_{mcg}}{M_{mc}} \cdot 100$$

where B is the yield of concentrates, %;

M_{mcg} is the mass of protein concentrate with Macgel MT 100, g;

M_{mc} is the mass of protein concentrate without the functional mixture, g.

The amount of protein concentrates (g) obtained from 4 l of rennet whey under the corresponding conditions was determined by the gravimetric method.

The organoleptic properties of protein concentrates were evaluated in accordance with the requirements of regulatory and technical documentation. Appearance and color were assessed visually; taste and odor, as well as consistency, were evaluated organoleptically at a sample temperature of 18–20 °C.

The mass fraction of moisture and the dynamics of moisture evaporation of protein concentrates were measured by the thermogravimetric method using laboratory electronic moisture-analyzer scales of the ADS series manufactured by AXIS (Poland).

The water-holding capacity of protein concentrates was determined by the mass of water released from the sample under slight pressing and absorbed by filter paper (Chubenko et al., 2025).

Results and discussion

Effect of functional mixture Macgel MT 100 on yield of protein concentrates

The change in the yield of protein concentrate depending on the amount of the functional mixture Macgel MT 100 added is shown in Figure 1. The control was a protein concentrate obtained by classical technology without the use of a functional mixture. The obtained results regarding the yield of protein concentrate were adjusted depending on the amount of dry matter of the added functional mixture.

According to the results (Figure 1), the addition of the functional mixture Macgel MT 100 to rennet whey in an amount of 0.5 % increases the yield of protein concentrate by an average of 16.4±0.2% compared to the control under the same conditions of thermoacid coagulation. This can be explained by the fact that transglutaminase in rennet whey forms strong chemical bonds between individual whey protein molecules, combining them into a stable network, in particular β-lactoglobulin and α-lactalbumin, both with each other and with casein residues, which results in the formation of a stable three-dimensional protein matrix (Ceren Akal, 2023; El Kiyat et al., 2021). Such enzymatic modification reduces protein losses in whey and increases the water-holding capacity of the protein concentrate, which leads to a significant increase in its yield and improvement of the rheological and structural characteristics of the product (Kim et al., 2023).

Thus, the use of the functional mixture Macgel MT 100 ensures more efficient incorporation of whey proteins into the total volume of the concentrate and increases the technological and economic efficiency of production. The addition of the functional mixture Macgel MT 100 in an amount of 0.2–0.4% increases the yield of protein concentrate to a lesser extent, while the addition of 0.6–0.7% is irrational, since only a 0.5–0.6% increase in mass yield is observed.

ISSN: 2409-4951 (Online), 2310-1008(Print)

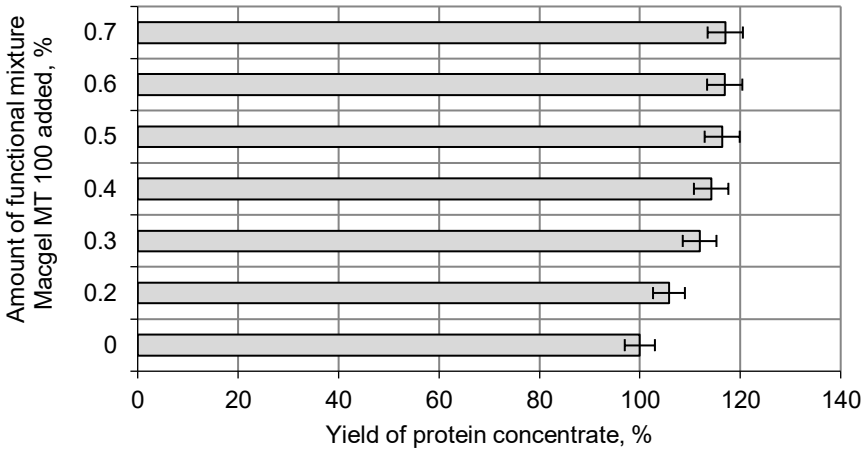

Figure 1. Effect of functional mixture Macgel MT 100 on yield of protein concentrate

Protein concentrate accumulation depending on the duration of protein denaturation

Figure 2 presents the dynamics of protein concentrate accumulation depending on process duration under constant conditions (t = 90–95 °C, pH = 4.6–4.4). The amount of the functional mixture Macgel MT 100 added was 0.5%.

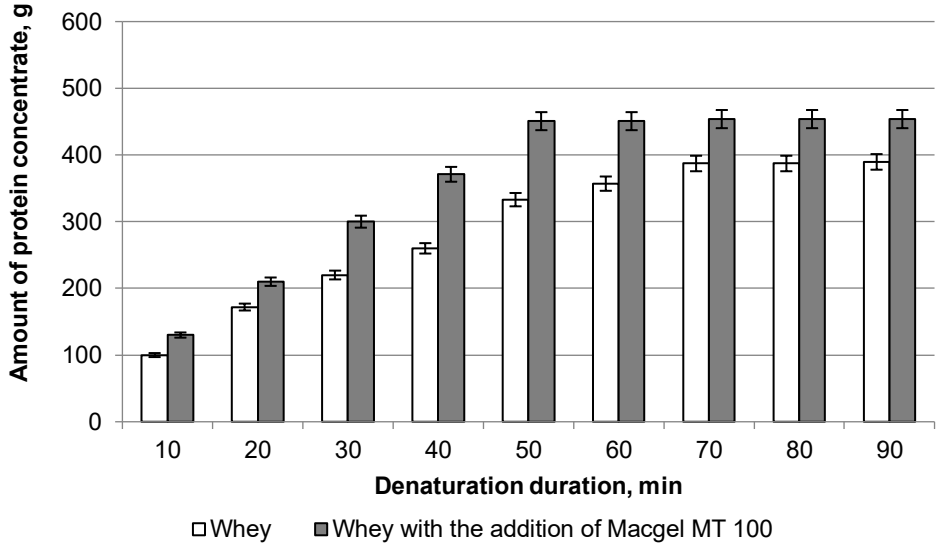

Figure 2. Protein concentrate accumulation depending on the duration of protein denaturation

ISSN: 2409-4951 (Online), 2310-1008(Print)

An increase in denaturation time led to a marked rise in protein concentrate yield for both samples; however, the rate of product accumulation was significantly higher in whey supplemented with Macgel MT 100. Thus, after 50±2 min of thermal treatment, the yield of concentrate in the sample with the additive reached 450.7±1.1 g, after which a further increase in heating duration was not accompanied by a significant increase in product mass.

For the control sample, the maximum effective increase in concentrate yield was observed up to 70±2 min of denaturation, while the absolute yield was 387.2±1.1 g. Further thermal treatment was inefficient and resulted only in a slight increase in concentrate mass.

The effective denaturation time for whey with Macgel MT 100 is 50±2 min, whereas for the control it is (70±2) min. Further thermal treatment up to 90±1 min is impractical, since the additional product yield is insignificant and amounts to only 453.8±1.1 g for the sample with Macgel and 389.6±1.0 g for the control.

The obtained data are consistent with scientific studies indicating a significant effect of time and thermal treatment conditions on whey protein denaturation. Modification of protein systems through the addition of specific protein or functional components can change the kinetics of denaturation and aggregation, affecting the technological parameters of the final product (Pu et al., 2024; Wang et al., 2024). This is consistent with the experimental values obtained, where the introduction of Macgel MT 100 leads to faster denaturation and higher product yield at a shorter heating time.

Therefore, the use of the functional mixture Macgel MT 100 makes it possible to reduce the duration of effective thermal treatment by 20±1 min compared to the control, while simultaneously ensuring a significantly higher absolute yield of protein concentrate.

Quality parameters of protein concentrates

Table 1 presents the results of the effect of the functional mixture Macgel MT 100 on the quality parameters of the protein concentrate.

Table 1

Quality parameters of protein concentrate with the functional mixture Macgel MT 100

Parameters	Characteristics of protein concentrate	
	Control	With the addition of Macgel MT 100
Organoleptic parameters		
Consistency	Homogeneous, delicate	Homogeneous, delicate, slightly buttery
Taste and odor	Clean, fresh with an albumin aftertaste	
Color	White	
Physicochemical parameters		
Titratable acidity, °T	93.0±1.7	81.0±1.1
Mass fraction of moisture, %	77.4±1.5	74.8±0.8
Water-holding capacity, %	48.8±1.2	52.1±1.3

The control sample of the concentrate was characterized by a homogeneous, delicate consistency, a clean and fresh taste with a characteristic albumin aftertaste, and a white color. The taste, odor, and color of the product remained appropriate for a protein concentrate, without foreign flavors.

ISSN: 2409-4951 (Online), 2310-1008(Print)

The introduction of Macgel MT 100 contributed to the formation of a more homogeneous structure and a slightly buttery consistency. These results are likely related to the fact that the enzyme transglutaminase, which catalyzes the formation of cross-links between amino acids of proteins, is able to modify the structure of whey proteins, improving their physicochemical properties such as gel formation, emulsion stability, and microstructure of products after thermal treatment (Chen J. et al., 2025). Similarly, enzymatic modification of whey proteins using transglutaminase improves the mechanical properties and microstructure of protein gels, indicating strengthening of intermolecular bonds in protein aggregates (Zhang et al., 2023).

Analysis of physicochemical indicators showed that the use of the functional mixture Macgel MT 100 significantly affects the acidity and moisture content of the concentrate. The mass fraction of moisture in the concentrate with Macgel MT 100 decreased by 2.6±0.3% compared to the control sample. Titratable acidity in the sample with the additive was 81±1.1 °T, which is lower by 12±1.1 °T compared to the control.

The decrease in acidity may be associated with stabilization of the protein matrix and changes in the course of denaturation–aggregation processes during thermal treatment of proteins in the presence of modifying agents, which corresponds to general patterns of changes in protein properties under the influence of enzymatic modifications (Ma et al., 2025).

It was found that the water-holding capacity of the protein concentrate sample in the presence of Macgel MT 100 increased by 3.3±0.7% compared to the control. This is likely related to the mechanism of action of transglutaminase, which is a component of Macgel MT 100 and catalyzes the formation of covalent ε-(γ-glutamyl)-lysine bonds between protein chains, strengthening the three-dimensional gel structure and limiting water mobility within the protein matrix (Chen X. et al., 2025).

Modern studies confirm that the use of transglutaminase increases the density of protein gels and improves water retention capacity in protein systems, in particular in starch–meat composite gels (Wu et al., 2023) and in plant protein isolates (Min et al., 2025), as well as forms a homogeneous and compact network that promotes molecular water retention (Zhan et al., 2022).

The sample with Macgel MT 100 is characterized by increased water-holding capacity. This is explained by the fact that the protein matrix effectively retains water inside the gel, which potentially improves the structural properties of the product.

The use of the functional mixture Macgel MT 100 makes it possible not only to preserve high sensory paramenters of the protein concentrate but also to improve its structural characteristics, reduce acidity, and optimize moisture content, which is important from the standpoint of technological stability and quality of the final product.

Effect of the functional mixture Macgel MT 100 on the dynamics of moisture evaporation from protein concentrates

The dynamics of moisture evaporation from model samples of protein concentrates are shown in Figure 3.

Measurements showed that the main portion of moisture (free water) was removed faster from the protein concentrate without the functional mixture 7.0–8.0 min than from the sample with Macgel MT 100 (9.0–10.0 min). This slower moisture evaporation in the Macgel-containing sample indicates a higher water-holding capacity, likely due to the formation of more stable gel-forming protein structures that bind water within the matrix (Liu et al., 2025).

ISSN: 2409-4951 (Online), 2310-1008(Print)

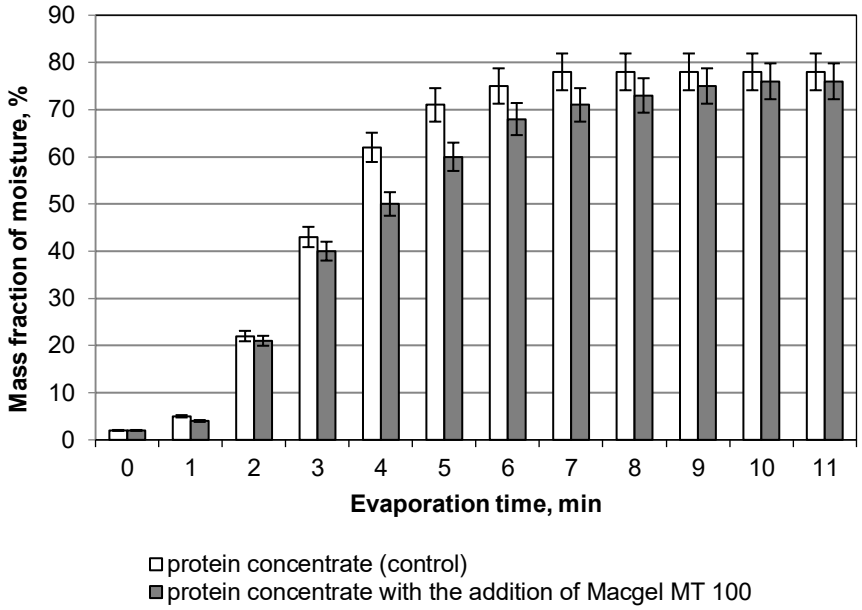

Figure 3. Moisture evaporation dynamics of model protein concentrate samples with and without Macgel MT 100

At the molecular level, thermoacid treatment of whey protein causes unfolding of polypeptide chains that were folded in the native molecule, resulting in the exposure of hydrophobic and charged polar groups on the surface (Freire et al., 2022). This allows the formation of new cross-links between protein molecules and with water, creating a dense, partially gel-forming matrix (Seddiek et al., 2025). As a result of these structural changes, free water partially transitions into a bound form, being firmly retained in the protein matrix, which slows its evaporation (Ozel et al., 2021).

In the initial evaporation phase (up to 2 min), removal of free water is observed, with the difference between samples being about 1–2 min. In the middle phase 3–7 min, the sample with Macgel MT 100 shows a more pronounced lag compared to the control (difference up to 10 min). This indicates delayed diffusion of water within the protein structure and a higher proportion of bound water. By the end of the experiment 8–11 min, the mass fraction of moisture stabilizes at the level of 76–78 % for both samples, indicating the achievement of equilibrium moisture content.

Thus, the addition of Macgel MT 100 promotes the formation of a more stable and dense protein matrix that retains moisture and slows the evaporation process. This confirms the prospects of using the functional additive to enhance the water-holding and textural properties of protein concentrate under thermoacid treatment conditions.

Conclusions

It was established that the addition of 0.5% of the functional mixture Macgel MT 100 to milk whey increased the yield of protein concentrate by an average of 16.4±0.2% compared to the control under the same thermoacid coagulation conditions and shortened the

ISSN: 2409-4951 (Online), 2310-1008(Print)

process duration. The effective coagulation time for whey with Macgel MT 100 was 50±2 min, whereas for the control it was 70±2 min. Quality indicators of protein concentrates were also investigated, showing that the addition of Macgel MT 100 contributed to more pronounced structural homogeneity and a slightly buttery consistency of the product. The mass fraction of moisture and titratable acidity of the experimental sample decreased by 2.6±0.3% and 12±1.1 °T, respectively, compared to the control, while water-holding capacity increased by 3.3±0.7%. Thermogravimetric analysis revealed that during the middle phase of evaporation, the difference between the experimental and control samples reached 10 min, and at the end of the process, the moisture content of the concentrates remained at 76–78%. These results confirm the formation of a denser and more stable protein matrix in the protein concentrate.

References

Alam M., Majid I., Kaur S., Dar B.N. (2025), An updated review on exploring hydrocolloids application in food matrix: Current insights into fruit, bakery, meat, and dairy based products, *Journal of Texture Studies,* 56*,* e70020, https://doi.org/10.1111/jtxs.70020

Bao H., Wang Y., Huang Y., Zhang Y., Dai H. (2025), The beneficial role of polysaccharide hydrocolloids in meat products: A review, *Gels,* 11(1), 55, https://doi.org/10.3390/gels11010055

Besediuk V., Yatskov M., Korchyk N., Kucherova A., Maletskyi Z. (2024), Whey – from waste to a valuable resource, *Journal of Agriculture and Food Research*, 18*,* 101280, https://doi.org/10.1016/j.jafr.2024.101280

Ceren Akal H. (2023), Transglutaminase induced whey cheese production: Impact of different ratios on yield, texture, and sensory properties, *Mljekarstvo*, 73(4), pp. 225–237, https://doi.org/10.15567/mljekarstvo.2023.0402

Chen G., Qu Y., Gras S., Kentish S. (2023), Separation technologies for whey protein fractionation, *Food Engineering Reviews*, 15, pp. 1–28, https://doi.org/10.1007/s12393-022-09330-2

Chen J., Chen Y., Cao W., Yang T., Li L., Liu W., Duan X., Ren G. (2025), Characterization of whey protein isolate–soymilk complexes modified by transglutaminase and their application inyuba film, *Foods*, 14(16), 2916, https://doi.org/10.3390/foods14162916

Chen X., Zhu X., Ning F., Wang S., Zhao Q. (2025), Effect of transglutaminase-mediated cross-linking on physicochemical properties and structural modifications of rice dreg protein, *Foods*, 14(21), 3719, https://doi.org/10.3390/foods14213719

Chubenko L., Grek V., Tymchuk A., Solovyov N. (2025), Effect of ground psyllium on the quality characteristics of dairy-plant concentrates, *Ukrainian Food Journal*, 14(1), pp. 36–53, https://doi.org/10.24263/2304-974X-2025-14-1-6

Czarniecka-Skubina E., Pielak M., Neffe-Skocińska K., Kajak-Siemaszko K., Karp-Październerska S., Głuchowski A., Moczkowska-Wyrwisz M., Rosiak E., Rutkowska J., Antoniewska-Krzeska A., Zielińska D. (2025), Whey – a valuable technological resource for the production of new functional products with added health-promoting properties, *Foods*, 14(24), 4258, https://doi.org/10.3390/foods14244258

El Kiyat W., Laurenthia E., Michaela J., Pari R. (2021), Recent advances in the use of transglutaminase in cheese production, *ASEAN Journal on Science and Technology for Development*, 38, https://doi.org/10.29037/ajstd.675

El-Sayed M. I., El-Deeb A. M., Elwahsh N. A. (2025), The combined effect of ultrasonic treatment and transglutaminase on the yield, textural, microbiological, physicochemical, and sensory characteristics of camel milk cheese*, Discover Food*, 5, 422, https://doi.org/10.1007/s44187-025-00738-3

Escobedo-Monge M. F., Parodi-Román J., Escobedo-Monge M. A., Marugán-Miguelsanz J. M. (2025), The biological value of proteins for pediatric growth and development: a narrative review, *Nutrients*, 17(13), 2221, https://doi.org/10.3390/nu17132221

ISSN: 2409-4951 (Online), 2310-1008(Print)

Freire P., Zambrano A., Zamora A., Castillo M. (2022), Thermal denaturation of milk whey proteins: A comprehensive review on rapid quantification methods being studied, developed and implemented, *Dairy*, 3(3), pp. 500–512, https://doi.org/10.3390/dairy3030036

Ivanov V., Shevchenko O., Marynin A., Stabnikov V., Gubenia O., Stabnikova O., Shevchenko A., Gavva O., Saliuk A. (2021), Trends and expected benefits of the breaking edge food technologies in 2021–2030, *Ukrainian Food Journal*, 10(1), pp. 7-36, https://doi.org/10.24263/2304-974X-2021-10-1-3

Kim W., Wang Y., Ye Q., Yao Y., Selomulya C. (2023), Enzymatic cross-linking of pea and whey proteins to enhance emulsifying and encapsulation properties, *Food and Bioproducts Processing*, 139, pp. 103–112, https://doi.org/10.1016/j.fbp.2023.03.011

Kochubei-Lytvynenko O., Bilyk O., Bondarenko Y., Stabnikov V. (2022), Whey proteins in bakery products, In: O. Paredes-López, O. Shevchenko, V. Stabnikov, V. Ivanov (Eds.), *Bioenhancement and Fortification of Foods for a Healthy Diet* (pp. 67-88), CRC Press, Boca Raton, https://doi.org/10.1201/9781003225287-5

Kochubei-Lytvynenko O., Bilyk O., Stabnikov V., Dubivko A. (2023), Milk whey enriched with magnesium and manganese for food production, In: O. Stabnikova, O. Shevchenko, V. Stabnikov, O. Paredes-López (Eds.) *Bioconversion of Waste to Value-Added Products*, (pp. 113-128), CRC Press, Boca Raton, https://doi.org/10.1201/9781003329671-4

Liu Q., Yeboah G. B., Wang S., Zhang H., Wu J., Wang Q., Cheng Y. (2025), Gel characteristics and digestion of composite protein emulsion-filled gels with varying soy and whey protein ratios in the matrix, *Gels*, 12(1), 37, https://doi.org/10.3390/gels12010037

Ma J., Mu Z., Zhang M., Jiang Z., Hou J. (2025), Mechanistic insights into cysteine-mediated transglutaminase crosslinking of whey protein isolate: modulation of functional properties and antigenicity, *Food Chemistry,* 496, 146626, https://doi.org/10.1016/j.foodchem.2025.146626

Min C., Wang Y., Li Y., Zhu Z., Li M., Chen W., Yi J., Liu M., Feng L., Cao Y. (2025), Effects of transglutaminase on the gelation properties and digestibility of pea protein isolate with resonance acoustic mixing pretreatment, *Food Chemistry*, 469, 142534, https://doi.org/10.1016/j.foodchem.2024.142534

Minj S., Anand S. (2020), Whey proteins and its derivatives: bioactivity, functionality, and current applications, *Dairy*, 1(3), pp. 233-258, https://doi.org/10.3390/dairy1030016

Mirzakulova A., Sarsembaeva T., Suleimenova Z., Kowalski Ł., Gajdzik B., Wolniak R., Bembenek M. (2025), Whey: composition, processing, application, and prospects in functional and nutritional beverages-a review, *Foods*, 14(18), 3245, https://doi.org/10.3390/foods14183245

Ozel B., Kruk D., Wojciechowski M., Osuch M., Oztop M. H. (2021), Water dynamics in whey-protein-based composite hydrogels by means of nmr relaxometry, *International Journal of Molecular Sciences*, 22(18), 9672, https://doi.org/10.3390/ijms22189672

Pu Y., Long Y., Xu D., Niu Y., Wu Q., Chen S., Wang R., Ge R. (2024), Influence of thermal denaturation on whey protein isolates in combination with chitosan for fabricating pickering emulsions: a comparison study, *Frontiers in Nutrition*, 11, 1418120, https://doi.org/10.3389/fnut.2024.1418120

Puryhin I., Nazarenko Y., Synenko T., Bolhova N., Demydova Y. (2025), Determining the effect of nanofiltration on the nutritional and biological value of whey, *Eastern-European Journal of Enterprise Technologies*, 5(11(137), pp. 71–78, https://doi.org/10.15587/1729-4061.2025.339914

Seddiek A.S., Chen K., Zhou F., Esther M. M., Elbarbary A., Golshany H., Uriho A., Liang L. (2025), Whey protein hydrogels and emulsion gels with anthocyanins and/or goji oil: Formation, characterization and in vitro digestion behavior, *Antioxidants*, 14(1), 60, https://doi.org/10.3390/antiox14010060

Shevchenko O., Mykhalevych A., Polischuk G., Buniowska-Olejnik M., Bass O., Bandura U. (2022), Technological functions of hydrolyzed whey concentrate in ice cream, *Ukrainian Food Journal*, 11(4), pp. 498-517, https://doi.org/10.24263/2304-974X-2022-11-4-3

Sukmana H., Rizwana I., Dobozi R., Al-Tayawi A., Szabó B., Ozer B., Kertész S. (2025), A review of various protein separation techniques and valorization of cheese whey and buttermilk, *European Food Research and Technology*, 251, pp. 4263–4279, https://doi.org/10.1007/s00217-025-04877-w

ISSN: 2409-4951 (Online), 2310-1008(Print)

Sychevskyi M., Romanchuk I., Minorova A. (2019), Milk whey processing: Prospects in Ukraine, *Food Science and Technology International,* 13*,* pp. 58–68, https://doi.org/10.15673/fst.v13i4.1557

Tsygankov S., Ushkarenko V., Grek O., Tymchuk A., Popova I., Chepel N., Onopriichuk O., Savchenko O. (2018), Influence of grain processing products on the indicators of frozen milk-protein mixtures, *Eastern-European Journal of Enterprise Technologies*, 6(11(96), pp. 51–58, https://doi.org/10.15587/1729-4061.2018.147854

Velazquez-Dominguez A., Hiolle M., Abdallah M. (2023), Transglutaminase cross-linking on dairy proteins: functionalities, patents, and commercial uses*, International Dairy Journal*, 143, 105688, https://doi.org/10.1016/j.idairyj.2023.105688

Wang Y., Xiao R., Liu S., Wang P., Zhu Y., Niu T., Chen H. (2024), The impact of thermal treatment intensity on proteins, fatty acids, macro/micro-nutrients, flavor, and heating markers of milk – A comprehensive review, *International Journal of Molecular Sciences*, *25*(16), 8670, https://doi.org/10.3390/ijms25168670

Wu M., Yin Q., Bian J., Xu Y., Gu C., Jiao J., Yang J., Zhang Y. (2023), Effects of transglutaminase on myofibrillar protein composite gels with addition of non-meat protein emulsion, *Gels*, 9(11), 910, https://doi.org/10.3390/gels9110910

Yiğit A., Bielska P., Cais-Sokolińska D., Samur G. (2023), Whey proteins as a functional food: Health effects, functional properties, and applications in food, *Journal of the American Nutrition Association*, 42(8), pp. 758-768, https://doi.org/10.1080/27697061.2023.2169208

Zhan F., Tang X., Sobhy R., Li B., Chen Y. (2022), Structural and rheology properties of pea protein isolate-stabilised emulsion gel: Effect of crosslinking with transglutaminase, *International Journal of Food Science and Technology,* 57(2), pp. 974–982, https://doi.org/10.1111/ijfs.15446

Zhang H., Wu J., Cheng Y. (2023), Mechanical properties, microstructure, and in vitro digestion of transglutaminase-crosslinked whey protein and potato protein hydrolysate composite gels, *Foods*, 12(10), 2040, https://doi.org/10.3390/foods12102040

Author identifiers ORCID

Alla Tymchuk	0000-0002-2052-2768
Nikita Solovyov	0000-0003-2734-4367
Volodymyr Lisnyuk	0009-0009-4222-8429
Olena Grek	0000-0001-6974-8162

Cite:

Ukr J Food Sci Style

Tymchuk A., Solovyov N., Lisnyuk V, Grek O., Bogachuk A. (2025), Effect of Macgel functional mixture on whey protein denaturation, *Ukrainian Journal of Food Science*, 13(2), pp. 125–135, https://doi.org/10.24263/2310-1008-2025-13-2-3

APA Style

Tymchuk, A., Solovyov, N., Lisnyuk, V, Grek, O., & Bogachuk, A. (2025). Effect of Macgel functional mixture on whey protein denaturation. *Ukrainian Journal of Food Science, 13*(2), 125–135. https://doi.org/10.24263/2310-1008-2025-13-2-3

Modeling of hydrodynamic processes in rotor-pulsation apparatus

Victor Voroshchuk[1], Maria Shynkaryk[1], Pawel Drozdziel[2], Oleh Kravets[1]

1 – Ternopil Ivan Puluj National Technical University, Ternopil, Ukraine
2 – Lublin University of Technology, Lublin, Poland

Keywords:

Rotor
Pulsation
Hydrodynamics
Pressure
Velocity
Simulation
Modelling

Article history:

Received 18.05.2025
Received in revised form 23.10.2025
Accepted 31.12.2025

Corresponding author:

Victor Voroshchuk
E-mail: voroschuk@gmail.com

DOI: 10.24263/2310-1008-2025-13-2-4

Abstract

Introduction. A mathematical model is developed to describe the unsteady flow in the gap between the rotating and stationary elements of a rotor–pulsation apparatus. The model accounts for pressure pulsations and the non-Newtonian behavior of the processed material.

Materials and methods. This study investigates the unsteady flow of a non-Newtonian curd mass in the rotor–stator gap of a rotor–pulsation apparatus using an axisymmetric model in cylindrical coordinates. The flow is governed by the continuity and Navier–Stokes equations, while rheology is described by the Herschel–Bulkley law with a structural parameter accounting for shear-induced breakdown and recovery. Pressure pulsations due to rotor–stator interaction are represented by a harmonic pressure-drop function, and the equations are solved using the finite-volume method in SolidWorks Flow Simulation with local mesh refinement in the rotor–stator gap.

Results and discussion. The numerical results show that, in the rotor speed range of 2000–3500 revolutions per minute, an unsteady flow develops in the rotor–stator gap with a dominant tangential motion. Over a 3.5 s operating cycle, the mean tangential velocity increases with speed, whereas axial transport remains strongly pulsatory. Tangential velocity pulsations are about 3%, axial oscillations reach ~10% of the mean value, and the radial component remains secondary (1–3%). A systematic reduction in throughput is observed with increasing rotor speed: the mean flow rate decreases from 0.00156 to 0.00066 m^3/s, and the processed volume per cycle from 0.00549 to 0.00229 m^3/cycle. The flow rate exhibits periodic oscillations due to rotor–stator interaction; for a twelve-channel rotor, the pulsation frequency increases from approximately 400 to 700 Hz with an amplitude of 5–10% of the mean value. Energy demand increases with speed: the calculated torque rises from 1.13 to 1.98 N·m and power from 223 to 553 W. The nondimensional axial contribution decreases from 0.212 to 0.064, indicating a shift toward a predominantly tangential regime and explaining the reduced throughput. Comparison with experimental data confirms model adequacy, with discrepancies below 10% for power and below 20% for torque.

Conclusions. An integrated unsteady-flow model for the rotor–stator gap was developed. The model captures the twelve-channel pressure pulsations in the frequency range of 400–700 Hz and predicts power consumption with an accuracy better than 10%. The proposed model can be used for hydrodynamic analysis and optimization of rotor-pulsation apparatus operating conditions.

Introduction

Hydrodynamic rotor-pulsation apparatuses (RPAs) are increasingly recognised as effective tools for dispersion, homogenization, emulsification, and the intensification of heat and mass transfer (Samoichuk et al., 2024). Their performance arises from the combined action of turbulent mixing, periodic pressure pulsations, and cavitation within the working chamber, creating a highly dynamic flow environment that is difficult to capture with conventional modelling approaches (Voroshchuk, 2010). Despite notable advances in studying RPA operation, existing mathematical models remain incomplete (Håkansson, 2018; Vashisth et al., 2021). Most assume Newtonian fluid behaviour, which does not represent the complex rheology typical of many food systems (Ahmed et al., 2018; Vashisth et al., 2021). Current modelling efforts can be broadly grouped into three directions (Håkansson, 2018; Vashisth et al., 2021): rheological models describing viscous and structured media (Barnes, 1999); models based on dimensionless criteria and similarity analysis (John et al., 2019); and CFD (Computational Fluid Dynamics) approaches capable of resolving detailed flow fields, pressure distributions, and turbulence characteristics (Minnick et al., 2023; Mortensen et al., 2018).

However, each of the existing modelling strategies captures only a limited part of the hydrodynamic behaviour (Mortensen et al., 2018). Rheological models typically neglect the spatial and temporal structure of the flow, whereas CFD approaches, despite their capabilities, rarely incorporate sufficiently accurate descriptions of non-Newtonian behaviour (Ahmed et al., 2018; Minnick et al., 2023). Methods based on dimensionless groups reveal general trends but are unable to resolve local effects associated with cavitation development or pulsation-induced instabilities (Zheng et al., 2022). These limitations create a clear need for more integrated modelling frameworks that combine rheological and hydrodynamic representations to enhance the predictability of RPA performance under real processing conditions (Samoichuk et al., 2024).

In computational fluid dynamics analyses of rotor-stator systems, the Reynolds-averaged Navier-Stokes formulation is widely used, decomposing velocity and pressure into mean and fluctuating components (Zemanová and Rudolf, 2019). Turbulence closure is most commonly performed using the k-ε and k-ω models, which may differ in accuracy when predicting energy dissipation and the localization of high-gradient zones (Wilcox, 2006) (Table 1). The k-ε model is often selected for its robustness and computational efficiency (Adanta, 2020). The k-ω model, particularly its SST modification (Table 1), provides a more reliable description of near-wall behavior and flow separation (Adanta, 2020). Simulation results supported by experimental observations, including velocity-field validation using particle image velocimetry, have confirmed the applicability of these approaches to rotor-stator mixing flows and to estimating energy dissipation characteristics (Mortensen et al., 2018). These findings also indicate that the geometry of the apparatus can strongly influence mixing efficiency and hydrodynamic behavior (Wang et al., 2023). This effect is consistent with broader analyses of hydrodynamic reactor design and performance trends (Zheng et al., 2022).

Additional insights into flow structure and energy dissipation were presented in (Utomo, 2008), where velocity fields and turbulent energy characteristics were successfully reproduced. For rotor-pulsation apparatuses with axial discharge, the LES (Large Eddy Simulation) approach was applied in (Minnick et al., 2023), yielding detailed predictions of velocity profiles, turbulence statistics, pressure distribution, particle transport, and energy dissipation patterns. Other studies focused on energetic aspects governed by the rotor-stator configuration (Badve et al., 2013) linked the turbulent dissipation rate E_k to the rotor-stator gap, while (Zheng et al., 2022) examined the relationship between power consumption and flow hydrodynamics.

ISSN: 2409-4951 (Online), 2310-1008(Print)

Table 1

Comparison of RANS-based turbulence models

Model type	Advantages	Limitations	Typical applications
k-ε (turbulence model)	Suitable for evaluating energy-related characteristics; simple in formulation; accurate for turbulent flows.	Inaccurate in regions with flow separation; large deviations from experimental data may occur.	Numerical studies of energy dissipation and design improvement (Utomo and Pacek, 2009).
k-ω (turbulence model)	More accurate near-wall predictions; improved evaluation of energy dissipation zones.	Sensitive to boundary and initial conditions; numerical stability may vary.	Analysis of hydrodynamics in rotor-stator gaps (Zemanová & Rudolf, 2019).
SST k-ω (shear-stress transport model)	Combines advantages of k-ε and k-ω; better performance for separated flows and adverse pressure gradients.	Requires extensive input data for proper setup.	CFD model validation (Launder et al, 1974) and model comparison (Mortensen et al., 2018).
RNG k-ε (renormalization-group variant)	Better representation of medium-scale turbulent fluctuations than the standard k-ε model.	Limited applicability for highly turbulent or strongly anisotropic flows.	Studies of rotor-based mixing devices (Vashisth et al., 2021).

As noted earlier, many existing studies (Badve et al., 2013; Ranade, 2022; Wang et al., 2023; Zheng et al., 2022) address Newtonian fluids, underscoring the need for modelling approaches suitable for non-Newtonian media and for capturing the geometric specifics of RPAs. In response to this, the present study develops a hydrodynamic model that incorporates both apparatus design features and experimentally observed rheology. The model is then evaluated through comparison with published data, followed by the formulation of practical recommendations based on the numerical findings.

This study aims to develop an integrated unsteady hydrodynamic model of a rotor-pulsation apparatus that incorporates non-Newtonian rheology and pressure pulsations, and to assess its adequacy by comparing it with published torque and power data.

Materials and methods

Rotor-pulsation apparatus

The study was performed for a rotor-pulsation apparatus (RPA) comprising a rotor and a stator equipped with a system of radial channels, with an annular clearance (gap) formed between the interacting surfaces (Figure 1).

ISSN: 2409-4951 (Online), 2310-1008(Print)

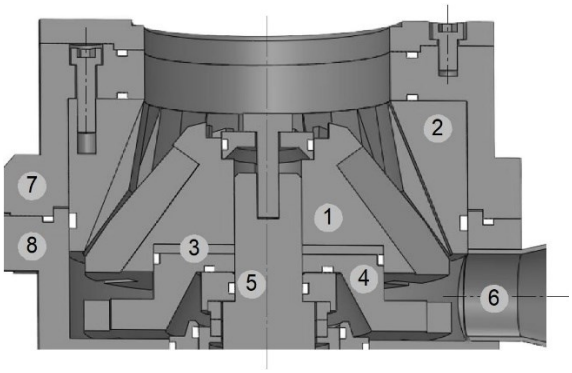

Figure 1. Schematic diagram of the rotor-pulsation apparatus (RPA):
1 – rotor;
2 – stator;
3 – adjustment shim;
4 – pump element;
5 – shaft;
6 – circulation channel;
7 – inlet chamber;
8 – outlet chamber.

The following parameters were used in the calculations: rotor radius R=0.038m, rotor-stator gap δ=1.5mm, number of radial channels z=12. The rotor speed range was 2000–3500 rpm, and the computational cycle duration was 3.5 s. The flow in the rotor-stator clearance was interpreted as the motion of a non-Newtonian medium in an annular gap between two coaxial cylinders. During rotor rotation, the curd mass is sheared in a Couette-type regime; the resulting tangential stresses govern the rotor torque and, consequently, the mechanical power demand (John et al., 2019; Mortensen et al., 2018; Utomo and Pacek, 2009).

Modelling approach and numerical implementation

Hydrodynamic characteristics of the RPA working zone were determined by numerical simulation of unsteady flow in the rotor-stator gap. In addition to circumferential shear, an oscillatory axial component driven by a pulsating pressure drop along the channel axis was considered. The modelling framework was formulated based on the conservation of mass and momentum, while accounting for the non-Newtonian rheological response of the curd mass (Adanta, 2020; Wilcox, 2006; Voroshchuk, 2010; Zemanová and Rudolf, 2019). The non-Newtonian behaviour of the medium was represented using a Herschel-Bulkley-type rheological description with a structural parameter. To represent pulsations, a harmonic time dependence of the imposed pressure drop was prescribed and characterised by its mean value, amplitude, angular frequency, and phase shift. The simulations were carried out using the finite-volume method with semi-implicit time integration in SolidWorks Flow Simulation. Local mesh refinement was applied in the rotor-stator gap.

Processed material (curd mass)

A laboratory-prepared curd mass was used as the working medium. The sample was obtained by thoroughly mixing the components until a homogeneous mass was formed. The formulation (mass fractions) was: curd base – 67.4 wt%, water – 23.0 wt%, and flavor – 9.6 wt%. This curd mass was then used in the simulations and subsequent analysis of hydrodynamic parameters in the RPA working zone.

ISSN: 2409-4951 (Online), 2310-1008(Print)

Results and discussion

Governing equations and mathematical model of the flow

The continuity equation ensuring mass conservation for an axisymmetric flow is written as (Bird et al., 2002; White, 2006; Zemanová and Rudolf, 2019):

$$\frac{1}{r}\frac{\partial\left(rv_r\right)}{\partial r}+\frac{\partial v_z}{\partial z}=0\ , \tag{1}$$

where v_r is the radial velocity, v_z the axial velocity, and r the radial coordinate (m).

The term $\frac{\partial\left(rv_r\right)}{\partial r}$ represents the radial derivative of mass flux; $\frac{1}{r}\frac{\partial\left(rv_r\right)}{\partial r}$ expresses the relative variation of the radial flux per unit radius; and $\frac{\partial v_z}{\partial z}$ describes the axial change of velocity (1/s). According to this equation, any variation in axial velocity is compensated by the corresponding distribution of radial velocities, ensuring a steady flow in the gap.

To describe the flow dynamics, the Navier-Stokes equations with three velocity components are applied. Each equation governs momentum in the corresponding direction (Bird et al., 2002; White, 2006).

In the radial direction, inertial forces, the centrifugal term u_θ^2/r, the pressure gradient $\partial p/\partial r$, and viscous stresses are taken into account (White, 2006; Zemanová and Rudolf, 2019):

$$\rho\left(\frac{\partial v_r}{\partial t}+v_r\frac{\partial v_r}{\partial r}+v_z\frac{\partial v_r}{\partial z}-\frac{u_\theta^2}{r}\right)=-\frac{\partial p}{\partial r}+\frac{1}{r}\frac{\partial\left(r\tau_{rr}\right)}{\partial r}+\frac{\partial\tau_{rz}}{\partial z}-\frac{\tau_{\theta\theta}}{r}\ , \tag{2}$$

where u_θ is the tangential velocity; ρ the fluid density; p the pressure; τ_{rr} the radial normal stress; $\tau_{\theta\theta}$ the tangential normal stress; and τ_{rz} the shear stress in the r - z plane.

In the tangential direction, momentum transfer from the rotor to the working fluid is dominant (Hop et al., 2023; John et al., 2019; Utomo et al., 2008):

$$\rho\left(\frac{\partial u_\theta}{\partial t}+v_r\frac{\partial u_\theta}{\partial r}+v_z\frac{\partial u_\theta}{\partial z}+\frac{v_r u_\theta}{r}\right)=\frac{1}{r^2}\frac{\partial\left(r^2\tau_{r\theta}\right)}{\partial r}+\frac{\partial\tau_{\theta z}}{\partial z}\ , \tag{3}$$

where $\tau_{r\theta}$ the shear stress in the $r-\theta$ plane; and $\tau_{\theta z}$ the shear stress in the $\theta-z$ plane.

The left-hand side represents inertial transport of tangential momentum, while the right-hand side represents viscous forces. In the axial direction, a pressure drop is needed to drive the product through the channels (Utomo and Pacek, 2009; Utomo et al., 2008):

$$\rho\left(\frac{\partial v_z}{\partial t}+v_r\frac{\partial v_z}{\partial r}+v_z\frac{\partial v_z}{\partial z}\right)=-\frac{\partial p}{\partial z}+\frac{1}{r}\frac{\partial\left(r\tau_{rz}\right)}{\partial r}+\frac{\partial\tau_{zz}}{\partial z}\ , \tag{4}$$

where τ_{zz} is the axial normal stress.

Since the equations involve stresses, the rheological behaviour of the curd mass must be considered (Barnes, 1999).

ISSN: 2409-4951 (Online), 2310-1008(Print)

The Herschel-Bulkley model (Barnes, 1999; Voroshchuk, 2010) is used

$$\tau = \tau_0 + K\dot{;} \qquad (5)$$

where τ is shear stress (Pa); τ_0 the yield stress (Pa); K the consistency coefficient (Pa·s^n); n the flow index; and $\dot{;}$ $\overline{\mathfrak{D}_{ij}}$ the shear-rate intensity (1/s). Here n is the flow index of the Herschel–Bulkley model; the rotor rotational speed is denoted as n_{rot} (rpm) in the Results section.

Unlike Newtonian fluids, curd mass undergoes structural breakdown under shear, reducing effective viscosity, while partial recovery occurs in rest. To account for this behaviour, a structural parameter $\lambda \in [0,1]$ is introduced, modifying τ_0 and K depending on structural integrity. Its evolution follows:

$$\frac{d\lambda}{dt} = \frac{1-\lambda}{T_b} - k_d(\dot{;} \qquad (6)$$

where T_b is the recovery time and $k_d \propto |\dot{;}$ with temperature correction.

This formulation allows reproduction of both the pulsating nature of flow in the RPA and the gradual decrease in viscosity and shift of mean values of $\dot{;}$ and wall shear stress τ_w from cycle to cycle (Utomo et al., 2008; Samoichuk et al., 2024).

As the apparatus operates with periodic pressure fluctuations, the instantaneous pressure drop is described by (Utomo et al., 2008):

$$\Delta p(z,t) = \Delta p_0(z) + A(z)\sin(\omega_p t + \varphi), \qquad (7)$$

where $\Delta p_0(z)$ is the mean pressure-drop component, $A(z)$ the pulsation amplitude, ω_p the pulsation angular frequency (rad/s), and φ the phase shift.

Boundary conditions

Rotor (no-slip at rotating wall) (White, 2006; Zemanová and Rudolf, 2019):

$$u_\theta = \omega r,\ v_r = 0,\ v_z = 0. \qquad (8)$$

Stator (stationary wall):

$$u_\theta = 0,\ v_r = 0,\ v_z = 0. \qquad (9)$$

Outlet (fixed pressure):

$$p = p_{out}. \qquad (10)$$

The influence of axial flow is evaluated using the nondimensional parameter (Hop et al., 2023):

$$\varepsilon = \frac{(v_z)_{A_{out}}}{U_\theta}, \quad U_\theta = \omega R, \qquad (11)$$

where $(v_z)_{A_{out}}$ is the mean axial velocity at the outlet; ω is the rotor angular velocity (rad/s), $\omega = 2\pi n_{rot}/60$.

The mean axial velocity is defined as:

ISSN: 2409-4951 (Online), 2310-1008(Print)

$$\overline{v_z}(t) = \frac{1}{A_{out}} \int_{A_{out}} v \cdot n_z \, dA, \tag{12}$$

where A_{out} is the outlet area and n_z the axial normal.

Simulations were performed for an RPA with rotor radius R=0.038 m, gap δ=1.5mm, and 12 radial channels. The average channel area was $A_{ch,avr}=7.49 \cdot 10^{-5}$ m², and the total cross-sectional area $A_{tot}=8.988 \cdot 10^{-4}$m^2. Operational speeds ranged from 2000 to 3000 rpm. A technological cycle duration of 3.5 s was adopted. Computations were axisymmetric with inclusion of tangential velocity.

The continuity equation (1), momentum equations (2) - (5), and rheological model (6) were used. Pulsations were included according to (7), and boundary conditions followed (8) - (10). The finite-volume method with semi-implicit time integration was applied. Mesh refinement was used in the gap to resolve steep velocity gradients. SolidWorks Flow Simulation was employed as the CFD environment (Patankar, 2018; Versteeg and Malalasekera, 2007; John et al., 2019).

The velocity fields $v_r(r,z,t)$, $v_\theta(r,z,t)$, $v_z(r,z,t)$ together with the pressure distribution $p(r,z,t)$ were obtained by solving the governing equations (1)-(4). The effective viscosity η_{eff} was evaluated according to the Herschel-Bulkley relation (6), which incorporates the non-Newtonian rheology of the curd mass.

Based on the computed velocity fields, the instantaneous volumetric flow rate

$$Q(t) = \int_{A_o} utv \cdot n_z dA \tag{13}$$

and the mean axial velocity (12) were determined. The nondimensional parameter ε , characterising the relative contribution of axial transport, was subsequently evaluated. The hydrodynamic torque acting on the rotor was calculated from

$$M(t) = \int_{S_{rot}} r \, \tau_{r\theta} \, dS \text{ , with } \tau_{r\theta} = 2 \eta_{eff} D_{r\theta} \text{ ,} \tag{14}$$

where $D_{r\theta}$ is the r−θ component of the strain-rate tensor followed by evaluation of the instantaneous and mean mechanical power (John et al., 2019; Mortensen et al., 2018)**:**

$$N(t) = M(t)\omega \text{ , and } \bar{N} = \bar{M}\,\omega \text{ .} \tag{15}$$

Verification of the numerical solution included comparison with experimental flow-rate measurements, analysis of mesh and time-step sensitivity, assessment of mass conservation between the gap and the outlet section, and evaluation of the overall energy balance (John et al., 2019; Mortensen et al., 2018):

$$\bar{N} \approx \overline{\Delta p \, Q} + \Phi_{\text{losses}} \text{ .} \tag{16}$$

Φ_{losses} represents additional hydraulic losses, including viscous dissipation and losses associated with vortex structures and secondary flows.

ISSN: 2409-4951 (Online), 2310-1008(Print)

Flow dynamics and cycle-resolved throughput over the operating cycle

Figure 2 presents the theoretical time dependences of the velocity components in the rotor-stator gap during a single 3.5-second operating cycle (results shown within a 0.1-second time window) for rotor rotational speeds n=2000-3500 rpm. The analysed For a rotor components are the tangential velocity $u_\theta(t)$, axial velocity $v_z(t)$, and radial velocity $v_r(t)$, where t denotes time (seconds). The mean tangential velocity u_θ increases with n, whereas its pulsations remain limited (3%). The axial velocity v_z (t) exhibits more pronounced oscillations (10% of the mean value), and its mean value decreases as n increases. The radial velocity v_r remains minor (1–3% of v_z), confirming its secondary contribution to overall transport.

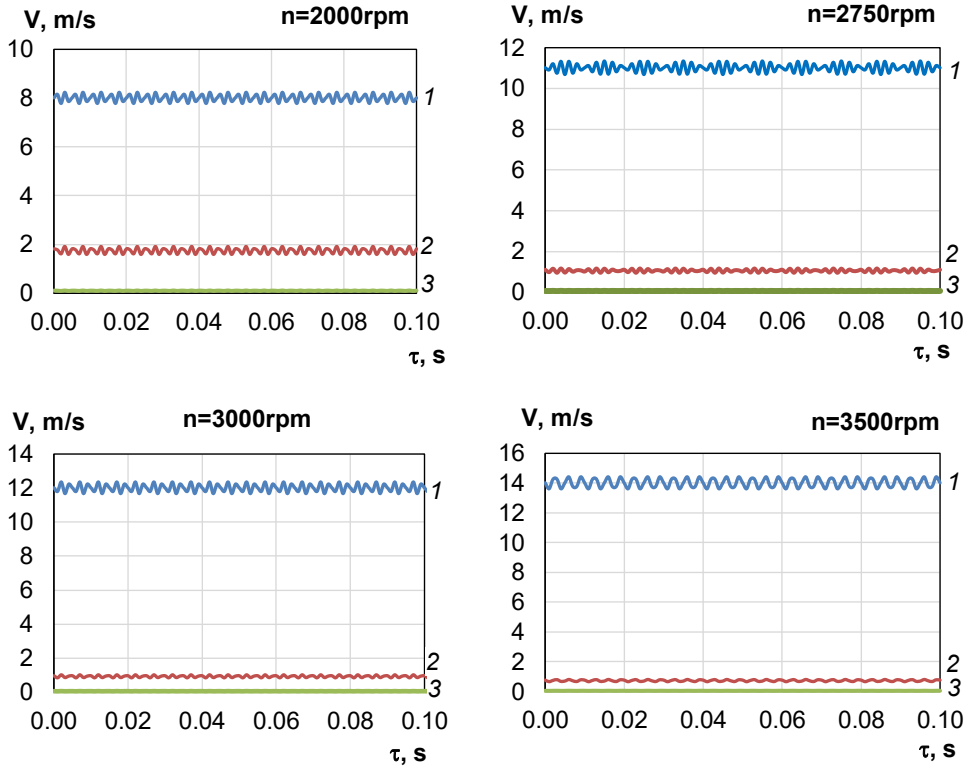

Figure 2. Theoretical time dependences of the velocity components within a single 3.5-second operating cycle (results shown within a 0.1-second time window); 1 – tangential velocity $u_\theta(t)$; 2 – axial velocity $v_z(t)$;3 – radial velocity $v_r(t)$.

From the graphical dependencies (Figure 2), it is observed that the mean tangential velocity u_θ increases proportionally with the rotational speed n (2000–3500 rpm). The pulsations of u_θ are about 3 percent, which is consistent with the 2-5 percent reported in (Utomo et al., 2008; Mortensen et al., 2018). The axial velocity $v_z(t)$ exhibits oscillations of

ISSN: 2409-4951 (Online), 2310-1008(Print)

approximately 10 percent of its mean value, which corresponds to the 8-12 percent range noted in (Mortensen et al., 2018). Although the mean value of v_z decreases with increasing n, the pulsatory behaviour remains. The radial velocity v_r accounts for only 1–3 percent of v_z, confirming its minor contribution, as also indicated in (Samoichuk et al., 2024) and (Launder et al., 2010; Utomo and Pacek, 2009).

Using the calculated velocity functions $u_\theta(t)$, $v_z(t)$, and $v_r(t)$, the instantaneous flow rate was determined as:

$$Q(t) = v_z(t) \cdot A_{\text{tot,}} \tag{16}$$

where A_{tot} is the total cross-sectional area.

Integration of $Q(t)$ over one 3.5-second operating cycle yields the total processed volume per cycle V_{tot}:

$$V_{\text{tot}} = \int_0^T Q(t)\,dt,$$

where T = 3.5 seconds is the cycle duration.

Figure 3 presents the variations of the instantaneous flow rate Q(t) and the accumulated volume $V_{tot}(t)$ over a single operating cycle for rotor rotational speeds n=2000–3500 rpm.

As shown in Figure 3, the instantaneous flow rate $Q(t)$ exhibits a clearly pronounced periodic pattern. The oscillations are quasi-regular and reflect the periodic interaction between the rotor channels and the stator (blade-passing effect), which modulates the axial velocity component and, consequently, the instantaneous throughput. The relative amplitude of the flow-rate oscillations is about 5–10%, which is consistent with LES/CFD studies (Mortensen et al., 2018; Utomo et al., 2008).

The accumulated volume $V_{tot}(t)$ shows an almost linear increase over the cycle, confirming that the net transport remains stable despite the pulsations of Q(t). Importantly, the slope of $V_{tot}(t)$ (i.e., the cycle-averaged throughput) decreases as n increases, indicating a weakening of axial transport at higher rotor speeds. This behaviour is consistent with Taylor-Couette type flows, where exceeding a critical rotational speed promotes stable vortex structures that reduce axial transport (Hop et al., 2023; Launder et al., 2010).

Experimental validation of hydraulic and energy characteristics of the rotor-stator system

To assess the adequacy of the proposed model, the predicted mean characteristics were compared with experimental data (Voroshchuk, 2010), including the mean liquid flow rate *Q*, torque M, and power N as functions of the rotor rotational speed *n*. As shown in Figure 4, the mean liquid flow rate decreases with increasing rotor speed. The predicted values agree well with the experimental dataset, supporting the adequacy of the model. The reduction in Q with increasing n is explained by the rise in hydraulic resistance and the development of vortex structures within the rotor-stator gap, which decreases the contribution of the axial flow component to transport (Zheng et al., 2022).

ISSN: 2409-4951 (Online), 2310-1008(Print)

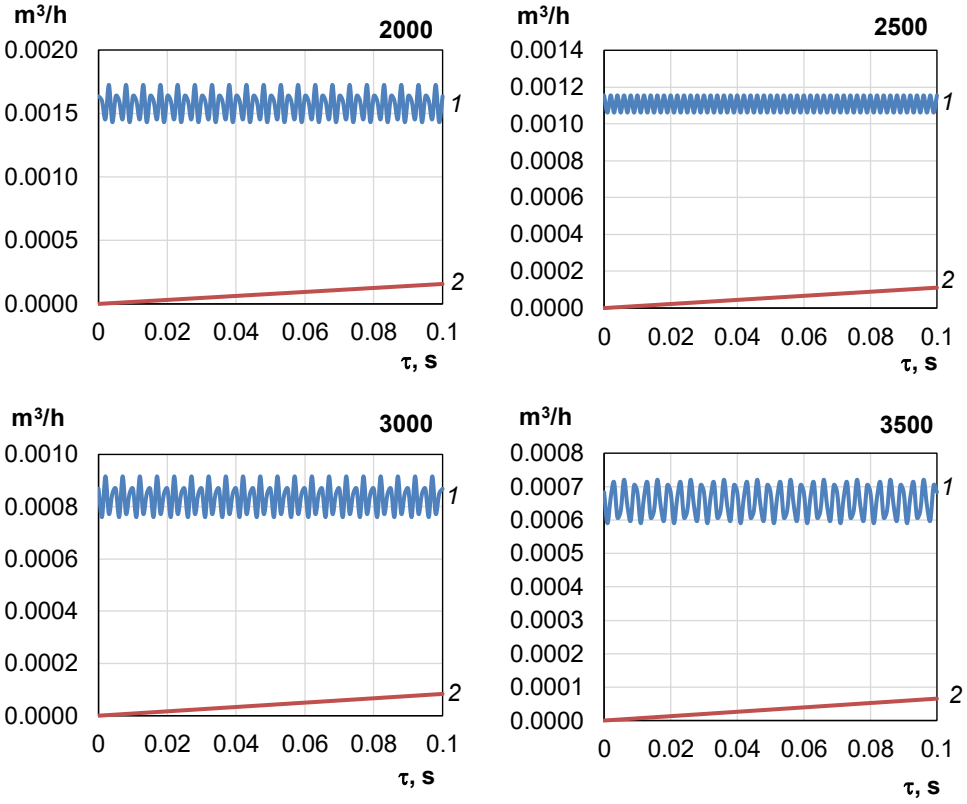

Figure 3. Instantaneous flow rate $Q(t)$ and accumulated (processed) volume $V_{tot}(t)$ over a single 3.5-second operating cycle: 1 – $Q(t)$; 2 – $V_{tot}(t)$

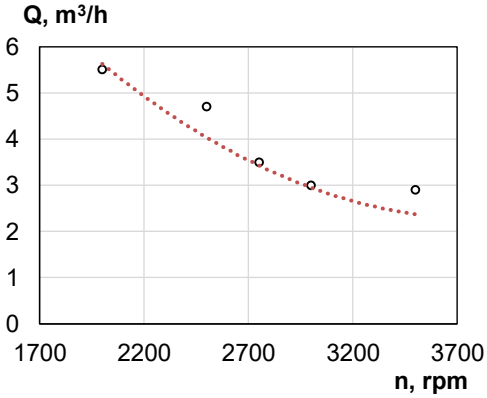

Figure 4. Mean liquid flow rate Q as a function of rotor rotational speed n:
—— calculated (theoretical) values;
◦ experimental values
(Voroshchuk, 2010).

ISSN: 2409-4951 (Online), 2310-1008(Print)

The results presented in Figure 4 demonstrate a decrease in the mean liquid flow rate Q with increasing rotor rotational speed n. The predicted mean values agree well with the experimental data (Voroshchuk, 2010), which confirms the adequacy of the model. The reduction in the mean liquid flow rate Q with increasing rotor rotational speed n is explained by the rise in hydraulic resistance, the formation of vortex structures within the rotor-stator gap, and, consequently, the decrease in the contribution of the axial flow component to overall transport. This observation is consistent with the findings of Zheng et al. (2022).

CFD studies of rotor-cavitation devices also indicate that, as the rotor rotational speed increases, the tangential flow components increasingly dominate the hydrodynamics, whereas the contribution of the axial component diminishes (Ranade, 2022). Similar hydrodynamic behaviour is observed in classical Taylor-Couette-type flows, where exceeding the critical rotational speed leads to the formation of stable vortex structures that weaken the axial flow and the corresponding transport (Hop et al., 2023).

The results for the torque M and power N reflect the increase in energy consumption associated with overcoming viscous resistance and generating circulating flow structures. It should be noted that the axial-flow contribution coefficient ε\varepsilonε decreases from 0.21 to 0.064, which is attributed to the transition in the flow structure-from a combined pattern (axial and tangential components) at low rotor rotational speeds to a predominantly tangential pattern at higher nnn.

Figures 5 and 6 present graphical comparisons between the values calculated using the proposed model and the corresponding experimental data (Voroshchuk, 2010).

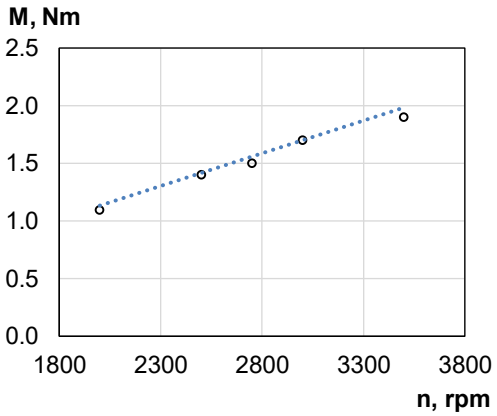

Figure 5. Dependence of torque M on rotor rotational speed n:
—— calculated (theoretical) values;
◦ experimental values
(Voroshchuk, 2010)

The torque M increases with rotor rotational speed n, consistent with intensified shear in the rotor-stator gap. The model-predicted (calculated) mean torque agrees well with the experimental data, and the calculated (n) trend is close to linear, indicating an approximately proportional relationship between the tangential flow velocity and viscous resistance. The deviation between experiment and model does not exceed 5-7% at n=2000-2500 rpm and remains below 20% at n=3000-3500 rpm. The remaining discrepancy is attributed to additional losses related to vortex structures and secondary flows that are difficult to capture analytically; similar effects at higher n have been reported in Wang et al. (2023), Zheng et al. (2022), and Ranade (2022).

ISSN: 2409-4951 (Online), 2310-1008(Print)

Figure 6 presents a comparison of the calculated and experimental power values.

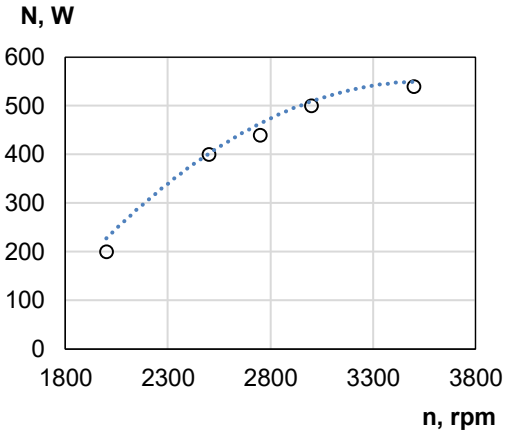

Figure 6. Comparison of calculated and experimental power N as function of rotor rotational speed n:
—— calculated (theoretical) values;
◦ experimental values
(Voroshchuk, 2010).

The predicted mean power values show good agreement with experiments, indicating that the adopted model adequately reproduces the energy consumption of the apparatus. The relationship $N = f(n)$ exhibits an almost linear trend over the investigated range, and the discrepancy between theoretical and experimental data does not exceed 10%. This deviation may be attributed to additional energy losses not fully captured by the model (Wang et al., 2023; Utomo et al., 2008; Zheng et al., 2022).

Conclusions

Existing approaches to describing rotor–pulsation devices are not fully universal: rheological models capture material behavior but ignore flow structure, while CFD methods reconstruct velocity and pressure fields but are mainly for Newtonian fluids. To address this, an integrated approach was developed, incorporating the non-Newtonian nature of curd mass via a structural parameter for shear-induced breakdown and recovery, and a harmonic function to represent flow oscillations. It was found that increasing rotor speed decreases mean flow rate and processed volume, while tangential flow dominates the hydrodynamic pattern. Flow pulsations, determined by rotor channel number and speed, reach 5–10% of the mean value, consistent with prior studies. Comparison with experimental data shows good agreement for performance and energy characteristics, confirming model adequacy. The results suggest operating at lower speeds to maximize processed volume and at higher speeds to intensify shear, dispersion, or homogenization. Further work could extend design parameters, refine rheological models, and apply 3D CFD (LES/URANS) to study secondary flows and vortex structures.

ISSN: 2409-4951 (Online), 2310-1008(Print)

References

Adanta D., Fattah I.M.R., Muhammad N.M. (2020), Comparison of standard k-ε and SST k-ω turbulence model for breastshot waterwheel simulation, *Journal of Mechanical Science and Engineering*, 7(2), pp. 39–44, https://doi.org/10.36706/jmse.v7i2.44

Ahmed U., Michael V., Hou R., Mothersdale T., Prosser R., Kowalski A., Martin P. (2018), An energy transport based evolving rheology in high-shear rotor–stator mixers, *Chemical Engineering Research and Design*, 133, pp. 398–406, https://doi.org/10.1016/j.cherd.2018.02.019

Badve M., Gogate P.R., Pandit A.B., Csoka L. (2013), Hydrodynamic cavitation as a novel approach for wastewater treatment in wood finishing industry, *Separation and Purification Technology*, 106, pp. 15–21, https://doi.org/10.1016/j.seppur.2012.12.029

Barnes H.A. (1999), The yield stress – a review or 'panta rei' – everything flows?, *Journal of Non-Newtonian Fluid Mechanics*, 81(1–2), pp. 133–178, https://doi.org/10.1016/S0377-0257(98)00094-9

Bird R.B., Stewart W.E., Lightfoot E.N. (2002), *Transport Phenomena*, 2nd ed., John Wiley & Sons, New York.

Hakansson A. (2018), Rotor-stator mixers: from batch to continuous mode of operation – a review, *Processes*, 6(4), 32, https://doi.org/10.3390/pr6040032

Hop C.J.W., Jansen R., Besten M., Chaudhuri A., Baltussen M.W., van der Schaaf J. (2023), Hydrodynamics of a rotor–stator spinning disk reactor, investigations by large-eddy simulation, *Physics of Fluids*, 35(3), 035105, https://doi.org/10.1063/5.0137405

John T.P., Panesar J.S., Kowalski A., Rodgers T.L., Fonte C.P. (2019), Linking power and flow in rotor-stator mixers, *Chemical Engineering Science*, 207, pp. 504–515, https://doi.org/10.1016/j.ces.2019.06.039

Launder B.E., Poncet S., Serre E. (2010), Laminar, transitional, and turbulent flows in rotor-stator cavities, *Annual Review of Fluid Mechanics*, 42, pp. 229–248, https://doi.org/10.1146/annurev-fluid-121108-145514

Launder B.E., Spalding D.B. (1974), The numerical computation of turbulent flows, *Computer Methods in Applied Mechanics and Engineering*, 3(2), pp. 269–289, https://doi.org/10.1016/0045-7825(74)90029-2

Minnick B.A., Janz E.E., Calabrese R.V. (2023), CFD simulation of an axial discharge rotor-stator mixer, LES versus RANS predictions, *Chemical Engineering Research and Design*, 198, pp. 413–430, https://doi.org/10.1016/j.cherd.2023.08.047

Mortensen H.H., Arlov D., Innings F., Hakansson A. (2018), A validation of commonly used CFD methods applied to rotor stator mixers using PIV measurements of fluid velocity and turbulence, *Chemical Engineering Science*, 177, pp. 340–353, https://doi.org/10.1016/j.ces.2017.11.037

Patankar S.V. (2018), *Numerical Heat Transfer and Fluid Flow*, CRC Press, Boca Raton, https://doi.org/10.1201/9781482234213

Ranade V.V. (2022), Modeling of hydrodynamic cavitation reactors, reflections on present status and path forward, *ACS Engineering Au*, 2(6), pp. 461–476, https://doi.org/10.1021/acsengineeringau.2c00025

Samoichuk K., Yalpachyk V., Kholobtseva I., Dmytrevskyi D., Chervonyi V. (2024), Design improvement of the rotary-pulsation device by resonance phenomena, In: *Advances in Design, Simulation and Manufacturing VII, Lecture Notes in Mechanical Engineering*, Springer Nature Switzerland, Cham, pp. 74–83, https://doi.org/10.1007/978-3-031-63720-9_7

Utomo A., Baker M., Pacek A.W. (2009), The effect of stator geometry on the flow pattern and energy dissipation rate in a rotor–stator mixer, *Chemical Engineering Research and Design*, 87(4), pp. 533–542, https://doi.org/10.1016/j.cherd.2008.12.011

ISSN: 2409-4951 (Online), 2310-1008(Print)

Utomo A.T., Baker M., Pacek A.W. (2008), Flow pattern, periodicity and energy dissipation in a batch rotor–stator mixer, *Chemical Engineering Research and Design*, 86(12), pp. 1397–1409, https://doi.org/10.1016/j.cherd.2008.07.012

Versteeg H.K., Malalasekera W. (2007), *An Introduction to Computational Fluid Dynamics, The Finite Volume Method,* 2nd ed., Pearson Education, Harlow.

Vashisth V., Nigam K.D.P., Kumar V. (2021), Design and development of high shear mixers, fundamentals, applications and recent progress, *Chemical Engineering Science*, 232, 116296, https://doi.org/10.1016/j.ces.2020.116296

Voroshchuk V.Ya. (2010), *Hidrodynamichni protsesy obrobky syrkovykh mas v rotorno-vykhorovomu emulsori*, *PhD thesis*, Kyiv.

Wang Y., Li M., Liu H.L., Chen J., Lv L.L., Wang X.L., Zhang G.X. (2023), Optimized geometric structure of a rotational hydrodynamic cavitation reactor, *Journal of Applied Fluid Mechanics*, 16(6), pp. 1218–1231, https://doi.org/10.47176/jafm.16.06.1495

White F.M. (2006), *Viscous Fluid Flow*, 3rd ed., McGraw-Hill, New York.

Wilcox D.C. (2006*), Turbulence Modeling for CFD, 3rd ed.,* DCW Industries, La Canada, CA.

Zemanova L., Rudolf P. (2019), Turbulence models for simulation of the flow in a rotor-stator cavity, *EPJ Web of Conferences*, 213, 02104, https://doi.org/10.1051/epjconf/201921302104

Zheng H., Zheng Y., Zhu J. (2022), Recent developments in hydrodynamic cavitation reactors, cavitation mechanism, reactor design, and applications, *Engineering*, 19, pp. 180–198, https://doi.org/10.1016/j.eng.2022.04.027

Author identifiers ORCID

Victor Voroshchuk	0000-0002-8943-1493
Maria Shynkaryk	0000-0003-3489-9803
Pawel Drozdziel	0000-0003-2187-1633
Oleh Kravets	0000-0002-3309-9962

Cite:

Ukr J Food Sci Style

Voroshchuk V., Shynkaryk P., Drozdziel P., Kravets O. (2025), Modeling of hydrodynamic processes in rotor-pulsation apparatus, *Ukrainian Journal of Food Science*, 13(2), pp. 136–149, https://doi.org/10.24263/2310-1008-2025-13-2-4

APA Style

Voroshchuk, V., Shynkaryk, P., Drozdziel, P., & Kravets, O.(2025). Modeling of hydrodynamic processes in rotor-pulsation apparatus. *Ukrainian Journal of Food Science, 13*(2), 136–149. https://doi.org/10.24263/2310-1008-2025-13-2-4

ISSN: 2409-4951 (Online), 2310-1008(Print)

Tomato powder as natural colorant and lycopene source in toast bread

**Olena Bilyk, Anastasiia Kukhar,
Artem Zabroda, Liudmyla Burchenko**

National University of Food Technologies, Kyiv, Ukraine

Keywords:

Toast bread
Tomato powder
Colorant
Lycopene
Antioxidant
Sensory

Article history:

Received 20.09.2025
Received in revised form 17.10.2025
Accepted 31.12.2025

Corresponding author:

Olena Bilyk
E-mail: bilyklena@gmail.com

DOI: 10.24263/2310-1008-2025-13-2-5

Abstract

Introduction. Toast bread is among the most widely consumed bakery products. This study aimed to justify the incorporation of tomato powder into toast bread formulations to expand the range of colored bakery products and enhance their nutritional value.

Materials and methods. Tomato powder was incorporated into toast bread formulations. The baked products were evaluated using sensory and physicochemical indicators, followed by calculation of a composite quality index. Dough structural and rheological properties were assessed using a Brabender farinograph and alveograph, along with monitoring dough diameter changes during proofing. Gas-producing capacity was determined volumetrically and by measuring dough ball floating velocity, while product color parameters were measured using a colorimeter.

Results and discussion. The feasibility of incorporating tomato powder into toast bread technology was substantiated. It was established that the addition of 5% powder (based on flour weight) ensured stable technological properties of the dough and enhanced the nutritional value of the final products without impairing their sensory characteristics. Alveograph and farinograph analyses demonstrated an increase in dough stability from 7.5 to 14.0 min and a reduction in softening from 110 to 50 BU, while maintaining an appropriate balance between dough elasticity and extensibility. The addition of tomato powder contributed to more controlled fermentation behavior: total gas production decreased from 616 to 588 ml CO_2/100 g, and the gas production peak shifted to a later stage, indicating improved gas retention capacity of the dough matrix. Pre-hydrated tomato powder further improved the quality attributes of the baked products: crumb porosity increased to 82%, crumb crumbliness after 72 h decreased from 11.3 to 9.2%, loaf shape stability was preserved, and sensory scores ranged from 8.2 to 8.5 points, confirming good consumer acceptability. The color difference (ΔE^*) reached 15.29 for the crust and 17.33 for the crumb, confirming the effectiveness of tomato powder as a natural colorant and functional ingredient, attributable to its high carotenoid content, particularly lycopene, and its contribution to the development of visually attractive bakery products.

Conclusions. The use of steamed tomato powder positively influences the quality of toast bread and ensures diversification of the assortment of colored bakery products enriched with antioxidants. Tomato powder can be considered a promising natural ingredient for the development of functional bakery products with improved nutritional and sensory properties.

ISSN: 2409-4951 (Online), 2310-1008(Print)

Introduction

Toast bread is one of the most popular bakery products intended for mass consumption due to its stable demand, convenience of use and regular presence in the daily diet. It is consumed by people of different ages and social groups, in particular as a component of breakfast or as an element of fast meals. This determines the significant role of toast bread in providing the body with energy and basic nutrients. However, the traditional formulation of toast bread is primarily oriented towards energy value and is characterised by an insufficient content of biologically active compounds, which creates prerequisites for its improvement (Falsafi et al., 2025).

The use of natural dyes in colored bakery products enhances their visual appeal while also supplying bioactive compounds such as anthocyanins, polyphenolic pigments, chlorophyll, and β-carotene. Natural colorants including elderberry pomace powder, blackthorn and hawthorn fruit extracts, purple sweet potato, and black carrot concentrate have been tested in bakery and dairy products (Stabnikova et al., 2003; 2025). In addition, barberry fruit powder has been applied as natural dye in caramel production (Sema et al., 2025), while chokeberry and hibiscus extracts have been incorporated into marshmallow formulations (Artamonova et al., 2025). This approach enables the preservation of traditional sensory properties while increasing nutritional value, thereby contributing to the development of a healthy eating culture and meeting the modern demand for original, nutritious, and aesthetically appealing products (Çolak and Karaduman, 2025). Moreover, it addresses consumer demand for bakery products manufactured without the use of synthetic food dyes (Boiko and Bilyk, 2025).

In modern food production, considerable attention is paid to the use of natural functional ingredients, particularly vegetable and fruit powders, in bakery and confectionery technologies. The chemical composition of vegetable and fruit powders is a key factor that determines their functional effects in bakery products (Naknaen and Angsombat, 2016). Tomatoes and other fruits processed into powders contain natural sugars (glucose, fructose, sucrose), organic acids (citric, malic), dietary fibre and pectin, as well as various polyphenols and carotenoids (including lycopene and β-carotene) (Lau and Shafie, 2021). Owing to this combination of bioactive compounds, vegetable powders modify dough texture: dietary fibre and pectin increase water-binding capacity and make the dough more viscous; organic acids reduce pH, stimulate yeast activity and improve crumb porosity. Polyphenols and carotenoids act as natural pigments, providing products with vivid colour, while their antioxidant activity protects lipid components from oxidation and extends shelf life (Djeghim and Zidoune, 2021). Powders also enrich the final product with vitamins (C, A) and minerals, increasing its nutritional value and technological performance during baking (Salanță and Fărcaş, 2024).

The introduction of vegetable powders such as carrot and pumpkin into bakery products significantly influences the technological properties of dough and the quality of the final product. In particular, the use of black carrot powder enriches bread with polyphenols, improves colour and increases antioxidant activity, which enhances the sensory characteristics of the product (Pandey et al., 2024). Pumpkin powder, due to its high content of dietary fibre and β-carotene, improves dough structure, increases loaf volume and imparts a pleasant colour and flavour to bread (Rakcejeva et al., 2011). Partial substitution of wheat flour (5–15%) with pumpkin cellulose resulted in a 1.1–1.4-fold increase in protein content and a 1.4–2.2-fold increase in dietary fiber compared with the control bread (Stabnikova et al., 2023). Replacement of wheat flour, 5%, with rosehip flour improved dough stabilithy, decrease baking loss and had a positive influence on bread aroma (Chochkov et al., 2022). Incorporation of 10% flour obtained from extruded sunflower seed kernels into muffin

ISSN: 2409-4951 (Online), 2310-1008(Print)

formulations increased the protein, fat, fiber, and ash contents by 24.7%, 16.9%, 23.3%, and 16.9%, respectively, while reducing total carbohydrates and sugars by 5.2% and 16.2%, respectively. The enriched muffins also exhibited improved textural properties, characterized by a smooth, crack-free surface and a soft, elastic crumb with well-developed porosity and small, and uniformly distributed thin-walled pores (Tsykhanovska et al., 2024).

The use of tomato powder in bread technology improves the rheological properties of dough, reduces stickiness and increases elasticity, which contributes to better shaping of the products. In addition, tomato powder is a rich source of lycopene, a potent antioxidant that reduces oxidative processes in dough and prolongs the shelf life of the final product (Eslami and Ferrari, 2022). Compared with other powders, such as beetroot or carrot powder, tomato powder gives products a more intense colour and improves their sensory characteristics without the need to add synthetic colourants or flavourings (Chabi and Kayodé, 2024; Mehta and Yadav, 2018). This makes it an attractive ingredient for consumers seeking natural and functional products.

The intense colour of bread with tomato powder is positively perceived by consumers; sensory studies showed that such samples received higher scores for crust attractiveness and appetising crumb appearance. In products with 3–5 % tomato powder, most tasting panel participants (approximately 70 %) noted that the new crust colour was vivid and conveyed a "fresh" impression without the need for additional colourants. At the same time, excessively high concentrations (8 % or more) produced an overly dark crust that slightly reduced overall acceptability; however, sensory tests demonstrated that most consumers still preferred the moderate darkening and distinct contrast between crumb and crust (Galvão et al., 2018).

The addition of dried tomato pomace significantly changes the indicators of water absorption capacity of dough and its structure. The addition of 6 % tomato pomace to flour mass increases the water absorption capacity of dough and finished bread, as well as increases titratable acidity due to the presence of organic acids in the powder (Amero and Collar, 1996). In this case, the specific volume of bread decreases by approximately 8 % compared to the control sample without additives, and crumb porosity decreases by 12 % due to the strengthening of the crumb framework by tomato pomace fibres. In addition, the increase in acidity and the presence of soluble compounds from tomato powder moisten the dough, prolonging proofing time by 10–15 %. The introduction of 3 % tomato powder into flour mass increases the water absorption capacity of flour by 5–7 % compared to the control sample, as dietary fibres adsorb more moisture and a denser gluten network is formed (Brighina and Restuccia, 2024). Despite the decrease in overall elasticity due to the strengthening of the gluten framework, a more stable bond between tomato powder fibres and gluten is formed, which ensures better dough stability during deformation in the moulding stage (Guimarães et al., 2025).

The use of tomato powder as a colouring raw material and a source of lycopene in bakery technology is economically justified due to the low cost of the starting material. Tomato pomace, from which tomato powder is produced, is a by-product of tomato paste and juice production and costs 20–30 % less than purchased tomato extract. The inclusion of tomato powder in toast bread technology does not require significant changes: standard equipment and conventional dosing systems can be used to ensure uniform distribution in flour blends (Arias et al., 2025).

The use of tomato powder allows replacement of waste from tomato processing in bakery technologies due to increased water absorption capacity of dough and improved crumb porosity. The growing demand for products with natural functional ingredients makes tomato powder an economically attractive innovation for industrial applications in the baking sector due to its low cost. Thus, tomato powder not only improves the colour and sensory

ISSN: 2409-4951 (Online), 2310-1008(Print)

profile of products, but also enables manufacturers to implement strategies for sustainable production, reducing waste and use of raw materials and minimising environmental impact (Chabi et al., 2024).

Therefore, the assessment of the feasibility of using tomato powder as a raw material with colouring capacity will ensure the expansion of the assortment of coloured toast bread products with increased nutritional value.

Materials and methods

Materials

Dough samples were prepared according to the formulation, % to flour mass: wheat flour of top grade – 100.0; compressed bakery yeast – 5.0; salt – 1.5; margarine with a fat content of 82 % – 5.0; granulated sugar – 8.0; skimmed milk powder – 2.0.

Preparation of dough samples

Dough was kneaded using a straight dough method with moisture content of 44.0 %. Dough fermentation lasted 20 minutes. Dough was kneaded again using the straight dough method, with fermentation time of 15 minutes. Dough kneading was performed in a two-speed dough mixer Escher (Italy), with kneading duration of 2 minutes at the first speed and 10 minutes at the second speed. Dough pieces weighing 0.275 kg were shaped as elongated rolls and placed in baking tins. Proofing was carried out in a proofing cabinet at a temperature of 35–40 °C for 45 minutes. Baking was performed without lids in Sveba-Dahlen (Italy) ovens at a temperature of 180–200 °C for 10–15 minutes. Tomato powder of TM "Pryanyi Svit" was used in the study. According to the manufacturer's data, the chemical composition of the tomato powder is as follows: moisture content – 4.5%, protein content – 12.9%, fat content – 0.43%, carbohydrate content – 74.7%, dietary fiber – 16.5%, ash content, % – 8.9%, calcium – 161 mg/100 g, magnesium – 176 mg/100 g, phosphorus – 296 mg/100 g, potassium – 1931 mg/100 g, iron – 4.65 mg/100 g, vitamin C – 115.0 mg/100 g, tocopherol (vitamin E) – 12.0 mg/100 g, lycopene – 46.260 mg/100 g.

Methods

Specific volume of bread

The grain is filled with the excess, which is raked with the edge of the ruler into the receiving container and removed through the hole. After that, the curtains of the main capacity with grain are opened manually and put through the hole into the bucket. This grain is used for determination. A small amount of grain is put into the main container, bread is put on it, carefully, without passing the grain, and the rest of grain is put in excess of the capacity. Grain is raked with the edge of the ruler and put into the receiving container, and then, after opening the latch – into the measuring cylinder. The volume of grain in a cylinder (ml) is equal to the volume of bread. Measurements are performed twice, deviations between parallel determinations should not exceed 5%.

The specific volume of bread is determined by dividing the volume of bread by its weight and expressed to the nearest 0.01 ml/g (Zhu et al., 2016).

ISSN: 2409-4951 (Online), 2310-1008(Print)

Porosity of bread

The porosity of bread reflects the volume of the pores in a certain volume of the crumb, expressed as a %age to the total volume (Verheyen et al., 2015).

Comprehensive quality index

The evaluation of finished products was carried out according to sensory and physico-chemical quality indicators of bakery products, and a comprehensive quality index was calculated. The comprehensive quality index represents the total score obtained by the test sample during its assessment. For its calculation, each product was evaluated according to the following indicators: shape accuracy; specific volume; crust colour; crust surface condition; crumb colour; crumb porosity structure; crumb rheological properties; staling after 72 hours; bread aroma; bread taste, and crumb chewability.

The obtained values were evaluated using a five-point scale, taking into account the weighting coefficient determined for each indicator by expert assessment. The assigned score was multiplied by the weighting coefficient, after which the sum of the resulting values was calculated. The higher the total score obtained by the sample, the better its quality indicators (Lebedenko et al., 2014). The expert commission included five candidates of technical sciences, one Doctor of Philosophy, two PhD candidates and twelve higher education students specialising in Food Technologies.

Determination of structural and mechanical properties of dough

The influence of tomato powder on the structural and rheological properties of the dough was assessed using a Brabender farinograph (Germany) and a Chopin alveograph (Drobot et al., 2015)

Falling number. The method is based on measuring the time (in seconds) during which a metal stirrer falls through a gelatinised mixture formed from water and flour (or cereal grain flour), preheated to boiling in a glass test tube (Lebedenko et al., 2014).

Gas production. Gas production capacity was determined volumetrically using an AG-1M device according to the standard methodology (Blazhenko and Falendysh, 2024)

Dough expansion. Dough expansion during fermentation was determined by changes in dough ball diameter at a temperature of 30 °C in a thermostat (Makhynko, 2021).

Dough rising capacity. Dough rising capacity was determined by measuring the duration of dough ball flotation in water at 35–30 °C in a thermostat (Drobot, 2015).

Crust and crumb colour. Colour measurements were performed according to the methodology described by the authors (Coelho and Salas-Mellado, 2015) a chroma meter CR-200 (Minolta, Osaka, Japan) with a Hunter Lab system was used. Lightness (L*) represents sample lightness with values from 0 (black) to 100 (white). The psychometric tone a* characterises red (+a*) to green (–a*) shades, while the psychometric tone b* characterises yellow (+b*) to blue (–b*) shades. The a* and b* values are obtained after instrument calibration. The overall colour difference ΔE describes the total colour difference and is calculated according to formula:

ISSN: 2409-4951 (Online), 2310-1008(Print)

$$\Delta E = \sqrt{(L^* - L_0^*)^2 + (a^* - a_0^*)^2 + (b^* - b_0^*)^2},$$

where L_0*, a_0*, b_0* are the values for the control sample, and L*, a*, b*– are the values for the test sample. Each parameter was measured at five points, and the mean value was used for calculations.

Statistical analysis

The experiments were carried out in five replicates, and the results were reported as arithmetic means.

Results and discussions

Selection of optimal tomato powder dosage for toast bread formulation

The initial studies concerned the feasibility of using tomato powder in toast bread technology. For this purpose, laboratory baking trials were carried out. Dough was prepared using the straight dough method according to the toast bread formulation (this sample served as the control). Tomato powder was added in dosages of 1.0; 2.0; 3.0; 4.0; 5.0; 6.0 and 7.0% to flour mass. Bread quality was evaluated according to physico-chemical, sensory indicators and the comprehensive quality index. The results are presented in Table 1 and in Figure 1.

Analysis of physico-chemical indicators (Table 1) demonstrated that the introduction of tomato powder within the range of 1.0–5.0% did not impair specific volume. At a dosage of 5.0%, its value increased to 408 ml/100 g compared with the control sample (394 ml/100 g), which may be attributed to the positive effect of dietary fibres and pectic substances from tomato powder on the gas-holding capacity of dough. Further dosage increase to 6.0–7.0% did not provide any significant improvement of this indicator.

It was established that at tomato powder dosages of 1.0–3.0%, crumb porosity characteristics approached the control sample, although pores were less homogeneous and insufficiently compacted for toast bread requirements. The most optimal fine-porosity characteristics were formed at 4.0–5.0 %: the crumb was dense with fine and medium pores evenly distributed throughout the entire volume. With an increase in dosage to 6.0–7.0%, excessive crumb compaction and disruption of porosity uniformity were observed. Despite the quantitative increase in porosity index, qualitative structural characteristics deteriorated, negatively affecting rheological properties, chewability and overall consumer perception.

Investigation of crumb staling after 72 h of storage revealed a progressive decrease in staling intensity with increasing levels of tomato powder. The most pronounced effect was observed at a 5.0% addition level, indicating delayed crumb firming and enhanced moisture-retention capacity. Further increases in tomato powder content did not result in significant additional improvements.

Sensory evaluation demonstrated that at tomato powder dosages up to 5.0% inclusive, acceptable crust and crumb colour, correct shape and surface condition were maintained. Starting from 6.0–7.0%, crumb colour became excessively dark and taste and aroma exhibited dominant tomato notes, which are undesirable for toast bread with a standard consumer profile.

ISSN: 2409-4951 (Online), 2310-1008(Print)

Table 1

Effect of tomato powder on dough quality and physico-chemical quality characteristics of bread

Quality indicator of toast bread	**Control**	**Tomato powder dosage, % to flour**						
		1.0	**2.0**	**3.0**	**4.0**	**5.0**	**6.0**	**7.0**
Specific volume, ml per 100 g of bread	394	396	392	394	396	396	398	408
Shape accuracy	Bread with dome-shaped crust							
Porosity, %	82	82	86	87	89	90	94	95
Staling after 72 h, %	11.3	10.9	10.5	10.1	9.7	9.1	8.7	8.2
Crust colour	Light brown				Brown		Dark brown	
Crust surface condition	Smooth, without bubbles or cracks, glossy							
Crumb colour	Light	Light brown to brown, acceptable for perception					Dark colour	Too dark, less acceptable
Crumb porosity structure	Small, thin-walled pores, evenly distributed throughout the crumb, typical for toast bread baked without a lid						Medium and small pores, thick-walled, evenly distributed, typical for toast bread baked without a lid	
Crumb rheological properties	Very soft, tender, elastic						Soft, elastic	
Bread aroma	Aroma characteristic of toast bread						Intense aroma of toast bread, with a tomato note	
	Slightly creamy	Creamy	Creamy, a light tomato aroma					
Bread taste	Taste characteristic of toast bread							
	Slightly creamy	Pronounced, creamy, with a slight tomato note	Pronounced, creamy, with a tomato note				Pronounced, creamy, with an intense tomato flavour	
Crumb chewability	Tender, single-bite chew						Fairly tender	
Comprehensive quality indicator	**96.4**	**96.8**	**96.8**	**96.0**	**95.4**	**95.0**	**81.0**	**80.9**

The integral quality assessment confirmed these patterns: the comprehensive quality index for samples with 1.0–5.0% dosage remained at a high level (95.0–96.8 points), whereas at 6.0 and 7.0% it sharply decreased to 81.0 and 80.9 points, respectively.

ISSN: 2409-4951 (Online), 2310-1008(Print)

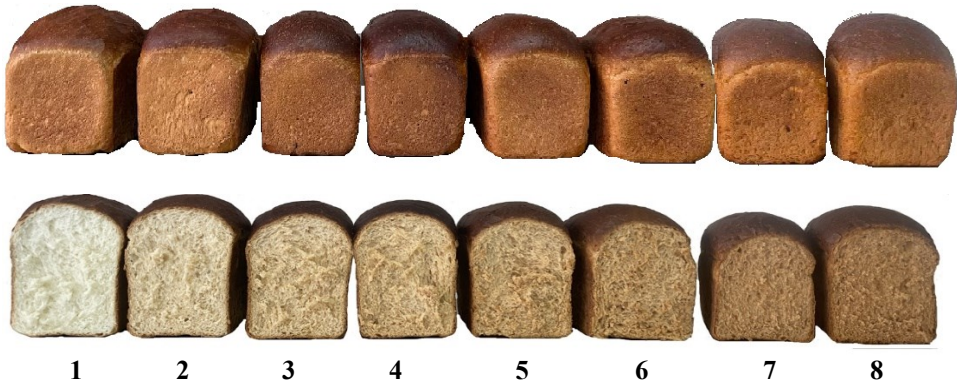

Figure 1. Images of finished toast bread products:
1 – control without additives; bread with tomato powder, %, to flour:
2 – 1.0; 3 – 2.0; 4 – 3.0; 5 – 4.0; 6 – 5.0; 7 – 6.0; 8 – 7.0.

Therefore, the optimal dosage of tomato powder is 5.0% to flour mass, without deterioration of physico-chemical and sensory indicators, with the formation of a fine-porous, dense and uniform crumb structure characteristic of toast bread, as well as a high comprehensive quality index.

Influence of tomato powder on structural and mechanical properties of dough

To conduct a more detailed investigation of the influence of tomato powder on baking properties of dough, instrumental analysis was carried out using an alveograph (Chopin) and a farinograph (Brabender). The research results are presented in Table 2.

According to alveograph data (Table 2), the addition of tomato powder improves the mechanical properties of dough. Dough elasticity (P) increased from 117 to 121 mm, indicating increased resistance to deformation. This may be attributed to interactions between tomato powder components, particularly dietary fibres and pectic substances, and wheat flour proteins, forming a denser and more stable gluten network. Dough extensibility (L) also slightly increased from 31 to 32 m), while the P/L ratio remained unchanged – 3.8, indicating preservation of elastic–plastic properties. Deformation energy (W) increased from 160 to 165 a.u., confirming enhanced flour strength and improved potential dough gas retention. A slight increase in extensibility index (G) from 12.4 to 12.6, with unchanged elasticity index (Ie), also indicates structural stabilisation of dough.

Farinograph analysis revealed a slight decrease in dough water absorption (from 53.3 to 53.1%), which can be explained by the formation of new colloidal bonds in the presence of pectin, binding part of the water and reducing its overall availability for gluten development. Dough development time increased from 1.5 to 2.0 min, indicating slower protein hydration, likely due to competitive water binding by tomato powder fibre. Dough stability remained at zero, although dough formation time also increased to 2.0 min, confirming the above assumption. Meanwhile, dough stability nearly doubled from 7.5 to 14.0 min, indicating structural strengthening and improved resistance to mechanical stress. Dough softening decreased from 110 to 50 B.U., indicating reduced dough weakening and increased dough stability during kneading.

ISSN: 2409-4951 (Online), 2310-1008(Print)

Table 2

Effect of tomato powder on structural and mechanical properties of dough

Indicator	Control sample (without additives)	With tomato powder (5.0 % to flour mass)
Alveograph		
Dough elasticity, P, mm	117	121
Dough extensibility, L, mm	31	32
Elasticity to extensibility ratio, P/L	3.8	3.8
Deformation energy (flour strength), W, a.u.	160	165
Elasticity index, Ie, %	0	0
Extensibility index, G	12.4	12.6
Farinograph		
Water absorption, %	53.3	53.1
Dough development time, min	1.5	2.0
Dough stability, min	0.0	0.0
Dough formation time, min	1.5	2.0
Stability, min	7.5	14.0
Softening, B.U.	110.0	50.0

These changes are explained by the physico-chemical effects of dietary fibres, pectins and other biologically active components of tomato powder, which interact with flour protein and starch structures, affecting dough rheology. As a result, a stronger and more stable structure is formed, positively influencing toast bread preparation technology.

Evaluation of tomato powder's impact on dough biochemical processes

The study of the influence of tomato powder on the Falling Number makes it possible to evaluate how the introduction of a plant-based additive modifies the enzymatic state of the flour system. Tomato powder contains organic acids, low-molecular-weight carbohydrates, pectic substances and mineral components, which may indirectly affect α-amylase activity by altering medium acidity, starch hydration and substrate availability for enzymes.

For enriched dough, the Falling Number also has additional importance, as it allows prediction of gas production and gas retention intensity. A decrease in the Falling Number indicates increased amylolytic activity, which may lead to excessive formation of fermentable sugars, weakening of the dough structure and formation of sticky crumb. Conversely, an excessively high Falling Number indicates insufficient starch hydrolysis, which restricts yeast nutrition and negatively affects product volume and porosity.

In the control sample, the Falling Number was 328 s, which corresponds to flour with moderate amylolytic activity sufficient for the formation of fermentable sugars and normal fermentation progress. This value is typical for flour suitable for the production of pan and toast bread with stable structural properties.

When 5% tomato powder was added to the flour, the Falling Number significantly increased — up to 484 s, indicating a decrease in the amylolytic activity of the system. The obtained increase can be explained by several interrelated factors.

Firstly, tomato powder contains neither starch nor amylase, therefore its incorporation

ISSN: 2409-4951 (Online), 2310-1008(Print)

causes a diluting effect on the enzymatically active flour fraction. Secondly, dietary fibre and pectic substances in tomato powder intensely bind water, reducing its availability for starch gelatinisation and limiting its accessibility as a substrate for enzymatic reactions (Wang and Janaswamy, 2001). Thirdly, organic acids in tomato may modify the structure of starch granules and indirectly reduce the hydrolysis rate (Rosell et al., 2001).

The increase of the Falling Number to 484 s indicates a reduction in the intensity of amylolytic processes, which is particularly relevant for enriched dough systems with initially elevated sugar content. In such systems, excessive α-amylase activity is undesirable, as it may lead to excessive starch degradation, dough weakening and formation of sticky crumb. Therefore, the increase in the Falling Number upon addition of tomato powder may be considered a stabilising factor that ensures controlled fermentation progress.

Thus, the obtained Falling Number values indicate that the incorporation of 5 % tomato powder reduces the amylolytic activity of the flour system without suppressing dough fermentation and creates prerequisites for the formation of a dense, fine-porosity crumb structure characteristic of toast bread.

Further investigations concerned the influence of tomato powder on gas production in dough. Dough was prepared using the straight dough method, 5 % tomato powder was added, and dough water content was 38%. Considering that dough rest lasted 15 min, dough proofing of shaped pieces lasted approximately 60 minutes, and gas production was measured during 120 min of fermentation. The results are shown in Figures 2 and 3.

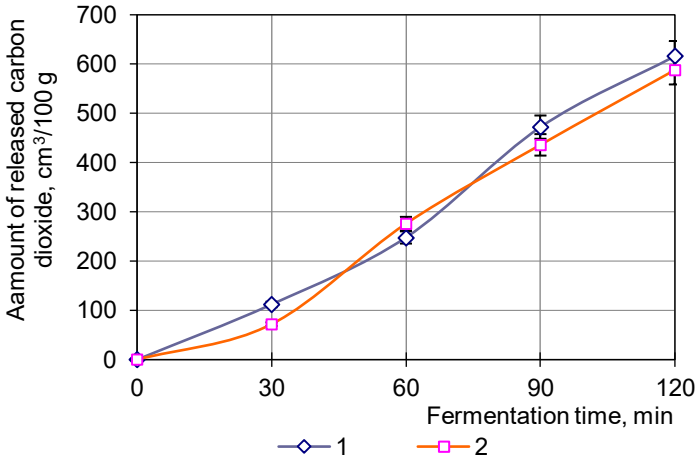

Figure 2. Gas production capacity of dough:
1 – control (without additives); 2 – with tomato powder, 5.0% to flour weight

The results of the investigation of gas production intensity in enriched dough for toast bread with the addition of 5% tomato powder demonstrate regular changes in the amount of carbon dioxide released during 120 min of fermentation. The total quantity of CO_2 released in dough with tomato powder reached 588 ml/100 g, which only slightly differed from the control sample (616 ml/100 g). The obtained data indicate that the addition of tomato powder does not cause a significant inhibition of gas production in dough, but provides moderate and controlled CO_2 release.

ISSN: 2409-4951 (Online), 2310-1008(Print)

From a technological point of view, such gas production is optimal for toast bread, as it promotes the formation of a fine-porous, uniform and dense crumb structure without the risk of excessive aeration. Controlled gas production intensity combined with stable dough structure creates prerequisites for obtaining products with predictable consumer properties and high quality.

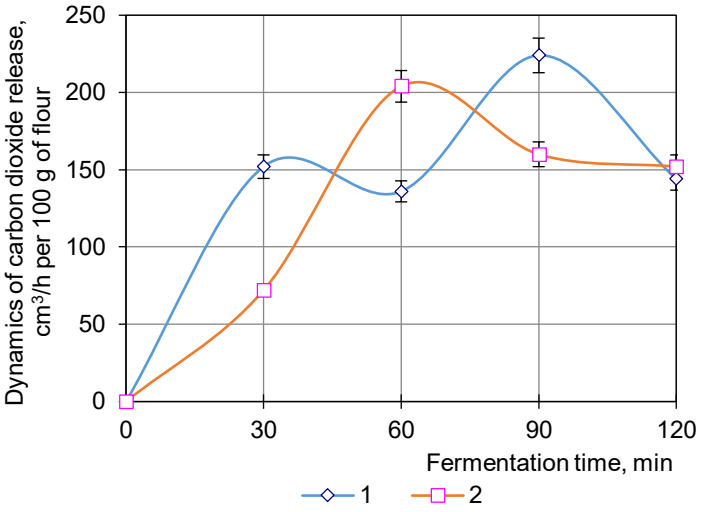

Figure 3. Dynamics of gas production during 2 hours of dough fermentation: 1 – control (without additives); 2 – with tomato powder, 5.0% to flour weight

Analysis of CO_2 release over a 120-min fermentation period showed that the control dough reached its first gas-production peak earlier, at 30 min, with a value of 152 ml/100 g. In contrast, dough containing 5% tomato powder exhibited substantially lower CO_2 release at 30 min (72 ml/100 g), and the maximum was shifted to 60 min, reaching 204 ml/100 g. These results indicate that the incorporation of tomato powder delays the onset of intensive fermentation while ultimately promoting a higher peak level of CO_2 production.

The early peak in the control enriched dough is explained by faster yeast activation in a medium where sugar is readily available as a substrate and water is not bound by additional hydrophilic components. After the initial peak at 60 minutes, the control sample demonstrated a decrease in gas production intensity (136 ml/100 g), which can be interpreted as the completion of the initial phase of fermentation of readily accessible sugars and a transition to another fermentation mode.

In dough containing tomato powder, the shift of the gas-production peak to 60 min is expected and can be attributed to the high water-binding capacity of dietary fiber and pectic substances present in tomato, which increase the viscosity of the dough system. In enriched formulations containing sugar and fat, these effects further hinder initial hydration and yeast adaptation, resulting in reduced CO_2 formation at 30 min. Following yeast adaptation and stabilization of enzymatic activity, CO_2 release increases, reaching 204 ml/100 g at 60 min, indicating that the main fermentation activity in the experimental dough occurs at a later stage.

ISSN: 2409-4951 (Online), 2310-1008(Print)

At 90 min, the control dough continues to intensify gas production (224 ml/100 g), whereas the tomato powder–enriched dough shows a lower value (160 ml/100 g), reflecting more pronounced, peak-type fermentation kinetics in the control and a more moderated fermentation profile in the experimental sample during the later stages. By 120 min, CO_2 production values in both systems become comparable (144 ml/100 g in the control and 152 ml/100 g in the tomato-enriched dough), suggesting similar fermentation intensity at the final stage.

Overall, the delayed gas-production peak observed in dough enriched with tomato powder is technologically advantageous for toast bread manufacture, as it supports controlled gas accumulation and ensures maximal CO_2 release during the dough-piece proofing stage.

Improvement of toast bread technology and investigation of consumer properties

The addition of tomato powder alters enzymatic, rheological and fermentation processes in enriched dough: amylolytic activity decreases (Falling Number increases), gas production kinetics changes and dough rising rate slightly decreases. Without adjustment of technological parameters, this may lead to deviations in crumb structure formation, specific volume and porosity uniformity.

For this purpose, laboratory baking trials were carried out, in which 5 % tomato powder (to flour mass) was dosed in dry form, soaked form and scalded form. The soaked powder was prepared at a tomato powder to water ratio of 1:2, with swelling duration of 30 minutes. The scalded powder was prepared at a tomato powder to water ratio of 1:2, using water at 95–97 °C followed by cooling to 28–30 °C. The results of laboratory baking trials are presented in Table 3 and Figure 4.

The obtained results indicate that the form in which tomato powder is incorporated (dry, soaked or scalded) differently affects dough development processes and the formation of toast bread quality, for which controlled gas production, limited dough spreading and the formation of a fine- to medium-pored, uniform crumb are essential.

The reduction of dough gas production in the experimental samples compared with the control from 616 to 568–588 ml/100 g is technologically desirable for toast bread, as excessive gas formation in enriched dough may lead to coarse-porous crumb. The lowest gas production was observed in the sample with scalded tomato powder.

The indicator of specific dough volume increase demonstrated notable differences depending on the powder preparation method. In the case of dry powder addition, volume increase was lower than the control, whereas the use of soaked and especially scalded tomato powder ensured notably higher volume increase relative to the dry powder sample. For toast bread, this means that preliminary hydration of tomato powder promotes more efficient and uniform expansion of gas cells without structural collapse.

The increased proofing time of dough pieces and the increase in dough rising strength (up to 62–66 min and 10 min, respectively) indicate delayed CO_2 release at the initial fermentation stage, which is favourable for toast bread.

The reduction of dough spreading from 172 to 160% in the case of scalded tomato powder confirms enhanced dough shape stability, which is critically important for pan-baked toast bread and uniform slice cutting.

From the perspective of finished products, specific volume, porosity and crumb texture are the most informative indicators. The use of scalded tomato powder ensured the highest bread specific volume (388 ml/100 g) and porosity (82%), which correspond to toast bread requirements with a light but not excessively developed crumb structure.

ISSN: 2409-4951 (Online), 2310-1008(Print)

Table 3

Effect of tomato powder on quality indicators of toast bread,

Indicator	Control (without additives)	Experimental samples		
		1	2	3
		with 5% tomato powder (to flour mass)		
		Dry	Soaked	Scalded dough
Dough				
Gas production, ml CO_2/100 g	616	588	580	568
Increase in specific dough volume, % to initial	324	308	373	378
Proofing time to readiness, min	50	62	62	66
Increase in ball diameter, % to initial	172	170	166	160
Dough rising strength, min	7	8	10	10
Finished products				
Specific volume, ml/100 g	385	372	376	388
Porosity, %	76	68	68	82
External appearance	Correct shape, surface uniform			
Crumb texture	Tender, single-bite chew			
Crumb porosity structure	Fine, thin-walled pores evenly distributed throughout the crumb, typical for toast bread baked without a lid	Medium and fine, thin-walled pores evenly distributed throughout the crumb, typical for toast bread baked without a lid	Medium and fine, thin-walled pores evenly distributed throughout the crumb, typical for toast bread baked without a lid	Medium and fine, thin-walled pores evenly distributed throughout the crumb, typical for toast bread baked without a lid
Crust colour	Dark brown		Brown	Light brown
Crumb colour	White with creamy shade	Light brown		
Taste and aroma	**Characteristic of toast bread**			
	Creamy	Pronounced, creamy, with light tomato note		Pronounced, , creamy, with tomato note

ISSN: 2409-4951 (Online), 2310-1008(Print)

Figure 4. Dough rising strength:
1 – control (without additives); 2 – with dry tomato powder, 5.0% to flour mass;
3 – with soaked tomato powder, 5.0% to flour mass;
4 – with scalded tomato powder, 5.0% to flour weight

Crumb porosity characteristics in all experimental samples corresponded to toast bread (fine to medium pores, thin walls), although scalded tomato powder ensured the most uniform and stable crumb structure, which was confirmed by sensory assessment ("very tender, single-bite chew").

Colour changes in crust and crumb are consistent: the use of dry powder resulted in darker colouring, while scalded tomato powder produced a light brown crust and pleasant light-brown crumb colour, which is desirable for toast bread and does not interfere with toasting of slices in a toaster.

Sensory evaluation of taste and aroma showed that all tomato powder forms impart a characteristic tomato note, although the scalded powder ensured the most harmonious flavour and aroma with a subtle tomato note that does not dominate over the creamy bread profile of toast bread.

The positive results of using tomato powder made it possible to develop a new product – "TomatoToast" toast bread.

To determine the influence of tomato powder on crust and crumb colouring, colour measurements were carried out using a digital colourimeter (Chroma Meter CR-200). The influence on the parameters L* (lightness, where L* = 0 and L* = 100 are taken as black and white, respectively), a* (psychometric tone ranging from green (−) to red (+) from −120 to120) and b* (psychometric chromaticity ranging from blue (−) to yellow (+) from −120 to 120) was determined, and the colour difference relative to the control sample (ΔE*) was calculated (Abdulazeez et al., 2023). The research results are presented in Table 4.

One of the most important quality indicators of bakery products is colour, which directly influences consumer perception and overall product appeal. In this study, the effect of tomato powder on colour characteristics of toast bread was evaluated using the CIELAB colour model, which allows quantitative assessment of changes in lightness (L*), red/green component (a*) and yellow/blue component (b*), as well as general colour difference expressed as ΔE*.

ISSN: 2409-4951 (Online), 2310-1008(Print)

Table 4

Colour characteristics of bread samples in the CIELAB model

Bread sample	Colour characteristics			
	L_0*	a_0*	b_0*	ΔE_0*
Crust				
Toast bread	38.39	7.8	6.87	-
"TomatoToast" bread	48.43	11.37	17.82	15.29
Crumb				
Toast bread	73.57	1.37	12.77	-
"TomatoToast" bread	63.77	11.01	23.31	17.33

The results indicate that the addition of tomato powder to the formulation substantially changes the colour of both crust and crumb. For the "TomatoToast" sample, the L* value of crust increased by 10.04 units, indicating increased surface lightness. Simultaneously, a* and b* values increased by 3.57 and 10.95 units, respectively, indicating enrichment with red and yellow tones. A similar trend was observed in the crumb: lightness decreased (by 9.8 units), while a* and b* increased by 9.64 and 10.54 units, respectively.

The overall colour difference ΔE* was 15.29 for the crust and 17.33 for the crumb, which exceed the threshold of perceptible visual difference (ΔE* > 3) and indicate a significant change in colour profile. This confirms the effectiveness of tomato powder as a natural colourant. The pronounced colouring is determined by carotenoid pigments (primarily lycopene), which are natural antioxidants. Their thermal stability allows retention of intense colouring even after baking, making tomato powder a promising functional additive for bakery products with not only aesthetic but also physiological and sensory value.

Thus, the application of tomato powder in toast bread formulation allows controlled colouring of the product without deterioration of technological or sensory properties, and potentially enhances its biological value, which is relevant under the growing demand for functional bakery products.

Conclusions

The feasibility of incorporating tomato powder at 5% of flour mass in toast bread was demonstrated, ensuring stable dough properties and enhanced nutritional value without compromising sensory quality. Alveograph and farinograph analyses showed improved dough stability (from 7.5 to 14.0 min) and reduced softening (from 110 to 50 B.U.), while maintaining the elasticity-to-extensibility ratio. Tomato powder also promoted a more controlled fermentation, with a slight decrease in total gas production (from 616 to 588 ml CO_2/100 g) and a later gas peak, contributing to a fine-porous, uniform crumb. The Falling Number increased from 328 to 484 s, indicating reduced amylolytic activity and stabilisation of the starch–protein matrix, advantageous for doughs with higher sugar content. Scalded tomato powder proved most effective, ensuring better hydration of dietary fibres and pectic substances and stabilising the protein–polysaccharide matrix. Colour measurements (ΔE*) of 15.29 for crust and 17.33 for crumb confirmed a significant colour change, attributed to carotenoids, mainly lycopene, which also provide antioxidant activity.

ISSN: 2409-4951 (Online), 2310-1008(Print)

Acknowledgement
This study was carried out within the framework of the state-funded research project "Scientific justification and development of resource-efficient technologies of targeted food products as an imperative of food security", project No. 0123U102060.

References

Abdulazeez Z.M., Mustafa A.M.I., Yazici F. (2023), Correlation between acrylamide content and colour in some baked products, *Czech Journal of Food Sciences*, 41(2), pp. 137–143, https://doi.org/10.17221/244/2022-CJFS

Amero E., Collar C. (1996), Antistaling additives effects on fresh wheat bread quality, *Food Science and Technology International,* 2, pp. 323–333, https://doi.org/10.1177/108201329600200506

Arias A., Feijoo G., Moreira M.T. (2025), Agri-food waste to phenolic compounds: Life cycle and eco-efficiency assessments, *Journal of Environmental Management*, 380, 124935, https://doi.org/10.1016/j.jenvman.2025.124935

Artamonova M., Piliugina I., Aksonova O., Stabnikova O. (2025), Chokeberry and hibiscus as natural food additives in confectionery, In: S. Gubsky, O. Stabnikova, V. Stabnikov, O. Paredes-López (Eds.), *Wild Edible Plants: Improving Foods Nutritional Value and Human Health through Biotechnology* (pp. 201-219), CRC Press, Boca Raton, London, New York, https://doi.org/10.1201/9781003486794-7

Blazhenko M., Falendysh N., Shpak V. (2024), Effect of hemp seed by-products on wheat dough fermentation, *Ukrainian Food Journal*, 13(4), pp. 737–752, https://doi.org/10.24263/2304-974X-2024-13-4-8

Boiko I., Bilyk O., Skryhun N., Kapinus L., Bilokhatniuk V. (2025), Marketing communications of enterprises of Ukrainian food market to improve consumer attitudes towards food additives, *Ukrainian Food Journal*, 14(2), pp. 354–374, https://doi.org/10.24263/2304-974X-2025-14-2-12

Brighina S., Pulvirenti L., Siracusa L., Arena E., Faulisi M. V., Restuccia C. (2024), Small-sized tomato pomace: Source of bioactive compounds and ingredient for sustainable production of functional bread, *Foods*, 13(21), 3492, https://doi.org/10.3390/foods13213492.

Chabi I.B., Zannou O., Dedehou E.S.C.A., Ayegnon B.P., Odouaro O.B.O., Maqsood S., Galanakis C.M., Kayodé A.P.P. (2024), Tomato pomace as a source of valuable functional ingredients for improving physicochemical and sensory properties and extending the shelf life of foods: A review, *Heliyon*, 10(3), e25261, https://doi.org/10.1016/j.heliyon.2024.e25261

Chochkov R., Zlateva D., Ivanova P., Stefanova D. (2022), Effect of rosehip flour on the properties of wheat dough and bread, *Ukrainian Food Journal*, 11(4), pp. 558-572, https://doi.org/10.24263/2304-974X-2022-11-4-6

Coelho M.S., Salas-Mellado M. M. (2015), Effects of substituting chia (*Salvia hispanica* L.) flour or seeds for wheat flour on the quality of the bread, *LWT – Food Science and Technology*, 60(2), pp. 729–736, https://doi.org/10.1016/j.lwt.2014.10.033

Çolak B., Karaduman Y. (2025), Bioactive components of colored grain wheat and its use in food products, *European Food Science and Engineering*, 6(2, Part 1), pp. 26–33, https://doi.org/10.55147/efse.1663061

Djeghim F., Bourekoua H., Różyło R., Bieńczak A., Tanaś W., Zidoune M.N. (2021), Effect of by-products from selected fruits and vegetables on gluten-free dough rheology and bread properties, *Applied Sciences*, 11(10), 4605, https://doi.org/10.3390/app11104605

Drobot V.I., Yurchak V.H., Bilyk O.A., Bondarenko Yu.V., Hryshchenko A.M. (2015), *Techno-Chemical Control of Raw Materials and Bakery and Pasta Products,* Kondor Publishing, Kyiv.

Eslami E., Carpentieri S., Pataro G., Ferrari G. (2022), A comprehensive overview of tomato processing by-product valorization by conventional methods versus emerging technologies, *Foods*, *12*(1), 166, https://doi.org/10.3390/foods12010166

ISSN: 2409-4951 (Online), 2310-1008(Print)

Falsafi S.R., Aaliya B., Demirkesen I., Kemerli-Kalbaran T., Dehnad D., Şahin S., Yildirim-Yalcin M., Alarcon-Rojo A.D. (2025), Recent trends in fortifying bread with nutrients: Comprehensive insights into chemical, physical, functional, and nutritional attributes, *Future Foods*, 11, 100674, https://doi.org/10.1016/j.fufo.2025.100674

Galvão A.M.M.T., Zambelli R.A., Araújo A.W.O., Bastos M.S.R. (2018), Edible coating based on modified corn starch/tomato powder: Effect on the quality of dough bread, *LWT*, 89, pp. 518–524, https://doi.org/10.1016/j.lwt.2017.11.027

Guimarães D.J.S., Zambelli R.A., Afonso M.R.A., Pontes D.F. (2025), Cryoprotective potential of vegetable powders and polydextrose in frozen bread doughs, *International Journal of Refrigeration*, 172, pp. 108-119, https://doi.org/10.1016/j.ijrefrig.2025.01.010.

Lau K.Q., Sabran M.R., Shafie S.R. (2021), Utilization of vegetable and fruit by-products as functional ingredient and food, *Frontiers in Nutrition*, 8, 661693, https://doi.org/ 10.3389/fnut.2021.661693

Lebedenko T., Pshenyshnyuk H., Sokolova N. (2014), *Bakery Production Technology. Practical Training Manual,* Osvita Ukrainy Publishing, Odesa.

Makhynko R. (2021), The upgraded dough running measurement device, *Scientific Look into the Future*, 1(19-01), pp. 28–31, https://doi.org/10.30888/2415-7538.2020-19-01-025

Mehta D., Prasad P., Sangwan R.S., Yadav S.K. (2018), Tomato processing byproduct valorization in bread and muffin: improvement in physicochemical properties and shelf life stability, *Journal of Food Science and Technology*, 55(7), pp. 2560–2568, https://doi.org/10.1007/s13197-018-3176-0

Naknaen P., Itthisoponkul T., Sondee A., Angsombat N. (2016), Utilization of watermelon rind waste as a potential source of dietary fiber to improve health promoting properties and reduce glycemic index for cookie making, *Food Science and Biotechnology*, *25*(2), pp. 415–424, https://doi.org/10.1007/s10068-016-0057-z

Pandey P., Grover K., Dhillon T. S., Chawla, N., Kaur, A. (2024), Development and quality evaluation of polyphenols enriched black carrot (*Daucus carota* L.) powder incorporated bread, *Heliyon*, 10(3), e25109, https://doi.org/10.1016/j.heliyon.2024.e25109

Rakcejeva T., Galoburda R., Cude L., Strautniece E. (2011), Use of dried pumpkins in wheat bread production, *Procedia Food Science*, 1, pp. 441–447, https://doi.org/10.1016/j.profoo.2011.09.068

Rosell C.M., Rojas J.A., de Barber C.B. (2001), Influence of hydrocolloids on dough and bread quality, *Food Hydrocolloids,* 15(1), pp. 75-81, https://doi.org/10.1016/s0268-005x(00)00054-0

Salanță L.C., Fărcaş A.C. (2024), Exploring the efficacy and feasibility of tomato by-products in advancing food industry applications, *Food Bioscience*, 62(01), 105567, https://doi.org/10.1016/j.fbio.2024.105567

Sema O., Stabnikova O., Sachko A., Gubsky S. (2025), Barberry as an ingredient for functional food production, In: S. Gubsky, O. Stabnikova, V. Stabnikov, O. Paredes-López (Eds.), *Wild Edible Plants: Improving Foods Nutritional Value and Human Health through Biotechnology* (pp. 185-200), CRC Press, Boca Raton, London, New York, https://doi.org/10.1201/9781003486794-5

Stabnikova O., Shevchenko A., Stabnikov V., Paredes-López O. (2023), Utilization of plant processing wastes for enrichment of bakery and confectionery products, *Ukrainian Food Journal*, 12(2), pp. 299-308, https://doi.org/10.24263/2304-974X-2023-12-2-11

Stabnikova O., Stabnikov V., Paredes-López O. (2024), Fruits of wild-grown shrubs for health nutrition, *Plant Foods for Human Nutrition*, 79(1), pp. 20–37, https://doi.org/10.1007/s11130-024-01144-3

Stabnikova O., Stabnikov V., Paredes-López O. (2025), Wild edible plants, berries, mushrooms and seaweeds in food production, In S. Gubsky, O. Stabnikova, V. Stabnikov, O. Paredes-López (Eds.), *Wild Edible Plants: Improving Foods Nutritional Value and Human Health through Biotechnology* (pp. 1-47), CRC Press, Boca Raton, London, New York, https://doi.org/10.1201/9781003486794-1

ISSN: 2409-4951 (Online), 2310-1008(Print)

Tsykhanovska I., Stabnikova O., Riabchykov M., Lazarieva T., Korolyova N. (2024), Effect of partial replacement of wheat flour by flour from extruded sunflower seed kernels on muffins quality, *Plant Foods for Human Nutrition*, 79(4), pp. 769-778, https://doi.org/10.1007/s11130-024-01232-4

Verheyen C., Albrecht A., Elgeti D., Jekle M., Becker T. (2015), Impact of gas formation kinetics on dough development and bread quality, *Food Research International*, 76(3), pp. 860–866, https://doi.org/10.1016/j.foodres.2015.08.013

Wang S., Janaswamy S. (2001), Effects of wheat bran and its particle size on mixing and bread-making quality of white wheat flour, *Cereal Chemistry*, 78(2), pp. 181–186.

Zhu F., Sakulnak R., Wang S. (2016), Effect of black tea on antioxidant, textural, and sensory properties of Chinese steamed bread, *Food Chemistry*, 194, pp. 1217–1223, https://doi.org/10.1016/j.foodchem.2015.08.110

Author identifiers ORCID

Olena Bilyk	0000-0003-3606-1254
Anastasiia Kukhar	0009-0000-8428-5768
Artem Zabroda	0009-0001-2100-1235
Liudmyla Burchenko	0000-0002-5413-961X

Cite:

Ukr J Food Sci Style

Bilyk O., Kukhar A., Zabroda A., Burchenko L. (2025), Tomato powder as natural colorant and lycopene source in toast bread, *Ukrainian Journal of Food Science*, 13(2), pp. 150–167, https://doi.org/10.24263/2310-1008-2025-13-2-5

APA Style

Bilyk, O., Kukhar, A., Zabroda, A., & Burchenko, L. (2025). Tomato powder as natural colorant and lycopene source in toast bread. *Ukrainian Journal of Food Science, 13*(2), 150–167. https://doi.org/10.24263/2310-1008-2025-13-2-5

ISSN: 2409-4951 (Online), 2310-1008(Print)

Influence of sweet potato puree and soybean addition on the quality characteristics of gluten-free biscuits

Emmanuel Kehinde Oke[1], Abiodun Aderoju Adeola[2], Oluwakemi Abosede Ojo[2], Odunayo Rhoda Adebayo[2], Saheed Adewale Omoniyi[3], Femi Fidelis Akinwande[4]

1 – University of Medical Sciences, Ondo City, Nigeria
2 – Federal University of Agriculture, Abeokuta, Nigeria
3 – Federal University, Gashua, Nigeria
4 – Yaba College of Technology, Yaba, Nigeria

Keywords:

Biscuit
Gluten-free
Sweet potato puree
Soybean
Quality

Article history:

Received 11.10.2025
Received in revised form 29.11.2025
Accepted 31.12.2025

Corresponding author:

Emmanuel Kehinde Oke
E-mail: kennyoke35@gmail.com

DOI:
10.24263/2310-1008-2025-13-2-6

Abstract

Introduction. This study aims to investigate the effects of sweet potato puree and soybean addition on the quality characteristics of gluten-free biscuits.

Materials and methods. Blends of wheat, sweet potato puree and soybeans flour at varying ratios were used to produce biscuit through D-optimal mixture design. The produced biscuits were subjected to proximate, minerals, physical, textural and sensory analysis.

Results and discussion. The weight, diameter, and spread ratio of the biscuits increased with the addition of sweet potato puree and soybean flour in the blends. The observed ranges were 9.52–15.22 g for weight, 7.21–10.17 mm for thickness, 41.89–47.85 mm for diameter, 45.42–51.16 for lightness (L*), 2.83–5.03 for redness (a*), 17.73–22.34 for yellowness (b*), 10.44–13.99 for energy value, and corresponding increases in spread ratio. The changes in colour parameters indicate enhanced browning reactions and pigment contribution from sweet potato puree.

Moisture content, crude protein, and crude fat increased with increasing levels of sweet potato puree and soybean flour in the formulation. The ranges obtained were 9.08–18.87% for moisture, 12.85–17.08% for crude protein, 17.11–19.63% for crude fat, 1.47–1.92% for ash, 4.85–6.85% for crude fibre, and 44.08–46.44% for carbohydrates. The increase in dietary fibre and protein suggests an improvement in the nutritional quality of the gluten-free biscuits compared to conventional formulations.

The incorporation of soybean flour and sweet potato puree had a significant ($p < 0.05$) positive effect on the mineral content of the biscuits. Calcium, potassium, magnesium, iron, and zinc contents ranged from 23.66–28.77 mg/100 g, 110.90–128.90 mg/100 g, 12.74–16.12 mg/100 g, 0.28–0.34 mg/100 g, and 0.39–0.43 mg/100 g, respectively.

Textural properties, including peak force, adhesiveness, gumminess, springiness, and cohesiveness, varied within the ranges of 2572–6555 N, 5.46–16.68 N·s, 3403–6477.5 N, 0.13–1.07, and 0.05–1.11, respectively.

Conclusion. Despite variations among formulations, all biscuit samples achieved acceptable sensory scores. However, the biscuit produced with 72.5% wheat flour, 20.0% sweet potato puree, and 7.5% soybean flour was the most preferred by the panellists.

Introduction

Biscuits are small, thin, low-moisture, crispy baked products made from unleavened dough, packaged and sold as ready-to-eat foods, and consumed by individuals of all ages worldwide (Ariyo et al., 2022). Biscuit production requires key ingredients such as water, sugar, fat, and wheat flour; additional ingredients may include milk, salt, aerating agents, flavouring substances, and other food additives (Zuljevic and Akagic, 2021). The classification of biscuits is based on their ingredient composition and the processing methods employed during manufacture.

Wheat is one of the most important cereal crops and is heavily relied upon by a large proportion of the world's population (Erenstein et al., 2022). Wheat flour (*Triticum aestivum* L.) is the primary ingredient used in the production of baked products such as biscuits and contributes nearly half of the global caloric intake (Masood, 2021). However, wheat is deficient in essential amino acids such as lysine and threonine and is also implicated in coeliac disease due to the presence of gluten in wheat grains (Oke et al., 2023; Serwaa et al., 2021). Consequently, several efforts have been made to partially substitute wheat flour with non-wheat flours to improve nutritional quality, promote the utilization of indigenous crops in Nigeria, and help reduce the production costs of bakery products (Olagunju et al., 2020). Regarding the common plant foods that constitute the main source of the world population in their diets, soybeans are highest in terms of nutrition because they contain considerable amounts of the known hematinic minerals and vitamins, which play vital roles in the formations of red blood cells (Mile et al., 2024). In addition to its nutritional composition, soybean possesses notable medicinal and therapeutic properties (Maske, 2020). As a functional food, soybeans have been reported to lower triglyceride and blood cholesterol levels, both of which are major risk factors of cardiovascular diseases. Furthermore, research has shown that soybean consumption alleviates malnutrition and contributes to the regulation of blood glucose and body weight (Ijarotimi et al., 2021). Soybeans are also characterized by low cholesterol content and are rich sources of protein and dietary fibre (Ali et al., 2020)

Sweet potato (*Ipomoea batatas*) is another critical staple crop in Nigeria and many other developing countries and is recognized as one of the most important food crops globally (Onyiba et al., 2023). It belongs to the family *Convolvulaceae* and is classified as a dicotyledonous root crop among major staple foods. Sweet potato roots are rich in starch, sugars, vitamin C, β-carotene, iron, and other essential minerals (Hossain et al., 2022). Sweet potatoes can be processed into a wide range of liquid and semi-solid food products, including milk analogues, soups, baked goods, breakfast cereals, snacks, and dessert formulations (Laveriano-Santos et al., 2022). To ensure year-round availability, the tubers are often converted into purées in the food industry, which may subsequently be aseptically packaged, frozen, or canned to enhance storage stability.

Nevertheless, the use of composite flour blends comprising wheat, soybean flour, and sweet potato purée in biscuit production offers a viable approach to enhancing the nutritional value of biscuits. This strategy may also promote increased utilization and consumer acceptance of biscuits produced from wheat–soybean–sweet potato composite formulations. Therefore, this study aimed to evaluate the quality attributes of biscuits produced from composite flours of wheat, soybean, and sweet potato purée.

ISSN: 2409-4951 (Online), 2310-1008(Print)

Materials and methods

Materials

All of the ingredients namely: wheat flour (Honey well brand), sweet potato of white fleshed, soybeans and the rest of the ingredients like: sugar, margarine, baking powder, salt, egg, vanilla flavour were purchased in a retail supermarket at Eleweran, Abeokuta, Nigeria

Methods

Preparation of Soybean flour

Soybean flour was produced following the method of Alabi and Anuonye (2007) with slight modifications. One thousand grams (1000 g) of soybean seeds were sorted to remove defective seeds, stones, and other foreign materials. The seeds were thoroughly washed with tap water and boiled in 1250 mL of water for 30 min to soften the hulls and facilitate dehulling. The soybeans were then dehulled, washed, and blanched in water for 10 min. After draining, the seeds were oven-dried at 80 °C for 6 h using a hot air oven (Gallenkamp SG3-08-169, UK). The dried soybeans were subsequently roasted in a steel frying pan at low temperature for 20 min until a light golden-brown colour was obtained. The roasted seeds were dry-milled using a laboratory hammer mill (Fritsch, D-55743, Idar-Oberstein, Germany), sieved through a 100 μm mesh, and packed in airtight containers until further use.

Preparation of sweet potato puree

Sweet potato purée was prepared following the method of Chilungo et al. (2019). The sweet potato roots were thoroughly washed, peeled, and cut into cubes. The cubes were steamed in boiling water for 1 h, allowed to cool, and then mashed using a Kenwood food processor to obtain a smooth purée.

Blend formulation

The formulation of the flour blends is presented in Table 1 and was developed using a D-optimal mixture design. A total of fourteen experimental runs were prepared, with 100% wheat flour serving as the control. The flour blends were packaged and stored until required for biscuit production.

Production of biscuits

Biscuits were prepared using the fourteen flour blends with slight modifications to the procedure described by Ifeh and Chioke (2024). The ingredients were accurately weighed. The measured flour blends, sugar, milk powder, and baking powder were mixed using a Kenwood hand mixer until homogeneous. Eggs were then incorporated to form a cohesive dough, which was rolled into sheets of uniform thickness. A cutter was used to shape the biscuits to the desired size, and they were baked in a preheated oven at 220 °C for 15 minutes. The baked biscuits were allowed to cool for 30 minutes at room temperature and subsequently stored in polythene bags. The formulation for biscuit production (per batch) was as follows: sugar, 150 g; margarine, 150 g; baking powder, 2.84 g; salt, 1.42 g; egg, 1.00 g; and vanilla flavour, 2.84 g.

ISSN: 2409-4951 (Online), 2310-1008(Print)

Table 1

Composite flour from wheat, soybean and sweet potato purée using D-optimal mixture design

Experiment	Wheat flour (%)	Sweetpotato puree (%)	Soybean flour (%)
1	72.50	22.50	5.00
2	70.83	20.83	8.34
3	75.00	20.00	5.00
4	70.00	20.00	10.00
5	72.50	22.50	5.00
6	70.83	23.33	5.83
7	73.33	20.83	5.83
8	71.67	21.67	6.67
9	72.50	20.00	7.50
10	75.00	20.00	5.00
11	70.00	22.50	5.00
12	72.50	22.50	5.00
13	70.00	20.00	10.000
14	100	0	0

Proximate composition of biscuits

Moisture content was determined using a hot air oven method. Crude fat was measured by Soxhlet extraction, while total ash was determined gravimetrically by ashing the samples in a preheated muffle furnace at 600 °C for 6 h until a constant weight was achieved. Crude fibre was analyzed following extraction with petroleum ether. Crude protein content was determined using the Kjeldahl method (AOAC, 2016), and total carbohydrate was calculated by difference.

Mineral composition of biscuits

The mineral content of the biscuit samples was determined following the AOAC (2006) method. Briefly, 0.5 g of each biscuit sample was digested with a mixture of perchloric, nitric, and sulphuric acids on a hot plate until white fumes appeared. After cooling, the digest was diluted with distilled water, filtered, and made up to volume in a volumetric flask. The concentrations of calcium, potassium, iron, magnesium, and zinc were then determined using an Atomic Absorption Spectrophotometer (AAS).

Physical properties of biscuits

Biscuit physical attributes were evaluated following the approach of Adeola and Ohizua (2018). Four biscuits from each sample were placed side by side, and their diameter (width, W) and thickness (T) were measured using a digital vernier caliper (0.01 mm, Cappera Precision, China). The spread ratio (SR) was calculated as the ratio of diameter to thickness. The weight of the baked biscuits was determined using a digital weighing balance (AD, EK-4100i, Japan) after cooling, and the values for each sample were recorded (Oke et al., 2017).

ISSN: 2409-4951 (Online), 2310-1008(Print)

Colour properties of biscuits

The colour of the biscuits was determined following the method of Oke et al. (2019). A Minolta Chroma Meter (CR-410, Japan) was used for the analysis. Prior to measurement, the instrument was calibrated using a white calibration plate and a zero calibration mask. Biscuit samples were placed on a Petri dish, and readings were taken to obtain the colour parameters: lightness (L*), redness (a*), and yellowness (b*).

Textural properties of biscuits

The texture of the biscuits was evaluated using a three-point bending test following the method of Da Silva and Moreira (2008). Each biscuit sample was placed on two parallel supports, and a central load was applied. Measurements were performed using a Texture Analyzer (Model TA-XT2i, Stable Micro Systems, Haslemere, UK) equipped with a 2.5 mm thick flat-edged steel blade and a support span of 90.00 mm. The test was conducted at a constant crosshead speed of 30.00 mm/min until fracture occurred. The maximum force (N) at the point of fracture, corresponding to the peak value on the force–deflection (N vs. mm) curve, was recorded as an indicator of the sample's resistance to breakage.

Sensory evaluation of biscuits

Ethical approval for the sensory evaluation was obtained from the Ethical Committee of the Department of Food Science and Technology, Federal University of Agriculture, Abeokuta. Participation was entirely voluntary and panellists were provided with comprehensive information regarding the study objectives, requirements and potential risks prior to participation. Participant's retained the right to withdraw from the sensory evaluation at any stage without penalty. Sixty Panellists from Federal University of Agriculture Abeokuta including staff and student evaluated the biscuit samples through sensory testing. The test panellist's evaluated product attributes including colour, texture, taste and aroma and overall acceptability through their hedonic ratings which ranged from 1 to 9 (extremely dislike to extremely like).

Statistical analysis

All analyses were performed in triplicate and results were expressed as mean values. The data were subjected to statistical analysis using analysis of variance (ANOVA). The means were separated using the Duncan multiple range test at $p \leq 0.05$ probability level (SPSS version 23.0).

Result and discussion

Proximate composition of biscuit from wheat, soybean and sweetpotato puree composite flour

The proximate composition of biscuit using wheat, soybean and sweetpotato puree composite flour (Table 2) indicated that the addition of wheat, soybeans and sweetpotato puree had a significant ($p<0.05$) influenced the proximate composition of the biscuits. Based on the results, it was seen that moisture contents varied between 9.08 and 18.87 % whereby the sample consisting of (75:20:5) was reported to have lowest moisture content amongst samples whereas sample (70.83:20.83:8.34) had the highest moisture content. When the percentage levels of sweet potato puree and soybeans flour blend were added together, the moisture content of the sample, had shown an increase. Moisture content of the food is one of the critical and most popular indices when it comes to defining the quality of processed goods that are dried (Bakare et al., 2020).

ISSN: 2409-4951 (Online), 2310-1008(Print)

Depending on the thermal characteristics of the ingredients, the rate of moisture loss during baking is determined. Both sweet potatoes and soybeans have ingredients that can hinder the rate of water evaporation much faster than when using wheat flour on its own. It implies that the less moisture can be lost in the course of baking, the higher the amount of moisture contained in it in the end will be provided that the inclusion level of these ingredients is high. The values of the moisture content of the biscuit measured in this study were differed significantly ($p<0.05$) with one another and resemble values obtained by Passos et al. (2013) on biscuits brand of different kinds.

The biscuits had crude fat content between 17.11 and 19.63%. Fat serves multiple critical physiological functions: it acts as a solvent for lipophilic hormones and is essential for steroid hormone synthesis and cellular signaling (Agu et al., 2021). Additionally, it provides essential fatty acids that serve as precursors for eicosanoid synthesis and acts as the carrier vehicle for fat-soluble vitamins A, D, E and K. From an energetic perspective, lipids provide 9 kcal/g, representing the highest caloric density among the macronutrients, surpassing both proteins and carbohydrates which yield 4 kcal/g (Roth, 2011). The relatively narrow variation in fat content across formulations can be explained by the similar quantities of added fats (margarine) in the recipe, as shown in Table 2. However, soybean flour as a legume-based ingredient contributes substantial endogenous lipids to the biscuit formulation, containing approximately 18-22% oil by dry weight (Ali et al., 2020). The lipid fraction in soybean flour is predominantly composed of polyunsaturated fatty acids, particularly linoleic acid (omega-6) and linolenic acid (omega-3), which contribute to the nutritional quality of the final product. This explains why formulations with higher soybean flour content, such as the 10% SF formulation (which recorded the highest fat content of 19.63%), demonstrate elevated total lipid levels. The fat content is further concentrated during baking as moisture evaporates, leading to a relative increase in the proportion of all other constituents, including lipids, on a dry weight basis. This concentration effect explains why samples with lower moisture content often exhibit higher fat percentages. The fat content of the biscuits falls within the standard range of 15-20% characteristic of soft dough biscuits (Hama-Ba et al., 2018). These findings are consistent with other researchers such as Asif-Ul-Alam et al. (2014) and Silky and Tiwari (2014), who reported similar values of 15.10%-18.10% in biscuits prepared using composite flours with varying blend proportions.

The total ash values ranged from 1.47-1.92%. Ash content serves as a reliable proxy indicator of the total mineral constituents present in food materials. During ash determination, the sample is subjected to high-temperature combustion in the presence of atmospheric oxygen, resulting in the complete oxidation and volatilization of organic components (water, proteins, lipids, and carbohydrates), leaving behind the inorganic mineral residue (Sanni et al., 2008). From a nutritional standpoint, these minerals function as essential cofactors and activators for numerous enzymatic reactions involved in the catabolism of macronutrients, including lipid oxidation and carbohydrate metabolism.

The significant increase in ash content observed with higher inclusion levels of soybean and sweet potato puree can be attributed to their superior mineral profiles compared to wheat flour. Soybeans are particularly rich in minerals such as calcium, magnesium, iron, and potassium (Ali et al., 2020), while sweet potato contains substantial amounts of potassium, manganese, and copper (Hossain et al., 2022). The observation of this study aligns with the reporting of Guyih et al. (2020) who documented increased ash contents in biscuits produced from composites of wheat, almond seeds and carrot flour. However, this observation contradicts the report by Bello et al. (2008) who observed reduction in total ash content of biscuits made using blends of wheat, yellow yam, unripe plantain and pumpkin flour. These contradictory findings can be explained by variations in the inherent mineral composition of the raw materials used in the flour blend formulations, as well as potential differences in processing methods that may affect mineral retention.

ISSN: 2409-4951 (Online), 2310-1008(Print)

Crude fibre content ranged from 4.85-6.85%. Fibre comprises primarily indigestible polysaccharides including hemicelluloses, cellulose, and lignin, along with resistant starch and oligosaccharides. These components exert profound physiological effects on gastrointestinal health and metabolic regulation in humans (Atobatele and Afolabi, 2016). Fibre increases fecal bulk, reduces gastrointestinal transit time, modulates glucose absorption kinetics, reduces postprandial glycemic response, lowers serum cholesterol levels through bile acid sequestration, and promotes beneficial gut microbiota proliferation.

The addition of soybean and SPP flour to wheat flour had significant ($p<0.05$) effects on the fibre content of biscuit samples. This enhancement can be mechanistically explained by the high fiber content of both soybean (containing approximately 15-20% total dietary fiber) and sweet potato (containing 3-5% fibre in fresh weight, concentrated in puree form), which substantially exceeds that of refined wheat flour (typically 2-3% fibre). Similar findings were reported by Eke et al. (2019) who observed increased fiber content in cookies formulated with sweetpotato and cashew nut flour blended with wheat. Guyih et al. (2020) documented comparable results in wheat, almond seed and carrot flour blend cookies. The fibre content obtained in this research indicates that biscuits produced from wheat, soybean and sweetpotato puree blends would provide meaningful dietary fiber contributions when consumed, potentially aiding in meeting recommended daily fiber intake of 25-30 g/day.

The values of crude protein were 12.85-17.08%. The protein contents of the biscuits prepared with different flour blends varied significantly ($p<0.05$). These findings align closely with those provided by Passos et al. (2013). The results indicated that sample (75:20:5) contained the highest percentage of protein. This can be attributed to the superior protein content of both soybean (approximately 35-40% protein) and wheat (10-14% protein) compared to sweet potato (1-2% protein on fresh weight basis).

The biological value of the protein is also enhanced through complementary protein effects: wheat protein is limiting in lysine but adequate in methionine, while soybean protein is rich in lysine but limiting in methionine, thus creating a more complete amino acid profile when combined (Ijarotimi et al., 2021). Beyond their primary role as structural and functional proteins, these macromolecules serve as transport vehicles for micronutrients, facilitating the absorption and distribution of lipids, vitamin A (via retinol-binding protein), iron (via transferrin), sodium and potassium (through various carrier proteins) throughout the body (Mahan and Escott-Stump, 2008).

The total carbohydrate content was found to be 44.08- 46.44%. The carbohydrate content decreased significantly ($p<0.05$) with the incorporation of soybeans and SPP flour in the blends. This reduction can be explained by the displacement of high-carbohydrate wheat flour (which contains approximately 70-75% carbohydrate) with lower-carbohydrate ingredients. Soybean flour contains only 30-35% carbohydrate due to its high protein and fat content, while sweet potato puree, though containing significant carbohydrates, has lower carbohydrate concentration on a dry weight basis compared to wheat flour due to its moisture content and fiber composition. The carbohydrate values in the present study (44.08-46.44%) were considerably lower than the 77.11-81.18% described by Guyih et al. (2020), which can be attributed to the low carbohydrate content of soybean flour and the high level of reducing sugars rather than complex carbohydrates in sweetpotato flour used in this study (Adeola and Ohizua, 2020; Ayo-Omogie and Ogunsakin, 2013). Similar trends of carbohydrate reduction were reported by Ndife et al. (2020) when almond seed and carrot flour were added as partial substitutes for wheat in biscuit formulations.

ISSN: 2409-4951 (Online), 2310-1008(Print)

Table 2

Proximate composition of biscuit from wheat, soybean and sweet potato puree

WF %	SPP %	SF %	Moisture Content %	Crude Fat %	Total Ash %	Crude Fibre %	Crude Protein %	Total CHO %
72.50	22.50	5.00	12.93±0.04^{e}	18.63±0.03^{d}	1.63±0.01^{c}	6.08±0.04^{cd}	14.91±0.02^{d}	45.83±0.00^{d}
70.83	20.83	8.34	18.87±0.04^{g}	17.11±0.02^{a}	1.47±0.02^{a}	4.85±0.02^{a}	12.85±0.02^{a}	44.88±0.12^{b}
75.00	20.00	5.00	9.08±0.03^{a}	19.63±0.03^{h}	1.92±0.02^{f}	6.85±0.03^{g}	17.08±0.03^{g}	45.59±0.18^{c}
70.00	20.00	10.00	11.22±0.02^{b}	18.89±0.04^{f}	1.92±0.02^{e}	6.59±0.01^{f}	16.68±0.01^{f}	44.85±0.03^{b}
72.50	22.50	5.00	12.75±0.02^{d}	18.14±0.02^{c}	1.83±0.02^{e}	6.04±0.03^{c}	14.91±0.02^{d}	46.35±0.07^{e}
70.83	23.33	5.83	12.20±0.04^{c}	19.08±0.03^{g}	1.64±0.02^{c}	6.24±0.02^{e}	16.14±0.02^{e}	44.72±0.09^{b}
73.33	20.83	5.83	18.67±0.03^{f}	17.64±0.02^{a}	1.54±0.04^{b}	5.08±0.03^{b}	13.00±0.03^{b}	44.08±0.01^{a}
71.67	21.67	6.67	11.93±0.04^{d}	18.11±0.02^{c}	1.74±0.01^{d}	5.04±0.03^{b}	13.91±0.03^{cd}	44.32±0.02^{a}
72.50	20.00	7.50	11.74±0.02^{c}	17.14±0.04^{ab}	1.73±0.02^{c}	6.65±0.02^{f}	13.85±0.02^{c}	45.47±0.01^{bc}
75.00	20.00	5.00	10.08±0.03^{b}	18.63±0.03^{d}	1.82±0.04^{e}	6.49±0.01^{f}	15.78±0.01^{de}	44.90±0.09^{b}
70.00	25.00	5.00	13.30±0.04^{d}	17.89±0.02^{b}	1.80±0.02^{e}	5.24±0.03^{bc}	15.91±0.01^{e}	45.78±0.08^{c}
70.00	20.00	10.00	10.22±0.02^{b}	17.90±0.01^{c}	1.82±0.03^{e}	6.35±0.03^{cd}	15.14±0.03^{de}	46.20±0.02^{e}
72.50	22.50	5.00	13.93±0.03^{d}	19.14±0.02^{f}	1.53±0.02^{b}	5.08±0.02^{b}	14.73±0.02^{d}	45.47±0.12^{c}
100	0.00	0.00	12.75±0.04^{d}	18.31±0.01^{c}	1.72±0.02^{d}	6.14±0.02^{d}	14.66±0.03^{c}	46.44±0.12^{e}

Means in same column with different superscripts are significantly ($p<0.05$) different.
WF = Wheat flour, SF = Soybean flour, SPP = Sweetpotato puree.

Mineral content of the biscuit from wheat, soybean and sweetpotato puree

Table 3 revealed mineral composition of the biscuit using wheat, soybean and sweetpotato puree flour mixes.

Table 3

Mineral content of biscuit from wheat, soybean and sweet potato puree

No	Potassium mg/100 g	Calcium mg/100 g	Magnesium mg/100 g	Iron mg/100 g	Zinc mg/100 g
1	118.71±0.02^{c}	24.86±0.01^{c}	14.65±0.01^{e}	0.33±0.00^{de}	0.42±0.01^{de}
2	120.69±0.01^{d}	27.10±0.01^{g}	16.12±0.01^{h}	0.30±0.01^{ab}	0.40±0.01^{bc}
3	114.70±0.01^{b}	25.12±0.01^{d}	14.91±0.00^{f}	0.31±0.00^{cd}	0.43±0.01^{e}
4	123.72±0.01^{f}	23.66±0.00^{a}	12.74±0.01^{a}	0.31±0.01^{bc}	0.39±0.01^{ab}
5	128.90±0.01^{h}	28.77±0.01^{h}	16.05±0.00^{g}	0.28±0.01^{a}	0.41±0.01^{cd}
6	125.10±0.01^{g}	26.91±0.00^{f}	13.79±0.00^{c}	0.29±0.01^{a}	0.43±0.00^{e}
7	110.90±0.01^{a}	24.09±0.01^{b}	14.19±0.00^{d}	0.34±0.01^{e}	0.39±0.01^{a}
8	119.49±0.01^{c}	25.09±0.00^{d}	13.74±0.01^{c}	0.30±0.01^{ab}	0.41±0.01^{cd}
9	124.57±0.02^{g}	24.95±0.01^{c}	15.00±0.01^{fg}	0.29±0.01^{a}	0.40±0.00^{c}
10	115.80±0.01^{b}	27.30±0.00^{h}	15.05±0.00^{g}	0.32±0.00^{d}	0.39±0.00^{bc}
11	121.70±0.01^{fg}	24.66±0.01^{c}	15.12±0.00g	0.34±0.01^{e}	0.42±0.01^{e}
12	120.72±0.02^{f}	23.86±0.01^{b}	13.98±0.01^{c}	0.32±0.01^{de}	0.43±0.01^{de}
13	119.71±0.02^{e}	24.83±0.01^{c}	14.50±0.01^{d}	0.34±0.00^{e}	0.42±0.01^{d}
14	122.66±0.01^{e}	26.19±0.01^{e}	12.98±0.00^{b}	0.29±0.01^{a}	0.42±0.01^{de}

Means in same column with different superscripts are significantly ($p<0.05$) different.
WF = Wheat flour, SF = Soybean flour, SPP = Sweetpotato pure

ISSN: 2409-4951 (Online), 2310-1008(Print)

The findings indicated that, potassium, whose value was between 110.90 and 128.90 mg/100 g, showing a significant ($p<0.05$) increase with higher inclusion levels of soybeans and SPP flour. Sample (72.5:20:7.5) exhibited the highest potassium content while sample (73.33:20.83:5.83) showed the lowest. Potassium functions as the primary intracellular cat-ion, playing crucial roles in maintaining cellular osmotic pressure, regulating acid-base balance, facilitating nerve impulse transmission, enabling muscle contraction (including cardiac muscle), and modulating blood pressure through antagonistic effects on sodium (Bolarinwa et al., 2016). The elevated potassium levels can be attributed to the inherently high potassium content of sweet potato puree; Badila et al. (2009) reported potassium concentrations of 243 mg/100 g in sweetpotato. This finding is consistent with the value of 110.9-128.9 mg/100 g reported by Roger et al. (2022) in biscuits prepared using wheat and sweet potato flour blends. Guyih et al. (2020) similarly documented enhancement of potassium content in cookies formulated from wheat, almond seed and carrot flour blends. The potassium levels in both control and composite flour biscuits remained substantially below the Recommended Daily Allowance (RDA) of 3500 mg/day (USDA, 2018). The amounts of calcium measured was between 23.66 to 28.77mg/100 g. The content of calcium in the samples of the biscuit was significantly ($p < 0.05$) different. There was a progressive increase in calcium content with the addition of soybeans and SPP flour to the blends. Calcium serves multiple critical physiological functions including skeletal mineralization, blood coagulation, neurotransmitter release, muscle contraction, enzyme activation, and cellular signaling as a secondary messenger (Bakare et al., 2020). The gradual increase in calcium content can be attributed to the relatively high calcium levels in both soybean flour (approximately 200-280 mg/100 g) and sweet potato puree (30-50 mg/100 g), which substantially exceed the calcium content of refined wheat flour (15-20 mg/100 g). This finding aligns with observations by Bakare et al. (2020), who documented increased calcium content in biscuits formulated from breadfruit and wheat flour enriched with edible fish meal. In contrast, Adegbanke et al. (2020) reported markedly lower calcium contents (2.12-4.45 mg/100 g) in wheat and Bambara nut flour biscuits, suggesting variability based on ingredient selection and processing methods. The calcium content of all biscuit samples remained considerably below the US Department of Agriculture's recommended dietary allowance (RDA) of 800 mg/day, indicating that these biscuits would provide only modest contributions to daily calcium requirements.

Magnesium was within 12.74-16.12 mg/100 g respectively. Magnesium functions as an essential cofactor in over 300 enzymatic reactions, including those involved in ATP synthesis, DNA and RNA synthesis, protein synthesis, muscle contraction and relaxation, neurological function regulation, cardiac rhythm stabilization, blood glucose homeostasis, and blood pressure regulation (Bolarinwa et al., 2016). The incorporation of soybeans and SPP flour significantly ($p<0.05$) increased the magnesium content of the biscuits. This enhancement can be attributed to the high magnesium content of both soybean flour (approximately 280 mg/100 g) and sweet potato (25-30 mg/100 g fresh weight basis), compared to wheat flour (20-25 mg/100 g). The results contrast with the higher values of 32-49 mg/100 g reported by Roger et al. (2022) in wheat and sweet potato flour blend biscuits, and 58.96-56.12 mg/100 g documented by Guyih et al. (2020) in biscuits prepared from wheat, almond seed and carrot flour blends. These discrepancies may be attributed to variations in raw material varieties, processing methods, and analytical techniques employed.

The outcomes have also indicated that the level of iron within the range between 0.28 and 0.34 mg/100 g. Iron plays indispensable roles in oxygen transport (as a component of hemoglobin and myoglobin), electron transport chain reactions within mitochondria, and numerous enzymatic reactions including those involved in energy metabolism and DNA synthesis (Elinge et al., 2012). The results indicated a progressive increase in iron content with higher inclusion levels of soybean and SPP flour in the biscuit formulations. This enhancement can be attributed to the addition of

ISSN: 2409-4951 (Online), 2310-1008(Print)

soybeans and SPP flour, which are micronutrient-dense ingredients. Soybeans contain approximately 6-8 mg iron/100 g, while sweet potato contains 0.6-1.0 mg/100 g, both exceeding the iron content of refined wheat flour (1.0-1.5 mg/100 g). The bioavailability of iron in these products is further influenced by the presence of phytic acid (which inhibits iron absorption) and ascorbic acid in sweet potato (which enhances non-heme iron absorption). This finding is consistent with Adegbanke et al. (2020) who reported iron contents of 0.97-1.21 mg/100 g in biscuits composed of wheat and Bambara nut flour. However, the iron content of all biscuit samples remained substantially below the RDA of 18 mg/day (USDA, 2018), indicating that these products would provide only minor contributions to daily iron requirements.

The range of value of zinc is 0.39-0.43 mg/100 g. Zinc functions as a cofactor for over 300 metalloenzymes, playing crucial roles in protein synthesis, nucleic acid metabolism, immune function, wound healing, taste perception, and antioxidant defense through superoxide dismutase activity (Elinge et al., 2012). The zinc content increased progressively with higher incorporation of soybeans and SPP flour in the biscuits. Sample (75:20:5) exhibited the highest zinc level compared to sample (100:0:0) and other flour blend formulations. This can be explained by the significantly higher zinc content in soybeans (3-5 mg/100 g) compared to wheat flour (0.7-1.2 mg/100 g), which leads to elevated zinc levels with increasing soybean inclusion. The bioavailability of zinc in these products may be limited by the presence of phytic acid, particularly from soybean flour, which can form insoluble complexes with zinc in the intestinal lumen. The findings contrast with those of Adegbanke et al. (2020), who observed that adding Bambara nut protein isolate to wheat-based biscuits resulted in decreased zinc content. The zinc content of all biscuit samples remained substantially below the RDA of 11 mg/day (USDA, 2020), suggesting these products would provide only modest contributions to daily zinc requirements.

Physical properties of biscuit from wheat, soybean and sweetpotato puree

Table 4 shows the data of the results of physical properties of biscuit. The physical properties of biscuit showed a significant difference ($p < 0.05$). The lightness, the redness and yellowness have ranges of L* (45.42 and 51.16), a* (2.83 and 5.03) and b* (17.73 and 22.34), respectively. One of the notable characteristics of colour is its potential to stimulate appetite in an individual (Adeola and Ohizua, 2018). In baking and roasting, one of the factors applied when it comes to the process control is colour, since the pigments in brown tend to become visible as the browning and caramelization chemical reactions occur (Oke et al., 2021; Pereira et al., 2013).

The lower lightness (L*) values in biscuits with higher concentrations of soybean flour and sweetpotato puree can be attributed to enhanced browning during baking, resulting from the increased availability of both reducing sugars (particularly in sweetpotato) and proteins rich in amino acids (particularly in soybean), which serve as Maillard reaction substrates. The positive values of redness (a*) and yellowness (b*) indicate predominance of these hues in the biscuit samples. Sweet potatoes contain substantial concentrations of carotenoid pigments, including beta-carotene, which impart characteristic orange-red coloration (Hossain et al., 2022). The redness (a*) values increased with higher sweetpotato puree inclusion due to the contribution of these thermostable natural pigments. Similarly, beta-carotene is the primary carotenoid responsible for the yellow-orange pigmentation of sweet potatoes. As the percentage of sweetpotato puree in the formulation increases, yellowness (b*) values rise due to the concentration of these pigments. Soy flour additionally contributes to yellowness through its content of lutein, zeaxanthin, and other minor carotenoids.

ISSN: 2409-4951 (Online), 2310-1008(Print)

Table 4

Physical properties of biscuit from wheat, soybean and sweet potato puree

WF %	SPP %	SF %	Lightness L*	Redness a*	Yellowness b*	Weight g	Diameter mm	Thickness mm	Spread Ratio
72.50	22.50	5.00	47.04 ±0.04^{c}	4.39 ±0.02^{b}	17.73 ±0.42^{a}	9.52 ±0.02^{a}	41.89 ±0.04^{a}	7.21 ±0.01^{a}	5.81 ±0.01^{e}
70.83	20.83	8.34	45.42 ±0.01^{a}	4.83 ±0.01^{d}	20.58 ±0.01^{f}	15.22 ±0.03^{h}	46.22 ±0.03^{b}	9.84 ±0.01^{g}	4.70 ±0.00^{a}
75.00	20.00	5.00	48.54 ±0.02^{d}	4.54 ±0.02^{c}	19.16 ±0.03^{c}	14.72 ±0.02^{g}	46.57 ±0.03^{c}	10.17 ±0.02^{h}	4.58 ±0.01^{a}
70.00	20.00	10.00	46.63 ±0.01^{b}	5.03 ±0.01^{e}	19.99 ±0.01^{e}	13.61 ±0.01^{d}	47.43 ±0.03^{d}	8.68 ±0.02^{e}	5.47 ±0.01^{c}
72.50	22.50	5.00	50.08 ±0.01^{f}	4.54 ±0.01^{c}	18.51 ±0.01^{b}	13.14 ±0.01^{b}	47.57 ±0.04^{e}	7.76 ±0.02^{b}	6.14 ±0.02^{f}
70.83	23.33	5.83	48.63 ±0.01^{e}	4.36 ±0.01^{b}	19.52 ±0.01^{d}	13.40 ±0.00^{c}	47.85 ±0.01^{f}	8.46 ±0.02^{c}	5.66 ±0.01^{d}
73.33	20.83	5.83	47.06 ±0.01^{c}	4.53 ±0.01^{c}	20.40 ±0.01^{f}	14.58 ±0.01^{f}	46.25 ±0.03^{b}	9.73 ±0.02^{f}	4.87 ±0.18^{b}
71.67	21.67	6.67	46.05 ±0.04^{b}	4.46 ±0.01^{c}	18.83 ±0.02^{b}	11.52 ±0.01^{a}	42.89 ±0.02^{b}	8.21 ±0.02^{e}	4.81 ±0.01^{b}
72.50	20.00	7.50	46.42 ±0.01^{b}	4.43 ±0.01^{b}	21.58 ±0.04^{g}	14.22 ±0.03^{de}	45.22 ±0.03^{b}	8.84 ±0.01^{f}	5.70 ±0.01^{d}
75.00	20.00	5.00	49.54 ±0.02^{f}	4.64 ±0.01^{b}	20.16 ±0.03^{f}	13.72 ±0.02^{d}	47.57 ±0.04^{b}	9.17 ±0.01^{g}	5.58 ±0.00^{d}
70.00	25.00	5.00	45.63 ±0.01^{a}	4.03 ±0.02^{b}	20.99 ±0.01^{g}	14.61 ±0.01^{g}	46.43 ±0.03^{cd}	9.68 ±0.01^{g}	4.60 ±0.02^{c}
70.00	20.00	10.00	51.08 ±0.00^{g}	5.03 ±0.02^{e}	19.51 ±0.02^{e}	14.14 ±0.02^{fg}	46.57 ±0.03^{c}	8.76 ±0.02^{e}	5.14 ±0.18^{cd}
72.50	22.50	5.00	48.06 ±0.01^{d}	4.39 ±0.01^{b}	20.52 ±0.01^{f}	14.40 ±0.01^{g}	45.25 ±0.01^{b}	9.46 ±0.02^{g}	4.66 ±0.01^{b}
100	0.00	0.00	51.16 ±0.00^{g}	2.83 ±0.01^{a}	22.34 ±0.01^{g}	14.32 ±0.01^{e}	47.51 ±0.02^{e}	8.62 ±0.02^{d}	5.52 ±0.01^{cd}

Means in same column with different superscripts are significantly ($p<0.05$) different.
WF = Wheat flour, S = Soybean flour, SPP = Sweetpotato puree.

The biscuits weighed between 9.52 -15.22 g, with significant ($p<0.05$) increases observed with higher inclusion levels of soybeans and SPP flour. According to Bello et al. (2008), variations in biscuit weight can be explained by differential water-holding capacities of the flours, which influence moisture retention during baking and consequently affect final product weight. The water-holding capacity is determined by the protein composition, fibre content, and starch characteristics of each flour component. This finding contrasts with Uboor et al. (2022), who reported cookies weight increases from 14.33 g to 16.13 g when cassava and pumpkin were incorporated into wheat flour blends. Eke et al. (2019) similarly observed weight increases in biscuit samples with the addition of sweet potato and African yam bean flour to wheat flour blends. Biscuit diameter was 41.89 - 47.85 mm, increasing significantly with the addition of soybeans and SPP flour. Sample (72.5:22.5:5) exhibited greater diameter than both flour blend and control biscuits. This finding aligns with Bello et al. (2008), who

ISSN: 2409-4951 (Online), 2310-1008(Print)

noted diameter increases upon addition of 10% yellow yam and unripe plantain flour to wheat flour biscuits. The increase in diameter can be explained by the dilution of wheat gluten. Soyflour is gluten-free and contains high protein levels, but these proteins do not form the viscoelastic gluten network characteristic of wheat proteins. Consequently, soyflour addition weakens the gluten structure, resulting in reduced dough elasticity and increased extensibility. During baking, this leads to greater lateral spreading before the structure sets, producing biscuits with larger diameters.

The spread ratios were within 4.58 -5.81, with values increasing as soybeans and SPP flour were incorporated. According to Eke et al. (2019), spread ratio is influenced by dough viscosity, with lower viscosity dough exhibiting more rapid spreading in the oven before structure fixation occurs. The increased spreading with soybean and SPP flour addition can be attributed to alterations in the dough's viscoelastic properties. These findings are consistent with Jothi et al. (2014), who reported elevated spread ratios (3.31 - 4.43) in blends incorporating soybeans and orange-fleshed sweet potato (OFSP) flour. The highest spread ratio was observed in sample (72.5:22.0:5). The optimal spread ratio was recorded in the sample containing 20.83% SPP and 8.34% soybeans flour. Lower spread ratios are generally associated with enhanced crispness and improved overall acceptability in baked products, as they indicate a more compact structure with better texture development. Accordingly, biscuits formulated with 20.83% soybean and 8.34% SPP flour are expected to exhibit superior consumer acceptability characteristics.

Textural properties of biscuit from wheat, soybean and sweet potato puree flour

Table 5 shows a difference in the peak force values of 2572-6555 N. Sample 71.67:21.67:6.67 had the lowest value compared to sample 71.67:21.67:6.67 which had the highest value but the difference was not significant ($p>0.05$). During baking starch swells by the absorption of water and the result is a change in texture to a tender product. Due to the high content of starch found in sweetpotato, its addition into the dough would denote low gelatinization, subsequently, destabilizing the entire integrity of the biscuit and leading to low peak force. The chewiness value was found to be between 2174.50 and 5635.50N. Sample 75:20:5 and 73.33:20.83:5.83 indicated the lowest value whereas sample ratio 75.00:20.00:5.00 had the highest value, and there was a significant difference ($p<0.05$) among the samples in terms of chewiness. Chewiness-requires sufficient energy to chew solid food until it is ready to swallow. It is at times approximated as multiplication of the hardness, cohesiveness and elasticity (Guo, 2021). The hydration of the dough is known to affect chewiness. The elevated moisture level leads to the decrease in the level of stiffness and the decrease of chewiness since the dough is less strong and easy to dissolve during the chewing process. Soyflour and sweetpotato purees have very high water absorption capacities. Incorporated into the dough, they will be less dry and therefore biscuits will be less chewy.

The adhesiveness value was 5.46 to 16.68 N·s. Sample (72.50:22.50:5.00) exhibited the lowest value while sample (71.67:21.67:6.67) showed the highest, with significant differences ($p<0.05$) among samples. Adhesiveness quantifies the degree of stickiness, representing the work required to overcome attractive forces between the probe surface and the sample surface during texture analysis (Trinh and Glasgow, 2012).

ISSN: 2409-4951 (Online), 2310-1008(Print)

Table 5

Textural properties of biscuit from wheat, soybean and sweet potato puree

WF	SPP	SF	Peak Force N	Chewiness N	Adhesiveness N·s	Gumminess N	Springiness	Cohesiveness
72.50	22.50	5.00	6456.00 ±4.24^{b}	5635.50 ±4.94^{g}	5.46 ±0.04^{a}	6477.50 ±10.61^{f}	0.89 ±0.03^{cd}	1.11 ±0.15^{f}
70.83	20.83	8.34	3595.00 ±5.66^{ab}	3677.50 ±1.26^{f}	14.04 ±0.04^{cd}	3684.50 ±6.36^{ab}	0.95 ±0.08^{d}	1.02 ±0.01^{f}
75.00	20.00	5.00	3588.50 ±3.53^{ab}	2311.50 ±1.15^{c}	10.85 ±0.06^{bc}	5326.00 ±4.24^{e}	0.48 ±0.04^{b}	0.40 ±0.08^{b}
70.00	20.00	10.00	4068.50 ±1.92^{ab}	2283.00 ±2.83^{bc}	6.65 ±0.05^{ab}	3858.50 ±4.95^{abc}	0.58 ±0.01^{b}	0.90 ±0.03^{f}
72.50	22.50	5.00	6555.00 ±4.24^{b}	2444.00 ±4.24^{d}	15.36 ±0.05^{cd}	6448.50 ±10.61^{f}	1.07 ±0.10^{d}	0.83 ±0.05^{e}
70.83	23.33	5.83	5483.50 ±7.77^{ab}	2804.50 ±6.36^{e}	14.54 ±0.04^{cd}	4683.00 ±2.83^{cde}	1.06 ±0.04^{d}	0.65 ±0.05^{c}
73.33	20.83	5.83	3546.50 ±2.12^{ab}	2174.50 ±0.71^{a}	15.18 ±0.01^{cd}	3511.50 ±2.12^{ab}	0.91 ±0.01^{d}	1.07 ±0.02^{f}
71.67	21.67	6.67	2572.00 ±1.79^{a}	2223.50 ±3.54^{ab}	16.68 ±0.05^{d}	3403.00 ±4.24^{a}	0.13 ±0.18^{a}	0.05 ±0.07^{a}
72.50	20.00	7.50	3837.50 ±4.66^{ab}	2223.50 ±3.54^{ab}	15.15 ±0.01^{cd}	4189.00 ±5.44^{abcd}	0.53 ±0.04^{b}	1.02 ±0.03^{f}
75.00	20.00	5.00	4766.00 ±4.00^{ab}	2174.50 ±0.71^{a}	16.02 ±0.95^{d}	4904.00 ±4.49^{de}	1.00 ±0.01^{d}	0.48 ±0.04^{b}
70.00	25.00	5.00	4554.50 ±5.46^{ab}	2806.00 ±4.24^{e}	11.00 ±0.17^{bc}	4607.00 ±3.96^{cde}	0.89 ±0.19^{cd}	0.68 ±0.04^{cd}
70.00	20.00	10.00	5050.00 ±3.54^{ab}	2444.00 ±4.24^{d}	14.30 ±0.35^{cd}	4260.50 ±3.86^{bcd}	1.03 ±0.23^{d}	0.47 ±0.05^{b}
72.50	22.50	5.00	5000.50 ±5.44^{ab}	2282.00 ±1.41^{bc}	6.07 ±0.86^{a}	4949.00 ±3.25^{de}	0.85 ±0.13^{cd}	0.78 ±0.04^{cde}
100	0.00	0.00	4439.00 ±4.35^{ab}	2261.50 ±5.45^{bc}	13.77 ±4.12^{cd}	4541.00 ±6.94^{cde}	0.65 ±0.01^{bc}	0·78 ±0.01^{de}

Means in same column with different superscripts are significantly ($p<0.05$) different.
WF = Wheat flour, S = Soybean flour, SPP = Sweetpotato puree.

At higher moisture contents, biscuit dough becomes increasingly cohesive and adhesive as water acts as a plasticizer, increasing molecular mobility and promoting intermolecular interactions. Enhanced moisture retention associated with higher percentages of sweetpotato puree or soyflour increases adhesiveness by facilitating greater contact between ingredients and promoting sticky characteristics. Excessively adhesive biscuits require more extensive jaw movements during oral processing and increased masticatory effort, even when compressive hardness remains constant (Cakir et al., 2012).

The gumminess value ranged between 3403 and 6477.50 N where the sample 71.67:21.67:6.67 had the least value and there was significant different ($p<0.05$) when compared to the sample 72.50:22.50:5.00 which had the highest value. Gumminess represents the energy required to disintegrate a semi-solid food product to a state ready for swallowing (Trinh and Glasgow, 2012). Higher wheat flour percentages, which contribute gluten proteins, generally increase gumminess due to the elastic and cohesive nature of the gluten network formed by glutenin and gliadin proteins through disulfide bonds and hydrogen bonding. Conversely, sweetpotato puree and soyflour are

ISSN: 2409-4951 (Online), 2310-1008(Print)

gluten-free ingredients that dilute the gluten network, resulting in softer, less cohesive structures with reduced gumminess.

The springiness was within the range of 0.13 to 1.07, with sample (71.67:21.67:6.67) exhibiting the lowest value and sample (72.50:22.50:5.00) the highest, showing significant differences ($p<0.05$). Springiness represents the rate and extent of recovery when compressive force is removed, indicating the elastic properties of the sample. The springiness values obtained in this work exceed those reported in other cookie studies (Pereira et al., 2013), suggesting enhanced elastic recovery properties. Cohesiveness values ranged from 0.05 to 1.11, with sample (71.67:21.67:6.67) showing the lowest and sample (72.50:22.50:5.00) the highest value, with significant differences ($p<0.05$). Cohesiveness quantifies the strength of internal bonds holding the structure together, measuring the material's ability to withstand a second deformation relative to its resistance during initial deformation. Higher cohesiveness values indicate stronger intermolecular forces and more integrated structural networks within the biscuit matrix.

Sensory properties of biscuit from wheat, soybean and sweet potato puree flour

Sensory properties like colour, texture, flavour, aroma and overall acceptability can be applicable in the identification of food products. Table 7 indicated that colour varied between 7.02 and 7.64. The colour had the least value in sample 72.50:22.50:5.00 and highest in sample 72.5:22.5:5 with no significant difference ($p >0.05$). Makanjuola and Adebowale (2020) also noted that the colour of biscuit samples reduced with addition of water yam flour in blends. The result of this study is not similar to the report of Afari, (2023) that the addition of tigernut flour and pineapple puree in blends reduced the colour rating. All the samples had colour rating within the limit of acceptability. The texture was measured as 6.22-7.22. There was no significant difference ($p>0.05$) among the samples in terms of the texture, sample 72.5:22.5:5 had the least value and sample 75:20:5 and 100:0:0 had the highest value. The taste values were between 7.00 and 7.66. Sample 70.83:20.83:8.34 had the lowest value whereas sample 70.83:23.33:5.83 had the highest value, and there were significant differences ($p<0.05$) among the samples in the taste. The resultant effects of the high concentration of soybean and SPP flour in the blends might be that it influenced the flavor of the biscuit sample. The result does not concur with the report by Makanjuola and Adebowale, (2020) and Afari (2023) on wheat-water yam and wheat-tigernut cookies supplemented with pineapple purée respectively because they did not report high acceptability ratings. This could be due to the high level of taste rating of samples containing high level of wheat since consumers could be used to bake products that contain wheat. The aroma value was recorded in the range of 6.04 and 7.98. The sample 72.5:22.5:5 had the lowest score and the sample 72.5:20:7.5 had the highest score, there was a significant different ($p<0.05$) among the samples regarding the aroma. The Aroma and overall acceptability score of flour blends biscuit samples also slightly decreased as soybeans and SPP flour was added in the blends. This might be as a result of the incorporation of soybeans and incorporation of SPP flour in the mix. This corroborates the findings of Iweh et al. (2017) who found out that aroma and overall acceptability rating of the biscuits sample decreased with the addition of almond seed and carrot flour in the blends. The overall acceptability was between 7.14 and 7.56. The overall acceptability of sample 72.5:22.5:5 was the least in value compared with the high value of the overall acceptability of the sample 72.5:20.00:7.50 and there was no significant difference ($p>0.05$) among the samples. These differences in the overall acceptability of different composite cookies may be explained by the variation in the likeness with regards to taste, colour, aroma and texture. The overall acceptability rating of the control biscuit and biscuit made using wheat, soybean and sweet potato puree flour blends samples was however within the acceptable score rating. The study revealed that it is possible to obtain biscuit of acceptable quality by using blends of wheat, soybeans and SPP flour.

ISSN: 2409-4951 (Online), 2310-1008(Print)

Table 6

Sensory properties of biscuit from wheat, soybean and sweet potato puree

WF	SPP	SF	Colour	Texture	Aroma	Taste	OA
72.50	22.50	5.00	7.02±1.41[a]	6.84±1.97[a]	6.88±1.51[a]	7.34±1.45[a]	7.14±1.63[a]
70.83	20.83	8.34	7.26±1.58[a]	6.72±2.38[a]	6.98±1.62[a]	7.00±1.84[a]	7.18±1.87[a]
75.00	20.00	5.00	7.12±1.12[a]	7.02±1.41[a]	6.90±1.17[a]	7.48±1.04[a]	7.30±1.06[a]
70.00	20.00	10.00	7.10±1.56[a]	6.82±2.18[a]	6.96±1.73[a]	7.32±1.60[a]	7.18±1.77[a]
72.50	22.50	5.00	7.54±1.07[a]	7.06±1.89[a]	7.26±1.28[a]	7.32±1.50[a]	7.14±1.34[a]
70.83	23.33	5.83	7.24±1.17[a]	7.06±1.53[a]	7.04±1.29[a]	7.66±0.98[a]	7.36±1.06[a]
73.33	20.83	5.83	7.44±1.51[a]	6.86±2.32[a]	7.04±1.81[a]	7.14±1.87[a]	7.26±1.89[a]
71.67	21.67	6.67	7.06±1.36[a]	6.94±1.44[a]	7.98±1.71[a]	7.23±1.50[a]	7.24±1.53[a]
72.50	20.00	7.50	7.16±1.27[a]	6.52±1.55[a]	7.78±1.29[a]	7.08±1.74[a]	7.38±1.78[a]
75.00	20.00	5.00	7.22±1.26[a]	7.22±1.63[a]	6.70±1.43[a]	7.46±1.34[a]	7.25±1.45[a]
70.00	25.00	5.00	7.20±1.32[a]	7.36±1.79[a]	6.76±1.27[a]	7.38±1.35[a]	7.19±1.47[a]
70.00	20.00	10.00	7.34±1.48[a]	7.16±2.28[a]	6.26±1.52[a]	7.24±0.99[a]	7.22±1.07[a]
72.50	22.50	5.00	7.64±1.61[a]	6.22±1.87[a]	6.04±1.41[a]	7.37±1.32[a]	7.14±1.99[a]
100	0.00	0.00	7.47±1.16[a]	7.22±1.65[a]	7.30±1.22[a]	7.58±1.42[a]	7.30±1.28[a]

Means in same column with different superscripts are significantly ($p<0.05$) different; OA = Overall Acceptability, W = Wheat, S = Soybeans, SPP = Sweet Potato Puree

Conclusions

The quality attribute of biscuit formulated from composite flours of wheat, soybeans, and sweet potato puree were evaluated. Moisture content of the biscuits showed significant variation, indicating that inclusion of soybean flour and sweetpotato puree enhanced moisture retention during baking, a key factor for product quality. Crude protein content increased significantly with the addition of soybean and sweetpotato puree, while total carbohydrate content decreased. The incorporation of these flours also improved the mineral composition of the biscuits, particularly potassium, magnesium and zinc. Colour properties revealed that higher levels of soybean flour and sweetpotato enhanced redness and yellowness. Biscuit weight and diameter increased with higher substitution levels. Sensory evaluation indicated that all samples were acceptable with the formulation containing wheat: soybean: sweet potato puree at 72.5:20.0:7.5 demonstrating the highest overall acceptability. These findings suggest that partial substitution of wheat with soybean flour and sweetpotato puree can improve the nutritional profile and sensory properties of biscuits without compromising product quality.

References

Adegbanke O.R., Osundahunsi O.F., Enujiugha V.N. (2020), Chemical and mineral composition of biscuit produced from wheat and Bambara groundnut flour, *Acta Scientific Nutritional Health*, 4(10), pp. 3-9.

Adeola A.A., Ohizua, E. R. (2018), Physical, chemical, and sensory properties of biscuits prepared from flour blends of unripe cooking banana, pigeon pea, and sweet potato. *Food Science and Nutrition*, 6, Pp. 532–540. https://doi.org/10.1002/fsn3.590

Afari A.A. (2023), Sensory qualities and proximate composition of composite cookies from wheat flour (*Triticum*), tigernut flour (*Cyperus esculentus* L.) and pineapple puree (*Anana comosus*). B.Tech Project Report Submitted to Department of Hotel, Catering and Institutional Management, Koforidua Technical University, Ghana.

ISSN: 2409-4951 (Online), 2310-1008(Print)

Agu H.O., Yunana R., Jideani A.I.O. (2021), Development and acceptability of snacks from yellow-fleshed sweet potato and wheat flours, *Journal of Food Processing and Preservation*, 45(1), e14851, https://doi.org/ 10.1111/jfpp.14851

Alabi M.O., Anunye J.C. (2007), Nutritional and sensory attributes of soy-supplemented cereal meals, *Nigerian Food Journal*, 25(1), pp. 100-110, https://doi.org/10.4314/nifoj.v25i1.33658

Alı W., Ahmad M., İftakhar F., Qureshi M., Ceyhan A. (2020), Nutritive potentials of soybean and its significance for humans' health and animal production: A Review, *Eurasian Journal of Food Science and Technology*, 4 (1), pp. 41-53.

AOAC. (2006), *Official Methods of Analysis, Association of Official Analytical Chemists*, 18th edn. USA, Washington DC.

AOAC. (2016), *Official Methods of Analysis (17th edn). Association of Official Analytical Chemists* (AOAC), International, 20th ed. Gaithersburg, MD, USA.

Ariyo O., Dudulewa B.I., Atojoko M.A. (2022), Nutritional and sensory properties of biscuits based on wheat (*Triticum aestivum*), beniseed seed (*Sesamum indicum*) and sweet potato (*Ipomoea batatas*) composite flour, *Agro-Science*, 21(2), pp. 66-73, https:// doi.org/ 10.4314/as.v21i2.7

Asif-Ul-Alam,, S.M., Islam,, M.Z., Hoque,, M.M., Monalis K. (2014), Effect of drying on the physicochemical and functional properties of green banana (*Musa sapientum*) flour and development of baked product, *American Journal of Food Science and Technology*, 2, pp. 128–133, https://doi.org/10.12691/ajfst-2-4-4

Atobatele O.B., Afolabi M.O. (2016), Chemical composition and sensory evaluation of cookies baked from the blends from the blends of soya bean and maize flours, *Applied Tropical Agriculture*, 21(2), pp. 8-13.

Bakare A.H., Adeola A.A., Otesile I., Obadina A.O., Afolabi W.A., Adegunwa M.O., Alamu E.O. (2020), Nutritional, texture, and sensory properties of composite biscuits produced from breadfruit and wheat flours enriched with edible fish meal, *Food Science and Nutrition*, 8, pp. 6226-6246, https://doi.org/10.1002/fsn3.1919

Bello M.O., Falade O.S., Adewusi S.R.A., Olawore N.O. (2008), Studies on the chemical compositions and anti-nutrients of some lesser-known Nigeria fruits, *African Journal of Biotechnology*, 7, pp. 3972-3979.

Çakir E., Koç H., Vinyard C.J., Essick G., Daubert C.R., Drake M., Foegeding E.A. (2012), Evaluation of texture changes due to compositional differences using oral processing, *Journal of Texture Studies,* 43, pp. 257–267, https://doi.org/10.1111/j.1745 4603.2011.00335.x

Chilungo S., Muzhingi T., Truong V.D., Allen J.C. (2019), Effect of processing and oil type on carotene bio accessibility in traditional foods prepared with flour and puree from orange-fleshed sweetpotatoes, *International Journal of Food Science and Technology*, 54, pp. 3285-3293, https://doi.org/10.1111/ijfs.14106

Da Silva P., Moreira R. (2008), Vacuum frying of high-quality fruit and vegetable based snacks, *Lebensmittel – Wissenschaft und Technologie*, 41(10), pp. 1758–1767, https://doi.org/10.1016/j.lwt.2008.01.016

Eke M.O., Ahure D., Donaldben N.S. (2019), Effect of Acha and sprouted soybeans flour on the quality of wheat based cookies, *Asian Food Science Journal,* 7(2), pp. 1-12, https://doi.org/10.9734/afsj/2019/v7i229969

Elinge C.M., Muhammad A., Atiku F.A., Itodo A.U., Peni I.J., Sanni O.M., Mbongo A.N. (2012), Proximate, mineral and anti-nutrient composition of pumpkin (*Cucurbita pepo* L) seeds extract, *International Journal of Plant Research,* 2(5), pp. 146-150, https://doi.org/ 10.5923/j.plant.20120205.02

Erenstein O., Jaleta M., Mottaleb K.A., Sonder K., Donovan J., Braun, H.J. (2022), Global trends in wheat production, consumption and trade. In: M.P. Reynolds, H.J. Braun, *Wheat Improvement: Food Security in a Changing Climate*, pp. 47-66, Cham: Springer International Publishing, https://doi.org/ 10.1007/978-3-030-90673-3_4

Guo Q. (2021), Understanding the oral processing of solid foods: Insights from food structure, *Comprehensive Reviews in Food Science and Food Safety*, 20(3), pp. 2941-2967, https://doi.org/10.1111/1541-4337.12745

ISSN: 2409-4951 (Online), 2310-1008(Print)

Guyih M.D., Dinnah A., Eke M.O. (2020), Production and quality evaluation of cookies from wheat, almond seed and carrot flour blends, *International Journal of Food Science and Biotechnology*, 5(4), pp. 45-51, https://doi.org/10.11648/j.ijfsb.20200504.11

Hossain M.M., Rahim M.A., Moutosi H.N., Das L. (2022), Evaluation of the growth, storage root yield, proximate composition, and mineral content of coloured sweet potato genotypes, *Journal of Agriculture and Food Research*, 8, 100289, https://doi.org/10.1016/j.jafr.2022.100289

Ifeh C., Chioke A. (2024), Quality evaluation of biscuits produced from wheat, high-quality cassava and African walnut composite flours, *Journal of Sustainable Agriculture and Environmental Research*, 11(1), pp. 32-40, https://doi.org/10.5281/zenodo.10620530

Ijarotimi O.S., Fakayejo D.A., Oluwajuyitan T.D. (2021), Nutritional characteristics, glycaemic index and blood glucose lowering property of gluten-free composite flour from wheat (*Triticum aestivum*), soybean (*Glycine max*), oat-bran (*Avena sativa*) and rice-bran (*Oryza sativa*), *Applied Food Research*, 1(2), 100022, https://doi.org/10.1016/j.afres.2021.100022

Laveriano-Santos E.P., López-Yerena A., Jaime-Rodríguez C., González-Coria J., Lamuela-Raventós R.M., Vallverdú-Queralt A., Romanyà J., Pérez M. (2022), Sweetpotato is not simply an abundant food crop: A comprehensive review of its phytochemical constituents, biological activities, and the effects of processing, *Antioxidants*, 11(9), 1648, https://doi.org/10.3390/antiox11091648

Mahan L.K., Escott-Stump S. (2008), *Krause's Food and Nutrition Therapy*, 12th ed., Canada, Saunders Elsevier.

Makanjuola O.M., Adebowale J.O. (2020), Vitamins, functional and sensory attributes of biscuit produced from wheat-cocoyam composite flour, *Journal of Scientific and Innovative Research*, 9(2), pp. 77-82, https://doi.org/ 10.31254/jsir-2020.9207

Mile M.T., Ahure D., Eke M.O. (2024), Chemical and sensory properties of biscuits produced from wheat, soybean and orange fleshed sweet potato, *European Journal of Nutrition and Food Safety*, 16(2), pp. 1-12, https://doi.org/10.9734/ejnfs-2024/v16i21383

Ndife J., Linus-Chibuezeh A., Alozie E.N., Olaoye A.O. (2020), Comparative evaluation of enriched biscuits made from selected cereals and groundnut (*Arachis hypogaea*) composite flours, *Nigerian Journal of Agriculture, Food and Environment*, 16(2), pp. 140-151.

Oke E.K., Idowu M.A., Sobukola O.P., Bakare H.A. (2017), Quality attributes and storage stability of bread from wheat–tigernut composite flour, *Journal of Culinary Science and Technology*, 17(1), pp. 75-88, https://doi.org/10.1080/15428052.2017.1404537

Oke E.K., Idowu M.A., Thanni N.O., Olorode O.O. (2019), Some quality attributes of sausage roll produced from wheat-tigernut composite flour, *Food and Environment Safety*, 18(4), pp. 287 – 297.

Oke E.K., Adeoye M.R., Adeola A.A., Ojo O.A., Omoniyi, S.A. (2023), Sensory acceptability and storage stability of pasta produced from yellow yam and kidney bean composite flour, *Food and Humanity*, 1, 1297, 1303https://doi.org/10.1016/j.foohum.2023.09.021

Onyiba P.O., Mbah T.N., Ikoro A.I., Okoh T., Achebe U., Ajisola J.K. (2023), *Suitability Assessment of Orange-Fleshed Sweet Potato for Sustainable Nutrition Security*, Centennial.

Olagunju A.I., Ekeogu P.C., Bamisi O.C. (2020), Partial substitution of whole wheat with acha and pigeon pea flours influences rheological properties of composite flours and quality of bread. *British Food Journal*, 122(11), pp. 3585-3600, https://doi.org/10.1108/BFJ-10-2019-0773

Passos M.E.A., Moreira C.F.F., Pacheco M.T.B., Takase I., Lopes M.L.M., Valente-Mesquita V.L. (2013), Proximate and mineral composition of industrialized biscuits, *Food Science and Technology*, 33(2), pp. 323–331, https://doi.org/10.1590/S010120612013005000046

Pereira D., Correia P.M., Guine R.P. (2013), Analysis of the physical-chemical and sensorial properties of maria type cookies, *Acta Chimica Slovaca*, 6(2), pp. 269–280, https://doi.org/10.2478/acs-2013-0040

Roger P., Bertrand B.M.M., Gaston Z., Nouhman B., Elie F. (2022), Nutritional composition of biscuits from wheat-sweet potato-soybean composite flour, *International Journal of Food Science,* 2022, 7274193, https://doi.org/10.1155/2022/7274193

Roth R.A. (2011), *Nutrition and Diet Therapy*, Cengage Learning.

ISSN: 2409-4951 (Online), 2310-1008(Print)

Sanni S.A., Adebowale A.A., Olayiwola I.O., Maziya-Dixon B. (2008), Chemical composition and pasting properties of iron fortified maize flour, *Journal of Food, Agriculture and Environment*, 6(3-4), pp. 172-175.

Serwaa A., Agamba D., Abayase R. (2021), Nutritional composition and sensory evaluation of wheat and millet flour pasta noodles, *International Journal of Academic and Applied Research*, 5(1), pp. 136–141.

Trinh K.T., Glasgow S. (2012), On the texture profile analysis test, https://pdfs.semanticscholar.org/da6a/1a997 b8e99059db ac3f6 d61c4 b2f42 87c682.pdf

Ubbor S.C., Agwo O.E., Elekeh R.I., Ekeh J.I., Linus-Chibuezeh A. (2022), Quality evaluation of cookies produced from wheat-yellow root cassava flours, enriched with pumpkin seed, *Nigerian Agricultural Journal*, 53(1), pp. 273-283.

USDA F. (2018), USDA food composition databases, United States Department of Agriculture (USDA), Nutrient lists from standard reference legacy 2018, in Food and Nutrition Information Center, National Agricultural Library, 2020, https://www.nal.usda.gov/fnic/nutrient-listsstandardreference-legacy-2018

Žuljević S.O., Akagić A. (2021), Flour-based confectionery as functional food, In: A.M. Grumezescu, A.M. Holban (Eds.), *Functional Foods*, pp. 281-312, https://doi.org/10.1016/B978-0-12-822410-6.00022-2

Author identifiers ORCID

Emmanuel Kehinde Oke	0000-0002-0045-9108
Abiodun Aderoju Adeola	0000-0003-0761-3507
Oluwakemi Abosede Ojo	0000-0001-9158-8089
Saheed Adewale Omoniyi	0000-0002-6204-8064
Femi Fidelis Akinwande	0000-0003-4501-0731

Cite:

Ukr J Food Sci Style

Oke E.K., Adeola A.A., Ojo O.A., Adebayo O.R., Omoniyi S.A., Akinwande F.F. (2025), Influence of sweet potato puree and soybean addition on the quality characteristics of gluten-free biscuits, *Ukrainian Journal of Food Science*, 13(2), pp. 168–185, https://doi.org/10.24263/2310-1008-2025-13-2-6

APA Style

Oke, E.K., Adeola, A.A., Ojo, O.A., Adebayo, O.R., Omoniyi, S.A., & Akinwande, F.F. (2025). Influence of sweet potato puree and soybean addition on the quality characteristics of gluten-free biscuits. *Ukrainian Journal of Food Science, 13*(2), 168–185. https://doi.org/10.24263/2310-1008-2025-13-2-6

ISSN: 2409-4951 (Online), 2310-1008(Print)

Biotechnological approaches and strategies for intensification of metanogenesis

Oleksandr Vorontsov, Viktor Stabnikov

National University of Food Technologies, Kyiv, Ukraine

Keywords:

Biogas
Biomethane
Digester
Design
Intensifiction
Methanogenesis
Stability

Article history:

Received 20.04.2025
Received in revised form 25.08.2025
Accepted 31.12.2025

Corresponding author:

Oleksandr Vorontsov
E-mail: VorontsovOleksandr@proton.me

DOI:
10.24263/2310-1008-2025-13-2-7

Abstract

Introduction. Biomethane production contributes to the development of a circular economy by enabling the generation of renewable energy through the efficient utilization of organic waste as a feedstock for the anaerobic conversion of organic matter into methane.

Materials and methods. A comprehensive review of scientific publications was conducted to analyze the main trends in digester design optimization, factors influencing microbial communities during biogas production, and methods for biogas upgrading to biomethane. The review was based on sources indexed in major scientific databases (Scopus, Web of Science, Google Scholar), as well as professional publications of the Higher Attestation Commission of Ukraine and official statistical data from the UN and the EU.

Results and discussion. By 2040, Europe aims to replace up to 10% of its natural gas consumption with biomethane. Biomethane is considered carbon-neutral, and its integration with CO_2 utilization technologies, such as biological methanation and Power-to-Gas systems, enables the potential achievement of "negative emissions," contributing to decarbonization of the energy sector. The core equipment for methanogenesis is the bioreactor (digester), whose design and operating parameters are critical for biogas optimization and long-term process stability. Advanced configurations, including Anaerobic Baffled Reactors (ABR) and Upflow Anaerobic Sludge Blanket (UASB) reactors, are widely used for treating municipal and industrial wastewater, as well as manure and agricultural residues.

Due to the high variability in substrate composition and properties, direct comparison of digester designs in terms of efficiency is limited, and the optimal configuration depends on process goals, economic feasibility, and local conditions. Methanogenesis is a multistage biotechnological process (hydrolysis, acidogenesis, acetogenesis, and methanogenesis) performed by syntrophically interacting bacterial and archaeal communities, requiring a holistic research approach that accounts for microbial structure and functionality. Emerging technologies, such as microbial electrolysis cells, system integration (e.g., with hydroponic farms), metal nanoparticles, and advanced monitoring combined with "omics" tools, aim to enhance process stability, productivity, and methane yield while reducing operational costs.

Conclusions. Future research should focus on molecular-biological modeling of anaerobic microbial communities to enable more precise adjustment of operating parameters (temperature, pH, nutrient dosing) based on microbiome state data, as well as on the development of advanced digester designs and intelligent control systems.

Introduction

Traditional microbial decomposition of organic matter is an ancient biotechnology for biogas production, which can be upgraded to biomethane. Methanogenesis produces biogas consisting mainly of methane (~60%) and carbon dioxide (~40%), with minor impurities (Li et al., 2017). However, conventional archaeal-driven bioconversion faces challenges, including low biodegradability of some agricultural feedstocks (e.g., animal manure and straw), relatively low methane content, long process times, and incomplete utilization of energy stored in lignin and cellulose (Ning et al., 2021).

Anaerobic digesters vary widely in complexity, ranging from simple cylindrical structures without moving parts to highly automated industrial installations. They are commonly classified according to their design and key operating parameters, including temperature regime, solids content, and substrate loading characteristics, such as batch substrate concentration (BSC) and continuous substrate concentration (CSC).

The most common digester configurations include cylindrical reactors; cylindrical reactors with internal partitions; inclined cylindrical reactors; egg-shaped digesters; and trench-type digesters constructed in the ground and covered with a rigid lid or gas-impermeable membrane. A fundamental requirement for all digester designs is structural tightness, as methane-producing microorganisms are obligate anaerobes (DelaVega-Quintero et al., 2025).

Anaerobic cultivation can be operated in either continuous or intermittent (batch) modes. In continuous systems, raw materials are supplied at regular intervals or continuously, while an equivalent volume of digestate is simultaneously withdrawn. The majority of modern industrial digesters operate under continuous feeding regimes due to their higher stability and process control (Yankovska et al., 2018). In contrast, intermittent systems are filled with substrate and operated for a fixed digestion period, after which the reactor is opened and completely emptied. Such systems are generally simpler and less expensive; however, they suffer from design limitations, lower technological efficiency, and reduced process stability, and are therefore considered functionally outdated. Based on the total solids content of the feedstock, anaerobic digestion systems are classified as wet or dry. Wet digestion systems process substrates with a dry solids (DS) content of 16% or less, whereas semi-dry and dry systems typically operate with substrates containing 22–40% DS.

Anaerobic conversion of organic matter into methane is a complex biotechnological process that occurs in the absence of oxygen and is mediated by a highly interdependent microbial consortium comprising diverse bacteria and archaea (DelaVega-Quintero et al., 2025). The efficiency of methanogenesis depends on the metabolic activity and balanced interactions among these microorganisms. Through the decomposition and mineralization of organic matter, microbial communities play a fundamental role in both natural and engineered ecosystems. In terms of chemical composition and energy value, biomethane is comparable to fossil natural gas, enabling its integration into existing gas distribution networks and its use for electricity and heat generation, as well as transportation fuel. To obtain biomethane, biogas produced via anaerobic conversion of organic matter must be purified. Biogas upgrading is performed using various technologies, including cryogenic separation and membrane-based processes. The large number of scientific studies currently being conducted, together with the wide diversity of equipment, feedstock pretreatment methods, and biogas purification technologies aimed at improving the efficiency of anaerobic conversion of organic matter to methane, indicates that an optimal and universally applicable biomethane production technology has not yet been established.

ISSN: 2409-4951 (Online), 2310-1008(Print)

Materials and methods

A comprehensive review of scientific publications was conducted to analyze the main trends in digester design optimization, factors influencing microbial communities during biogas production, and methods for biogas upgrading to biomethane. The review was based on sources indexed in major scientific databases (Scopus, Web of Science, Google Scholar), as well as official statistical data from the UN and the EU.

Results and discussion

Improving the design of biogas plants (digesters) is one of the most important areas of innovation. Digesters exist in single-, two- and multi-stage. The need to use two- and multi-stage systems arises due to the specific sequence of biochemical reactions of the methanogenesis process, which have different optimal conditions for cultivating the corresponding microbial consortia and for some raw materials are difficult to regulate in one-stage conditions. Two- and multi-stage systems provide higher energy efficiency and stability in the fermentation of raw materials of plant origin (Wang et al., 2005a, b). However, single-stage systems are simple to design, assemble and operate and are cheaper. Therefore, they are currently the most common and are used both for industrial biogas production and for small decentralized production. A comparative analysis of single-stage and two-stage systems demonstrates the advantages of the latter, especially when processing complex substrates. Modern bioreactors are significantly different from previous models and contribute to increasing biogas yield, improving process stability and expanding the types of raw materials used. The complexity of the biogas production process, which occurs in several stages, and the diversity of microflora necessitate the development of complex bioreactor designs. The design features of anaerobic bioreactors are determined by the type and volume of waste being processed, the required degree of degradation, optimization of energy yields and economic factors. The most commonly accepted classification of anaerobic reactors is based on the shape of the macrostructures of biomass methanogens in them. According to this principle, all designs can be divided into reactors with suspended-sedimented activated sludge, attached biomass (biofilm) and with a fluidized bed on a synthetic or natural carrier (Koniuszewska et al., 2020). The first type of digesters include a traditional methane tank, an anaerobic lagoon, an upflow reactor through an anaerobic sludge bed (UASB), and an aerated concrete reactor (ABR) (Mojiri et al., 2012).The second type includes downflow reactors (DSFF-reactor), an aerated fluidized bed reactor (AFB), biological filters. A number of designs - an upflow anaerobic biofilter (AF) and a hybrid reactor (AF+UASB) - combine elements of both types of reactors (van Lier, 2006).

Type 1 digesters are the simplest anaerobic bioreactors. The substrate is fermented at a low rate when it comes into contact with biomass pellets that settle at the bottom of the bioreactor. The design is simple, suitable for processing various types of waste with a load of 0.1 to 2 kg of COD/(m^3/day). However, the geometric parameters of such bioreactors require large areas for placement, the process is practically impossible to intensify and control (Douglas, 2017). The use of this technology is justified when wastewater contains solid particles that are difficult to digest and easily precipitate.

Traditional methane tanks are cylindrical tanks with a hermetic overlap and a conical or flat bottom. There are methane tanks with a floating overlap, methane tanks-gas holders and methane tanks-compacting. The best technological indicators are achieved in ovoid-shaped methane tanks, which have minimal heat loss, and less sand accumulation and cork formation (Alengebawy et al., 2024).

ISSN: 2409-4951 (Online), 2310-1008(Print)

The contact reactor is built together with a settling tank (Figure 1).

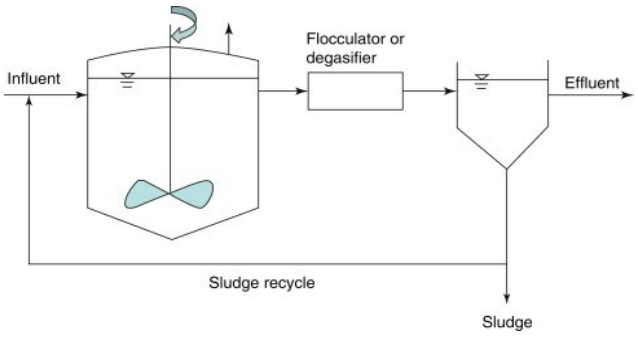

Figure 1. Anaerobic contact reactor

The contact reactor is built together with a settling tank. Contact reactors are characterized by a high concentration of activated sludge, and, accordingly, a relatively short residence time of biomass in the reactor. The advantages are a sufficiently high quality of processing, the ability to control the process. The disadvantages include a relatively low load, from 4 to 30 g/l of COD/m^3/day.

The anaerobic baffled reactor (ABR) is characterized by its simplicity of design and wide possibilities for improvement: the introduction of various types of loading, heat exchange devices and elements for biogas removal (Foxon et al., 2025). It consists of a series of vertical compartments or chambers, which forces wastewater to flow upward through a series of sludge layers, which is essentially a serial connection of UASB reactors. In modern models, the flow between the chambers occurs through small-diameter pipes, which provides a longer hydraulic retention time (HRT) in neighboring elements and a high flow rate (Figure 2).

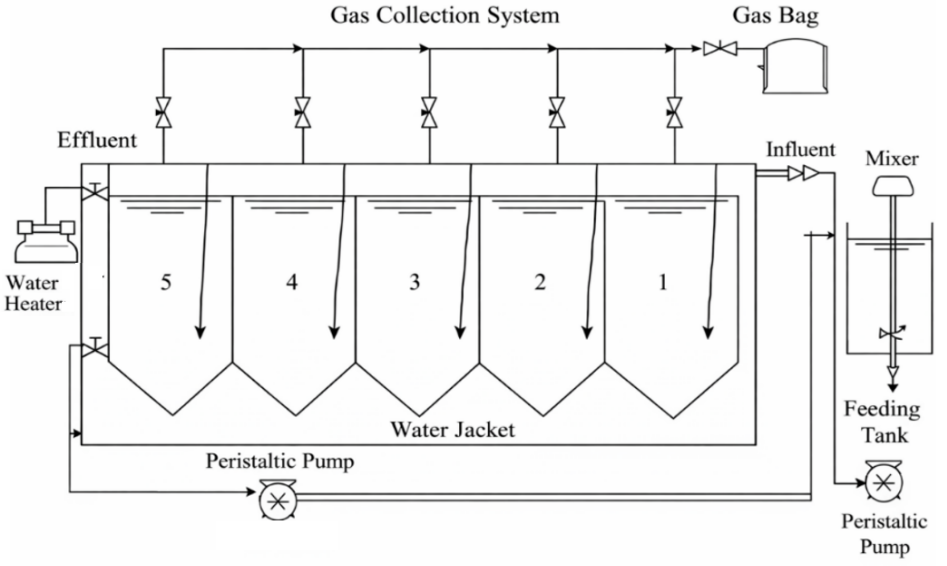

Figure 2. Anaerobic bafflet reactor

ISSN: 2409-4951 (Online), 2310-1008(Print)

The ABR design provides high purification efficiency, stability to organic and hydraulic shock loads. The principle of operation of the ABR is to separate the processes of acid formation and methanation by dividing the working volume into sections. The desirability of separating acid formation and methanation is based on different optimal conditions for these phases. By physically separating them in different compartments, the ABR creates conditions for more efficient methanogenesis and potentially higher biogas yields.

The disadvantages include insufficient mixing, leaching of biomass by the biogas flow and accumulation of volatile fatty acids (VFA). A number of modifications have been proposed to improve the characteristics of the reactor, including batch ABR (PABR), carrier ABR (CABR), separate-feed ABR (SABR), modified ABR (MABR), anaerobic-aerobic ABR (AABR) and granular sludge ABR (GRABBR). The list of ABR modifications suggests that the original design, while having advantages, has the potential for improvement.

Type 2 digesters use the principle of immobilizing microflora on natural (gravel) or synthetic (PVC rings) media. The media can be loaded either in an ordered or bulk manner. Structures with immobilized biomass have better resistance to toxic effluents and quickly adapt to changes in the composition of the raw material. The main difference between a biofilter and a biofilter is the loading of an inert media without the possibility of its removal by the flowing liquid flow. A biofilm is formed on the media, with which the substrate comes into contact. Anaerobic biofilters are classified according to the direction of substrate flow, loading, and media material.

A typical representative of type 2 digesters is downflow stationary fixed film reactor (Figure 3).

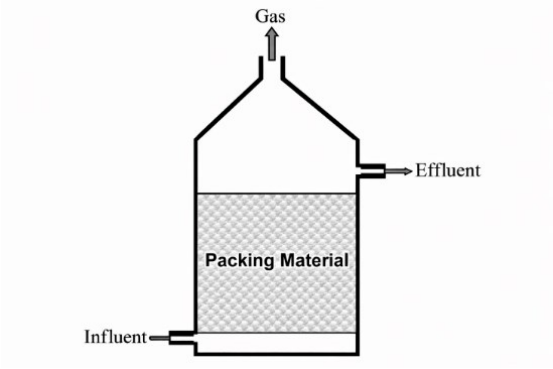

Figure 3. Downflow stationary fixed film reactor (DSFF)

Wastewater is fed into the upper part of the reactor and, flowing through the loading layer, is removed from the bottom. The design is simple, does not require much pumping equipment, but the biofilm requires meticulous selection of a carrier with the necessary surface properties. Soft materials with high internal porosity (not less than 200 m^2 per 1 m^3) are most often used. The flow of wastewater from top to bottom and biogas bubbles rising upwards will contribute to the mixing of biomass in the reactor. The biogas yield and its quality may be somewhat lower compared to other anaerobic bioreactors, since the removal of gas is complicated by the shape of the loading and the counterflow of liquid. The loading may become clogged with suspended particles.

In anaerobic filters with upward flow AF (Anaerobic Filter). wastewater is fed into the lower part of the reactor and rises upwards, biogas is removed from the top, and the surface

ISSN: 2409-4951 (Online), 2310-1008(Print)

of the carrier is effectively used. Biomass is present not only in the form of biofilm, but also in flocs and granules (Comparetti et al., 2013). The flow prevents the bottom of the anaerobic filter from growing and clogging, the occurrence of stagnant zones and ensures uniform distribution of biomass. Such bioreactors are suitable for working with sharp fluctuations in the concentration of pollutants in wastewater and are most often used in the treatment of wastewater from meat processing, dairy and textile industries (Rodrigues et al., 2024). To prevent the accumulation of sludge inside the digester, a tubular reactor with a fixed film is used, which is a biofilter with a planar loading. The reactor can be with an upward or downward flow. The carrier is pipes or plates arranged in such a way as to create vertical channels. The working load is up to 30 kg COD/m^3·day. This form of loading, in addition, will contribute to a more complete removal of biogas from the volume of the anaerobic filter. The principle of operation of another reactor of the second type is based on the self-immobilization of biomass in the form of granules (granulated sludge). Such devices are characterized by good decantation characteristics and high methanogenic activity. An example is devices with an upward flow of liquid with a suspended granular layer of sludge (Figure 4).

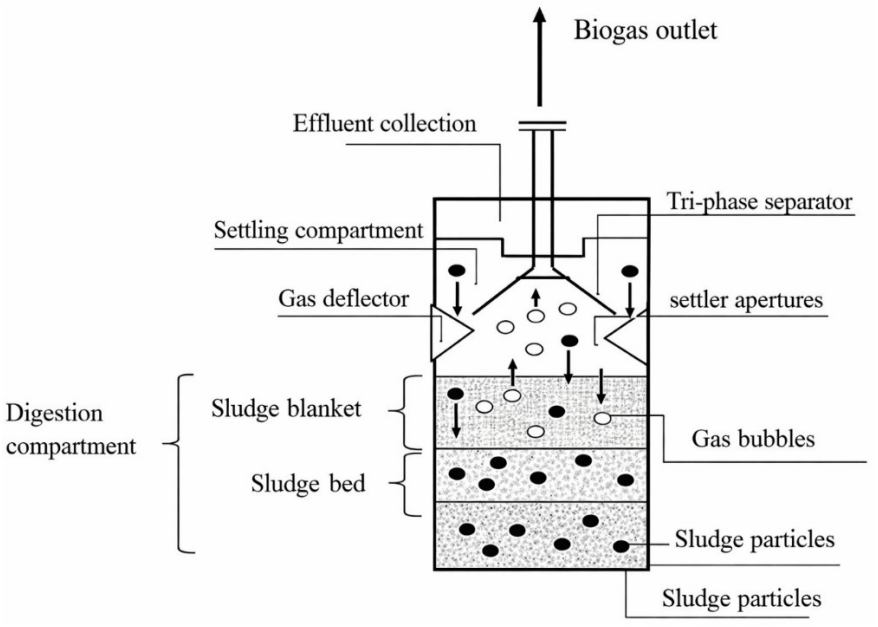

Figure 4. Upflow anaerobic sludge blancet reactor (UASB)

Since the reactor does not require an internal filling to fix the biomass, it is economically attractive, but its performance characteristics depend on the granulation of the biomass. In addition, the UASB reactor has a gas-liquid-solid separation system in its upper part, which prevents or limits the removal of suspended particles and promotes gas removal and sludge decantation. The separation of gas, treated water and granular biomass is carried out using a special sludge-gas separation device.

The retention of granular biomass is also carried out due to its high sedimentation capacity. UASB reactors are highly sensitive to the composition of the wastewater, especially

ISSN: 2409-4951 (Online), 2310-1008(Print)

the presence of solids and inhibitors in it, however, they are relatively compact and simple, providing good mixing conditions. UASB reactors are characterized by the ability to withstand high organic loads of up to 40 kg COD/m^3·day, short hydraulic retention time (HRT), low energy requirements, simple design and maintenance, and high solids retention time (SRT) due to the granular sludge. Similar to anaerobic filters, UASB reactors have been widely used in industry at the agro-food wastewater treatment level (Mainardis et al., 2020).

The phenomenon of sludge granulation is not fully understood, and makes it difficult to start up UASB reactors when the production does not have a suitable source of seed culture, such as sludge from another operating UASB reactor. There is currently no general theory of granulation, and the available data do not always correlate well with each other. Disadvantages include a long start-up period for the formation of granular sludge, the need for further processing, sensitivity to toxic compounds, potential leaching of sludge, sensitivity to pH and temperature, and problems with granulation. On an industrial scale, UASB reactors are widely used in large treatment plants, especially in tropical countries (China, India, BrADil).

Hybrid designs have also been developed that combine the advantages of a UASB reactor and an anaerobic filter: the UBF (Upflow Bed-Filter) reactor (Figure 5).

The lower part contains a layer of granular sludge, and the upper part, usually 25-30% of the volume, is filled with an inert carrier, fixed or floating. This allows the use of biomass of a higher concentration, provides high productivity and optimal mixing modes. Thus, it is possible to avoid the clogging of the lower layers of the carrier, which is typical for an anaerobic filter, and to reduce its amount.

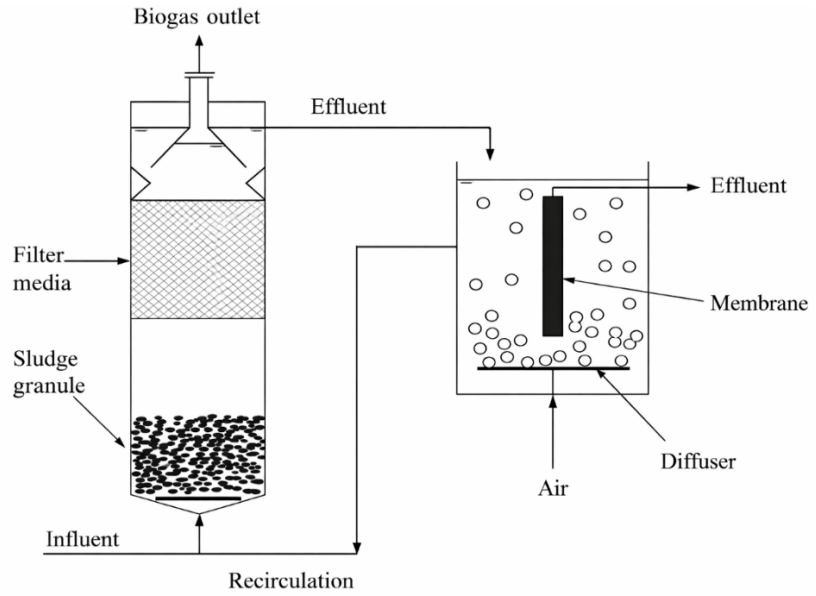

Figure 5. Upflow Bed-Filter reactor (UBF)

Type 3 digesters are characterized by the presence of a fluidized microbial layer on a synthetic or natural carrier. The contact area of the carrier is 200 m^2/m^3 and more, active mixing occurs during methanogenesis. Fluidized bed reactors have a degree of fluidization

ISSN: 2409-4951 (Online), 2310-1008(Print)

of more than 50%, and expanded sludge bed reactors - about 20%. The organic load can exceed 40 kg of COD/m^3·day. The hydraulic residence time is less than 12 hours. However, these reactors consume more energy, have a complex design, and are accordingly more expensive to build and operate compared to Type 1 and Type 2 reactors (Figure 6).

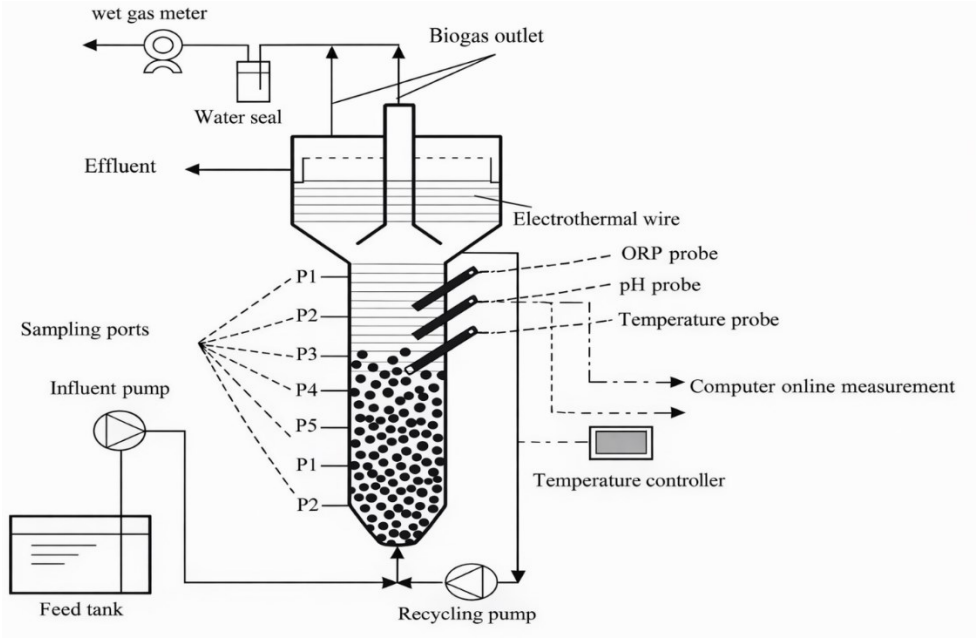

Figure 6. Bioreactor with expanded and suspended activated sludge bed (EGSB)

The fundamental difference of this type of reactor from UASB is the higher velocity of the upward flow of liquid due to recirculation and intensification of mass transfer between sludge granules and wastewater. Such reactors are suitable for processing low-concentration wastewater. A fluidized bed reactor is one of the most productive bioreactors with fixed microflora due to more complete contact of contaminants with biomass. Fluidization occurs due to the upward flow of liquid and the released biogas bubbles. At the same time, the contact surface between the active biomass and untreated waste increases significantly. In such bioreactors, low-concentration wastewater with dissolved or finely dispersed contaminants is treated. However, maintaining the fluidized bed requires significant energy consumption.

Digester with membrane filtration system **(**AnMBR). AnMBR combines anaerobic digestion with membrane filtration, which allows the hydraulic retention time (HRT) to be controlled independently of the solids retention time (SRT). The membrane retains biomass inside the reactor, while the treated liquid is removed as permeate. This enables operation at short HRT and long SRT, reduces reactor volume, and ensures high effluent quality.

The combination of a classic anaerobic digester with a membrane ultrafiltration (microfiltration) system allows to retain microbial biomass in the reactor, achieve a significant extension of SRT (solid retention time), which increases the stability of the process and contributes to a higher biogas yield (Liao et al., 2006). Membrane fouling and high energy costs for pumping remain the main disadvantages of the technology (Figure 7) (Benyahia et al.,2024; Stuckey, 2012).

ISSN: 2409-4951 (Online), 2310-1008(Print)

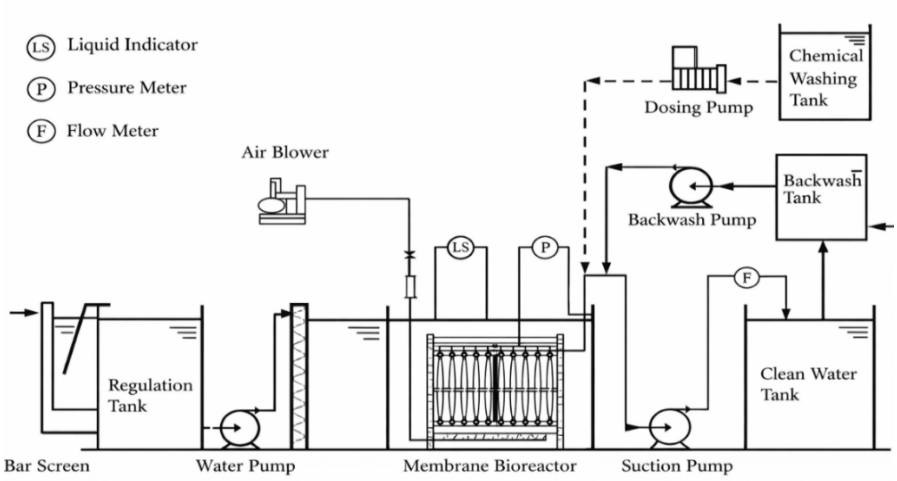

Figure 7. Digester with membrane filtration system (AnMBR)

However, the use of new module configurations (external/internal, electric) demonstrate encouraging results at the stage of laboratory experiments (Li et al., 2023).The use of various membrane modules (cross-flow, submerged, fluidized) reduces the degree of membrane surface contamination due to the turbulence of the substrate flow. Algorithms have been developed that allow predicting biokinetic parameters during membrane operation in different load regimes and biomass concentrations.

Two-phase systems. The classical anaerobic process consists of four stages: hydrolysis, acidogenesis, acetogenesis and methanogenesis. In a traditional reactor, all these processes occur simultaneously in one container, but the stages require different environmental conditions. Hydrolysis and acidogenesis are characterized by relatively rapid bacterial growth (several hours/day), resistance to load changes. Optimal pH 5.5–6.5 (phase 1). During methanogenesis, very slow growth of archaea (up to 15-30 days) is observed, and it is highly sensitive to the accumulation of volatile fatty acids (VFA). Optimal pH 7.0–8.0 (phase 2). Dividing the process into two consecutive reactors allows to optimize the hydrolysis of complex substrates and increase the methane yield due to stabilization of the methanogenic phase, ensuring better processability (Wang et al., 2005; Stabnikova et al., 2008a). In the acid reactor (phase 1), complex organic substances are converted into simple acids (acetic, propionic, etc.), and an optimally prepared substrate enters the methanation tank, where only CH_4 and CO_2 generation occurs (phase 2) (Tang et al., 2023). However, the stability of two-phase systems depends on the hydraulic retention time (HRT), C/N ratio in the substrate, pretreatment of substrate, temperature regime, and composition of the inoculum (Kabaivanova et al., 2024; Liu et al., 2008; Stabnikova et al., 2008b).

Combined systems: Two-phase + AnMBR. The combination of these two technologies creates a system where the first reactor acts as a buffer and hydrolyzer, and the second (AnMBR) is a highly efficient methane generator. In the first reactor, solid organic waste is solubilized (dissolved). Having greater resistance to changes in cultivation conditions, acetogens eliminate the negative consequences of a sharp drop in pH. This reduces the load of solid particles on the membrane in the second reactor, reduces the rate of formation of a gel layer on the membrane, and stabilizes methanogenesis. This combination ensures the stability of the load on the methanogenic phase, high permeate quality, and the possibility of

ISSN: 2409-4951 (Online), 2310-1008(Print)

nutrient recovery. Optimization of conditions for each group of microorganisms increases organic conversion (Gao et al., 2010). However, capital and operating costs for membrane modules and control systems are higher compared to other types of digesters, and the membranes still require periodic chemical washing and gas scouring for cleaning (Bueno et al., 2024; van Lier et al., 2015). Particularly promising are the systems with AnMBR + phototrophic MBR, which allow for additional CO_2 absorption, improve the quality of treated wastewater and increase the biogas yield (Fischer et al., 2024).

The main types of digesters used for anaerobic conversion of organic matter to methane:

- for liquids with a low solids content (<3%) - upflow reactors through anaerobic sludge (UASB);
- with a high solids content (6-12%) - induced bed reactors (IBR);
- for raw materials of a wide range of consistencies, from dilute to highly concentrated, - suspended bed reactors.

The variety of composition and properties of substrates does not allow for a clear comparison of different digester designs in terms of efficiency and manufacturability. Depending on the characteristics of the effluent, desired results, economic feasibility and local climatic conditions, any design of the above systems may be optimal.

Microbial communities and stages of methanogenic bioconversion of organic matter

Anaerobic digestion (AD) is a complex biotechnological process carried out by a diverse community of interdependent microorganisms, including bacteria and archaea, in the absence of oxygen. The efficiency of this process directly depends on the metabolic activity and complex interactions of these microorganisms (Alipoursarbani et al., 2025). The AD process includes several sequential stages: hydrolysis, acidogenesis, acetogenesis and methanogenesis. Each phase is provided by microbial consortia that are characterized by high specialization and interdependence (Pal et al., 2021).

Hydrolysis. Hydrolysis is the initial stage of AD, in which complex organic polymers (lipids, polysaccharides and proteins) are broken down into simpler, soluble ones, including sugars, amino acids and fatty acids. This process is carried out by hydrolytic bacteria that produce extracellular enzymes, including amylases, proteases, cellulases and lipases. Microbial groups involved in hydrolysis include the families *Clostridiaceae, Pseudomonadaceae and Syntrophomonadaceae*, as well as the genera *Streptococcus, Enterobacter, Clostridia, Micrococci, Bacteroides, Butyrivibrio, Fusobacterium and Selenomonas*. Hydrolysis is often rate-limiting for the digestion of complex organic wastes, especially for lignocellulosic biomass (Das and Mondal, 2016). The key enzymes involved in hydrolysis belong to the class of hydrolases, including esterases, glycosidases and peptidases. Glycosidases, for example, include cellulases (endo-1,4-beta-D-glucanase, cellulose 1,4-beta-cellobiosidase, beta-glucosidase) required for cellulose degradation, as well as xylanases, xylosidases, mannanases, mannosidases, alpha-galactosidases, and alpha-glucuronidase that break down hemicellulose (Pal et al., 2021).

Acidogenesis (Acid formation). In the acidogenesis stage, microorganisms convert sugars, amino acids, and fatty acids obtained during the hydrolysis step into short-chain organic acids such as formic, acetic, propionic, butyric, and pentanoic acids. In addition, alcohols (methanol, ethanol), aldehydes, carbon dioxide (CO_2), and hydrogen (H_2) are produced as intermediates. This step is carried out by acidogenic bacteria (acidogens), including members of the genera *Clostridium*, *Bacillus*, *Lactobacillus*, *Pseudomonas*, *Micrococcus*, and *Flavobacterium*. Acidogenic bacteria play an important role in creating

ISSN: 2409-4951 (Online), 2310-1008(Print)

favorable anaerobic conditions for the growth of obligate anaerobes involved in the later stages of the process. Approximately 20-30% of the total CO_2 is produced at this stage. Key enzymes in acidogenesis include hexokinase, phosphoglucose isomerase, phosphofructokinase, aldolase, triose phosphatase isomerase, glyceraldehyde-3-phosphate dehydrogenase, phosphoglycerate kinase, mutase, enolase, pyruvate kinase (for glycolysis); pyruvate:ferredoxin oxidoreductase (PFOR), NADH:ferredoxin oxidoreductase (NFOR) and ferredoxin hydrogenase (for H_2 production); as well as lactate dehydrogenase, phosphotransacetylase, acetate kinase, ethanol dehydrogenase, acetaldehyde dehydrogenase, acetyl-CoA acetyltransferase, and butyryl-CoA dehydrogenase (Pal et al., 2021).

Acetogenesis. In the acetogenesis stage, acetogenic bacteria (*Syntrophomonas* and *Syntrophobacter*) convert organic acids and alcohols formed during acidogenesis into acetate, H_2, and CO_2 (Quin et al., 2025). Homologous acetogenic bacteria can also reduce CO_2 and H_2 to produce acetate. The products of acetogenesis, acetate and hydrogen, are directly used by methanogenic microbes in the final stage of AD. Approximately 70% of methane production is associated with the reduction of acetate in this stage (Pal et al., 2021). Key enzymes include those involved in the oxidation of acetate (citrate synthase, aconitase, isocitrate dehydrogenase), butyrate (CoA transferase, butyryl-CoA dehydrogenase), propionate (pyruvate carboxylase, malate dehydrogenase, fumarate hydratase, fumarate reductase, succinate dehydrogenase, succinyl-CoA synthetase, methylmalonyl CoA mutase/epimerase/decarboxylase, propionate-CoA transferase), and ethanol (acetaldehyde dehydrogenase).

Methanogenesis. Methanogenesis is the final stage of anaerobic fermentation, in which methanogenic archaea (*Methanobacterium*) produce methane (CH_4). They use substrates formed in previous phases, in particular acetic acid, H_2, CO_2, methanol, methylamine or dimethyl sulfide. Thus, *Methanosarcina* is a universal methanogen capable of using acetoclastic, hydrogenotrophic and methylotrophic pathways (Mesquita et al., 2023). It should be noted that *Methanothrix* is an acetoclastic methanogen that is sensitive to high concentrations of ammonia. Among the hydrogenotrophic methanogens, *Methanoculleus, Methanobacterium, Methanoregula* and *Methanomassiliicoccus* are distinguished (Piercy et al., 2025). The main metabolic pathways of methanogenesis are the acetoclastic pathway, which involves the breakdown of acetate and is responsible for approximately 70-72% of CH_4 production, and the hydrogenotrophic pathway, which consists in the reduction of CO_2 with H_2 and accounts for about 28-30% of CH_4 production. There is also a methylotrophic pathway that uses methylated compounds (Siroka et al., 2018). Methanogens actively consume hydrogen, which helps maintain a low partial pressure of H_2. This thermodynamically enhances the fermentation stages, in particular the conversion of sugars to short-chain fatty acids, and prevents their excessive accumulation. Maintaining low hydrogen concentrations creates favorable conditions for the development of acidogenic bacteria and prevents the accumulation of short-chain organic acids during the acidogenesis stage. The vital activity of methanogens leads to a decrease in the content of H_2, which enhances fermentation in the previous stages, ensuring a sufficient level of volatile fatty acids (VFA).

The concept of "microbial consortia" is central to the efficiency of AD, which is driven by synergistic interactions between different microbial groups. This means that research should focus on optimizing the entire community, rather than simply introducing a single "supermicrobe". However, not all methanogens are equally beneficial. Significant increases in the abundance of *Methanomassiliicoccus* resulted in reduced biogas production at high butyric acid concentrations. Thus, the type of methanogen and its specific metabolic interactions in the consortium matter, and an increase in the abundance of certain

ISSN: 2409-4951 (Online), 2310-1008(Print)

methanogens may be an indicator of process instability rather than efficiency (Alipoursarbani et al., 2025). The main stages of anaerobic conversion of organic matter to methane are given in Table 1.

Table 1

The main stages of anaerobic conversion of organic matter to methane

Stage	Microbial groups	Main functions	Products
Hydrolysis	Hydrolytic bacteria	Breakdown of organic polymers	Monomers (sugars, amino acids)
Acidogenesis	Acidogenic bacteria	Conversion to organic acids, alcohols, H_2, CO_2	VFA, alcohols, H_2, CO_2
Acetogenesis	Acetogenic bacteria	Oxidation of VFA and alcohols to acetate, CO_2	Acetate, H_2, CO_2
Methanogenesis	Methanogenic archaea	Conversion of acetate, H_2, CO_2 to CH_4	CH_4, CO_2

Syntrophic relationships and interspecies electron transfer. Microbial consortia involved in anaerobic digestion function in synergistic and syntrophic relationships, where the metabolic products of one group of microorganisms serve as substrates for the next. This interaction is particularly critical between hydrogen-producing acetogenic bacteria and hydrogenotrophic methanogens. The close coupling and syntrophic association between acetogenesis and methanogenesis is a thermodynamic necessity. Many acetogenic reactions that produce H_2 are thermodynamically unfavorable unless H_2 is continuously consumed by methanogens. This explains why maintaining a healthy methanogenic population is so critical to the entire process (Siroka et al., 2018).

Factors affecting microbial communities in the biomethane production process. Operational parameters play a significant role in the formation of microbial communities and their metabolic activity in anaerobic digesters, which affects the biomethane yield.

Temperature. Depending on the operating temperature, mesophilic (30–40 °C) and thermophilic (45–60 °C) regimes are distinguished. Lower temperatures are not used, since the process duration becomes inadequately long. Mesophilic systems are considered more stable and require less energy than thermophilic ones. However, the higher the fermentation temperature, the higher the reaction rate and gas yield. In developing countries, including Ukraine, systems with lower heating costs (mesophilic temperature range) are mainly used in order to increase the profitability of production (Zhadan et al., 2023). Mesophilic conditions (30–40 °C) usually support a more diverse and tightly connected microbiome, ensuring greater process stability. In contrast, thermophilic conditions (50-65 °C) result in a limitation of microbial diversity, making the systems more sensitive to changes in operational parameters. With temperature changes, specific changes are observed in the dominant microbial genera, such as *Firmicutes, Bacteroidetes, Thermotogae, Methanobacteriales* and *Methanosarcinales*. An increase in temperature promotes higher metabolic activity, accelerating substrate degradation and leading to more intensive methane production. However, thermophilic systems tend to be less stable. A small increase in temperature (1-2 °C) can cause a significant decrease in methane production due to the accumulation of volatile fatty acids (VFA) and acidification of the reactor. Mesophilic systems, on the other hand, provide greater stability and are able to process a wider range of biomass, making them less vulnerable. This requires a trade-off in the design and operation of the AD: the higher

ISSN: 2409-4951 (Online), 2310-1008(Print)

productivity potential of thermophilic systems requires a careful weighing of the desired outcomes, e.g. high biogas yield, against stability (Costopolou et al., 2023).

pH plays a significant role in regulating the composition and activity of the microbial community. Acetoclastic methanogens, in particular, are extremely sensitive to pH, and their productivity will be reduced at pH values below 6.2. Changes in pH lead to changes in the relative abundance of various microorganisms, such as *Proteobacteria, Firmicutes* and *Bacteroidetes*, as well as the genera *Lactobacillus, Methanocorpusulum, Petrimonas, Proteiniphilum* and *Methanosarcina*. Excessive accumulation of VFA can lead to acidification of the reactor and a drop in pH, which limits the growth of methanogenic communities and potentially causes the AD to shut down. High protein content in substrates contributes to their enrichment with ammonium (NH_4+), preventing a sharp drop in pH (Costopolou et al., 2023).

Hydraulic retention time (HRT) and organic load (OL) significantly influence microbial communities and digester performance. Short HRT can reduce microbial diversity and acetogenic bacteria, while fluctuations in OL affect bacterial and archaeal community structure. High or unstable OL may decrease diversity further, causing shifts between Methanobacterium and Methanosarcina. HRT below a critical threshold and excessively high OL can lead to methanogen loss, VFA and hydrogen accumulation, and pH drop. Nevertheless, combining high OL with moderately reduced HRT can enhance methane production per unit reactor volume (Costopolou et al., 2023).

Substrate composition. The composition of the substrate is a key factor shaping microbial communities and determining biomethane production. Complex feedstocks favor more diverse microbial populations. Main bacterial phyla, such as Chloroflexi, Bacteroidetes, Firmicutes, and Proteobacteria, are prevalent regardless of substrate type, but specific feedstocks enrich particular populations. For example, Anaerolineaceae and Rikenellaceae dominate in food waste, while *Candidatus Methanoculleus thermohydrogenotrophicum* is more abundant in lipid-rich substrates. Substrate characteristics, including polysaccharide, protein, and lipid content, directly affect conversion and biogas yield, with lipids having the highest methane potential (94.8%), followed by proteins (71%) and carbohydrates (50.4%). Low C/N ratios can reduce AD efficiency and biogas production (Ivanov et al., 2002; Costopolou et al., 2023).

Inhibitory compounds. *Ammonia* concentration is a significant inhibitor in anaerobic digestion. Levels above 5 g/L, mainly as free ammonia nitrogen, passively diffuse into cells, disrupting metabolism, pH, and proton motive force. Acetoclastic methanogens are most sensitive, while microbial adaptation often involves syntrophic acetate oxidation coupled with hydrogenotrophic methanogenesis. *Methanothrix* is generally sensitive to NH_4^+, whereas *Methanosarcina, Methanoculleus*, and *Methanobacterium* are more resistant. Elevated ammonia leads to accumulation of VFAs, especially propionate and acetate, causing instability in AD. The addition of trace elements (Fe, Co, Se, Ni) or zeolite can alleviate inhibition and improve biomethanization. In a hybrid anaerobic solid–liquid (HASL) system enhanced with a submerged biofilter, food waste digestion was improved: COD and VFA generation increased in the acidogenic reactor, while total COD removal and methane production increased in the methanogenic reactor, reaching 99% COD removal and 26% higher methane production compared to conventional HASL (Wang et al., 2003).

Lipids are a major problem in municipal and food-industry wastewater because they are present in high amounts and are difficult to remove completely. Although most fats can be eliminated by physico-chemical methods, the remaining emulsified lipids must be treated biologically. During anaerobic digestion, fats are converted into long-chain fatty acids, which inhibit microbial activity and methane production. The addition of iron salts reduces this

ISSN: 2409-4951 (Online), 2310-1008(Print)

inhibition by binding long-chain fatty acids into insoluble compounds, thereby improving their degradation and overall anaerobic digestion performance (Ivanov et al., 2002, 2014; Tay et al., 2006; 2008).

Sulfate concentrations of 1–3 g/L in anaerobic systems decrease methane production due to sulfate reduction to sulfide by sulfate-reducing bacteria, which inhibit methanogens through toxicity, substrate competition, and trace element precipitation (Chelliapan and Sallis, 2015). Elevated sulfide levels can severely suppress biogas formation and cause corrosion, odor, and health hazards. The addition of ferric hydroxide during anaerobic digestion of sulfate-rich wastewater enhances treatment by stimulating iron-reducing bacteria, completely eliminating hydrogen sulfide from both biogas and liquid phases and reducing the sulfate-reducing bacteria-to-methanogen ratio sixfold (Stabnikov and Ivanov, 2006).

Volatile fatty acids (VFAs) accumulated in excessive amounts also has an inhibitory effect. This occurs due to high organic load, increased carbohydrate content or high concentrations of other obstructive compounds such as Na^+, total ammonia nitrogen (TAN) and lipids. Microorganisms responsible for the degradation of propionate and butyrate (*Syntrophobacter, Pelotomaculum, Smithella, Syntrophomonas*) can decrease in number with increasing organic load, leading to the accumulation of VFAs. *Methanothrix* concentrations may decrease, while *Methanoculleus* and acetate-oxidizing bacteria (*Tepidanaerobacter acetatoxydans*) may increase, indicating a shift in acetate consumption from acetoclastic methanogenesis to SAO. *Methanosarcina* abundance may increase with the increase in VFA in mesophilic reactors, as their growth promotes acetate accumulation.

VFA are positive for methane generation when their concentration remains within a certain range. *Proteiniphilum* plays a key role in the conversion of VFA to CO_2. The interplay of operational parameters and inhibitory compounds is critical. High organic loading can lead to the accumulation of VFA, which lowers pH, inhibits methanogens, and this in turn enhances VFA accumulation due to the lack of hydrogen consumption. This complex network of interactions highlights the need for holistic system management to prevent cascading failures. Microbial communities exhibit adaptability and resilience to stress. Understanding these adaptive mechanisms is key to developing more robust AD systems (Mills et al., 2024). The influence of the parameters of the anaerobic conversion of organic substances on the biomethane yield is analyzed in Table 2.

To increase the efficiency and stability of the anaerobic digestion process, various methods of influencing microbial populations are used.

Bioaugmentation is the introduction of specific stress-resistant or highly efficient microorganisms into AD systems. The main goal of this is to enhance the system's ability to produce biomethane and mitigate the effects of stressful conditions. The advantages of bioaugmentation: high efficiency, resistance to stress loads, overall enhancement of the AD process, reduction of toxic inhibition (e. g., ammonia) and overcoming the limitations of the psychrophilic regime. The metabolic activity of the microbial community is also improved, the adaptability of microbes to cultivation changes is increased, and the overall biogas production process is enhanced. Representatives of the *Clostridiaceae, Pseudomonadaceae* and *Syntrophomonadaceae* families are mainly used for bioaugmentation. However, there are difficulties associated with compatibility with the local microbiota, dosage and frequency of inoculum introduction (Alipoursarbani et al., 2025).

ISSN: 2409-4951 (Online), 2310-1008(Print)

Table 2

Influence of operational parameters and substrate composition on microbial communities and biomethane yield

Parameter	Impact on microbial community	Biomethane production
Operational parameters		
Temperature	Mesophilic (30-40 °C): diverse microbiome, stability. Thermophilic (50-65 °C): limited diversity, sensitivity to change, specific dominants (*Firmicutes, Bacteroidetes, Thermotogae, Methanobacteriales, Methanosarcinales*).	Increasing temperature accelerates biosynthesis CH_4.
pH	Critical for structure and activity. Acetoclastic methanogens are sensitive (<6.2). Changes in phyla (*Proteobacteria, Firmicutes, Bacteroidetes*) and genera (*Lactobacillus, Methanocorpusulum, Methanosarcina*).	Optimal pH is important for VFA degradation. A drop in pH limits methanogenesis.
HRT and OL	Short HRT reduces acetogenic diversity. Fluctuations in OL shape microbial community structure, with high OL decreasing diversity and causing shifts between *Methanobacterium* and *Methanosarcina*.	Short HRT leads to VFA and H_2 accumulation, pH decrease, and methanogenesis inhibition.
Substrate composition		
Substrate composition	Complex substrate: more complex microbiome, higher metabolic diversity. Major phyla (*Chloroflexi, Bacteroidetes, Firmicutes, Proteobacteria*). Specific substrates enrich different populations.	Low C/N ratio reduces methanogenesis efficiency.
Ammonia concentration	NH_4+>5 g/L inhibits AD (FAN-NH3). Acetoclastic methanogens are most sensitive. Adaptation: transition to SAO + hydrogenotrophic methanogenesis. *Methanothrix* is sensitive, *Methanosarcina* is resistant.	Micronutrients and zeolite can mitigate the negative effects of methanogenesis inhibition by excessive NH_4^+.
Lipids	Alters the microbial community structure by inhibiting acidogenic and methanogenic microorganisms due to the accumulation of long-chain fatty acids.	Reduce biomethane production by suppressing methanogenic activity.
Sulfate	Shifts the microbial community by promoting sulfate-reducing bacteria, which compete with methanogens for substrates and inhibit their activity through sulfide production.	High sulfate concentrations reduce biomethane production by inhibiting methanogens through sulfide formation.
Volatile fatty acids	Excessive accumulation inhibits AD. Propionate/butyrate decomposers may decrease. *Methanothrix* may decrease, *Methanoculleus* and SAOB increase. *Methanosarcina* may increase also.	VFA are precursors, but excessive accumulation causes acidification, pH drop and methanogen limitation.

Co-digestion involves mixing different organic substrates in different ratios. This approach is often preferable to mono-digestion due to numerous advantages. It allows for improved carbon to nitrogen ratio (C/N, optimum 25-30:1), increased biodegradability,

ISSN: 2409-4951 (Online), 2310-1008(Print)

efficient removal of solids (VS) and contributes to the sustainability of production. Co-digestion helps to achieve a balance of nutrient components, dilutes inhibitory compounds and provides buffer capacity of the system. As a result, an increase in methane yield and more efficient operation of the digester is observed. In addition, co-digestion contributes to increased microbial diversity and stability of the system. Examples of successful co-digestion are combinations of fruit/vegetable and food waste, as well as cow manure, chicken manure and whey. Lignocellulosic agricultural residues are also a priority feedstock for co-digestion (Quin et al., 2025).

Inoculation *i*s the introduction of microorganisms into the digester to initiate anaerobic fermentation. Traditional sources include cow manure from a manure pit or waste activated sludge from an operating digester. Marine sediment has also been found to be a promising microbial source for inoculation. Optimizing the process requires determining the optimal inoculum to substrate ratio. Typically, it is added in the range of 10–20%. Studies have shown that the initial inoculum adapts to the digester conditions, making further continuous addition of manure unnecessary once microbial adaptation is achieved. Proper inoculation enhances the bacterial community, leading to increased specific biogas production and methane content, as well as reduced hydraulic retention time. Timely and appropriate inoculations can also reduce the risks of acidification by maintaining a balance between acidogens and methanogens (Abouelenien et al., 2021).

Application BioIronTech process that is a microbial iron-based treatment in which Fe(III) is biologically reduced to Fe(II), transforming iron particles and forming ferrous/ferric compounds that adsorb and precipitate pollutants such as sulfides, lipids, and recalcitrant organics. By removing these inhibitory compounds, the process stabilizes anaerobic digestion and enhances biomethane production (Ivanov et al., 2014).

New and promising technologies. New, promising technologies are constantly emerging in the field of biogas production. One of them is the use of microbial electrolysis cells (MEC), which, in combination with anaerobic digestion, can increase the efficiency of biomethane production by using electricity to stimulate microbial processes. Another innovative direction is the integration of biogas plants with other systems, for example, with hydroponic farms, which allows the reuse of nutrient-rich by-products of anaerobic digestion for plant cultivation. The use of nanotechnology, in particular metal nanoparticles, is also considered as a way to increase the efficiency of biogas production by stimulating the activity of microorganisms. New approaches to biogas generation itself are also being developed, aimed at optimizing the process and increasing the yield of the target product. The effectiveness of implementing promising technologies for archaic bioconversion of organic matter into biogas is shown in Table 3.

Microbial electrolysis cells (MECs) are advanced bioelectrochemical systems that use an external electrical potential or current to produce hydrogen or biomethane from spent biomass or wastewater. This technology involves an anode that is functionally similar to microbial fuel cells (MFCs), but the cathode receives additional current from a DC source. Specially tuned for "electromethanogenesis," electroactive microorganisms known as electrotrophs attach to the anode. Here, they oxidize organic substrates to carbon dioxide using an electrode material, typically graphite-based, as the final electron acceptor.

The electrons generated by this anodic oxidation reaction flow through an external circuit. These electrons are then used to biocatalyze reduced target molecules such as hydrogen (H_2), acetate (CH_3COOH), or methane (CH_4). In particular, the oxidation of chemical oxygen demand (COD) in wastewater at the anode can be effectively combined with biogas upgrading to biomethane, creating an integrated and highly efficient process (Mers et al., 2023).

ISSN: 2409-4951 (Online), 2310-1008(Print)

Table 3

Development of promising technologies for archaic bioconversion of organic matter into biogas

Technology	Main advantage	Result	Key mechanism
Microbial electrolysis cells	Increased methane yield, process stability	Improved methanogenesis	Stimulation of microbial processes
Integrating bioconversion with hydroponics	Substrate optimization, environmental friendliness	Improvement of methanogenesis	Better nutrient balance
Nanotechnology	Stimulation of microorganisms	Improving biogas quality	Increasing metabolic activity
Process optimization	Reduction of operating costs, process stability	Increase of biogas yield	Control of parameters (temperature, pH)

The integration of MEC into anaerobic digestion (MEC-AD) systems significantly improves the overall efficiency of the digestion, which is manifested in an increase in methane content and its production rate. Studies have shown that the methane production rate and stabilization time in MEC-AD systems were on average 1.7 and 4.0 times higher than in traditional AD reactors. The increase in methane yield (up to 200%) and process stability (4 times faster stabilization) indicate that MEC is not just an additional technology, but a transformational one. They fundamentally change the microbial environment, providing more reliable and efficient anaerobic digestion, especially for complex, highly concentrated feedstocks. Demonstrate increased tolerance to adverse environmental factors such as high organic loads, the presence of inhibitors. Current research focuses on the optimization of cathode materials. Platinum is a highly efficient material for proton recovery, however, activated carbon is being studied as a suitable and cheaper alternative. Integration with carbon nanotubes (CNTs) for biocathodes is also a promising direction. The role of specific microbial populations such as *Geobacter* and *Shewanella* in electron transfer is crucial for optimizing both electricity and hydrogen/methane production in MEC (Noémi et al., 2023).

Integration of biogas plants with hydroponic farms. The integration of anaerobic digestion (AD) with aquaponics or hydroponics creates an innovative closed system that effectively manages waste and simultaneously generates energy, promoting circularity in food production. In such systems, the waste generated in aquaponic systems - uneaten fish feed, fish feces and dead fish - are sent to an anaerobic biodigester after a post-filtration process. This allows, together with the production of biogas, to avoid environmental pollution.

Co-digestion of aquaponic effluent with cattle manure has shown better biogas production results compared to mono-digestion. This integration leads to powerful synergistic effects, such as increased overall biogas production, improved organic load conversion and achieving a better nutrient balance, which contributes to the overall stability of the process. The mineral richness of tilapia sludge, which is a component of aquaponic effluent, can enhance the enzymatic activity of microorganisms in the manure, optimizing the fermentation process (Paes et al., 2025). The concept of a "closed system" goes beyond simple waste treatment, creating a self-sustaining cycle where waste from one process becomes a valuable input for another, reducing the need for primary resources and minimizing emissions to the environment.

ISSN: 2409-4951 (Online), 2310-1008(Print)

Nanotechnology. Nanoparticles (NPs) have unique properties such as large specific surface area and high reactivity, which makes them attractive for many applications, including bioenergy. In anaerobic digestion (AD), metal nanoparticles can significantly affect the activity of anaerobic microorganisms, stimulating both hydrogen and methane production. The mechanisms of this positive effect depend on the chemical formula of the nanoparticles. Nanoparticles based on trace elements such as iron, cobalt and nickel promote the synthesis of essential enzymes and coenzymes that are crucial for the metabolic activity of anaerobic microorganisms, thereby directly improving their productivity. For example, the optimal concentration of nickel nanoparticles (NiNPs) can increase the volume of biogas and methane by 1.7 - 2.0 times. The addition of magnetic nanoparticles (MNPs) up to 100 mg/L can increase biogas production by 1.9-2.1 times compared to the control. Nanoadditives without trace elements can absorb inhibitory factors, reducing their harmful effects on microbial activity. Studies have shown that methane production phases are more sensitive to the addition of these nanoparticles than hydrogen production phases. In addition, nanoparticles can improve biogas quality by significantly reducing or completely removing hydrogen sulfide concentrations (Zhu et al., 2021). The prospects for the application of nanotechnology in bioenergy are promising. Current trends include the development of specialized multifunctional nanomaterials that are stable and biodegradable. Nanomaterials are expected to lead to significant efficiency improvements, cost reductions in the bioenergy sector, and be integrated with other technologies, such as artificial intelligence, to further optimize bioenergy production.

Advanced monitoring methods and “omics” approaches

Advanced monitoring methods and “omics” approaches are being used to gain a deep understanding of microbial diversity, physiology, interactions, and metabolic networks in AD systems. This is crucial for optimizing the productivity and sustainability of bioprocesses. Key methods include high-throughput sequencing (e.g., 16S rRNA) for microbial community analysis. More comprehensive “omics” approaches, such as metagenomics, metatranscriptomics, metaproteomics, and metabolomics, provide unprecedented insights into microbial functionality (Ana et al., 2021). The advantages of these methods are to identify the functional importance of specific microorganisms and to elucidate complex microbial interactions, such as metabolic cross-feeding. They also allow the identification of key microorganisms and regulated functional proteins that influence the process. In addition, these approaches allow the evolution of the microbial community to be tracked in response to changing operating conditions. The application of this knowledge involves the integration of detailed chemical and biological fingerprinting with machine learning models. This creates a new approach to understanding the microbial ecology of the AD. Bioaugmentation, co-fermentation and microbial pretreatment - all these directions explore the principles of synergy in microbial communities. It is not just about adding more microbes or substrates, but about creating conditions under which different microbial groups complement each other's functions, leading to more reliable and effective cooperation. The increasing use of "omics" technologies and machine learning indicates a shift from an empirical trial-and-error approach to a more guided, predictive and mechanistic understanding of the AD. This is a significant trend in the field, moving towards the development of "smart" digesters (Song et al., 2021).

ISSN: 2409-4951 (Online), 2310-1008(Print)

Biogas purification and enrichment

Biogas, a product of anaerobic digestion of organic matter, is an important renewable energy source. However, for its effective use, in particular as biomethane - an analogue of natural gas, it is necessary to purify it from impurities and increase the concentration of methane. The main undesirable components of biogas are carbon dioxide (CO_2), hydrogen sulfide (H_2S), water (H_2O), as well as trace amounts of nitrogen (N_2), oxygen (O_2), ammonia (NH_3) and siloxanes (Figure 8).

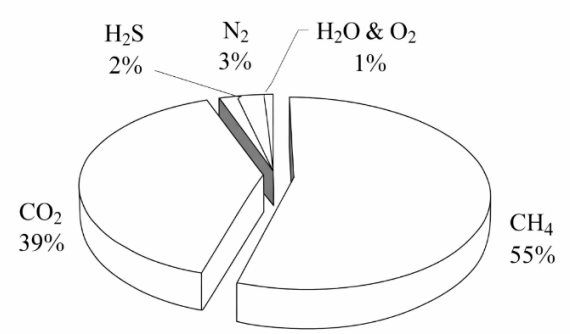

Figure 8. Chemical composition of biogas

The main technologies for cleaning and enriching biogas are: membrane (removal of carbon dioxide, hydrogen sulfide and other impurities); adsorption (purification using activated carbon, zeolites and other adsorbents); cryogenic (separation into methane and carbon dioxide using the method of using low temperatures).

Membrane technologies are one of the most promising and widely used for removing carbon dioxide, hydrogen sulfide and other impurities from biogas. The principle of operation is based on the different permeability of the components of the gas mixture through a selective membrane. Biogas is supplied under pressure to one side of the membrane. Components with higher permeability (for example, CO_2, H_2S, H_2O) pass through the membrane faster than methane (CH_4), which has a lower permeability. Thus, two streams are obtained at the exit of the membrane module: a methane-enriched retentate (product) and a permeate containing separated impurities. Polymer membranes are most commonly used, including polyimide, polysulfone, cellulose acetate, and polydimethylsiloxane. Each type of material has its own advantages and disadvantages in terms of selectivity, permeability, resistance to biogas components, and cost. In recent years, membranes based on inorganic materials (ceramic, metal) and mixed matrix membranes (Mixed Matrix Membranes, MMMs) have been actively developed and researched. Equipment for membrane biogas separation is compact, modular, easy to operate, and easily automated. For most processes, there is no need for chemical reagents (Kramer, 2023).

Disadvantages include the sensitivity of membranes to some impurities (H_2S, siloxanes, heavy hydrocarbons), which may require preliminary purification of biogas; methane losses with permeate (2-15 %); the need for periodic replacement of membrane modules (Aguilloso et al., 2024).

ISSN: 2409-4951 (Online), 2310-1008(Print)

Adsorption technologies are based on the ability of solid porous materials (adsorbents) to selectively absorb certain components of a gas mixture on their surface. Pressure swing adsorption (PSA) or vacuum pressure swing adsorption (VSA) technology is most often used for biogas purification. The PSA process includes four stages: adsorption, desorption (pressure reduction), purging and pressure equalization. Biogas under pressure is passed through a layer of adsorbent, which selectively absorbs CO_2, H_2S, N_2 and water vapor, while methane passes further. After saturation of the adsorbent, the pressure in the column is reduced (or a vacuum is created in the VSA), which leads to the desorption of the absorbed impurities. For continuous operation, several adsorption columns operating in parallel are used.

Types of adsorbents: (a) activated carbon: used to remove H_2S, siloxanes and volatile organic compounds. It has high porosity and a developed surface. Can be treated with special substances to increase selectivity to certain impurities; (b) zeolites (molecular sieves): these are synthetic or natural aluminosilicates with a regular microporous structure. Effective for the removal of CO_2, H_2S, N_2 due to the molecular sieve effect and different strengths of adsorption interaction. The type of zeolite is chosen depending on the size of the molecules to be removed; (c) other adsorbents: metal oxides (e.g. iron oxide for chemisorption of H_2S), silica gels (for desiccation), aluminogels and new materials such as metal-organic frameworks (MOFs), which demonstrate high selectivity and adsorption capacity (Awe at al., 2017).

The use of adsorption technologies ensures the production of high-purity methane (up to 99%), the possibility of simultaneous removal of several impurities and, with proper regeneration, a long service life of the adsorbents. However, their implementation requires relatively high capital costs, regeneration consumes a lot of energy, and some sorbents are sensitive to moisture and heavy hydrocarbons (Awe et al., 2017).

Cryogenic biogas separation technologies are based on the difference in boiling/condensation temperatures of its components. When gradually cooled to low temperatures, components with higher boiling points condense and are separated first. The biogas is first compressed and cleaned of water, H_2S and other impurities that can freeze and block equipment at low temperatures. The gas is then gradually cooled. Carbon dioxide (CO_2) is condensed and separated from methane (CH_4) at temperatures from -35 °C to -85 °C and elevated pressure (depending on the specific process scheme). High purity methane (over 99%) remains in the gaseous phase and can be liquefied (if necessary) by further cooling to approximately -162 °C. In addition, there is the possibility of obtaining a by-product - liquid CO_2, which has commercial value. (Tan et al., 2017). However, high capital and operating costs and significant energy consumption make these technologies cost-effective only for large-scale production.

The choice of the optimal technology for biogas purification and enrichment depends on many factors, including the required degree of methane purity, production volumes, economic indicators and environmental requirements. Often, hybrid systems are used to achieve optimal results, combining the advantages of different technologies. For example, H_2S removal by adsorption before feeding biogas to a membrane or cryogenic plant. Further research and development is aimed at creating more efficient, selective and cost-effective materials and processes for biogas purification.

ISSN: 2409-4951 (Online), 2310-1008(Print)

Conclusions

Methanogenesis is a complex, multifactorial process that can be intensified through the combined optimization of microbial consortia and digester design. Advanced reactor configurations, such as UASB, EGSB, AnMBR, and hybrid biofilm–membrane systems, enhance substrate solids concentration, mass transfer, and biomass retention, leading to shorter hydraulic retention times and higher biogas yields.

The efficiency and stability of methane production are largely determined by the composition and balance of microbial consortia, including methanogenic archaea and syntrophic bacteria. Targeted manipulation of the microbiota—through inoculation strategies, stimulation of direct interspecies electron transfer, and fine-tuning of operational parameters—can significantly improve process resilience and methane yield.

An integrated microbiological–engineering approach has been shown to increase methanogenesis productivity by 20–70%, depending on the type of feedstock. For small-scale biogas systems, simple and robust digester designs that maintain favorable conditions for microbial activity remain particularly important. Future research should focus on molecular-level modeling of microbial communities and the development of intelligent digester control systems to enable precise and adaptive process management.

References

Abouelenien F., Miura T., Nakashimada Y., Elleboudy N., Al-Harbi M., Esma F., Ali E., Shukry M. (2021), Optimization of biomethane production via fermentation of chicken manure using marine sediment: a modeling approach using response surface methodology, *International Journal of Environmental Research,* 18(22), 11988, https://doi.org/10.3390/ijerph182211988

Aguilloso G., Arpia K., Khan M., Sapico Z., Lopez E. (2024), Recent advances in membrane technologies for biogas upgrading, *The 3rd International Electronic Conference on Processes—Green and Sustainable Process Engineering and Process Systems Engineering*, 67(1), 57, https://doi.org/10.3390/engproc2024067057

Alengebawy A., Ran Y., Osman A., Jin K., Samer M., Ai P. (2024), Anaerobic digestion of agricultural waste for biogas production and sustainable bioenergy recovery: a review, *Environmental Chemistry Letters,* 22, pp. 2641–2668, https://link.springer.com/journal/10311

Alipoursarbani M., Tideman J., Loper M, Abendroth C. (2025), Bioaugmentation in anaerobic digesters: a systematic review*, bioRxiv,* Zenodo,1, https://doi.org/10.1101/2025.01.22.634285

Awe O., Zhao Y., Nzihou A., Minh D., Lyczko N. (2017), A review of biogas utilisation, purification and upgrading technologies, *Waste and Biomass Valorization*, 8(2), pp. 267-283, https://hal.science/hal-01619254/file/a-review-of-biogas-utilisation.pdf

Benyahia B., Charfi A., Lesage G., Heran M., Cherki B., Harmand J. (2024), Coupling a simple and generic membrane fouling model with biological dynamics: application to the modeling of an anaerobic membrane bioreactor (AnMBR). *Membranes*, 14(3), 69, https://doi.org/10.3390/membranes14030069

Bueno B., Brito A., Rea V., Kurnianto R., Zaiat M., van Lier J. (2024), Anaerobic membrane bioreactor (AnMBR) with external ultrafiltration membrane for the treatment of sugar beet vinass, *Frontiers in Bioengineering and Biotechnology*, 12, 1491974, https://doi.org/10.3389/fbioe.2024.1491974

ISSN: 2409-4951 (Online), 2310-1008(Print)

Cavaleiro A.J., Joana I., Alves J., Salvador A., Stams M., Madalena J., Alves M. (2023), Editorial: the microbiology of the biogas process, *Frontiers in Microbiology*, 14, 1235624, https://doi.org/10.3389/fmicb.2023.1235624

Chelliapan S., Sallis P.J. (2015), Anaerobic treatment of high sulphate containing pharmaceutical wastewater, *Journal of Scientific & Industrial Research*, 74, pp. 526-530.

Comparetti A., Febo P., Greco C., Orlando S. (2013), Current state and future of biogas and digestate production, *Bulgarian Journal of Agricultural Science,* 19(1), pp. 1-14, https://www.researchgate.net/publication/280882276_Current_state_and_future_of_biogas_and_digestate_production

Costopolou E., Chioti A., Tsioni V., Sfetsas T. (2023), Microbial dynamics in anaerobic digestion: a review of operational and environmental factors affecting microbiome composition and function, *Preprints Friendly Journals,* https://doi.org/10.20944/preprints202306.0299.v1

Das A., Mondal C. (2016), Biogas production from co-digestion of substrates: A review. *International Research Journal of Environment Sciences,* 5(1), pp. 49-57.

DelaVega-Quintero J.C., Nuñez-Pérez J., Lara-Fiallos M., Barba P., Burbano-García J.L., Espín-Valladares R. (2025), Advances and challenges in anaerobic digestion for biogas production: Policy, technological, and microbial perspectives, *Processes*, 13(11), 3648, https://doi.org/10.3390/pr13113648

Douglas W. (2017), Anaerobic digestion of animal manures: Types of digesters, Fact Sheet, *The Oklahoma State University Extension,* BAE-1750

Fischer J., Koss L., Saetta D., Bullard T., Smith A., Yeh D., Roberson L. (2024), Unleashing the power of anaerobic–phototrophic membrane bioreactors for sustainable bioregenerative life support, *53rd International Conference on Environmental Systems ICES-2024-347,* 21-25 July 2024*, Louisville,* Kentucky, USA https://ntrs.nasa.gov/api/citations/20240007366/downloads/ICES-2024-347.pdf?utm_source=chatgpt.com

Foxon K., Pillay S., Lalbahadur T., Rodda N., Holder F., Buckley C. (2007), The anaerobic baffled reactor (ABR): An appropriate technology for on-site sanitation, *Water SA*, 30(5), pp. 44-50, https://doi.org/10.4314/wsa.v30i5.5165

Gao W., Lin H., Leung K., Schormans D., Liao B. (2010), Membrane fouling control in anaerobic membrane bioreactors. *Journal of Membrane Science*, 364(1-2), pp. 183–193, https://doi.org/10.1016/j.memsci.2010.08.011

Ivanov V.N., Stabnikova E., Stabnikov V., Kim I.S., Zubair A. (2002), Effects of iron compounds on the treatment of fat-containing wastewaters, *Applied Biochemistry and Microbiology,* 38(3), pp. 255-258, https://doi.org/10.1023/A:1015475425566

Ivanov V., Stabnikov V., Guo C.H., Stabnikova O., Ahmed Z., Kim I.S., Shuy E.B. (2014), Wastewater engineering applications of BioIronTech process based on the biogeochemical cycle of iron bioreduction and (bio)oxidation, *AIMS Environmental Journal*, 1(2), pp. 53-66, https://doi.org/10.3934/environsci.2014.2.53

Kabaivanova L., Hubenov V., Dimitrov N., Petrova P. (2024), Anaerobic two-phase co-digestion for renewable energy production: Estimating the effect of substrate pretreatment, hydraulic retention time and participating microbial consortia, *Applied Sciences,* 14(12), 5311, https://doi.org/10.3390/app14125311

Koniuszewska I., Korzeniewska E., Harnisz M., Czatzkowska M. (2020), Intensification of biogas production using various technologies: A review, *International Journal of Energy Research*, 44(2), https://doi.org/10.1002/er.5338

Kramer V. (2023), Biogas upgrading technologies and their characteristics, *Thermophysics and Thermal Power Engineering,* 45(1), pp. 64-74, https://doi.org/10.31472/ttpe.1.2023.8

Li Y., Ren Y., Ji J., Li Y., Kobayashi T. (2023), Anaerobic membrane bioreactors for municipal wastewater treatment, sewage sludge digestion and biogas upgrading: A review, *Sustainability*, 15(20), 15129, https://doi.org/10.3390/su152015129

ISSN: 2409-4951 (Online), 2310-1008(Print)

Li H., Mehmood D., Thorin E., Yu Z. (2017), Biomethane production via anaerobic digestion and biomass gasification, *Energy Procedia,* 105, pp. 1172-1177, https://doi.org/10.1016/j.egypro.2017.03.490

Liao B., Kraemer J., Bagley M. (2006), Anaerobic membrane bioreactors: applications and research directions, *Critical Reviews in Environmental Science and Technology*, 36(6), pp. 489–530, https://doi.org/10.1080/10643380600678146

Liu X.Y., Ding H.B., Sreeramachandran S., Stabnikova O., Wang J.Y. (2008), Enhancement of food waste digestion in the hybrid anaerobic solid-liquid system, *Water Science and Technology*, 57(7), pp. 1369–1373, https://doi.org/10.2166/wst.2008.081

Mainardis M., Buttazzoni M., Goi D. (2020), Up-flow anaerobic sludge blanket (UASB) technology for energy recovery: a review on state-of-the-art and recent technological advances, *Bioengineering,* 7(2), 43, https://doi.org/10.3390/bioengineering7020043

Mers S., Sathish-Kumar K., Sánchez-Olmos L., Sánchez-Cardenas M., Caballero-Briones F. (2023), Microbial electrochemical technologies for fuel cell devices. In: Naushad Mu., Saravanan R., Al-Enizi A.M., *New Technologies for Electrochemical Applications*, pp. 83-104, Boca Raton, CRC, https://doi.org/10.1201/9780429200205

Mesquita C., Wu D., Tringe S. (2023), Methyl-based methanogenesis: An ecological and genomic review, *Microbiology and Molecular Biology Reviews,* 87(1), 000024, https://doi.org/10.1128/mmbr.00024-22

Mills S., Cao Q., Wu G. (2024), Microbial ecology of anaerobic digestion, In: *Green Energy and Technology*, pp. 57-81, Springer, Cham, https://doi.org/10.1007/978-3-031-69378-6_4

Mojiri A., Aziz H.A., Zaman N.Q., Aziz S.Q. (2012), A review on anaerobic digestion, bio-reactor and nitrogen removal from wastewater and landfill leachate by bio-reactor, *Advances in Environmental Biology*, 6(7), pp. 2143-2150.

Ning X., Lin R., O'Shea R., Wall D., Deng C., Wu B., Murphy J. (2021), Emerging bioelectrochemical technologies for biogas production and upgrading in cascading circular bioenergy systems, *iScience,* 24(9), 102998, https://doi.org/10.1016/j.isci.2021.102998

Noémi N., Horváth-Gönczi Z., Bagi Z., Szuhaj M., Rákhely G., Kovács K. (2023), Bioelectrochemical systems (BES) for biomethane production — Review, *Fermentation*, 9(7), 610, https://doi.org/10.3390/fermentation9070610

Paes J., Guimarães C., Gomes A., Valadão R., Cecchin D., Menino R. (2025), Circularity between aquaponics and anaerobic digestion for energy generation, *AgriEngineering,* 7(5), 129, https://doi.org/10.3390/agriengineering7050129

Pal A., Tripathi V., Kumar P., Kumar P. (2021), *Biomethane: Developments and Prospects*, Apple Academic Press, *Palm Bay, Florida,* USA, https://doi.org/10.1002/9781119717317.ch12

Piercy E., Sun X., Ellis P., Taylor M., Guo M. (2025), Temporal dynamics of microbial communities in anaerobic digestion: influence of temperature and feedstock composition on reactor performance and stability, *Water Research,* 284, 123974, https://doi.org/10.1101/2025.01.12.632589

Quin S., Chen L., Xu S., Zeng C., Lian X., Xia Z., Zou J. (2025), Research on methane-rich biogas production technology by anaerobic digestion under carbon neutrality: a review, *Sustainability,* 17(4), 1425, https://doi.org/10.3390/su17041425

Rodrigues B., Mello B., Grangeiro L., Dusan K., Sarti A. (2024), The most important technologies and highlights for biogas production worldwide, *Journal of the Air and Waste Management Association*, 75, pp. 87–108, https://doi.org/10.1080/10962247.2024.2393192

Siroka A., Detman A., Mielecki D., Chojnacka A., Btazczyk M. (2018), Searching for metabolic pathways of anaerobic digestion: A useful list of the key enzymes, In: J.R. Banu (Ed.), *Anaerobic Digestion*, IntechOpen, London, United Kingdom, https://doi.org/10.5772/intechopen.81256

ISSN: 2409-4951 (Online), 2310-1008(Print)

Song C., Li W., Cai F., Liu G., Chen C. (2021), Anaerobic and microaerobic pretreatment for improving methane production from paper waste in anaerobic digestion, *Frontiers in Microbiology*, 12, https://doi.org/10.3389/fmicb.2021.688290

Stabnikov V.P., Ivanov V.N. (2006), The effect of various iron hydroxide concentrations on the anaerobic fermentation of sulfate-containing model wastewater, *Applied Biochemistry and Microbiology*, 42(3), pp. 284 – 288, https://doi.org/10.1134/S0003683806030112

Stabnikova O., Liu X.Y., Wang J.Y. (2008a), Anaerobic digestion of food waste in a hybrid anaerobic solid-liquid system with leachate recirculation in an acidogenic reactor, *Biochemical Engineering Journal*, 41(2), 198–201, https://doi.org/10.1016/j.bej.2008.05.008

Stabnikova O., Liu X.Y., Wang J.Y. (2008b), Digestion of frozen/thawed food waste in the hybrid anaerobic solid–liquid system, *Waste Management*, 28(9), pp. 1654-1659, https://doi.org/10.1016/2007.05.021j.wasman

Stuckey D. (2012), Recent developments in anaerobic membrane reactors. *Bioresource Technology*, 122, pp. 137–148, https://doi.org/10.1016/j.biortech.2012.05.138

Surendra K., Takara D., Hashimoto A., Khanal S. (2020), A review of anaerobic digestion systems for biodegradable waste: Configurations, operating parameters, and current trends, *Environmental Engineering Research*, 25(1), pp. 1-17, https://doi.org/10.4491/eer.2018.334

Tang H., Tang C., Luo H., Wu J., Wu J., Wang J., Jin L., Sun D. (2023), Study on the effect of two-phase anaerobic co-digestion of rice straw and rural sludge on hydrogen and methane production, *Sustainability*, 15(22), 16112, https://doi.org/10.3390/su152216112

Tan Y., Nookuea W., Li H., Thorin E. (2017), Cryogenic technology for biogas upgrading combined with carbon capture - a review of systems and property impacts, *Energy Procedia*, 142, pp. 3741-3746, https://doi.org/10.1016/j.egypro.2017.12.270

Tay J.H., Tay S.T.L., Ivanov V., Stabnikova O., Wang J.Y. (2006), Singapore Patent 106658, Compositions and methods for the treatment of wastewater and other waste.

Tay J.H., Tay S.T.L., Ivanov V., Stabnikova O., Wang J.Y. (2008), US Patent 7 393452, Compositions and methods for the treatment of wastewater and other waste.

van Lier J.B. (2006), Anaerobic industrial wastewater treatment; Perspectives for closing water and resource cycles, https://edepot.wur.nl/39480

van Lier J., van der Zee F., Frijters C., Ersahin M. (2015), Celebrating 40 years anaerobic sludge bed reactors for industrial wastewater treatment, *Reviews in Environmental Science and Bio/Technology*, 14, pp. 681–702, https://doi.org/10.1007/s11157-015-9377-z

Wang J.Y., Zhang H., Stabnikova O., Tay J.H. (2003), Removal of ammonia in a modified two-phase food waste anaerobic digestion system coupled with an aerated submerged biofilters, *Waste Management and Research*, 21(6), pp. 527–534, https://doi.org/10.1177/0734242X0302100605

Wang J.Y., Zhang H., Stabnikova O., Ang S.S., Tay J.H. (2005a), A hybrid anaerobic solid-liquid (HASL) system for food waste digestion, *Water Science and Technology*, 52(1-2), pp. 223–228, https://doi.org/10.2166/wst.2005.0521

Wang J.Y., Zhang H., Stabnikova O., Tay J.H. (2005b), Comparison of lab-scale and pilot-scale hybrid anaerobic solid-liquid systems operated in batch and semi-continuous modes, *Process Biochemistry*, 40(11), pp. 3580–3586, https://doi.org/10.1016/j.procbio.2005.03.047

Ward A., Hobbs P., Holliman P., Jones D. (2008), Optimization of the anaerobic digestion of agricultural resources, *Bioresource Technology,* 99, pp. 7928–7940, https://doi.org/10.1016/j.biortech.2008.02.044

Yankovska K., Syrotyuk H., Syrotyuk S., Konieczny R. (2018), Unit cost of energy, obtained by the methane fermentation technology of agricultural biomass conversion, In: Renewable Energy Sources: Engineering, Technology, Innovation, pp. 241-251, Springer International Publishing. Zhu Z., Blanco E., Bhatti M., Borrion A. (2021), Impact of

ISSN: 2409-4951 (Online), 2310-1008(Print)

metallic nanoparticles on anaerobic digestion, *Science of The Total Environment*, 757, 143747, https://doi.org/10.1016/j.scitotenv.2020.143747
Zhadan S., Shapovalov Y., Salyuk A., Usenko S. (2023). Bioconversion of poultry waste into clean energy. In: O. Stabnikova, O. Shevchenko, V. Stabnikov, O. Paredes-López (Eds.), Bioconversion of Waste to Value-Added Products (pp. 221-243), CRC Press, Boca Raton, London, New York, https://doi.org/10.1201/9781003329671-8

Author identifiers ORCID
Oleksandr Vorontsov 0009-0005-1944-6947
Viktor Stabnikov 0000-0003-3738-8056

Cite:

Ukr J Food Sci Style

Vorontsov O., Stabnikov V. (2025), Biotechnological approaches and strategies for intensification of metanogenesis, *Ukrainian Journal of Food Science*, 13(2), pp. 186–210, https://doi.org/10.24263/2310-1008-2025-13-2-7

APA Style

Vorontsov, O., & Stabnikov, V. (2025). Biotechnological approaches and strategies for intensification of metanogenesis. *Ukrainian Journal of Food Science, 13*(2), 186–210. https://doi.org/10.24263/2310-1008-2025-13-2-7

Influence of chickpea flour sourdough on technological properties and quality of bakery products

Yevgen Godunko, Yuliia Bondarenko

National University of Food Technologies, Kyiv, Ukraine

Keywords:

Bread
Chickpea
Seeds
Flour
Sourdough
Lactic acid bacteria
Fermentation

Article history:

Received 01.10.2025
Received in revised form 20.12.2025
Accepted 31.12.2025

Corresponding author:

Yuliia Bondarenko
E-mail: bjuly@ukr.net

DOI:
10.24263/2310-1008-2025-13-2-8

Abstract

Introduction. To address the limited biological value of refined wheat bread, this study investigated the technological properties of chickpea flour sourdoughs prepared with selected lactic acid bacteria and their effects on the quality of wheat bakery products.

Materials and methods. Chickpea sourdoughs were prepared from chickpea flour and water (1:1) and inoculated with *Lactiplantibacillus plantarum*, *Lentilactobacillus buchneri*, and their mixed culture, followed by fermentation at 32–35 °C. Sourdough acidity and microbial activity were determined, and wheat bread quality was evaluated based on key technological, physicochemical, and sensory parameters in triplicate experiments.

Results and discussion. Chickpea sourdough fermentation was characterized by a slow initial increase in acidity followed by a sharp rise between 7 and 10 h, reflecting the adaptation and activation of lactic acid bacteria. Maximum microbial activity was observed after 14–16 h of fermentation, whereas further prolongation led to excessive acidification and deterioration of technological properties. Sourdoughs fermented with Lactobacillus buchneri exhibited the highest acidification and gas-forming capacity, indicating intense metabolic activity but with an increased risk of excessive acidity. In contrast, Lactobacillus plantarum showed lower activity under conditions of limited fermentable sugars, resulting in a milder and more neutral aromatic profile but less uniform crumb porosity in the final bread. The use of a mixed starter culture ensured balanced acidification and stable microbial activity. Bread produced with mixed-culture sourdough demonstrated the highest specific volume, improved crumb structure, and superior sensory characteristics. The optimal conditions for chickpea sourdough preparation were identified as 14–16 h of fermentation at 32–35 °C, under which high lactic acid bacteria activity was achieved at a moderate final acidity of 12–16°.

Conclusions. Chickpea flour sourdoughs prepared with selected lactic acid bacteria significantly influenced fermentation behavior and bread quality, with an optimal fermentation time of 14–16 h. A mixed culture of *Lactiplantibacillus plantarum* and *Lentilactobacillus buchneri* provided the most balanced technological and sensory properties, indicating its potential for producing wheat bread enriched with chickpea flour.

ISSN: 2409-4951 (Online), 2310-1008(Print)

Introduction

Analysis of the current bakery assortment reveals a predominance of products manufactured from refined wheat flour of the highest and first grades. Such products are characterized by limited biological value due to an unbalanced amino acid composition, particularly lysine deficiency, as well as a low content of dietary fiber (Buyalska et al., 2020).

With the growing consumer demand for foods with enhanced biological value and functional properties, the incorporation of non-traditional raw materials into bakery production has become increasingly important (Guiné and Florença, 2024; Stabnikova et al., 2021). Numerous studies have focused on enhancing the quality of bread and flour-based confectionery products through the partial replacement of wheat flour with plant ingredients rich in dietary fiber and bioactive compounds (Chochkov et al., 2022; Perea-Escobar et al., 2025; Sanfilippo et al., 2023; Shevchenko et al., 2023; Stabnikova et al., 2022).

In this context, the application of legume flours in bakery technology represents a promising approach to improving the nutritional and biological quality of bakery products, in line with current food industry trends focused on health-oriented foods (Sadohara et al., 2022; Stabnikova and Paredes-López, 2024).

One of the most promising types of legume raw materials for the enrichment of bakery products is chickpea flour (Shrivastava and Chakraborty, 2018; Xing et al., 2021). Chickpeas typically contain 19–29 g of protein per 100 g, which is more than twice the amount found in cereal grains. Of particular value is the high content of lysine, an essential amino acid that is deficient in wheat flour. In addition, chickpeas are rich in dietary fiber, the content of which may exceed 20 g/100 g depending on the biotype, as well as in unsaturated fatty acids such as linoleic and oleic acids. Chickpea flour is also characterized by a low glycemic index (Santos et al., 2018; Wang et al., 2021).

Partial replacement of wheat flour with chickpea flour in bread formulations improves the nutritional value of the product due to increased contents of dietary fiber and protein, as well as amino acid complementation between legumes and cereals. However, the incorporation of chickpea flour into bread formulations also leads to technological challenges, manifested by a reduction in loaf volume, deterioration of crumb texture, and the appearance of a characteristic legume flavor. In wheat bread formulations containing chickpea flour, it is advisable to limit the replacement level to up to 10% of wheat flour. At this level of substitution, the dough, despite reduced extensibility, is characterized by good resistance to mechanical stress. Higher levels of chickpea flour addition result in increased dough stickiness and decreased dough stability, leading to bread with a firmer crumb and a significantly reduced volume (Boukid et al., 2019; Ouazib et al., 2016). Such effects of chickpea flour are primarily due to a reduction in gluten content in the dough as a result of partial replacement of wheat flour, and secondarily to conformational changes in gluten proteins associated with a significant increase in β-sheet structures within the protein matrix (Kotsiou et al., 2022; Mohammed et al., 2012).

Chickpea flour, similarly, to flours derived from other legumes, contains a range of antinutritional compounds, including oligosaccharides (raffinose, stachyose), phytic acid, and trypsin inhibitors, which may negatively affect nutrient absorption and cause undesirable physiological responses such as flatulence. To reduce the content of these antinutritional compounds, the application of pretreatment methods to legume raw materials is considered advisable when they are used in bakery production. For this purpose, processes such as fermentation, soaking, and germination are commonly applied. Fermentation of raw materials in the form of sourdoughs is regarded as the most effective approach for improving their nutritional profile, owing to a reduction in antinutrient concentration and enhanced bioavailability of macro- and micronutrients (Kahala et al., 2021; Kaur and Prasad, 2021).

ISSN: 2409-4951 (Online), 2310-1008(Print)

In breadmaking, sourdoughs based on wheat or rye flour are traditionally used. The use of sourdoughs prepared from non-traditional crops represents a promising direction in the development of baking technologies, providing a range of functional and technological advantages (Cheliabiieva and Sosedova, 2018; Conte, 2018).

Advances in sourdough biotechnology highlight the functional roles of lactic acid bacteria and yeast and their symbiotic interactions, resulting in a complex microbial ecosystem that maximizes the use of flour components (Arora et al., 2021). Additionally, the establishment of a mature and functional sourdough is influenced by several factors, including flour type, water, additional ingredients (Gobbetti et al., 2016), enzymatic activity (Ercolini et al., 2013), and fermentation conditions (De Vuyst et al., 2014; Minervini et al., 2014). Among these factors, the type of flour used is considered a critical determinant (Pontonio et al., 2017; Rizzello et al., 2016).

The integration of legume fermentation processes into modern breadmaking is predominantly achieved through the use of spontaneously fermented sourdoughs Mykhonik and Hetman, 2022). However, in industrial bakery production, the application of spontaneously fermented sourdoughs has certain limitations. Such sourdoughs are characterized by slower and less predictable fermentation dynamics, which largely depend on environmental conditions, including temperature, humidity, and raw material composition. Moreover, during their maintenance, there is an increased risk of contamination by undesirable microorganisms, which may adversely affect the quality and stability of the final product (Arora et al., 2021).

In contrast, inoculated sourdoughs obtained by the addition of specifically selected yeast and lactic acid bacteria strains provide a higher level of control over the fermentation process. This approach enables faster and more reproducible fermentation, reduces the risk of microbiological contamination, and enhances the technological safety and stability of the process. Consequently, inoculated sourdoughs are particularly effective under industrial conditions, where consistent process parameters and controlled fermentation times are required (Lima et al., 2023).

Fermentation — both spontaneous (Type-I) and guided by selected lactic acid bacteria (Type-II) has been shown to improve the nutritional profile of legumes by degrading anti-nutritional factors and enhancing protein digestibility, fiber bioavailability, and phenolic compounds (Curiel et al., 2015; Gobbetti et al., 2019; Rizzello et al., 2017; Schettino et al., 2019). Moreover, fermentation positively affects the technological and sensory properties of legume flour, promoting their use in industrial applications.

Fermentation of chickpea flour using selected lactic acid bacteria strains is an effective biotechnological approach for the targeted modification of its nutritional, biological, and functional–technological properties. The application of *Lactiplantibacillus plantarum* (formerly *Lactobacillus plantarum*), *Limosilactobacillus fermentum*, *Pediococcus pentosaceus*, and *Levilactobacillus brevis* ensured active microbial development in the chickpea flour substrate and intensive acidification, resulting in a pH decrease from 6.2–6.5 to 4.0–4.5 after 24–48 h of fermentation at approximately 30 °C. The reduction in pH, combined with the proteolytic activity of lactic acid bacteria, leads to partial hydrolysis of chickpea proteins, manifested by an increased content of free amino acids and low-molecular-weight peptides. The most pronounced proteolytic effect was observed when *Lactiplantibacillus plantarum* was used, indicating its high potential for improving the digestibility and biological value of plant protein. At the same time, the degradation of protein–polyphenol complexes was observed, which limit amino acid availability in non-fermented chickpea flour. A significant outcome of lactic acid fermentation is the reduction of antinutritional compounds, particularly phytic acid, whose content decreases by 40–60% depending on the strain applied. This effect is attributed to the activation of endogenous chickpea phytases under acidic conditions, as well as

ISSN: 2409-4951 (Online), 2310-1008(Print)

to the phytase activity of certain lactic acid bacteria strains, primarily *Lactiplantibacillus plantarum* and *Pediococcus pentosaceus*. This leads to increased bioavailability of mineral elements, particularly iron, zinc, and calcium. In addition, fermentation contributes to the partial inactivation of protease inhibitors and a reduction in the content of raffinose and stachyose oligosaccharides. Lactic acid fermentation also has a positive effect on the antioxidant properties of chickpea flour. This is associated with the release of phenolic compounds from their bound forms as a result of enzymatic transformations, which further enhances the functional value of the product (Chiacchio et al., 2025; Di Biase et al., 2019; Sáez et al., 2022).

Thus, lactic acid fermentation is an effective biotechnological tool for modifying the protein and mineral composition of chickpea flour, reducing the content of antinutritional factors, and improving its technological properties. Fermented chickpea flour can therefore be considered a promising ingredient for the development of functional bakery products. At the same time, the use of chickpea flour fermented with selected lactic acid bacteria strains in breadmaking technology requires further investigation of the technological properties of chickpea sourdough and its influence on the quality characteristics of the finished products.

Materials and methods

Materials

Pure cultures of lactic acid bacteria *Lactiplantibacillus plantarum* (formerly *Lactobacillus plantarum*) UKM B-2694 (hereinafter *L. plantarum*) and *Lentilactobacillus buchneri* (formerly *Lactobacillus buchneri*) UKM B-2666 (hereinafter L. *buchneri*), obtained from the Ukrainian Collection of Microorganisms of the D.K. Zabolotny Institute of Microbiology and Virology of the National Academy of Sciences of Ukraine, were used for the preparation of chickpea sourdough. Chickpea flour (TM "Sto Pudov") with an initial acidity of 10° was used for dough preparation.

Preparation of chickpea sourdough samples

During the study, three sourdough samples were prepared and inoculated with different lactic acid bacteria cultures: sample 1 - *L. buchneri*; sample 2 - *L. plantarum*; sample 3 - a mixed culture of *L. plantarum* and *L. buchneri*.

To prepare the sourdough, chickpea flour and water at a temperature of 30–32 °C were mixed at a ratio of 1:1, and 1 ml of a suspension of lyophilized lactic acid bacteria culture was added per 100 g of the water–flour mixture (Table 1).

Table 1

Formulation for chickpea sourdough preparation

Raw material	Sample 1	Sample 2	Sample 3
Chickpea flour, g	100.0	100.0	100.0
Water, g	100.0	100.0	100.0
Pure culture of *L. buchneri*, ml	2.0	-	1.0
Pure culture of *L. plantarum*, ml	-	2.0	1.0

The samples were fermented at 32–35 °C. During fermentation, the acidity of the sourdough and the activity of lactic acid bacteria were monitored periodically.

ISSN: 2409-4951 (Online), 2310-1008(Print)

Preparation of dough samples

Wheat bread was baked with the addition of 10% chickpea flour (control) as a partial replacement for wheat flour. Experimental samples were prepared with the addition of chickpea sourdough containing the same amount of chickpea flour as in the control sample. Dough mixing was performed using an ESHER dough mixer (Italy) at first speed for 4–6 min and at second speed for 6–8 min. The initial dough temperature was 25–26 °C. The dough was left to ferment for 90 min at a temperature of 30–32 °C. After fermentation, dough pieces were shaped and placed in a proofing chamber (Sveba Dahlin AB DC-21, Sweden) at 35–38 °C, after which they were baked in a deck oven (Sveba Dahlin AB DC-21, Sweden) at 210–230 °C for 30–35 min.

Methods

Sourdough acidity. A 5 g sample of sourdough was triturated with 50 ml of distilled water in a porcelain mortar until a homogeneous suspension was obtained. Subsequently, 3–5 drops of a 1% alcoholic phenolphthalein solution were added, and the suspension was titrated with 0.1 mol/l NaOH until a pale pink coloration persisted for 20–30 s. The acidity value was calculated by multiplying the volume of 0.1 mol/l NaOH consumed by 2 (Godunko et al., 2024).

Lactic acid bacteria activity. A 20 g sample of sourdough was mixed with 40 ml of water at 40 °C until a homogeneous suspension was obtained. From this suspension, 10 ml aliquots were transferred into two test tubes. To the test sample, 1 ml of a 0.05% aqueous methylene blue solution was added, while the second test tube served as a control. The tubes were incubated at 40 °C.

The activity of lactic acid bacteria was assessed based on the time (in minutes) required for decolorization of the test sample. Activity was classified as low when decolorization occurred within 90–100 min, high at 35–50 min, and very high at 7–25 min (Godunko et al., 2024).

Specific volume of bread. Bread volume was determined using the traditional rapeseed displacement method. Measurements were performed in duplicate, and deviations between parallel determinations did not exceed 5%. The specific volume of bread was calculated by dividing the loaf volume by its weight and expressed to the nearest 0.01 ml/g (Zhu et al., 2016).

Porosity of bread. The porosity of bread reflects the volume of the pores in a certain volume of the crumb, expressed as a percentage to the total volume (Verheyen et al., 2015).

Bread shape stability (H/D). The height and diameter of hearth bread were measured using a ruler or a specialized measuring device. The shape stability index (H/D) was calculated as the ratio of product height (H) to product diameter (D) (Drobot et al., 2015).

Bread crumb moisture content. Two metal weighing dishes were each loaded with 5 g of ground bread crumb. The dishes containing the crumb were placed in a drying oven (SESh-3M) and dried for 45 min at a temperature of 130 °C. After drying, the dishes were transferred to a desiccator and cooled for 20–120 min. The cooled dishes were then weighed, and the mass fraction of moisture in the bread crumb was calculated (Drobot et al., 2015):

ISSN: 2409-4951 (Online), 2310-1008(Print)

$$W = ((m_1 - m_2)/m) \times 100\%,$$

where m is the mass of the bread crumb sample before drying; m_1 is the mass of the box with the sample before drying; m_2 is the mass of the box with the sample after drying.

Crust and crumb color of bread. The bread slice crumb and crust colour were analysed using a colorimeter Chroma meter CR-200 (Minolta, Osaka, Japan). Three colour-coordinates were recorded: (1) $L*$ (dark-light); (2) $a*$ (green-red) and (3) $b*$ (blue-yellow) as well as the total colour difference ($\Delta E*$) which was subsequently recorded to understand human perceivable differences (e.g., less than one: non-perceivable differences, one to three: minor perceivable differences and more than three: perceivable differences) (Norton et al., 2025):

$$\Delta E = \sqrt{(L^* - L_0^*)^2 + (a^* - a_0^*)^2 + (b^* - b_0^*)^2},$$

where L_0*, a_0*, and b_0* are the color parameters of the control sample, and L*, a*, and b* are those of the experimental sample. Each parameter was measured at five different points, and the mean value was used for calculations.

Statistical analysis

The reliability of the obtained results was ensured by performing the experiments in triplicate. The experimental data were subjected to statistical analysis using standard Microsoft Office software packages.

Results and discussions

Chickpea sourdough development using pure cultures of lactic acid bacteria

The study of the dynamics of acidity accumulation, as the main indicator characterizing sourdough maturation, showed that at the initial stage of sourdough development the accumulation of acidity in all sourdough samples occurred slowly and uniformly. The data on acidity accumulation in the sourdough samples are presented in Table 2.

Table 2

Acidity of sourdoughs during fermentation, degrees

Fermentation time, h	Sample 1 (*L. buchneri*)	Sample 2 (*L. plantarum*)	Sample 3 (mixture of *L. plantarum* and *L. buchneri*)
0	5.0	5.0	5.0
4	6.0	6.0	6.0
7	7.0	7.0	7.0
10	12.0	11.8	12.0
14	15.0	14.0	15.0
16	16.0	14.7	15.5
24	25.5	23.0	25.0

ISSN: 2409-4951 (Online), 2310-1008(Print)

During the first four hours of fermentation, an increase of 1 degree of acidity was observed in all sourdough samples. Further evaluation of acidity during sourdough fermentation showed that a significant increase in acidity occurred after seven hours of fermentation: in the period from 7 to 10 h of fermentation, that is, over three hours, the acidity increased by 5 degrees. After the 10th hour of fermentation, a change in the dynamics of acidity accumulation was observed. In the sourdough samples containing lactic acid bacteria *L. buchneri* and the mixed culture of *L. buchneri* and *L. plantarum*, acidity accumulation proceeded similarly, whereas in the sourdough containing *L. plantarum* the acidity at 14 h of fermentation reached 14 degrees, which was 1 degree lower than in the other samples. At 16 h of fermentation, the acidity in the sourdough sample containing *L. plantarum* was also lower than in the sample containing *L. buchneri* (by 1.3 degrees); a slightly lower rate of acidity accumulation was also observed in the sample containing the mixed culture of lactic acid bacteria.

Fermentation of the sourdough for 24 h demonstrated the preservation of the differences in acidity development among the samples. After 24 h, sourdoughs with high acidity values in the range of 23.0–25.5 degrees were obtained. Considering the aim of the study to obtain chickpea sourdough suitable for bread production with a lower acidity level, a parallel investigation of the activity of lactic acid bacteria in these sourdoughs was conducted. The results of this investigation are presented in Table 3.8.

Determination of the activity of lactic acid bacteria in the experimental sourdoughs showed that high and very high activity levels were reached after 14–16 h of fermentation. Prior to this time, the activity of lactic acid bacteria in the sourdoughs remained low.

During the study, it was found that in sourdoughs inoculated with *L. buchneri* and with the mixed culture of *L. buchneri* and *L. plantarum*, the activity of lactic acid bacteria was very high, whereas in the sourdough sample inoculated with *L. plantarum* the activity was high; moreover, the duration of indicator discoloration during the analysis of this sourdough was twice as long as in the other samples.

Table 3

Activity of lactic acid bacteria in sourdoughs during fermentation

Fermentation time, h	**Sample 1 (*L. buchneri*)**	**Sample 2 (*L. plantarum*)**	**Sample 3 (mixture of *L. plantarum* and *L. buchneri*)**
4	>100 min	>100 min	>100 min
7	>100 min	>100 min	>100 min
10	70-100 min (low)	70-100 min (low)	70-100 min (low)
14	21 min (very high)	48 min (high)	24 min (very high)
16	18 min (very high)	40 min (high)	21 min (very high)

The observed differences in the activity of lactic acid bacteria may be attributed to the different adaptability of these cultures to the chickpea flour substrate and to differences in their metabolic fermentation mechanisms. Chickpea flour contains a limited amount of sugars required for the growth and metabolic activity of *L. plantarum* strains. In particular, chickpea flour contains 0.05–0.2% glucose, 0.02–0.15% fructose, 0.3–1.2% sucrose, and 0.05–0.3% maltose. When the content of fermentable sugars in the sourdough is low, *L. plantarum* bacteria reduce their activity, in contrast to *L. buchneri*, which are heterofermentative cultures capable of metabolizing other nutrients.

ISSN: 2409-4951 (Online), 2310-1008(Print)

In addition, *L. buchneri* bacteria produce acetic acid as a result of fermentation processes, in contrast to *L. plantarum*, which predominantly produce lactic acid. This also contributes to the formation of higher acidity values (Di Biase et al., 2019). In the sourdough sample obtained using a combination of these two cultures, the lower activity of *L. plantarum* is compensated by the activity of *L. buchneri*, which promotes the achievement of acidity and lactic acid microbiota activity at a level comparable to that of the sample containing *L. buchneri* alone.

Chickpea flour is characterized by a relatively low content of simple sugars available for lactic acid fermentation, the total amount of which, according to literature data, does not exceed 0.4–1.8% of dry matter. The major proportion of carbohydrates is represented by raffinose-family oligosaccharides, which cannot be directly utilized by most lactic acid bacteria (Begum et al., 2023). The limited availability of fermentable sugars, combined with the high buffering capacity of chickpea raw material, determines the specific features of sourdough acidification and may explain the lower titratable acidity values observed in sourdoughs inoculated with homofermentative cultures of *L. plantarum*.

Therefore: (1) the duration of chickpea sourdough development using pure cultures of *L. plantarum* and *L. buchneri* was 14–16 h at 32–35 °C; (2) the final acidity of mature sourdoughs was 13–16 ° for sourdoughs inoculated with *L. buchneri*, 12–15 ° for sourdoughs inoculated with *L. plantarum*, and 13–16 ° for sourdoughs inoculated with the combined culture of *L. plantarum* and *L. buchneri*; (3) lactic acid bacteria activity at this stage was high or very high: very high for sourdoughs with *L. buchneri*, high for sourdoughs with *L. plantarum*, and very high for sourdoughs with the combined culture; (4) the mature sourdough exhibited the appearance of a well-aerated, loose mass.

It should be noted that the transformation of sourdough consistency into such a loosened structure occurred from the 14th hour of fermentation, since sensory evaluation at the 12th hour of fermentation indicated that the sourdough was still a rather viscous, flowable mass. Comparative visual evaluation of the consistency and appearance of the sourdoughs showed that, in the case of fermentation with *L. buchneri*, the sourdough exhibited the loosest and most aerated consistency, containing a large number of large gas cells in its structure. This is due to the fact that, in addition to organic acids, *L. buchneri* actively produce carbon dioxide. The sourdough sample prepared using *L. plantarum* had a less loose consistency; the gas cells in its structure were smaller in size and fewer in number, and the overall consistency was denser, since these bacteria predominantly produce lactic acid and only very small amounts of carbon dioxide. The sourdough sample prepared with the mixed culture of lactic acid bacteria exhibited a consistency similar to that of the *L. buchneri* sample; however, the gas cells were smaller, resulting in a lower degree of aeration. This effect was expected considering the influence of *L. plantarum* on sourdough consistency; thus, this sample occupied an intermediate position between the two above-mentioned sourdoughs.

The obtained mature sourdoughs were evaluated based on sensory characteristics (Table 4).

According to the sensory evaluation, the aroma of all sourdoughs was acceptable for this type of semi-finished product, with no signs of unpleasant odors; the aroma characteristics were within the range typical of sourdough products. It was established that the sourdough fermented with *L. buchneri* exhibited a pleasant alcoholic–acidic aroma, with slight fruity notes reminiscent of apple and legume nuances. The sourdough fermented with *L. plantarum* was characterized by a lactic aroma with pronounced legume notes. The sourdough prepared with the mixed culture exhibited the most intense and complex aroma, which was more difficult to characterize: a distinct alcoholic–acidic character with lactic acid notes was perceived, along with a slight aroma reminiscent of sauerkraut; legume notes similar to green pea aroma were also detected.

ISSN: 2409-4951 (Online), 2310-1008(Print)

Table 4

Quality indicators of chickpea sourdoughs

Indicator	Sample 1 (*L. buchneri*)	Sample 2 (*L. plantarum*)	Sample 3 (mixture of *L. plantarum and L. buchneri*)
Initial acidity, degrees	5.0	5.2	5.2
Final acidity, degrees	15.6	14.2	15.0
Aroma	Alcoholic–acidic with slight fruity notes; faint legume aroma	Pronounced lactic aroma initially, followed by the development of a chickpea–nutty aroma, more intense than in the *L. buchneri* sample	More intense than in the other samples; immediately perceived alcoholic–acidic aroma combined with lactic and slight sauerkraut notes, followed by chickpea–nutty notes
Taste	Sour, with a slight legume aftertaste	Sour, the perception of acidity diminishes rapidly, with a legume aftertaste	The sourest among all samples; no lingering aftertaste

Thus, it was established that the selected lactic acid bacteria cultures ensure the fermentation of chickpea flour during sourdough preparation and, within 14–16 h of fermentation of the semi-finished product, promote the production of a sourdough characterized by high lactic acid bacteria activity. However, this activity is not sufficient for the sourdough to fully perform the function of a leavening agent in the dough system. Therefore, when using these sourdoughs, it is advisable to include compressed yeast in the formulation of bakery products, while the sourdoughs will primarily serve as acidifying agents and carriers of aromatic compounds.

Effect of chickpea sourdoughs inoculated with different lactic acid bacteria strains on bread quality

Considering the technological recommendations for the preparation of chickpea sourdoughs established above, it became necessary to investigate the effect of sourdoughs produced under these conditions on the quality of wheat bread. The results of the analysis are presented in Table 5.

Figures 1 and 2 present the baked products: the control sample, the sample with the addition of chickpea flour, and the sample with the addition of sourdough.

According to the research results, the bread containing chickpea flour exhibited medium and fine porosity with pore walls of medium thickness. The crumb was elastic. In all samples containing sourdough, an increase in crumb elasticity was observed, and the crumb acquired a more cream-colored appearance.

ISSN: 2409-4951 (Online), 2310-1008(Print)

Table 5

Sensory and physicochemical characteristics of the bread

Parameter	Control with chickpea flour	*L. buchneri* sourdough	*L. plantarum* sourdough	Mixture of *L. plantarum* and *L. buchneri*
Shape	Regular, without cracks	Regular, without cracks	Regular, without cracks	Regular, without cracks
Surface	Smooth	Smooth	Smooth	Smooth
Crust color	Dark golden	Golden	Dark golden	Golden
Crumb characteristics	Cream-colored; non-uniform porosity, predominantly medium with inclusions of large pores; medium cell wall thickness; elastic	Cream-colored; non-uniform medium porosity; medium cell wall thickness, with inclusions of large pores; more elastic than the control	Cream-colored; uniform medium porosity; medium cell wall thickness; more elastic than the *L. buchneri* sample	Cream-colored; non-uniform fine porosity; thick cell walls, with inclusions of medium and large pores; more elastic than the *L. buchneri* and *L. plantarum* samples
Taste	Slight legume aftertaste	Slight acidity perceived at the beginning of mastication; very mild legume flavor; pleasant aftertaste	Less sour than the *L. buchneri* sample; legume flavor more pronounced	Slight sourness perceived at the beginning of mastication; flavor more harmonious and pleasant than in the *L. buchneri* sample
Aroma	More pronounced legume aroma	Acidic, with almost imperceptible legume notes	Less intense, with slight acidity and somewhat legume notes	More intense aroma with pronounced acidity
Moisture, %	42.6	42.3	42.2	42.4
Acidity, degrees	1.8	2.8	2.2	2.8
Porosity, %	67	66	67	69
Specific volume, ml/g	2.5	2.3	2.5	2.8
Shape stability, H/D	0.44	0.44	0.38	0.42

ISSN: 2409-4951 (Online), 2310-1008(Print)

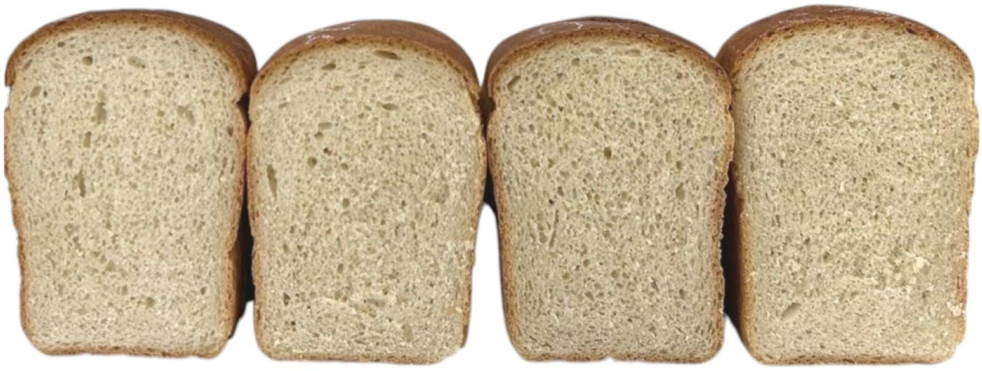

Control with chickpea flour | With *L. buchneri* sourdough | With *L. plantarum* sourdough | With *L. buchneri* + *L. plantarum* sourdough

Figure 1. Pan bread products

Control with chickpea flour | With *L. buchneri* sourdough | With *L. plantarum* sourdough | With *L. buchneri* + *L. plantarum* sourdough

Figure 2. Free-standing bread

In breads prepared with *L. buchneri* sourdough and with the mixed culture, the crumb structure became finer compared to the control, with the formation of pore walls of medium thickness. In breads prepared with *L. plantarum* sourdough, the porosity was markedly non-uniform, predominantly fine, with thicker pore walls and inclusions of large pores.

The control bread was characterized by a pleasant wheat bread aroma with slight notes of legume flour. In samples containing sourdough, the aroma was pleasant and more pronounced. Despite the use of an accelerated dough preparation method, the aroma of the products was rich, resembling that obtained by a long fermentation process. In breads with sourdough, a slight acidic aftertaste was perceived, while legume notes were not detected. The crumb of bread prepared with *L. plantarum* sourdough was coarser during mastication. Based on sensory evaluation, the breads prepared with *L. buchneri* sourdough and with the mixed-culture sourdough were more attractive.

To ensure a more objective evaluation of the color characteristics of the breads (crust and crumb), the colorimetric method in the CIELab system was applied (Table 6).

ISSN: 2409-4951 (Online), 2310-1008(Print)

Table 6

Colorimetric parameters of breads determined in the CIELab system

Bread with	L* (crust)	L* (crumb)	a* (crust)	a* (crumb)	b* (crust)	b* (crumb)	ΔE
Control with chickpea flour	47.45	65.10	15.10	0.55	21.83	14.32	-
sourdough (*L. buchneri*)	48.82	63.25	14.80	5.01	22.65	13.47	5.7
sourdough (*L. plantarum*)	48.93	64.18	14.44	2.50	21.59	10.65	4.0
sourdough (*L. buchneri* + *L. plantarum*)	47.85	62.43	15.60	3.14	21.07	14.34	6.2

The L* parameter was used to evaluate the degree of darkening of the crust and crumb within a range from 0 (black) to 100 (white). The L* values for the crust varied only slightly (47.45–48.93), indicating the absence of a significant effect of sourdough type on crust color intensity. All samples were subjected to similar conditions of non-enzymatic browning reactions during baking.

In the crumb, the L* value decreased slightly in samples prepared with sourdough, indicating moderate crumb darkening when sourdough was used; this effect was most pronounced for the mixed culture, which is consistent with the intensification of fermentation processes and acid formation.

The value of the parameter characterizing changes in the color spectrum within the green–red range (a*) indicates that the control bread containing chickpea flour exhibited a very low a* value (0.55), corresponding to an almost neutral, “cool” tone. The use of sourdoughs resulted in an increase in this parameter, indicating the formation of warmer cream–reddish hues in the crumb, most pronounced when the heterofermentative sourdough (*L. buchneri*) was used. This effect is associated with the formation of fermentation products and changes in the protein–starch matrix.

Evaluation of the b* parameter is related to the identification of color tones within the blue–yellow range. All chickpea-containing breads were characterized by elevated b* values, corresponding to the yellow hue inherent to legume raw materials. The *L. plantarum* sourdough significantly reduced the intensity of the yellow hue, whereas the mixed culture maintained it at a level comparable to the chickpea-containing control.

Thus, the color evaluation of the breads showed the following: control with chickpea flour: the lightest crumb, minimal red component (a*), and a pronounced yellow tone (b*), typical of non-fermented chickpea flour; *L. buchneri* sourdough: resulted in a warmer and slightly darker crumb color, with moderate retention of the yellow hue; *L. plantarum* sourdough: provided the smallest deviation in lightness compared to the control and reduced the yellow tone, forming a more neutral crumb color; mixed *L. buchneri* + *L. plantarum* sourdough: caused the greatest crumb darkening while preserving an intense yellow tone, indicating a synergistic effect of the cultures on the pigment profile.

ISSN: 2409-4951 (Online), 2310-1008(Print)

Evaluation of the physicochemical parameters showed that the largest product volume was characteristic of the bread prepared with the mixed-culture sourdough. This bread also exhibited good shape stability of the hearth bread.

Conclusions

It was established that the type of lactic acid bacteria significantly influences the dynamics of acid accumulation, microbial activity, and the properties of chickpea sourdoughs. Sourdough based on *Lentilactobacillus buchneri* exhibited the highest acidity and microbial activity, while sourdough prepared with *Lactiplantibacillus plantarum* showed lower acidity and moderate activity, producing a milder and more neutral aromatic profile. Sourdough prepared with the mixed culture combined the advantages of both strains, providing an optimal balance of acidity, aroma, and technological properties. The optimal conditions for chickpea sourdough preparation were 14–16 h of fermentation at 32–35 °C, under which high or very high lactic acid bacteria activity was achieved at a moderate final acidity of 12–16 °. Chickpea flour–based sourdoughs function primarily as acidifying agents and carriers of aromatic compounds rather than as complete leavening agents, making their use in combination with compressed baker's yeast advisable. The most balanced physicochemical and sensory characteristics of the finished bakery products were obtained using sourdough prepared with the mixed culture of *Lactiplantibacillus plantarum* and *Lentilactobacillus buchneri*.

References

Arora K., Ameur H., Polo A., Di Cagno R., Rizzello C.G., Gobbetti M. (2021), Thirty years of knowledge on sourdough fermentation: A systematic review, *Trends in Food Science & Technology,* 108, pp. 71–83. https://doi.org/10.1016/j.tifs.2020.12.008

Begum N., Khan Q.U., Liu L.G., Li W., Liu D., Haq I.U. (2023), Nutritional composition, health benefits and bio-active compounds of chickpea (*Cicer arietinum* L.), *Frontiers in Nutrition,* 10, 1218468, https://doi.org/10.3389/fnut.2023.1218468

Boukid F., Folloni S., Sforza S., Vittadini E., Prandi B., Lambri M. (2019), Pulses for bread fortification: A necessity or a choice? *Trends in Food Science & Technology*, 88, pp. 416–428, https://doi.org/10.1016/j.tifs.2019.04.007

Buyalska N.P., Humeniuk O.L., Denysova N.M., Cheliabiieva V.M. (2020), *Increasing the Nutritive Value of Bread and Flour-Based Confectionery Products,* Chernihiv, Chernihiv National University of Technology.

Cheliabiieva V., Sosedova E. (2018), Use of spontaneous fermentation starters and legume flours in bread production, *Technical Sciences and Technologies,* 3(13), pp. 251–257, https://doi.org/10.25140/2411-5363-2018-3(13)-251-257

Chiacchio M.F., Tagliamonte S., Pazzanese A., Vitaglione P., Blaiotta G. (2025), Lactic acid fermentation improves nutritional and functional properties of chickpea flours, *Food Research International,* 203*,* 115899, https://doi.org/10.1016/j.foodres.2025.115899

Chochkov R., Zlateva D., Ivanova P., Stefanova D. (2022), Effect of rosehip flour on the properties of wheat dough and bread, *Ukrainian Food Journal*, 11(4), pp. 558-572, https://doi.org/10.24263/2304-974X-2022-11-4-6

Conte P. (2018), Technological and nutritional challenges, and novelty in gluten-free breadmaking: A review, *Polish Journal of Food and Nutrition Sciences,* 69(1), pp. 5–21, https://doi.org/10.31883/pjfns-2019-0005

ISSN: 2409-4951 (Online), 2310-1008(Print)

Curiel J.A., Coda R., Centomani I., Summo C., Gobbetti M., Rizzello C.G. (2015), Exploitation of the nutritional and functional characteristics of traditional Italian legumes: The potential of sourdough fermentation, *International Journal of Food Microbiology,* 196*,* pp. 51–61, https://doi.org/10.1016/j.ijfoodmicro.2014.11.032

De Vuyst L., Van Kerrebroeck S., Harth H., Huys G., Daniel H.M., Weckx S. (2014), Microbial ecology of sourdough fermentations: Diverse or uniform? *Food Microbiology,* 37, pp. 11–29, https://doi.org/10.1016/j.fm.2013.06.002

Di Biase M., Bavaro A.R., Lonigro S.L., Pontonio E., Conte A., Padalino L., Minisci A., Lavermicocca P., Valerio F. (2019), *Lactobacillus plantarum* ITM21B fermentation product and chickpea flour enhance the nutritional profile of salt-reduced bakery products, *International Journal of Food Sciences and Nutrition,* 70(6), pp. 701–713, https://doi.org/10.1080/09637486.2019.1567699

Drobot V.I., Yurchak V.H., Bilyk O.A., Bondarenko Yu.V., Hryshchenko A.M. (2015), *Technochemical Control of Raw Materials in Bakery and Pasta Products,* Kyiv, Kondor.

Ercolini D., Pontonio E., De Filippis F., Minervini F., La Storia A., Gobbetti M., Di Cagno R. (2013), Microbial ecology dynamics during rye and wheat sourdough preparation, *Applied and Environmental Microbiology,* 79(24), pp. 7827–7836, https://doi.org/10.1128/AEM.02286-13

Gobbetti M., De Angelis M., Di Cagno R., Calasso M., Archetti G., Rizzello C.G. (2019), Novel insights on the functional and nutritional features of sourdough fermentation, *International Journal of Food Microbiology,* 302*,* pp. 103–113, https://doi.org/10.1016/j.ijfoodmicro.2018.05.018

Gobbetti M., Minervini F., Pontonio E., Di Cagno R., De Angelis M. (2016), Drivers for the establishment and composition of the sourdough lactic acid bacteria biota, *International Journal of Food Microbiology,* 239*,* pp. 3–18, https://doi.org/10.1016/j.ijfoodmicro.2016.05.022

Godunko Ye.V., Zabroda A.V., Bondarenko Yu.V., Bilyk O.A. (2024), Application of spontaneous flax sourdough in the production of rustic bread, *Scientific Works of the National University of Food Technologies,* 30(4), pp. 120–140, https://doi.org/10.24263/2225-2924-2023-29-3-1

Guiné R.P.F., Florença S.G. (2024), Development and characterisation of functional bakery products. *Applied Sciences,* 14(24), 12023, https://doi.org/10.3390/app142412023

Kahala M., Mäkinen S., Pihlanto A. (2021), Impact of fermentation on antinutritional factors, In: Grumezescu A.M., Holban A.M. (Eds.), *Bioactive Compounds in Fermented Foods,* pp. 185–206, CRC Press, https://doi.org/10.1201/9781003094930-8

Kaur R., Prasad K. (2021), Technological, processing and nutritional aspects of chickpea (*Cicer arietinum*): A review, *Trends in Food Science & Technology,* 109, pp. 448–463, https://doi.org/10.1016/j.tifs.2021.01.045

Kotsiou K., Tzia C., Oreopoulou V. (2022), Physicochemical and functional aspects of composite wheat–roasted chickpea flours in relation to dough rheology, bread quality and staling phenomena, *Food Hydrocolloids,* 124*,* 107322, https://doi.org/10.1016/j.foodhyd.2021.107322

Lima T.T.M., Hosken B.D.O., De Dea Lindner J., Menezes L.A.A., Pirozi M.R., Martin J.G.P. (2023), How to deliver sourdough with appropriate characteristics for the bakery industry? The answer may be provided by microbiota, *Food Bioscience,* 56, 103072, https://doi.org/10.1016/j.fbio.2023.103072

Minervini F., De Angelis M., Di Cagno R., Gobbetti M. (2014), Ecological parameters influencing microbial diversity and stability of traditional sourdough, *International Journal of Food Microbiology,* 171*,* pp. 136–146, https://doi.org/10.1016/j.ijfoodmicro.2013.11.021

Mohammed I., Ahmed A.R., Senge B. (2012), Dough rheology and bread quality of wheat–chickpea flour blends, *Industrial Crops and Products,* 36(1), pp. 196–202, https://doi.org/10.1016/j.indcrop.2011.09.006

Mykhonik L., Hetman I. (2022), The use of leaven of spontaneous fermentation of cereal flours in the technology of healthy and dietary bakery products, In: O. Paredes-López, O. Shevchenko, V. Stabnikov, V. Ivanov, (Eds.), *Bioenhancement and Fortification of Foods for a Healthy Diet* (pp. 135-154), CRC Press, Boca Raton, London, New York, https://doi.org/10.1201/9781003225287-9

ISSN: 2409-4951 (Online), 2310-1008(Print)

Norton V., Rodriguez-Garcia J., Wagstaff C., Lovegrove A., Shewry P., Charlton M., Gillett N., Tindall M., Prins A., Lignou S. (2025), Exploring the relationship between physical properties and sensory characteristics of newly developed white breads with improved nutritional composition – Initial insights, *LWT – Food Science and Technology*, 230, 118297, https://doi.org/10.1016/j.lwt.2025.118297

Ouazib M., Garzon R., Zaidi F., Rosell C. M. (2016), Effect of partial substitution of wheat flour by processed (germinated, toasted, cooked) chickpea on bread quality, *International Journal of Agricultural Science and Technology,* 4(1), pp. 8–18, https://doi.org/10.12783/ijast.2016.0401.02

Perea-Escobar C.D., Londoño-Hernández L., Benavente-Valdés J.R., Balagurusamy N., Contreras Esquivel J.C., Hernández-Almanza A.Y. (2025), Incorporation of protein alternatives in bakery products: Biological value and techno-functional properties, *Applied Sciences*, 15(20), 11279, https://doi.org/10.3390/app152011279

Pontonio E., Lorusso A., Gobbetti M., Rizzello C.G. (2017), Use of fermented milling by-products as functional ingredient to develop a low-glycaemic index bread, *Journal of Cereal Science,* 77, pp. 235–242, https://doi.org/10.1016/j.jcs.2017.08.022

Rizzello C.G., Coda R., Gobbetti M. (2017), Use of sourdough fermentation and nonwheat flours for enhancing nutritional and healthy properties of wheat-based foods, In: J. Frias, C. Martinez-Villaluenga, E. Peñas (Eds.), *Fermented Foods in Health and Disease Prevention* (pp. 433–452), Academic Press, https://doi.org/10.1016/B978-0-12-802309-9.00018-2

Rizzello C.G., Lorusso A., Montemurro M., Gobbetti M. (2016), Use of sourdough made with quinoa (*Chenopodium quinoa*) flour and autochthonous selected lactic acid bacteria for enhancing the nutritional, textural and sensory features of white bread, *Food Microbiology,* 56*,* pp. 1–13, https://doi.org/10.1016/j.fm.2015.11.018

Sadohara R., Ainsworth P., Boye J.I. (2022), Food industry views on pulse flour — Perceived intrinsic, processing, and environmental sustainability attributes, *Foods,* 11(14), 2146, https://doi.org/10.3390/foods11142146

Sáez G.D., Sabater C., Fara A., Zárate G. (2022), Fermentation of chickpea flour with selected lactic acid bacteria for improving its nutritional and functional properties, *Journal of Applied Microbiology,* 133(1), pp. 181–199, https://doi.org/10.1111/jam.15401

Santos F.G., Aguiar E.V., Centeno A.C.S., Rosell C.M., Capriles V.D. (2018), Mixture design applied to the development of chickpea-based gluten-free bread with attractive technological, sensory, and nutritional quality *Journal of Food Science,* 83(1), pp. 188–197, https://doi.org/10.1111/1750-3841.14009

Sanfilippo R., Canale M., Dugo G., Oliveri C., Scarangella M.C., Amenta M., Crupi A., Spina A. (2023), Effects of partial replacement of durum wheat re-milled semolina with bean flour on physico-chemical and technological features of doughs and breads during storage, *Plants*, 12(5), 1125, https://doi.org/10.3390/plants12051125

Schettino R., Pontonio E., Rizzello C. G. (2019), Use of fermented hemp, chickpea and milling by-products to improve the nutritional value of semolina pasta, *Foods,* 8(12), 604, https://doi.org/10.3390/foods8120604

Shrivastava C., Chakraborty S. (2018), Bread from wheat flour partially replaced by fermented chickpea flour: Optimizing the formulation and fuzzy analysis of sensory data, *LWT*, 90, pp. 215–223, https://doi.org/10.1016/j.lwt.2017.12.019

Shevchenko A., Litvynchuk S., Drobot V., Shevchenko O. (2023), Influence of pumpkin cellulose addition on conformational transformations in the structure of wheat flour dough and bread, *Ukrainian Food Journal*, 129(1), pp. 38-50, https://doi.org/10.24263/2304-974X-2023-12-1-5

Stabnikova O., Paredes-López O. (2024), Plant materials for the production of functional foods for weight management and obesity prevention, *Current Nutrition & Food Science*, 20(4), pp. 401–422, https://doi.org/10.2174/1573401319666230705110854

Stabnikova O., Marinin A., Stabnikov V. (2021), Main trends in application of novel natural additives for food production, *Ukrainian Food Journal*, 10(3), pp. 524–551, https://doi.org/10.24263/2304-974X-2021-10-3-8

ISSN: 2409-4951 (Online), 2310-1008(Print)

Stabnikova O., Shevchenko A., Stabnikov V., Paredes-López O. (2023), Utilization of plant processing wastes for enrichment of bakery and confectionery products, *Ukrainian Food Journal*, 12(2), pp. 299-308, https://doi.org/10.24263/2304-974X-2023-12-2-11

Tsykhanovska I., Stabnikova O., Riabchykov M., Lazarieva T., Korolyova N. (2024), Effect of partial replacement of wheat flour by flour from extruded sunflower seed kernels on muffins quality, *Plant Foods for Human Nutrition*, 79(4), pp. 769-778, https://doi.org/10.1007/s11130-024-01232-4

Verheyen C., Albrecht A., Elgeti D., Jekle M., Becker T. (2015), Impact of gas formation kinetics on dough development and bread quality, *Food Research International*, 76(3), pp. 860–866, https://doi.org/10.1016/j.foodres.2015.08.013

Wang J., Hu S., Nie S., Yu Q., Xie M. (2021), Nutritional constituents and health benefits of chickpea (*Cicer arietinum* L.): A review, *Food Research International,* 150*,* 110790, https://doi.org/10.1016/j.foodres.2021.110790

Xing Q., Kyriakopoulou K., Zhang L., Boom R.M., Schutyser M.A.I. (2021), Protein fortification of wheat bread using dry fractionated chickpea protein-enriched fraction or its sourdough, *LWT*, 142, 110931, https://doi.org/10.1016/j.lwt.2021.110931

Zhu F., Sakulnak R., Wang, S. (2016), Effect of black tea on antioxidant, textural, and sensory properties of Chinese steamed bread, *Food Chemistry*, 194, pp. 1217-1223, https://doi.org/10.1016/j.foodchem.2015.08.110

Author identifiers ORCID
Yevgen Godunko 0009-0002-8715-0695
Yuliia Bondarenko 0000-0002-3781-5604

Cite:

Ukr J Food Sci Style

Godunko Ye., Bondarenko Yu. (2025), Influence of chickpea flour sourdough on technological properties and quality of bakery products, *Ukrainian Journal of Food Science*, 13(2), pp. 211–226, https://doi.org/10.24263/2310-1008-2025-13-2-8

APA Style

Godunko Ye., & Bondarenko Yu. (2025). Influence of chickpea flour sourdough on technological properties and quality of bakery products. *Ukrainian Journal of Food Science, 13*(2), 211–226. https://doi.org/10.24263/2310-1008-2025-13-2-8

Evaluation of quality indicators of foam-structured beverages

Olga Pushka, Illia Shevchenko, Tetiana Sylchuk, Larysa Sharan

National University of Food Technologies, Kyiv, Ukraine

Keywords:
Beverage
Lemon balm
Brewing
Infusion
Egg white
Foam
Stability

Article history:

Received 9.09.2025
Received in revised form 28.11.2025
Accepted 31.12.2025

Corresponding author:

Tetiana Sylchuk
E-mail:
tsnuft@gmail.com

DOI:
10.24263/2310-1008-2025-13-2-9

Abstract

Introduction. The aim of the study was to evaluate the effect of lemon balm brewing methods and different types of chicken egg white on foam stability and sensory properties in model beverage systems, in order to substantiate the development of formulations and technologies for intended drinks.

Materials and methods. Infusions of lemon balm (*Melissa officinalis* L.), cherry juice, honey, native and reconstituted chicken egg white, and cinnamon were used in the study. Foam stability was assessed by measuring foam volume and the duration of foam height retention. Dry matter content was determined using the refractometric method, while titratable acidity was measured by acid–base titration.

Results and discussion. The method of preparing the lemon balm infusion significantly alters the taste characteristics, aroma, and color of the beverage. The hot lemon balm infusion was characterized by a more pronounced flavor and aroma, as well as a higher concentration of dry substances, whereas the cold infusion exhibited higher acidity and less intense sensory properties. These differences can be explained by enhanced extraction of volatile compounds and phenolic substances at elevated temperatures. To prepare drinks based on lemon balm infusions, a comparative assessment of the quality of native egg white (sample 1) and dry egg white (samples 2–4) from different manufacturers was conducted. The functional properties of egg white powders varied depending on their origin and processing conditions, which directly affected foaming behavior and stability. The sample 3 dry egg white demonstrated the best foam stability and the greatest increase in foam volume, reaching the highest volumetric expansion of 331.25%. In comparison, sample 2 egg white reached 325% at the sixth minute of whipping and 293.75% at the fourth minute, while native chicken egg white reached 217.65% at the fourth minute of whipping. In the model system, sample 3 egg white also showed the highest foam stability: its foam retained more than 50% of its initial volume even after 2 hours, whereas the native egg white lost more than 30% of its volume within 30 minutes, indicating weaker interfacial film formation.

The beverage with 10% egg white was found to be optimal in terms of sensory properties, achieving the highest complex quality indicator of 45.00 points, compared to 42.17 points for the sample with 12% egg white and 34.17 points for the sample with 7%. This concentration provided a balanced combination of foam stability, mouthfeel, and flavor perception without excessive protein-related off-notes.

Conclusions. Cold and hot lemon balm infusions, as well as dried egg whites, significantly influenced foam stability, taste, and texture. Optimal foam formation, sensory qualities and functional properties of the beverage were obtained when using 10% dried egg white.

Introduction

Modern society is increasingly oriented toward a healthy lifestyle, which drives the growing demand for functional beverages. These products not only quench thirst but also perform health-promoting functions by supporting physiological and psychological well-being.

In place of traditional bar menus, bar programs are increasingly being introduced–conceptual solutions that integrate beverage assortments with marketing strategies and service design. Unlike standard menus, bar programs are strategic in nature and focused on current consumer demands in the areas of health, biohacking, and mental well-being. Such programs contribute to shaping a culture of functional nutrition within the restaurant sector, positioning healthy beverages as part of everyday consumer choice. Each type of drink is developed according to a recipe adapted to specific physiological needs (Pushka et al., 2025).

These bar programs typically include: (a) *detox drinks*, aimed at supporting metabolic processes and facilitating the elimination of metabolic by-products; (b) *anti-stress drinks*, capable of reducing cortisol levels and stabilizing emotional state; (c) *immunostimulating drinks*, which support the body's protective functions through vitamins and minerals; (d) *sleep-enhancing drinks*, formulated with functional ingredients that may improve sleep quality; (e) *drinks for children and adolescents*, designed to supply essential vitamins and energy; (f) *drinks for athletes*, intended to enhance endurance and support post-exercise recovery.

Today, there is a significant increase in demand for healthy, natural, and functional products, accompanied by growing regulatory initiatives aimed at limiting the consumption of harmful ingredients (Stabnikova and Paredes-López, 2024). These trends encourage manufacturers to develop beverages with improved nutritional composition and enhanced health value.

Alexandropoulou et al. (2025) analyzed the impact of healthy dietary practices on physical and psycho-emotional well-being, demonstrating that diets enriched with functional foods are associated with improved health indicators, highlighting their technological and social relevance. Similarly, Aprilia et al. (2025) reported significant therapeutic and preventive potential of biologically active compounds derived from natural plant materials, underlining their importance for both pharmaceutical and food technologies.

Plant materials incorporated into functional foods can provide health benefits by serving as sources of bioactive compounds with antioxidant activity, including vitamin C, tocopherols, carotenoids, and phenolic compounds (Stabnikov et al., 2025). Numerous studies support the use of plant-based ingredients in functional beverage development (Gubsky et al., 2025; Stabnikova et al., 2021). Bomba et al. (2023) demonstrated the effectiveness of plant extracts in preventing metabolic disorders, while Karputina et al. (2022) and Tyshchenko et al. (2023) identified antioxidant, anti-inflammatory, and health-promoting effects of various herbal and plant materials, including amaranth, chia, ginger, and turmeric, added to non-alcoholic beverages. Priss et al. (2025) highlighted the potential of wild catnip (*Nepeta cataria* L.) extracts for producing beverages with high biological value and sensory quality. The addition of aqueous or aqueous–alcoholic infusions of spices, such as common rue (*Ruta graveolens* L.) and catmint (*Nepeta transcaucasica* L.), to alcoholic cocktails has been shown to enhance redox potential and and overall sensory appeal (Kuzmin et al., 2020).

The technological aspects of functional beverage formulation have also been widely investigated. It was showed that freeze-dried vegetable powders retain a high content of biologically active substances, making them suitable for non-alcoholic functional drinks

ISSN: 2409-4951 (Online), 2310-1008(Print)

(Ivanov and Schutuyk, 2012). Dulka et al. (2024) and Paska et al. (2024) demonstrated that chia mucilage formed during seed hydration improves beverage texture, stability, and microbiological safety without compromising sensory properties. Kurilenko et al. (2024) emphasized the importance of optimizing processing technologies to preserve active compounds during beverage enrichment.

In parallel, nutritional and regulatory challenges remain important considerations. Kersting et al. (2025) pointed out that plant-based milk alternatives may lack sufficient levels or bioavailability of calcium, vitamin D, vitamin B12, and protein, necessitating careful formulation and fortification strategies. Sugajski (2023) emphasized the role of water quality in functional beverages, as contamination can negate potential health benefits.

Legislative initiatives aimed at reducing sugar consumption, as discussed by Nikolenko (2024), further stimulate the development of nutritionally improved beverage formulations. Within this context, the development of functional beverages with balanced nutritional, technological, and sensory properties remains a relevant research direction.

The aim of this study was to evaluate the effect of different lemon balm (*Melissa officinalis* L.) brewing methods and native and dry chicken egg white protein on foam stability and sensory properties in model beverage systems, in order to substantiate the development of formulations and technologies for functional beverages.

Materials and methods

Materials

The object of the study was model systems of infusions of a mixture of lemon balm, chamomile, and lavender, reconstituted chicken egg whites, and the beverage "Mellow Raspberry Bliss" with different dosages of formulation components. The drink included natural ingredients with health-promoting properties: phytocomponents (lemon balm, chamomile, lavender), cherry juice, honey, egg white, and cinnamon. Preparation of the samples began with the reproduction of formulations according to the selected concepts.

A comparative characterization of two extracts of the dried mixture of lemon balm, chamomile, and lavender was carried out, prepared by two methods: hot (90–95 °C, time 15 min) and cold (- 4 – 6 °C, time, 12 h), followed by filtration. Based on the obtained infusions, the drink was formed by adding cherry juice, cinnamon, egg white, and honey. To ensure the foamy structure, chicken egg white was used.

Preparation of test samples

A comparative study of four samples was carried out: native egg white (hereinafter referred to as sample 1) and three dried egg white samples (samples 2, 3, and 4). Sample 1 was native chicken egg white obtained from fresh eggs and separated manually immediately before use. Samples 2–4 were industrially produced dried chicken egg white powders obtained by industrial dehydration and supplied by different manufacturers (Table 1).

The dried samples differed in production methods and functional characteristics, including foaming capacity and foam stability, which made it possible to assess the influence of the source and manufacturer of egg white on the quality characteristics of foam-structured beverages. Prior to use, the dried egg white powders were reconstituted with potable water in accordance with the manufacturer's instructions to obtain liquid egg white systems suitable for incorporation into beverage formulations.

ISSN: 2409-4951 (Online), 2310-1008(Print)

Table 1

Eggs used in the study

Samples	Characteristics	Manufacturer
1	Native egg white	Boyarka, Ukraine
2	Industrially produced powder by industrial dehydration of native chicken egg whites	produced by TM Oreshkino, Ukraine
3	Industrially produced powder by industrial dehydration of native chicken egg whites	produced by TM Cookit, Italy
4	Industrially produced powder by industrial dehydration of native chicken egg whites	produced by TM Zdorovo, Ukraine

Methods

Foam stability

A comparative analysis of the foam stability of native egg white and three reconstituted dried egg whites from different manufacturers was carried out, as well as their ability to form and maintain foam in the drink composition. Before being added, the egg whites were reconstituted in water to the required concentration and added to the mixture, after which the beverage was intensively mixed in a bar shaker for 4 minutes. The stability of the foam was studied by measuring the volume and duration of foam cap retention.

Functional beverage based on egg white

In the course of the research, a beverage aimed at improving sleep and reducing excitability, "Mellow Raspberry Bliss," was developed based on an infusion of lemon balm, chamomile, lavender, cherry juice, egg white, honey, and cinnamon. To determine the best method of lemon balm extraction, two techniques were studied – hot brewing and cold infusion (4–6 °C), comparing sensory properties, dry matter content, and acidity. When developing a mixed drink, it is important to consider not only the foaming agent's ability to create a stable foam but also its safety, storage conditions, and cost-effectiveness. The study of the effect of egg white content on the suitability of the beverage was carried out by varying its mass fraction within the range of 7%, 10%, and 12% of the total beverage mass.

Sensory properties

The sensory properties of the drinks were evaluated by a tasting commission using a 5-point scale. The obtained samples were subjected to sensory evaluation by a tasting panel, during which the intensity and quality of taste, aroma, and aftertaste were assessed. Based on the mean sensory scores and taking into account the assigned weighting coefficients, the complex quality index was calculated.

The complex quality index (CQI) was calculated based on the weighting coefficients of each parameter. The resulting CQI values were used to compare the samples and to determine the optimal level of egg white addition to the beverage formulation.

ISSN: 2409-4951 (Online), 2310-1008(Print)

Physico-chemical characteristics

Physicochemical characteristics were determined according to current standards: dry matter content was measured refractometrically, and titratable acidity was determined by acid–base titration.

Statistical analysis

Data analysis included calculation of arithmetic means and standard deviations.

Results and discussion

Characteristics of lemon balm infusions

The sensory and physicochemical indicators of lemon balm infusions (Table 2) demonstrate a significant dependence of the beverage quality on the preparation method. In particular, as a result of cold infusion, a light straw-colored, slightly cloudy drink with a mild, neutral taste and delicate aroma was obtained – such a beverage is well suited as a refreshing one, especially in combination with other ingredients.

Table 2

Quality indicators of lemon balm infusion

Quality indicators of lemon balm infusion	Experimental sample	
	Lemon balm infusion prepared by cold steeping	**Lemon balm infusion prepared by hot steeping**
Color	Golden, semi-transparent, with slight turbidity	Light golden with characteristic shine
Taste	Mild, weakly expressed	Moderately rich, with distinct minty notes
Aftertaste	Practically absent	Moderately expressed minty shade
Aroma	Light, floral-minty	Pronounced, with shades of roasted herbs
Appearance	Light straw with noticeable turbidity	Rich brown with shine
Consistency	Homogeneous, liquid	Homogeneous, liquid
Dry matter content, %	0.2	1
Titrated acidity, °	1.8	0.9
Color	Golden, semi-transparent, with slight turbidity	Light golden with characteristic shine
Taste	Mild, weakly expressed	Moderately rich, with distinct minty notes

Thus, each preparation method has its advantages: the hot infusion is more concentrated and aromatic, whereas the cold infusion is characterized by milder sensory properties. The choice of infusion method therefore depends on the desired characteristics of the final

ISSN: 2409-4951 (Online), 2310-1008(Print)

product. Based on lemon balm infusion, the recipe for the "Mellow Raspberry Bliss" beverage was developed, with the incorporation of egg white to form a stable foamy structure (Figure 1).

Figure 1. "Mellow Raspberry Bliss" beverage and its components

Research on functional beverages and their technological and physiological aspects has also been widely addressed in publications by other authors (Karputina et al., 2022; Paska and Mlynko, 2023).

The hot infusion, on the contrary, had an intense color, a pronounced aroma of essential oils, and a rich flavor with a minty aftertaste, which makes it attractive as a functional drink with a calming effect. The consistency of both samples remained stable.

However, the hot infusion contained five times more dry matter (1.0% vs. 0.2%), which indicates higher efficiency of bioactive compound extraction during thermal processing. As for acidity – the cold infusion had a higher value (1.8 degrees vs. 0.9 degrees), which is probably due to the preservation of organic acids that are partially destroyed under high temperatures. This contributes both to the improvement of taste and to the microbiological stability of the beverage.

These studies are consistent with those of the authors who used phytochemicals and antioxidant activities of decoction lemon balm and sage (Yaman, 2020) and green tea extract (Heydari et al., 2025).

Native chicken egg white has limitations in the bar industry due to microbiological risks and a short shelf life, so a promising alternative is dried egg white – it is more convenient to use, has a longer shelf life, and better stabilizes the foam. To determine the optimal manufacturer and dosage of egg white, foam stability tests were carried out using both the classical method and a shaker.

The most economically advantageous option is raw egg white; however, it has a limited shelf life (up to 3 weeks) and requires heat treatment due to the risk of microbial contamination, including salmonella. Dried egg whites are safer, easier to transport, and can be stored for up to 12 months. Sample 3 is the most expensive, sample 4 is the most affordable, and sample 2 is a compromise option. One kilogram of dry powder yields 7–8 kg of reconstituted product, equivalent to the amount of fresh egg white. Taking into account sanitary standards and economic aspects, dried egg whites have a number of advantages in many respects.

ISSN: 2409-4951 (Online), 2310-1008(Print)

Quality of egg whites

One of the criteria for assessing the quality of such a drink is the volume and stability of the foam, which depends on the specific properties of the selected egg white. The foam formation dynamics (Figure 2) show the rate at which the maximum foam expansion is achieved – a key parameter for service speed in food service establishments.

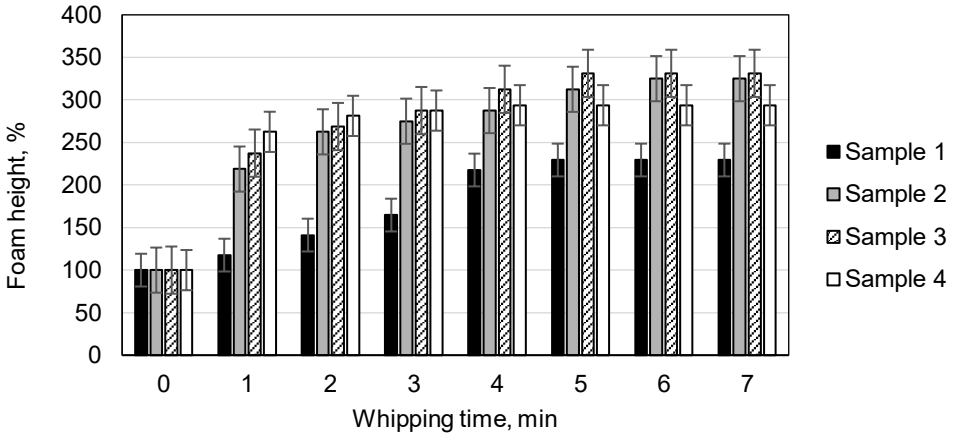

Figure 2. Foam volume increase during whisking of egg whites (native and dry from different manufacturers)

All test samples begin to form foam within the first minute of whisking; however, significant differences are observed afterward. The best results were demonstrated by Sample 3 egg white, reaching the highest volumetric increase of 331.25% already by the fifth minute, after which the values did not change. Sample 2 also showed a high increase – 325% by the sixth minute, but with lower stability. In Sample 4 egg white, foam formation occurs quickly, but stabilizes by the fifth minute at 293.75%, which may indicate lower structural strength. The worst performance was observed in native egg white – its volume increases slowly, reaching only 217.65% by the fourth minute, after which it remains unchanged.

This trend is due to the fact that chicken egg whites from different manufacturers had different initial physicochemical parameters (dry matter content, pH), which affected the results obtained. The results obtained coincide with the studies of the authors who analyzed the foam resistance of native egg white and dry egg white (Polovyk et al., 2019).

To determine foam stability, measurements of foam height reduction were conducted over 120 minutes after whisking using both the traditional method and a shaker (Figures 3–4). This made it possible to compare not only the initial volume but also the duration of foam retention depending on the method used.

The foam formed by native egg white was less stable compared to the dry analogues. The Sample 2 egg white showed the best stability when whipped with a mixer, while the Sample 3 egg white was more stable when using a shaker. Thus, foam stability depends on the type of egg white and the whipping method.

ISSN: 2409-4951 (Online), 2310-1008(Print)

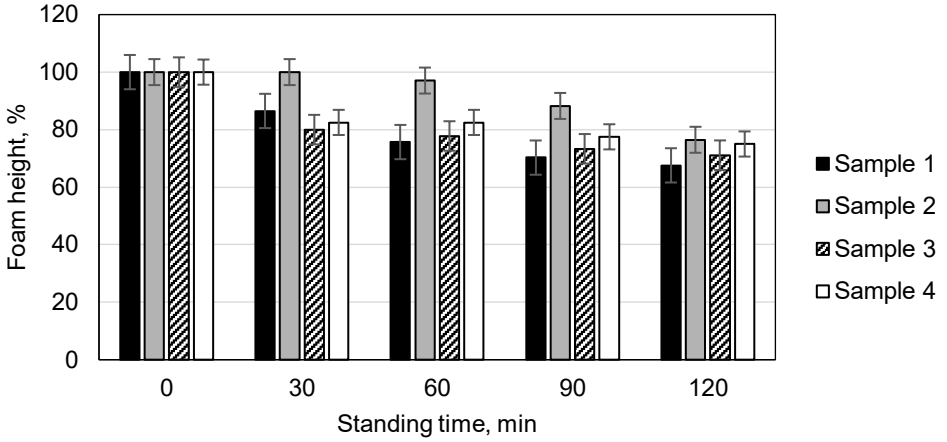

Figure 3. Foam column height of egg white during mixing with a mixer

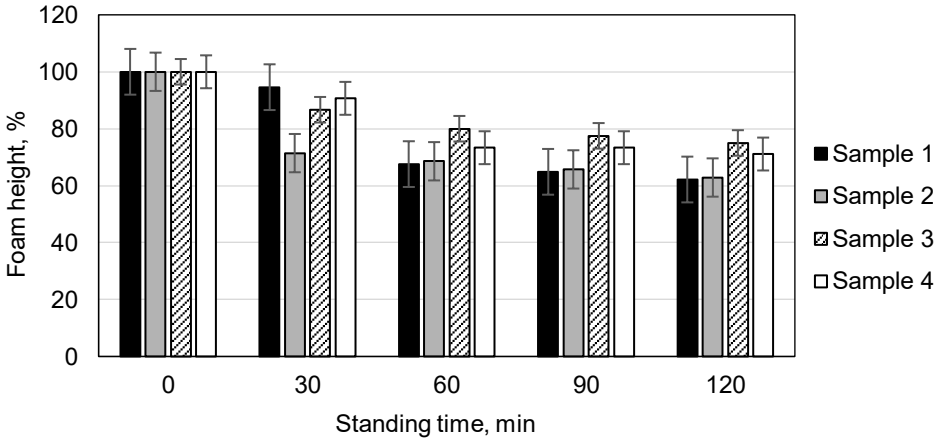

Figure 4. Foam column height of egg white during shaking

To evaluate the foaming ability of egg whites, generalized indicators of foam formation and foam stability (%) were calculated for samples whipped with a mixer and a shaker. The study covered 4 minutes of whipping and 30 minutes of standing (Table 3).

Table 3

Foaming ability and foam stability of egg whites

Indicator	Egg white							
	Sample 1		Sample 2		Sample 3		Sample 4	
	M	S	M	S	M	S	M	S
Foaming ability, %	129.41	135.29	187.50	118.75	212.50	400.00	193.75	400.00
Foam stability, %	82.05	92.50	93.48	77.14	90.00	83.75	85.11	83.75
Dry matter content in egg whites, %	18	18	10	10	9	9	8	8

Note: M - mixer; S - shaker

ISSN: 2409-4951 (Online), 2310-1008(Print)

The highest foaming ability during shaking was shown by sample 3 and sample 4 egg whites (400%), while the sample 2 egg white demonstrated the best foam stability when whipped with a mixer (93.48%). Sample 1, although it formed a relatively stable foam, was inferior in foaming properties to the dry analogues. To determine the relationship between dry matter content and foam stability of egg whites, their mass fraction in each sample was analyzed. This made it possible to identify a potential correlation between the concentration of dry matter and foam properties.

Sample 1 contained the highest amount of dry matter – 18%, but this was not decisive for achieving the highest foaming rate. The lowest dry matter content was found in the sample 4 egg white – 8%. Thus, the dry matter content does not always correlate with the ability of egg white to form and retain foam.

Since it is a multicomponent beverage, the ability of egg whites to form and retain foam within a model system was studied. For this purpose, four model samples were prepared using cold-brewed lemon balm infusion, lavender infusion, chamomile infusion, cherry juice, and one of the four tested egg whites. The ingredients were mixed in a bar shaker (Figure 5).

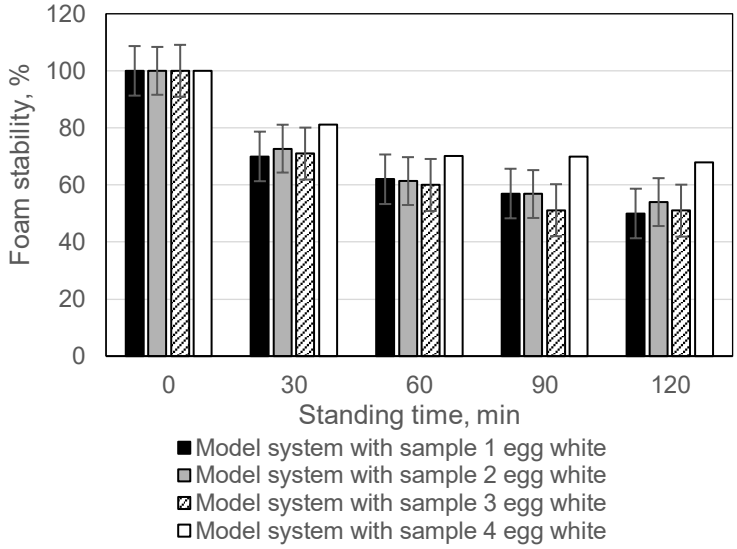

Figure 5. Foam stability of various egg whites in the model beverage system

The least stable foam was observed in the model system with sample 1, which lost more than 30% of its volume after just 30 minutes. The best stability was demonstrated by the sample 3 egg white, in the system with which the foam retained more than 50% of its initial volume even after 2 hours.

For guests of food service establishments, an important aspect is the visual presentation of the beverage, which includes the uniformity of structure, the presence of foam, and the overall impression of the drink in the glass. The color is evaluated in terms of naturalness, intensity, and correspondence to consumer expectations. The aroma should be balanced, without foreign or overly sharp odors, with clear notes of the used ingredients. The consistency determines the overall mouthfeel – whether the beverage is light and airy or, conversely, too thick. The taste should be balanced, with a clear sweet and sour composition that reveals all components of the

ISSN: 2409-4951 (Online), 2310-1008(Print)

recipe. The aftertaste is important for forming the overall impression – it should be pleasant and lasting, without bitterness or unpleasant notes.

According to the data in Table 4, the addition of different amounts of egg white significantly affects the sensory properties of the drink. The study showed that with an increase in egg white concentration, both the color (from dull pink to rich raspberry) and the flavor profile changed.

Table 4

Quality indicators of the "Mellow Raspberry Bliss" beverage with different dosage of reconstituted egg white, similar to sample 3

Indicator	7%	10%	12%
Appearance	Light infusion with fluffy white foam	Light infusion with fluffy white foam	Light infusion with fluffy white foam
Color	Dull pink	Light pink	Rich raspberry
Aroma	Fresh	Fresh	Refreshing
Consistency	Medium-thick, with foam and specks of berry puree	Medium-thick, with foam and specks of berry puree	Medium-thick, with foam and specks of berry puree
Taste	Distinctly sweet	Harmonious, with optimal combination of malt and bitterness	Slightly fruity
Aftertaste	Pronounced herbal	Moderately herbal	Herbal
Dry matter content, %	10.3%	8.9%	7%

The best results were obtained for the sample with 10% egg white with a balanced taste, pleasant aftertaste, and harmonious texture. The drink with 7% was too sweet, while the one with 12% had a less harmonious taste. The aroma in all samples remained stable, with characteristic notes of lemon balm. The appearance and consistency were also similar: a light drink with lush foam and medium density.

The complex quality indicator (CQI), calculated on a 5-point scale, made it possible to determine the optimal sample according to sensory and functional criteria.

As a result of the study, it was found that the inclusion of egg white at levels of 7%, 10%, and 12% affects the sensory characteristics of the test samples differently. The lowest value of the complex quality indicator (CQI = 34.17) was recorded for the sample containing 7% egg white, which was due to lower scores for taste and aftertaste. Increasing the proportion of egg white to 10% led to a noticeable improvement in sensory properties, resulting in the highest CQI value of 45.00. A further increase in egg white content to 12% did not allow for additional improvement of the complex quality indicator. The CQI value for this sample was 42.17, which can be attributed to a reduced balance of sensory characteristics.

Based on the analysis of the sensory and physicochemical parameters of the mixed functional drink "Mellow Raspberry Bliss" formulated with different levels of egg white, it was determined that the variant containing 10% egg protein exhibited the most harmonious sensory profile. This conclusion was drawn from the results of sensory evaluation, in which the attributes of appearance, aroma, taste, aftertaste persistence, and overall harmony were assessed using a five-point scale. The complex quality index (CQI) was calculated as a weighted sum of the mean sensory scores, with the weighting coefficients reflecting the relative importance of individual sensory attributes. The sample containing 10% egg white achieved the highest CQI value (45.0), indicating superior overall sensory quality compared to the samples containing 7% and 12% egg

ISSN: 2409-4951 (Online), 2310-1008(Print)

white. The optimality of the 10% egg protein level was confirmed by the simultaneous increase in the CQI value and the absence of undesirable sensory effects, such as excessive foam density or imbalances in taste and aftertaste, which were observed at lower or higher egg white concentrations.

Conclusions

The feasibility of developing functional beverages was confirmed as a promising direction for expanding bar assortments in HoReCa establishments. The investigation of the influence of specific ingredients on the sensory and physicochemical parameters of beverages made it possible to formulate scientifically substantiated principles for the development of recipes and production technologies for functional drinks with pronounced sensory appeal and health-promoting properties.

It was established that different methods of preparing lemon balm infusions significantly affect the sensory characteristics, acidity, and dry matter content of the final beverage. Cold infusion resulted in a dry matter content of 0.2%, whereas hot infusion increased this value to 1.0%; the corresponding titratable acidity values were 1.8° and 0.9°, respectively. Cold infusion formed a delicate taste profile with light acidity, while hot infusion produced a more intense taste and concentrated aroma, allowing the extraction process to be adjusted according to the intended functional purpose of the beverage.

The comparative study of egg white types (native and three dried variants) demonstrated the technological advantages of dried egg whites for use in bar practice. Dried egg white Sample 3 exhibited the highest foam stability and the greatest increase in foam volume, reaching a maximum volumetric expansion of 331.25%. In comparison, Sample 2 achieved 325% at the sixth minute of whipping, Sample 4 reached 293.75%, and native chicken egg white achieved only 217.65% at the fourth minute. Although native egg white is less expensive, it is characterized by lower microbiological safety and reduced technological efficiency.

The optimal dosage of reconstituted egg white for the “Mellow Raspberry Bliss” beverage was determined to be 10%. According to the complex quality indicator (CQI), this formulation achieved the highest score of 45.0 points, demonstrating excellent foaming capacity, prolonged foam stability, a pleasant mouthfeel, and the highest sensory evaluation scores.

Analysis of the chemical composition of the “Mellow Raspberry Bliss” beverage confirmed its functional orientation. Consumption of the beverage provides 31.7% of the recommended daily intake of tryptophan and 41.3% of bioflavonoids for adults, nutrients that play an important role in supporting sleep quality and overall psycho-emotional balance.

References

Alexandropoulou I., Gkouvi A., Kontouli K.M., Papadopoulou-Maniki S., Giannioti A., Bogdanos D.P., Vassilakou T., Mouchtouri V.A., Goulis D.G., Grammatikopoulou M.G. (2025), Sustainable Healthy Diet practices: A cross-sectional analysis of an adult Greek sample, *Nutrition Journal,* 24, 32, https://doi.org/10.1186/s12937-025-01096-7

Aprilia B.E., Fibri D.L.N., Rahayu E.S. (2025), Development and characterization of high-protein flakes made from *Spirulina platensis* in instant cereal drinks enriched with probiotic milk powder, *Food Production, Processing and Nutrition,* 7(1), 24, https://doi.org/10.1186/s43014-024-00298-6

Bomba M.Ya., Fedyna L.O., Masliichuk O.B., Maikova S.V. (2023), Non-traditional plant raw materials of the Carpathians in the technology of health-improving beverages, *Tavriya*

ISSN: 2409-4951 (Online), 2310-1008(Print)

Scientific Bulletin. Series: Technical Sciences, 6, pp. 42–51, https://doi.org/10.32851/tnv-tech.2022.6.6

Dudarev I. (2023), Development of beer mixed drinks compositions with "oat milk" and juices, *Restaurant and Hotel Consulting. Innovations,* 6*(*2), pp. 214–231, https://doi.org/10.31866/2616-7468.6.2.2023.291704

Dulka O.S., Prybylskyi V.L., Fedosov O.L., Kyrpichenkova O.M., Kuts A.M., Shydlovska O.B., Ishchenko T.I., Tsyrulnikova V.V., Bondar N.P. (2024), The use of chia seeds in the technology of non-alcoholic beverages, *Journal of Chemistry and Technologies,* 32(1), pp. 163–170, https://doi.org/10.15421/jchemtech.v32i1.276288

Gubsky S., Stabnikova O., Stabnikov V., Paredes-López O. (Eds.). (2025), *Wild Edible Plants: Improving Foods Nutritional Value and Human Health through Biotechnology*, CRC Press, Boca Raton, https://doi.org/10.1201/9781003486794

Heydari M., Pourahmad R., Hashemiravani M. (2025), The effect of green tea extract on the viability of *Lactobacillus casei* and the qualitative characteristics of a probiotic drink based on a mixture of celery, carrot and apple juice, *Journal of Food Science and Technology,* 156(21), pp. 125–135.

Ivanov Y., Schutuyk V. (2021), Functional drink from malt raw materials as a substitute for natural coffee, *Food Industry,* 29, pp. 42-52, https://doi.org/10.24263/2225-2916-2021-29-7

Karputina M., Khargeliya D., Vitriak O. (2022), Safety and quality of beverages based on sorghum, *Commodity Science. Technologies. Engineering,* 43(3), pp. 99–107, https://doi.org/10.31617/2.2022(43)08

Kersting M., Kalhoff H., Zahn K., Belgardt A.J., Sinningen K., Lücke T. (2025), Replacing cow's milk with plant-based drinks: Consequences for nutrient intake of young children on a balanced diet in Germany, *Journal of Health, Population and Nutrition, 44, 93*, https://doi.org/10.1186/s41043-025-00836-z

Kurylenko Y., Sukhenko V., Andronovych H., Kurakin O. (2024), Multinutrient functional beverage, *Innovations and Technologies in the Service Sphere and Food Industry,* 4(14), pp. 25–30, https://doi.org/10.32782/2708-4949.4(14).2024.4

Kuzmin O., Kucherenko V., Sylka I., Isaienko V., Furmanova Y., Pavliuchenko O., Hubenia V. (2020), Antioxidant capacity of alcoholic beverages based on infusions from non-traditional spicy-aromatic vegetable raw materials, *Ukrainian Food Journal*, 9(2), pp. 404-424, https://doi.org/10.24263/2304-974X-2020-9-2-12

Nikolenko V. (2024), International experience in the functioning of the soft drinks market, *Economics and Business Management,* 15(3), pp. 58–71, https://doi.org/10.31548/economics/3.2024.58

Paska M., Mlynko O. (2023), Technological aspects of the use of functional beverages in the restaurant business, *Economics and Society,* 52*,* https://doi.org/10.32782/2524-0072/2023-52-88

Paska M., Izhevska O., Makarovskyi N. (2024), Chia seeds and their role in creating functional beverages in restaurant establishments, *Economics and Society,* 68, https://doi.org/10.32782/2524-0072/2024-68-61

Polovyk V.V., Koretska I.L., Berezova H.O., Kravchuk N.M. (2019), The use of sweet organic amendments to improve the quality of the dessert, *Tavriya Scientific Bulletin. Series: Technical Sciences,* 30(69), pp. 126-132, https://doi.org/10.32838/2663-5941/2019.6-2/23

Pomalango Z.B., Paneo M.A., Pakaya N., Aman L.O., Hutuba A.H. (2025), Cholesterol-lowering effects of turmeric effervescent dosage in preventing atherosclerosis, *Science and Technology Indonesia,* 10(2), pp. 482–492, https://doi.org/10.26554/sti.2025.10.2.482-492

Priss O., Kolisnychenko T., Zahorko N. (2025), The catnip plant for beverage production, In: S. Gubsky, O. Stabnikova, V. Stabnikov, O. Paredes-López (Eds.), *Wild Edible Plants: Improving Foods Nutritional Value and Human Health through Biotechnology* (pp. 108-142), CRC Press, Boca Raton, https://doi.org/10.1201/9781003486794-4

Pushka O.S., Shevchenko I.V., Sylchuk T.A. (2025), Analysis of the marketing feasibility of introducing functional drinks in the hotel and restaurant business. *Market Infrastructure,* 82*,* pp. 299–303, https://doi.org/10.32782/infrastruct82-48

Schönenberger K.A., Ranzini C., Laval J., Bellenger P., Tenon M., Fança-Berthon P. (2025), The influence of food matrices on the bioavailability of curcuminoids from a dried colloidal

ISSN: 2409-4951 (Online), 2310-1008(Print)

turmeric suspension: A randomized, crossover, clinical trial, *Food & Function*, 16, pp. 774-784, https://doi.org/10.1039/d4fo03414g

Stabnikov V., Stabnikova O., Paredes-López O. (2025), Antioxidant compounds in wild edible berries. In: S. Gubsky, O. Stabnikova, V. Stabnikov, O. Paredes-López. (Eds.), *Wild Edible Plants: Improving Foods Nutritional Value and Human Health through Biotechnology* (pp. 143-184), CRC Press, Boca Raton, https://doi.org/10.1201/9781003486794-5

Stabnikova O., Marinin A., Stabnikov V. (2021), Main trends in application of novel natural additives for food production, *Ukrainian Food Journal*, 10(3), pp. 52–551, https://doi.org/10.24263/2304-974X-2021-10-3-8

Stabnikova O., Paredes-López O. (2024), Plant materials for the production of functional foods for weight management and obesity prevention, *Current Nutrition & Food Science*, 20(4), pp. 401–422, https://doi.org/10.2174/1573401319666230705110854

Sugajski M., Buszewska-Forajta M., Buszewski B. (2023), Functional beverages in the 21st century, *Beverages,* 9(1), 27, https://doi.org/10.3390/beverages9010027

Tyshchenko V.I., Bozhko N.V. (2023), Use of phytoextracts for fortification of functional purpose soft beverages, *Bulletin of Uman National University of Horticulture,* 1, pp. 123–127, https://doi.org/10.32782/2310-0478-2023-1-123-127

Tyshchenko V.I., Bozhko N.V. (2023), Analysis of modern trends in the production of non-alcoholic beverages using unconventional plant raw materials, *Tavriya Scientific Bulletin. Series: Technical Sciences,* 1, pp. 114–124, https://doi.org/10.32851/tnv-tech.2023.1.12

Yaman C. (2021), The effect of sample amount and decoction time on the phytochemicals and antioxidant activities of decoction lemon balm and sage, *Journal of Agriculture and Nature*, 24(4), pp. 725–732, https://doi.org/10.18016/ksutarimdoga.vi.810689

Author identifiers ORCID

Olga Pushka	0000-0001-8016-4889
Illia Shevchenko	0009-0006-6050-0914
Tetiana Sylchuk	0000-0001-8035-4957
Larysa Sharan	0000-0001-6404-0907

Cite:

Ukr J Food Sci Style

Pushka O., Shevchenko O., Sylchuk T., Sharan L. (2025), Evaluation of quality indicators of foam-structured beverages, *Ukrainian Journal of Food Science*, 13(2), pp. 227–239, https://doi.org/10.24263/2310-1008-2025-13-2-9

APA Style

Pushka, O., Shevchenko, O., Sylchuk, T., & Sharan, L. (2025). Evaluation of quality indicators of foam-structured beverages. *Ukrainian Journal of Food Science, 13*(2), 227–239. https://doi.org/10.24263/2310-1008-2025-13-2-9

ISSN: 2409-4951 (Online), 2310-1008(Print)

Surface microbiota of *Pinus sylvestris* seeds and its potential in biocontrol

Viacheslav Shopinskyi[1], Liudmyla Butsenko[1,2]

1 - National University of Food Technologies, Kyiv, Ukraine
2 - D.K. Zabolotny Institute of Microbiology and Virology, National Academy of Sciences of Ukraine, Kyiv, Ukraine

Keywords:

Pinus sylvestris
Seeds
Epiphytes
Bacteria
Biocontrol
Antagonism

Article history:

Received 21.10.2025
Received in revised form 14.12.2025
Accepted 31.12.2025

Corresponding author:

Viacheslav Shopinskyi
E-mail:
chemslava@gmail.com

DOI: 10.24263/2310-1008-2025-13-2-10

Abstract

Introduction. The study of plant-associated microbiota deepens our understanding of plant–microorganism interactions and is of considerable practical importance for the identification of strains suitable for the development of biotechnological preparations for crop production. This paper presents the results of an investigation into the epiphytic microbiota of Scots pine (*Pinus sylvestris* L.) seeds and its antagonistic potential.

Materials and methods. Epiphytic bacteria were isolated by washing seeds to preserve native surface communities. The isolates were characterized by morphological and cultural traits and identified using classical microbiological methods and MALDI-TOF mass spectrometry. Antagonistic activity was evaluated in vitro by the radial streak method against phytopathogenic bacteria (*Pseudomonas syringae* 8511, *P. fluorescens* 8573, *Xanthomonas campestris* 8003b, *Agrobacterium tumefaciens* 8628, and *Clavibacter michiganensis* subsp. *michiganensis* 10_2).

Results and discussion. It was found that the epiphytic bacterial microbiota is represented by three species: *Bacillus subtilis*/*B. amyloliquefaciens*, *Pantoea agglomerans* and *Micrococcus luteus*. Epiphytic bacterial isolates from Scots pine seeds were successfully identified using MALDI-TOF mass spectrometry with a high degree of reliability: 99.9%. Structural analysis of the epiphytic microbiome shows an even distribution between two taxa: *B. subtilis*/*B. amyloliquefaciens* and *P. agglomerans*, each of which accounts for 40% of the total number of identified isolates; one fifth of the microbial community (20%) is composed of *M. luteus.*

Bacillus subtilis/*amyloliquefaciens* strain E18 showed the highest antagonistic activity, forming growth inhibition zones of up to 35±1 mm against *X. campestris* and 15±2 mm against *C. michiganensis*. Isolate E15 showed selective activity against *P. syringae* (18±1 mm) and *C. michiganensis* (12±1 mm). Meanwhile, strains E17 and E20 did not inhibit the growth of any of the tested phytopathogens.

Thus, the results of the study confirmed the presence of bacteria with pronounced biocontrol potential among the epiphytic microbiota of *P. sylvestris* seeds. *Bacillus* spp. strains are particularly promising, as they are capable of producing a wide range of biologically active metabolites and demonstrating stable antagonistic activity.

Conclusions. The experimental data obtained provide a basis for the development of environmentally safe biological products that can be used in forestry to increase seed germination and protect seedlings from phytopathogens.

Introduction

Food safety is a priority area of research, with one of its key components being the achievement of stable crop yields and effective protection against plant pathogens. The plant microbiome plays a crucial role in maintaining plant health by contributing to pathogen suppression, growth stimulation, and tolerance to abiotic stresses. These microbial communities, inhabiting internal tissues (endophytes) and plant surfaces (epiphytes), are an integral part of plant life (Lindow et al., 2003; Turner et al., 2013).

Epiphytic bacteria are microorganisms that colonize the external surfaces of plants, including leaves, stems, flowers, and seeds, without penetrating host tissues. Unlike endophytic microorganisms, epiphytic microbiota form complex microbial communities on plant surfaces, collectively referred to as the phyllosphere (Lindow et al., 2003; Vorholt, 2012).

Among epiphytic bacteria, representatives of the genera *Pseudomonas, Bacillus, Pantoea, Sphingomonas, Methylobacterium*, and *Enterobacter* are the most common. These microorganisms exhibit antagonistic activity against phytopathogens and are capable of producing a wide range of biologically active substances, including antibiotics, siderophores, phytohormones, terpenes, and other metabolites that enhance plant resistance to biotic and abiotic stress factors (Achath et al., 2025; Gnanamanickam et al., 2006; Hirano et al., 2000; Lindow et al., 2003; Vorholt, 2012; Trias et al., 2012).

The microbiota associated with seeds is important and largely derived from rhizosphere microbial communities, although partial vertical transmission from the host plant has also been reported. These microorganisms can be beneficial, promoting seedling germination and development, or pathogenic, leading to seed degradation and damage to the host plant, depending on the species composition and functional characteristics of the microorganisms (Necajeva et al., 2023).

Scots pine (*Pinus sylvestris* L.) plays a key role in the formation of coniferous forest ecosystems in northern Europe. The cultivation of this species faces specific challenges, particularly infection of young plants by phytopathogenic fungi, such as *Fusarium* spp., which cause fusarium wilt and severely affect the germination capacity of seed material. Additional problems arise from adverse abiotic conditions, including temperature extremes, salt stress, and heavy metal exposure. The combined impact of these biotic and abiotic factors leads to reduced germination energy, lower percentages of viable seedlings, and slowed ontogenetic development of the young tree generation (Pirttila et al., 2011).

Conventional phytoprotection methods based on the use of chemical fungicides, bactericides and synthetic pesticides have limited effectiveness and are characterised by negative ecotoxicological potential, causing contamination of natural environments and inducing the formation of resistant strains of phytopathogenic microorganisms (Pal et al., 2006; Pirttila et al., 2011). Therefore, the search for environmentally safe alternatives based on the use of antagonistically active epiphytic bacteria is a relevant and promising area of research.

Although endophytic bacteria from Scots pine seeds have been extensively studied for their growth-stimulating and protective effects, the epiphytic bacterial community found directly on the surface of these seeds remains less studied. Due to their surface colonisation, epiphytic bacteria are the first line of microbial interaction with germinating seeds and young seedlings, potentially providing protective and growth-stimulating benefits. The study of epiphytes on seeds is extremely important for understanding the initial points of interaction and their response to external environmental factors. These microorganisms, which are found on the surface of the seed, are the first to interact with external stress factors during germination: moisture, temperature, ultraviolet radiation, and potential pathogens (e.g., soil fungi, airborne bacteria). The study of epiphytic bacteria is important for understanding the early interactions between plants and

ISSN: 2409-4951 (Online), 2310-1008(Print)

microorganisms and for developing targeted seed treatment methods that provide effective phytostimulant effects (Aachath et al., 2025; Gnanamanickam et al., 2006).

The plant microbiome has a significant impact on the health of the host plant, its growth and resistance to biotic and abiotic stresses. These microbial communities, which include bacteria and fungi, interact with plants in complex and dynamic ways, shaping their development and adaptation to stress factors (Turner et al., 2013). Epiphytic bacteria are a major component of the diverse microbiota that inhabits the surface of plants. They live predominantly non-parasitically on various plant organs, including seeds, forming aggregates or biofilms (Gnanamanickam et al., 2006; Thomas et al., 2024).

Epiphytic bacteria have significant potential in sustainable agriculture due to their ability to promote plant growth. This is often achieved through the production of phytohormones (auxins, cytokinins, and gibberellins), which are important for plant development. For example, some *Bacillus* species are known to produce gibberellins (Aachath et al., 2025; Turner et al., 2013). They can also solubilise essential nutrients (zinc, potassium, phosphorus), making them bioavailable to plants. Some bacterial species are also capable of fixing atmospheric nitrogen, providing additional symbiotic benefits (Aachath et al., 2025).

Epiphytic bacteria can effectively suppress phytopathogens through various mechanisms. Key mechanisms include competitive exclusion, where beneficial microbes outcompete pathogens for essential nutrients (carbon, nitrogen, hydrogen, oxygen, sulphur, phosphorus) and space on the plant surface. In addition, many epiphytic species secrete antimicrobial compounds (e.g., antiviral, antibacterial, and antifungal bios compounds) that directly inhibit pathogen growth (Gnanamanickam and Immanuel, 2006).

Studies of the *Pinus sylvestris* microbiome have mostly focused on endophytic communities, especially in the roots. These studies have shown that factors such as geographical origin and season significantly influence the composition and nature of interactions between root endophytic fungal and bacterial communities, correlating with the biochemical properties of the host plant's roots and climatic factors (Maitra et al., 2024).

In the context of studying the epiphytic microbiota of Scots pine (*Pinus sylvestris* L.) seeds, it is important to consider the specific conditions of these microorganisms. The surface of conifer seeds is characterised by low moisture content, the presence of resinous substances and other secondary plant metabolites, which creates selective pressure for the formation of a specific microbial community (Pirttila et al., 2011).

Particular attention in studies is paid to epiphytic bacteria of the genus *Bacillus*, which demonstrate high efficiency as biological control agents and are characterised by their ability to produce various antimicrobial compounds, lipopeptides and surface-active substances (Aachath et al., 2025; Monteiro et al., 2005).

Studies have also shown that epiphytic bacteria *Bacillus subtilis*, *Bacillus megaterium* and *Bacillus cereus*, isolated from cabbage and radishes, exhibit significant antagonistic activity against the phytopathogen *Xanthomonas campestris*. The authors noted that inoculation of plants with epiphytic bacteria contributed to increased germination and reduced pathogen infection of seedlings (Monteiro et al., 2005).

Scientists have established that the microbiota of seeds of plants of the *Brassicaceae* family contains endophytic and epiphytic microorganisms of the genera *Bacillus*, *Massilia*, *Pseudomonas* and *Pantoea*, which exhibit growth-stimulating activity on the germination and initial development of the host plant (Barret et al., 2015).

An important aspect is the study of factors that influence the formation of epiphytic seed microbiota. According to scientific research, the composition of the microbiota depends on the plant genotype, environmental conditions, seed storage methods and other factors (Compant et al., 2019).

ISSN: 2409-4951 (Online), 2310-1008(Print)

In the field of forestry, the study of conifer seed microbiota is particularly relevant. The authors note that conifer seeds are often characterised by low germination and high sensitivity to pathogens, which makes the search for natural antagonists among the microbiota a promising area of research (Pirttila et al., 2011).

Fusarium filamentous ascomycete fungi are well-known pathogens of *Pinus sylvestris* seeds, capable of significantly reducing germination rates (Davydenko, 2019; Davydenko et al., 2018; Yusipovich et al., 2018). This highlights the need for effective biological control strategies. Despite active research into phytomicrobiome interactions and recognition of the importance of seed microbial associations, there is insufficient study of the epiphytic bacterial community of *Pinus sylvestris* seeds and its functional characteristics. Therefore, comprehensive characterisation, study of the species diversity of epiphytic bacteria in pine seeds, and experimental determination of their antagonistic activity against phytopathogenic microorganisms is a relevant scientific task that can contribute to the development of environmentally safe methods for protecting and stimulating the growth of this important forest species.

The aim of the present work is to study epiphytic bacteria isolated from the seed material of Scots pine (*Pinus sylvestris* L.); to establish the taxonomic affiliation of surface microflora, characterise its morphological and cultural features, and assess the bioantagonistic potential of identified epiphytic isolates against phytopathogenic microorganisms.

Materials and methods

Materials

For the study, first-class Scots pine (*Pinus sylvestris* L.) seeds harvested in 2023 from the Bucha Forestry Enterprise (Kyiv region) were used. The seed material was stored under optimal conditions to preserve its quality until laboratory analysis.

Phytopathogenic bacteria strains

To study the antagonistic activity of epiphytic bacteria isolated from Scots pine (*Pinus sylvestris* L.) seeds, a collection of well-characterised strains of phytopathogenic bacteria was used: *Pseudomonas syringae* 8511; *Pseudomonas fluorescens* 8573; *Xanthomonas campestris* 8003b; *Agrobacterium tumefaciens* 8628; *Clavibacter michiganensis* subsp. *michiganensis* 10_2.

Test cultures of the phytopathogenic bacteria were obtained from the collection of the Department of Phytopathogenic Bacteria of the D. K. Zabolotny Institute of Microbiology and Virology of the National Academy of Sciences of Ukraine.

Isolation of epiphytic bacteria

For selective isolation of epiphytic bacteria, a "soft" washing method was used, which ensured the preservation of surface microorganisms without the use of harsh sterilisation procedures characteristic of endophyte isolation. This methodological difference is critical for differentiating between epiphytic and endophytic microbial communities.

A washing method was used to isolate epiphytic bacteria from the surface of Scots pine seeds (Baruco et al., 2020; Golub et al., 2012; Sanchez-Lopez et al., 2018). A seed sample (50 seeds) was placed in 100 ml of sterile 10 mM $MgSO_4$ solution and intensively stirred on a mechanical shaker for 20 minutes at 200 rpm to desorb surface-associated microbial cells

ISSN: 2409-4951 (Online), 2310-1008(Print)

(Necajeva et al., 2023). The resulting wash solution containing the epiphytic microbial community was thoroughly mixed to ensure uniform distribution of cells and serial tenfold dilutions (10^{-1}, 10^{-2}, 10^{-3}) were prepared. Aliquots of 0.1 ml from the corresponding dilutions were transferred with a sterile pipette to the surface of agarised nutrient media: potato agar (for fungi) and LB medium (for bacteria). The inoculum was evenly distributed over the surface of the medium using a sterile L-shaped spatula. The Petri dishes were labelled, turned upside down and incubated at a temperature of 27 ± 1°C. The development of bacterial colonies was monitored every 24 hours for 72 hours. Morphologically distinct and representative bacterial colonies were selected for further purification by repeated transfer to fresh nutrient media until pure cultures were obtained for further identification and characterisation.

Nature of isolated bacteria

The isolated epiphytic bacterial strains were characterised using classical microbiological methods (Patika et al., 2014; 2017). This included assessment of colony morphology (size, shape, colour, transparency, surface texture, edge characteristics), cell morphology (shape, arrangement), Gram reaction, and endospore presence. Physiological and biochemical tests were performed to determine key metabolic properties: catalase and oxidase activities, ability to grow on media with different NaCl concentrations (2%, 5%, 7%, 10%), aerobic and anaerobic growth on glucose; hydrolysis of gelatin, starch, casein and esculin. Nitrate reduction, tyrosine hydrolysis, citrate utilisation and the Voges-Proskauer reaction (acetoine production) were also evaluated. The optimal, minimum and maximum temperatures and pH ranges for growth were determined.

Use of MALDI-TOF-MS for the identification of epiphytic bacteria

Taxonomic identification of purified epiphytic bacterial isolates was performed using matrix-assisted laser desorption/ionisation (MALDI-TOF) mass spectrometry using the VITEK MS system. The study included the preparation of a calibration curve using Escherichia coli ATCC 8739. Pure cultures of test bacteria, grown for 18-24 hours, were applied in a thin layer to the MALDI-TOF target well of the plate. A matrix solution (α-cyano-4-hydroxycinnamic acid) was then added to each target well and allowed to air dry. The prepared slide was placed in the VITEK MS device and the identification process was started. Bacteria identification was achieved by comparing the obtained mass spectra of unknown isolates with an extensive database of reference spectra. The system provides a percentage of identification reliability, with a range from 60% to 100% indicating correct identification (Ashfaq et al., 2022; Cevik et al., 2021; Tsuchida et al., 2020).

Antagonistic activity of epiphytic bacteria

The antagonistic activity of epiphytic bacteria isolated from Scots pine seeds against bacterial phytopathogens was evaluated in vitro using the radial streak method (co-culture test) on appropriate agar media. A streak of the antagonist (epiphytic isolate) was made on an agar plate, and then streaks of phytopathogens were made perpendicular to the isolates. The plates were incubated at 27°C for 24-48 hours. Antagonistic activity was quantitatively assessed by measuring the growth inhibition zone (in millimetres) of the phytopathogen around the antagonist streak (Butsenko et al., 2010; Patyk et al., 2017).

ISSN: 2409-4951 (Online), 2310-1008(Print)

Assessment of experimental results

Experimental studies were conducted with three replicates for each variant. Mathematical and statistical analysis of the obtained data was performed using the Statistica 6.0 software package with standard Microsoft Excel statistical tools.

Results and discussion

Isolation and characterisation of epiphytic bacteria from Scots pine seeds

During the study of the epiphytic microbiota of Scots pine (*Pinus sylvestris* L.) seeds, bacterial isolates were isolated and characterised from the seed surface without sterilisation. The method used effectively isolated microorganisms associated with the seed surface and allowed the natural epiphytic microbiota of pine seeds to be preserved for further study of its species composition and functional properties.

Bacteria forming colonies of various morphologies were isolated from the surface of Scots pine seeds. Significant variability in the morphological and cultural characteristics of the isolated isolates (their size, shape, transparency, surface texture, and others) was observed, indicating a high biodiversity of the epiphytic microbiota of the seeds. For detailed study and characterisation, the most typical isolates demonstrating various morphological and cultural characteristics were selected: E13, E16, E17, E18 and E20 (Figure 1).

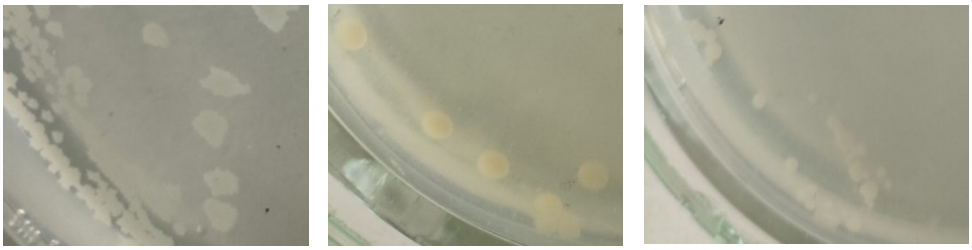

a **b** **c**

Figure 1. Colonies of epiphytic bacteria from Scots pine seeds: isolate E15 (a), isolate E16 (b), and isolate E17 (c)

Morphological and cultural analysis showed that among the isolated isolates (E15, E16, E17, E18, E20), Gram-positive rods predominate, which are capable of growing on various nutrient media under aerobic conditions. most isolates showed a positive reaction to the catalase test and the ability to hydrolyse gelatin (Table 1).

As shown in Table 1, various morphological, cultural, physiological, and biochemical properties were found among the isolated epiphytes. Isolates E15 and E18, identified as *B. subtilis* (or *B. amyloliquefaciens*), formed rounded or irregular colonies with a diameter of 2-4 mm, with wavy or fringed edges, opaque, with a wrinkled surface, whitish in colour. They are Gram-positive, motile, straight rods that form ellipsoidal and cylindrical spores. These isolates showed positive results for catalase activity, hydrolysis of gelatin, starch, casein and esculin, as well as the ability to reduce nitrates and utilise citrate. They demonstrated growth at NaCl concentrations up to 10% and aerobic growth on glucose, with an optimal growth temperature of 28-30 °C and a pH range of 5.5-8.5.

ISSN: 2409-4951 (Online), 2310-1008(Print)

Table 1

Properties of epiphytic isolates isolated from Scots pine (*Pinus sylvestris* L.) seeds

Property	Isolates from Scots pine seeds			Properties of typical representatives of species according to literature data			
	E15, E18	E16, E20	E17	*B. subtilis*[1]	*B. amyloliquefaciens*[2]	*P. agglomerans*[3]	*M. luteus*[4]
Cell shape	Rods	Rods	Cocci	Rods	Rods	Rods	Cocci
Spore formation	+	-	-	+	+	-	-
Gram staining	+	-	+	+	+	-	+/-
Mobility	-	+	-	+	+	+	-
Catalase activity	+	+	+	+	+	+	+
Oxidase activity	+	-	+	+/-	-	-	+
Growth in a medium with 2% NaCl	+	+	+	+	+	+	+
Growth in a medium with 7% NaCl	+	-	-	+	+	+/-	-
Growth in a medium with 10% NaCl	+	-	-	+/-	+/-	N/A	-
Growth in glucose medium aerobically	+	+	+	+	+	+	+
Growth in glucose medium anaerobically	-	+	-	+/-	+/-	+/-	-
Gelatin hydrolysis	+	+	-	+	+	+	-
Starch hydrolysis	+	-	-	+	+	-	-
Casein hydrolysis	+	-	-	+	+	N/A	+
Esculin hydrolysis	+	+	-	+	+	+/-	-
Nitrate reduction	+	+	-	+	+	+	-
Citrate utilization	+	+	-	+	+	+	-
Voges-Proskauer reaction	+\-	+	-	+	+	+	+/-

Note: N/A – not found; 1 – according to Logan et al., 2015; Rooney et al., 2009; Satapute et al., 2012; 2 – according to Baudu et al., 2025; Afrin et al., 2023; 3 – according to Mardaneh et al., 2013; Acioly et al., 2017; 4 – according to Shi et al., 2023; Greenblatt et al., 2004; Environment and Climate Change Canada, 2018.

Isolates E16 and E20, identified as *Pantoea agglomerans*, formed smooth, translucent, convex colonies with intact edges and a pale yellowish colour. They are Gram-negative, motile, straight rods that do not form spores. They are characterised by catalase activity,

ISSN: 2409-4951 (Online), 2310-1008(Print)

gelatin hydrolysis, nitrate reduction and citrate utilisation. They are capable of growing at 7% NaCl, with an optimal temperature of 25-30 °C and a pH range of 4.5–9.0.

Isolate E17, identified as *Micrococcus luteus*, formed round, smooth, creamy-yellow colonies approximately 4 mm in diameter. The cells are coccoid, Gram-positive, immotile, and do not form spores. This isolate exhibited catalase and oxidase activity, casein hydrolysis, but did not hydrolyse gelatin and starch. Growth was observed at 5% NaCl. The optimal growth temperature was 25–30 °C and the pH range was 7.0–9.0.

This characterization confirmed the greater taxonomic and functional diversity of the epiphytic community compared with the predominantly bacillary endophytic community described by Shopinskyi and Butsenko (2025).

MALDI-TOF MS-based identification of epiphytic bacteria

The identification of epiphytic bacteria was also carried out using the MALDI-TOF mass spectrometry method, which ensured high accuracy of taxonomic determination.

Taxonomic identification of the studied bacterial isolates was performed using the matrix-assisted laser desorption/ionisation mass spectrometry method.

Based on the results of MALDI-TOF mass spectrometric analysis, the taxonomic affiliation of five epiphytic bacterial strains (E15, E16, E17, E18 and E20) isolated from the surface of *Pinus sylvestris* seeds was established. The dominant taxa were representatives of *B. subtilis*/*B. amyloliquefaciens* and *P. agglomerans*. A single isolate of *M. luteus* was also identified.

Five separate epiphytic bacterial isolates (E15, E16, E17, E18, E20) were successfully identified using MALDI-TOF mass spectrometry with a high degree of reliability: 99.9% (Table 2).

Table 2

Results of identification of epiphytic bacterial isolates using MALDI-TOF

Isolate	Identified epiphytic bacteria	Identification accuracy, %
E15	*Bacillus subtilis/amyloliquefaciens/vallismortis*	99.9
E16	*Pantoea agglomerans*	99.9
E17	*Micrococcus luteus*	99.9
E18	*Bacillus subtilis/amyloliquefaciens/vallismortis*	99.9
E20	*Pantoea agglomerans*	99.9

Diversity of the epiphytic microbiota of Scots pine seeds

The epiphytic bacterial microbiota of *Pinus sylvestris* L. seeds is characterised by limited taxonomic diversity and is represented by three dominant species: *B. subtilis*/ *B. amyloliquefaciens* (for isolates E15 and E18), *P. agglomerans* (for E16 and E20) and *M. luteus* (for E17).

Structural analysis of the epiphytic microbiome shows an even distribution between two taxa: *B. subtilis*/*B. amyloliquefaciens* and *P. agglomerans*, each of which accounts for 40% of the total number of identified isolates; one fifth of the microbial community (20%) is composed of *M. luteus* (Figure 4).

ISSN: 2409-4951 (Online), 2310-1008(Print)

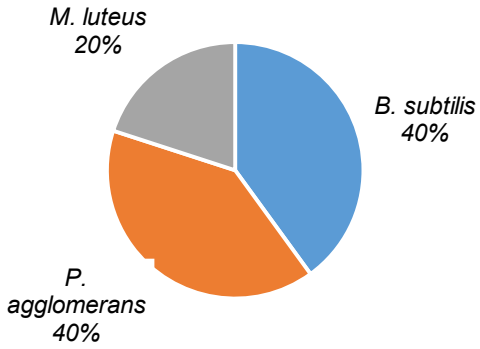

Figure 4. Species distribution of epiphytic bacteria isolated from Scots pine (*Pinus sylvestris* L.) seeds

The identified structure of the epiphytic microbiome reflects the selective adaptation of bacterial taxa to the specific ecological conditions of the surface of conifer seeds. The dominance of *Bacillus* spp. reflects their high resistance to stress factors and ability to form spores, which ensures survival in conditions of variable humidity and temperature fluctuations. The presence of *P. agglomerans* may be associated with their phytostimulating properties and ability to colonise plant surfaces, while *M. luteus* is characterised by high resistance to UV radiation and water deficiency.

Biocontrol potential of Scots pine epiphytes against phytopathogenic bacteria

The results of determining the antagonistic activity of epiphytic bacterial isolates isolated from *Pinus sylvestris* L. seeds in relation to collection strains of phytopathogenic microorganisms are presented in Table 3.

Table 3

Antagonistic activity of epiphytic bacteria isolated from *Pinus sylvestris* L. seeds against phytopathogenic bacteria

Epiphytic bacteria	***P. syringae* 8511**	***P. fluorescens* 8573**	***X. campestris* 80036**	***A. tumefaciens* 8628**	***C. michiganensis subsp. michiganensis* 10_2**
	Growth inhibition zones, mm				
E15	18±1	17±1*	N/A	5±1	12±1
E16	0	9±1	0	0	0
E17	0	0	0	0	0
E18	14±1	14±1	35±1	12±1	15±2
E20	0	0	0	0	0

Notes: * – no complete absence of growth was observed, only its delay; N/A – not studied

The data obtained indicate significant variability in the antagonistic activity of the studied epiphytes. Isolates E15 and E18 (*B. subtilis*/*B. amyloliquefaciens*) showed antagonistic activity, forming the largest growth inhibition zones against most of the

ISSN: 2409-4951 (Online), 2310-1008(Print)

collected phytopathogenic strains: *X. campestris* (35±1 mm), *C. michiganensis* subsp. *michiganensis* (15±2 mm), *P. syringae* (14±1 mm) and *P. fluorescens* (14±1 mm). This indicates a broad spectrum of antimicrobial activity of this isolate and its potential as an effective biological control agent.

Strain E15 showed selective antagonistic activity, exhibiting high efficacy only against *P. syringae* (18±1 mm) and moderate activity against *C. michiganensis* subsp. *michiganensis* (12±1 mm). It was also found that strain E15 has moderate bioantagonistic activity against *P. fluorescens* (17±1 mm) and only inhibits the growth of the phytopathogen, but does not completely eliminate it, indicating a bacteriostatic rather than bactericidal effect.

Isolate E16 was characterised by a narrow spectrum of antagonistic activity, exhibiting an inhibitory effect only against *P. fluorescens* (9±1 mm). Such selectivity may indicate a specific mechanism of antimicrobial action or a limited spectrum of antibiotic compounds produced.

Strains E17 and E20 did not show antagonistic activity against any of the tested phytopathogens. This may indicate that these strains are unable to produce antimicrobial compounds that are effective against the studied phytopathogens, or that they have other mechanisms of interaction with the host plant that are not related to direct antagonism.

Compared to endophytic bacteria, epiphytic isolates show more variable antagonistic activity with less characteristic efficacy indicators. However, strain E18 was characterised by a pronounced inhibitory effect on *X. campestris*, where the growth inhibition zone (35±1 mm) exceeded the results obtained for endophytic bacteria.

The results confirmed the potential of epiphytic bacteria isolated from Scots pine seeds as biocontrol agents, especially strains E15 and E18, which may be promising for further study as potential agents of biological control of phytopathogenic bacteria in forestry.

Conclusions

The isolated epiphytic bacteria of Scots pine (*Pinus sylvestris* L.) seeds, identified as *Bacillus subtilis*/*amyloliquefaciens*, *Pantoea agglomerans* and *Micrococcus luteus*, are characterised by significant biocontrol potential for suppressing phytopathogenic microorganisms. The established taxonomic structure of the epiphytic microbiome demonstrates the dominance of bacillary forms and the presence of phytostimulating taxa adapted to the specific ecological conditions of the surface of coniferous seeds. The antagonistic activity of *Bacillus* spp. strains against a wide range of phytopathogens confirms the promise of their use in the creation of environmentally safe biological products for forestry. Further research should be aimed at studying the molecular mechanisms of antagonistic action, identifying antimicrobial metabolites, and evaluating the effectiveness of selected epiphytic isolates in field conditions for protecting seedlings and increasing seed germination.

References

Aachath R.S., Rupawalla Z.H. (2025), Epiphytic bacteria and their uses in sustainable agriculture: A review, *Current Agriculture Research Journal*, 13(1), pp. 38–53, https://doi.org/10.12944/CARJ.13.1.04

Acioly L.M.L., Carlos V.J., da Silveira A.B., de Almeida F.C.G., de Lima e Silva T.A., de Campos-Takaki G.M. (2017), Isolation, identification, characterization and enzymatic

ISSN: 2409-4951 (Online), 2310-1008(Print)

profile of the new strain of *Pantoea agglomerans*, *International Journal of Current Microbiology and Applied Sciences*, 6(11), pp. 4152–4163, https://doi.org/10.20546/ijcmas.2017.611.487

Afrin S., Bhuiyan M.N.I. (2023), Antagonistic activity of *Bacillus amyloliquefaciens* subsp. *amyloliquefaciens* against multidrug resistant *Serratia rubidaea*, *Current Research in Microbial Sciences*, 5, 100206, https://doi.org/10.1016/j.crmicr.2023.100206

Ashfaq M.Y., Da'na D.A., Al-Ghouti M.A. (2022), Application of MALDI-TOF MS for identification of environmental bacteria: A review, *Journal of Environmental Management*, 305, 114359, https://doi.org/10.1016/j.jenvman.2021.114359

Banoo A., Shahnaz E., Banday S., Rasool R., Bashir T., Latif R. (2020), Plant pathology & microbiology studies on predominant epiphytic micro-flora as antagonists to post-harvest pathogens of apple, *Journal of Plant Pathology & Microbiology*, 11(9), 512, https://doi.org/10.35248/2157-7471.20.11.512

Barret M., Briand M., Bonneau S., Preveaux A., Valiere S., Bouchez O., Hunault G., Simoneau P., Jacquesa M.A. (2015), Emergence shapes the structure of the seed microbiota, *Applied and Environmental Microbiology*, 81(4), pp. 1257–1266, https://doi.org/10.1128/AEM.03722-14

Baudu E., Raspaud E., Fontagne-Faucher C., Nait Chabane Y., Marcato-Romain C.-E. (2025), Morphogenesis and mechanical properties of *Bacillus amyloliquefaciens* biofilms: A comparative study of rough and smooth morphotypes, *Current Research in Microbial Sciences*, 8, 100403, https://doi.org/10.1016/j.crmicr.2025.100403

Benjamin S., Surekha Y., Moolakkariyil S.J., Pradeep S. (2016), *Micrococcus luteus* strain BAA2, a novel isolate produces carotenoid pigment, *Electronic Journal of Biology*, 12(1), pp. 83–89

Butsenko L.M., Penchuk Yu.M., Pyroh T.P. (2010), *Technologies of Microbial Synthesis of Medicinal Products,* Textbook, Kyiv, NUHT.

Cevik Y.N., Ogutcu H. (2021), Identification of bacteria in soil by MALDI-TOF MS and analysis of *Bacillus* spp., *Paenibacillus* spp. and *Pseudomonas* spp. with PCA, *Analytical Chemistry Letters*, 10(6), pp. 784–797, https://doi.org/10.1080/22297928.2021.1877194

Clark D., Youngblood C., Taplin M., Brown E., Williams B.S., Phillips C., Garner B. (2014), Impact of iron availability on *Bacillus amyloliquefaciens* growth, *Advances in Microbiology*, 4(9), pp. 962–967, https://doi.org/10.4236/aim.2014.413107

Costa E., Usall J., Teixido N., Delgado J., Vinas I. (2003), Water activity, temperature, and pH effects on growth of the biocontrol agent *Pantoea agglomerans* CPA-2, *Canadian Journal of Microbiology*, 48(12), pp. 1082–1088, https://doi.org/10.1139/w03-001

Davydenko K., Nowakowska J. A., Kaluski T., Gawlak M., Sadowska K., Martin-Garcia J., Diez J.J., Okorski A., Oszako T. (2018), A comparative study of the pathogenicity of *Fusarium circinatum* and other *Fusarium* species in Polish provenances of *Pinus sylvestris* L., *Forests*, 9(9), 560, https://doi.org/10.3390/f9090560

Davydenko K.V. (2019), Preliminary assessment of pathogenicity of *Fusarium circinatum* on germlings of *Pinus sylvestris* in Ukraine, *Forestry and Forest Melioration*, 134, 117, https://doi.org/10.33220/1026-3365.134.2019.117

De Vos P., Garrity G.M., Jones D., Krieg N.R., Ludwig W., Rainey F.A. Whitman W.B. (2009), *Bergey's Manual of Systematic Bacteriology*, 2nd Edition, Vol. 3, Springer, https://doi.org/10.1007/b92997

Environment and Climate Change Canada. (2018), *Final Screening Assessment of Micrococcus luteus Strain ATCC 4698*, *Government of Canada*, Available at: https://publications.gc.ca/site/eng/9.850899/publication.html

Gnanamanickam S., Immanuel E. (2006), Epiphytic bacteria, their ecology and functions, *Plant-Associated Bacteria*, pp. 131–153, https://doi.org/10.1007/978-1-4020-4538-7_4.

ISSN: 2409-4951 (Online), 2310-1008(Print)

Greenblatt C.L., Baum J., Klein B.Y., Nachshon S., Koltunov V., Cano R.J. (2004), *Micrococcus luteus* – survival in amber, *Microbial Ecology*, 48(1), pp. 120–127, https://doi.org/10.1007/s00248-003-2016-5

Hirano S.S., Upper C.D. (2000), Bacteria in the leaf ecosystem with emphasis on *Pseudomonas syringae* – a pathogen, ice nucleus, and epiphyte, *Microbiological Reviews*, 64(3), pp. 624–653, https://doi.org/10.1128/mmbr.64.3.624-653.2000

Holub S.M., Holub V.O., Melnichuk Yu.V. (2012), Microbiology: methodological guidelines for laboratory works for students of the 3rd year of the biology faculty, *Volyn State University named after Lesya Ukrainka*, Biology Faculty, Department of Botany and Garden-Park Management. Lutsk, Private Enterprise Ivanyuk.

Lee H.B., Hong J.P., Kim S.B. (2010), First report of leaf blight caused by *Pantoea agglomerans* on rice in Korea, *Plant Disease*, 94(11), 1372, https://doi.org/10.1094/PDIS-05-10-0374.

Lindow S.E., Brandl M.T. (2003), Microbiology of the phyllosphere, *Applied and Environmental Microbiology*, 69(4), pp. 1875–1883, https://doi.org/10.1128/AEM.69.4.1875-1883.2003

Ling J., Zhang G., Sun H., Fan Y., Ju J., Zhang C. (2011), Isolation and characterization of a novel pyrene-degrading *Bacillus vallismortis* strain JY3A, *The Science of the Total Environment*, 409(10), pp. 1994–2000, https://doi.org/10.1016/j.scitotenv.2011.02.020

Logan N.A., De Vos P. (2015), *Bergey's Manual of Systematics of Archaea and Bacteria*, John Wiley & Sons, Inc., in association with Bergey's Manual Trust, https://doi.org/10.1002/9781118960608.gbm00530

Loncaric I., Heigl H., Licek E., Moosbeckhofer R., Busse H.J., Rosengarten R. (2009), Typing of *Pantoea agglomerans* isolated from colonies of honey bees (*Apis mellifera*) and culturability of selected strains from honey, *Apidologie*, 40(1), pp. 40–54, https://doi.org/10.1051/apido/2008062

Maitra P., Hrynkiewicz K., Szuba A., Niestrawska A., Mucha J. (2024), The effects of *Pinus sylvestris* L. geographical origin on the community and co-occurrence of fungal and bacterial endophytes in a common garden experiment, *Microbiology Spectrum*, 12(10), e00807-24, https://doi.org/10.1128/spectrum.00807-24

Mardaneh J., Soltan Dallal M.M. (2013), Isolation, identification and antimicrobial susceptibility of *Pantoea* (*Enterobacter) agglomerans* isolated from consumed powdered infant formula milk (PIF) in NICU ward, *Iranian Journal of Microbiology*, 5(3), pp. 263–267.

Monteiro L., Mariano R. de L.R., Souto-Maior A.M. (2005), Antagonism of *Bacillus* spp. against *Xanthomonas campestris* pv. *campestris*, *Brazilian Archives of Biology and Technology*, 48(1), pp. 23–29, https://doi.org/10.1590/S1516-89132005000100004

Necajeva J., Boroduske A., Nikolajeva V., Senkovs M., Kalnina I., Roga A., Skinderskis E., Fridmanis D. (2023), Epiphytic and endophytic fungi colonizing seeds of two *Poaceae* weed species and *Fusarium* spp. seed degradation potential *in vitro*, *Microorganisms*, 11(1), 184, https://doi.org/10.3390/microorganisms11010184

Ngalimat M.S., Yahaya R.S.R., Baharudin M.M.A., Yaminudin S.M., Karim M., Ahmad S.A., Sabri S. (2021), A review on the biotechnological applications of the operational group *Bacillus amyloliquefaciens*, *Microorganisms*, 9(3), 614, https://doi.org/10.3390/microorganisms9030614

Pal K.K., McSpadden Gardener B. (2006), Biological control of plant pathogens, *Plant Health Instructor*, 2, https://doi.org/10.1094/PHI-A-2006-1117-02

Patyka V.P., Pasichnyk L.A., Dankevych L.A., Moroz S.M., Butsenko L.M., Zhytkevych N.V., Gnatiuk T.T., Zakharova O.M., Savenko O.A., Shkatula Yu.M., Kyrylenko L.V., Alekseiev O.O. (2014), *Diagnosis of Phytopathogenic Bacteria, Methodical Recommendations*, LLC Komprint, Kyiv.

ISSN: 2409-4951 (Online), 2310-1008(Print)

Patyka V.P., Pasichnyk L.A., Hvozdyak R.I., Petrychenko V.F., Kalinichenko A.V., Butsenko L.M., Hnatyuk T.T. (2017), *Phytopathogenic Bacteria. Research Methods*, LLC Vindruk, Vinnytsia.

Pirttila A.M., Frank A.C. (2011), *Endophytes of Forest Trees: Biology and Applications*, Springer, https://doi.org/10.1007/978-94-007-1599-8

Priest F.G., Goodfellow M., Shute L.A., Berkeley R.C.W. (1987), *Bacillus amyloliquefaciens* sp. nov., nom. rev, *International Journal of Systematic Bacteriology*, 37(1), pp. 69–71, https://doi.org/10.1099/00207713-37-1-69

Priest F.G., Goodfellow M., Todd C. (1988), A numerical classification of the genus *Bacillus*. *Journal of General Microbiology*, 134(7), pp. 1847–1882, https://doi.org/10.1099/00221287-134-7-1847

Roberts M.S., Nakamura L.K., Cohan F.M. (1996), *Bacillus vallismortis* sp. nov., a close relative of *Bacillus subtilis*, isolated from soil in Death Valley, California, *International Journal of Systematic and Evolutionary Microbiology*, 46(2), pp. 470–475, https://doi.org/10.1099/00207713-46-2-470

Rooney A.P., Price N.P.J., Ehrhardt C., Swezey J.L., Bannan J.D. (2009), Phylogeny and molecular taxonomy of the *Bacillus subtilis* species complex and description of *Bacillus subtilis* subsp. *inaquosorum* subsp. nov, *International Journal of Systematic and Evolutionary Microbiology*, 59(10), pp. 2429–2436, https://doi.org/10.1099/ijs.0.009126-0

Sanchez-Lopez A.S., Gonzalez-Chavez M. del C.A., Solis-Dominguez F.A., Carrillo-Gonzalez R., Rosas-Saito G.H. (2018), Leaf epiphytic bacteria of plants colonizing mine residues: Possible exploitation for remediation of air pollutants, *Frontiers in Microbiology*, 9, 3028, https://doi.org/10.3389/fmicb.2018.03028

Satapute P.P., Olekar H.S., Shetti A.A., Kulkarni A.G., Hiremath G.B., Patagundi B.I., Shivsharan C.T., Kaliwal B.B. (2012), Isolation and characterization of nitrogen fixing *Bacillus subtilis* strain AS-4 from agricultural soil, *International Journal of Recent Scientific Research*, 3(9), pp. 762–765.

Shi X., Qiu S., Ji L., Lu H., Wu S., Chen Q., Zou X., Hu Q., Feng T., Chen S., Cui W., Xu S., Jiang M., Cai R., Geng Y., Bai Q., Huang D., Liu P. (2023), Pathogenetic characterization of a *Micrococcus luteus* strain isolated from an infant, *Frontiers in Pediatrics*, 11, https://doi.org/10.3389/fped.2023.1303040

Shopinskyi V., Butsenko L. (2025), Endophytic bacteria from seeds of scots pine, *Scientific Works of NUFT*, 31(2), pp. 61-72, https://doi.org/10.24263/2225-2924-2025-31-2-7

Thomas G., Kay W.T., Fones H.N. (2024), Life on a leaf: The epiphyte to pathogen continuum and interplay in the phyllosphere, *BMC Biology*, 22, 168, https://doi.org/10.1186/s12915-024-01967-1

Trias R., Garcia-Lledo A., Sanchez N., Lopez-Jurado J.L., Hallin S., Baneras L. (2012), Abundance and composition of epiphytic bacterial and archaeal ammonia oxidizers of marine red and brown macroalgae, *Applied and Environmental Microbiology*, 78(2), pp. 318–325, https://doi.org/10.1128/AEM.05904-11

Tsuchida S., Hiroshi U., Tomohiro N. (2020), Current status of matrix-assisted laser desorption/ionization-time-of-flight mass spectrometry (MALDI-TOF MS) in clinical diagnostic microbiology, *Molecules*, 25(20), 4775. https://doi.org/10.3390/molecules25204775

Turner T.R., James E.K., Poole P.S. (2013), The plant microbiome, *Genome Biology*, 14(6), 209, https://doi.org/10.1186/gb-2013-14-6-209

Vorholt J.A. (2012), Microbial life in the phyllosphere, *Nature Reviews Microbiology*, 10(12), pp. 828–840, https://doi.org/10.1038/nrmicro2910

Wieser M., Denner E.B.M., Kampfer P., Schumann P., Tindall B., Steiner U., Vybiral D., Lubitz W., Maszenan A.M., Patel B.K.C., Seviour R.J., Radax C., Busse H.J. (2002), Emended

ISSN: 2409-4951 (Online), 2310-1008(Print)

description of the genus *Micrococcus*, *Micrococcus luteus* (Cohn 1872) and *Micrococcus lylae* (Kloos et al. 1974), *International Journal of Systematic and Evolutionary Microbiology*, 52, pp. 629–637, https://doi.org/10.1099/ijs.0.01901-0

Yusypovych Yu.M., Kovaliova V.A., Hut R.T. (2018), Diagnosis of fungi of the *Fusarium* in Scots pine seedlings by polymerase chain reaction, *Scientific Works of the Forestry Academy of Sciences of Ukraine*, 13, pp. 55–58, https://doi.org/10.15421/411506

Author identifiers ORCID

Viacheslav Shopinskyi 0009-0006-9050-8896

Liudmyla Butsenko 0000-0002-3575-4289

Cite:

Ukr J Food Sci Style

Shopinskyi V., Butsenko L. (2025), Surface microbiota of *Pinus sylvestris* seeds and its potential in biocontrol, *Ukrainian Journal of Food Science*, 13(2), pp. 240–253, https://doi.org/10.24263/2310-1008-2025-13-2-10

APA Style

Shopinskyi, V., & Butsenko, L. (2025). Surface microbiota of *Pinus sylvestris* seeds and its potential in biocontrol. *Ukrainian Journal of Food Science, 13*(2), 240–253. https://doi.org/10.24263/2310-1008-2025-13-2-10

ISSN: 2409-4951 (Online), 2310-1008(Print)

Biological inducers as regulators of secondary metabolite biosynthesis in actinobacteria

Anastasiia Okhmakevych[1], Tetiana Pirog[1,2]

1 – National University of Food Technologies, Kyiv, Ukraine
2 – Institute of Microbiology and Virology, National Academy of Sciences of Ukraine, Kyiv, Ukraine

Keywords:

Actinobacteria
Biological inducer
Secondary metabolites
Biological activity

Article history:

Received 20.10.2025
Received in revised form 17.12.2025
Accepted 31.12.2025

Corresponding author:

Tetiana Pirog
E-mail: tapirog@nuft.edu.ua

DOI:
10.24263/2310-1008-2025-13-2-11

Abstract

Introduction. The aim of this review is to summarise available information on secondary metabolite production by actinobacteria in the presence of biological inducers in culture media.

Materials and methods. A systematic search of scientific publications was conducted, primarily using PubMed and Google Scholar, to identify studies on the cultivation of actinobacteria in the presence of biological inducers from the earliest available reports up to 2025.

Results and discussion. With the development of biotechnology, unconventional methods of cultivating producers alongside other microorganisms or inducers are attracting increasing attention. Cultivating actinobacteria with biological inducers can lead to increased concentration and/or activity of synthesised secondary metabolites, as well as to the production of practically valuable metabolites that are not characteristic of monocultures.

Actinobacteria, bacteria, fungi, and yeasts are used as biological inducers, mainly in the form of living cells, although supernatants and inactivated cells are also employed. Among the possible mechanisms of induction, the most commonly highlighted are intercellular interactions between producers and inducers, as well as the effect of inducer signalling molecules on the biosynthesis of secondary metabolites; however, this aspect remains insufficiently studied and requires deeper molecular and physiological investigation.

Actinobacteria are cultivated with inducers in the laboratory mainly in flasks on shakers, although some researchers also use laboratory bioreactors, indicating the potential for process scale-up. Different nutrient media are often applied for the preparation of microbial inocula and for biosynthesis, which requires further optimisation for scaling-up to the industrial level. Not all authors provide a detailed description of preparing inocula of actinobacteria and other microorganisms, which makes it difficult to determine whether the cultivation was indeed performed with an inducer and limits reproducibility of the results. Furthermore, not all studies investigate the biological activity of the secondary metabolites obtained, which requires further study, as the feasibility of their industrial production and their potential practical applications largely depend on this.

Conclusions. The co-cultivation of actinobacteria with biological inducers represents a promising biotechnological strategy for enhancing and diversifying the production of secondary metabolites. However, the underlying mechanisms of induction and intercellular interactions remain insufficiently understood and further study is needed to identify effective inducers and optimise conditions.

ISSN: 2409-4951 (Online), 2310-1008(Print)

Introduction

Microbial products are increasingly being explored for medical applications, as it has been established that only 0.1–1% of all microorganisms have been successfully cultivated under laboratory conditions, while their diversity remains virtually limitless (Adnani et al., 2017; Alhadrami et al., 2021). Actinobacteria are prolific producers of secondary microbial metabolites and can be classified into members of the genus *Streptomyces* and rare, non-*Streptomyces* actinomycetes, possessing dozens of biosynthetic genes (Hoshino et al., 2018a; Liang et al., 2020). Their metabolic repertoire includes, among others, antibiotics (Boruta et al., 2021; Shamikh et al., 2020), alkaloids (Maglangit et al., 2020; Shamikh et al., 2020), and polyketides (Hoshino et al., 2016; Wang et al., 2014).

A considerable number of valuable microbial metabolites are now known; however, some exhibit low biological activity, occur at low concentrations, or are not synthesised at all under standard laboratory conditions, making it important to explore strategies to overcome these limitations (Maimone et al., 2021).

Conventional approaches to modulating the biosynthesis process include altering the composition of the nutrient media, adjusting temperature and pH (Alam et al., 2022), as well as refining strains through metabolic engineering techniques (Singh et al., 2023). Concurrently, with the advancement of applied biotechnologies, the use of mixed cultures has attracted increasing attention (Khedkar et al., 2025). In our study (Pirog et al., 2023), we have highlighted that the concepts of co-cultivation "with competitive microorganisms" and "with biological inducers" are distinct: in the former, inocula are introduced at nearly equal concentrations, whereas in the latter, the producer is applied at a substantially higher concentration than the inducer. In our previous review (Pirog et al., 2025), we examined the impact of competitive microorganisms on the synthesis of secondary metabolites by actinobacteria; in this review, we focus on the role of biological inducers.

The earliest reports on the impact of biological inducers on the synthesis of secondary metabolites by actinobacteria date back to 2008–2011. Initially, these were sporadic studies (Kurosawa et al., 2008; Onaka et al., 2011); however, in recent years, there has been a noticeable increase in such research (Selegato et al., 2023).

Cultivation of producers of antimicrobial secondary metabolites with competitive microorganisms or inducers may result in (Wang et al., 2021): alterations in metabolite concentration and/or antimicrobial activity; production of metabolites not typically observed in monocultures; or absence of metabolites normally formed in monoculture. Studies (Liang et al., 2020; Song et al., 2020) indicate that producers respond differently to various inducers in the culture media, and no consistent patterns in secondary metabolite formation have been identified, meaning that the induction mechanism underlying co-cultivation remains poorly understood. Furthermore, there is no guarantee that the metabolites obtained will possess the desired biological activity, so each approach to co-cultivating microorganisms or cultivating them with inducers should be thoroughly investigated and analysed.

The aim of this study is to summarise the literature on the biosynthesis of practically important secondary metabolites by actinobacteria in the presence of biological inducers, considering their various physiological states (living cells, inactivated cells, or supernatant).

The objectives of this study are to search for, analyse, and summarise the findings of international colleagues regarding the influence of biological inducers on the synthesis of secondary metabolites by actinobacteria and their biological activity, as well as on the production of metabolites not typically observed in the producer monoculture.

ISSN: 2409-4951 (Online), 2310-1008(Print)

Materials and methods

A systematic search of scientific publications was conducted, primarily using PubMed and Google Scholar databases, with keywords including “actinobacteria,” “secondary metabolites,” “co-culture,” “inducer,” “elisitor,” and “microbial interactions.” Articles published from 2008 to 2025 were selected. Only studies reporting secondary metabolite production in the presence of biological inducers were included. Relevant studies were summarised and analysed.

Results and discussion

Synthesis of metabolites not characteristic of monocultures

In the available literature, the vast majority of studies on the cultivation of actinobacteria with inducers, resulting in the synthesis of new metabolites, focus on the use of other actinobacteria containing mycolic acids and belonging to the genera *Tsukamurella*, *Rhodococcus*, *Gordonia*, and *Nocardia* (see Table 1).

Table 1

Cultivation of actinobacteria in the presence of inducers: synthesis of metabolites not characteristic of monocultures

Producer + inducer	Synthesised metabolites	Antimicrobial activity	Cytotoxic and other activity	Sources
Inducers - other actinobacteria				
Streptomyces lividans TK23 + *Tsukamurella pulmonis* TP-B0596 (living cells)	Red pigment UPG*	–	–	Onaka et al., 2011
S.coelicolor S522 + *T. pulmonis* TP-B0596 (living cells)	Antibiotic alchivemycin A	MIC (μg/mL) against: *Micrococcus luteus* TP-B100 – 0.06; *Bacillus subtilis* ATCC 6633 – 40; *Staphylococcus aureus* 209P JC-1, *Escherichia coli* NIHJ JC-2, *Candida albicans* TP-F0176 - > 50	–	Onaka et al., 2011
Gordonia sp. KMC005 + *S. tendae* KMC006 (living cells)	Gordonic acid (yellow polyketide glycosid)	GIZ (mm) 10 μg/disc: *M. luteus* KCCM11548 – 2.5; *Enterococcus hirae* KCCM11768 -1.5	–	Park et al., 2017
Umezawaea sp. RD066910 + *T. pulmonis* TP-B0596 (living cells)	Antibiotic umezawamide A	GIZ, 5 μg/disc: *C. albicans* – 1.7 mm; Diameter of GIZ (10 μg/disc): *B. cereus, S. aureus* sensitive to methicillin, *E. coli* (not reported)	–	Hoshino et al., 2018b

ISSN: 2409-4951 (Online), 2310-1008(Print)

Producer + inducer	Synthesised metabolites	Antimicrobial activity	Cytotoxic and other activity	Sources
	Antibiotic umezawamide B	Diameter of GIZ (10 µg/disc): *C. albicans, B. cereus, S. aureus* sensitive to methicillin, *E. coli* - not reported	–	
Actinosynnema mirum NBRC 14064 + *T. pulmonis* TP-B0596 (living cells)	Antibiotics mirilactams C, D, E	Absence of antimicrobial activity against *C. albicans, B. cereus, S. aureus* sensitive to methicillin (strain numbers not specified)	Cytotoxic activity against cervical cancer, MCF-7 breast cancer, A549 lung cancer cells, starting from 100 µM	Hoshino et al., 2018c
Micromonospora sp. WMMB-235 + *Rhodococcus* sp. WMMA-185 (living cells)	Antibiotic keyicin	Inhibition of growth of *Mycobacterium* sp. WM MB-235, *Rhodococcus* sp. WMMA-185 (degree of inhibition not reported); MIC (µg/mL) against *B. subtilis* – 8; *S. aureus* sensitive to methicillin (strain numbers not specified) - 2	–	Adnani et al., 2015, 2017
Streptomyces nigrescens HEK616 + *T. pulmonis* TP-B0596 (living cells)	Lipidic metabolite SA-9n*	GIZ, mm (30 µg/disc): *B. subtilis* NBRC 3134 – 12; *S. aureus* NBRC 13276 – 10. Growth inhibition zone, mm (100 µg/disc): *E. coli* NBRC 3972 - 10	–	Sugiyama et al., 2016
Streptomyces sp. CJ5 + *T. pulmonis* TP-B0596 (living cells)	Chojalactones A, B and C (butanolides)	Absence of antimicrobial activity against *B. subtilis, S.aureus,* and *C. albicans* (strain numbers not specified)	IC_{50} 18–28 µM Moderate cytotoxic activity against P388 mouse leukemia cells	Hoshino et al., 2015a
Catenuloplanes sp. RD067331 + *T. pulmonis* TP-B0596 (living cells)	*Catenulobactin* A (heterocyclic peptide)	–	Moderate cytotoxic activity against P388 mouse leukemia cells (IC_{50} 22.4 µM)	Hoshino et al., 2018a
	Catenulobactin B (heterocyclic peptide)	–	Cytotoxic activity against P388 mouse leukemia cells ($IC_{50} \geq 100$ µM)	
Streptomyces padanus MITKK-103 + *Rhodococcus fascians* 307 (living cells)	Antibiotic RSM* A	GIZ, mm (30 µg/disc): *S. padanus* MITKK-103 – 15; *E. coli*-8; *S. aureus*-9; *B. subtilis*–8; *Helicobacter pylori* -10	Absence of activity against HL-60 human leukemia cells	Kurosawa et al., 2008; 2010

ISSN: 2409-4951 (Online), 2310-1008(Print)

Producer + inducer	Synthesised metabolites	Antimicrobial activity	Cytotoxic and other activity	Sources
S. padanus MITKK-103 +*R. fascians* 307 (living cells)	Antibiotic RSM* B	GIZ, mm (30 µg/disc): *S. padanus* MITKK-103 – 18; *E. coli*–12; *S. aureus*-14; *B. subtilis*–14; *H. pylori* -18	Absence of activity against HL-60 human leukemia cells	Kurosawa et al., 2008; Kurosawa et al., 2010
Streptomyces sp. RKND-216 + *Mycobacterium smegmatis* ATCC 12051 (living and inactivated cells)	CBQ* G	Absence of antimicrobial activity against *S. aureus* resistant to methicillin ATCC 33591, *E. faecium* F379 resistant to vancomycin E, *S. warneri* ATCC 17917, *Proteus vulgaris* ATCC 12454, and *C. albicans* ATCC 14035	Selective cytotoxic activity against MCF-7 and HTB26 breas cancer cells (IC_{50} 3.07 and 3.67 µM)	Liang et al., 2020
Streptomyces sp. NZ-6 + *T. pulmonis* TP-B0596 (living cells)	Niizalactams A, B (multicyclic macrolactams)	Absence of GIZ against *C. albicans*, *B. subtilis*, and *Saccharomyces cereviciae*	Absence of activity against P388 mouse leukemia cells	Hoshino et al., 2015b
Streptomyces sp. TAKO-2 + *T. pulmonis* TP-B0596 (living cells)	Aromatic polyketides julichrome Q_6 and julichrome $Q_{8.8}$	–	–	Hoshino et al., 2016
S. nigrescens HEK616 + *T. pulmonis* TP-B0596 (living cells)	Alkaloids 5aTHQs*	MIC (µM) against *Schizosaccharomyces pombe* JY1 – 6.3	–	Sugiyama et al., 2015
Streptomyces sp. KUSC_F05 + *T. pulmonis* TP-B0596 (living cells)	LCA* A-D (cyclic hexapeptides)	MIC (µM) against *B. subtilis* IFO3134 -100; absence of antimicrobial activity against *S. aureus* IFO13276, *E. coli* IFO3972, *Pseudomonas aeruginosa* IFO169	Absence of activity against HT1080 human fibrosarcoma cells at 100 µM	Jiang et al., 2021
Streptomyces cinnamoneus NBRC 13823 + *T. pulmonis* (strain number not specified) (living cells)	*Arcyriaflavin* E (alkaloid)	–	Cytotoxic activity against P388 mouse leukemia cells (IC_{50} 39 µM)	Hoshino et al., 2015c
Micromonospora wenchangensis HEK-797 + *T. pulmonis* TPB0596 (living cells)	Dracolactams A i B (macrolactams)	Absence of antimicrobial activity against *C. albicans*, *B. cereus, S. aureus* resistant to methicillin, *T. pulmonis* (strain numbers not specified)	Absence of activity against P388 mouse leukemia cells	Hoshino et al., 2017

ISSN: 2409-4951 (Online), 2310-1008(Print)

Producer + inducer	Synthesised metabolites	Antimicrobial activity	Cytotoxic and other activity	Sources
Micromonospora sp. UA17 + *Gordonia* sp. UA19 (living cells)	Complex of metabolites, including piperidine derivative MY 336a, antibiotic *chlorocardicin,* antibiotic WS 5995-A, neocopiamycin A	MIC (μg/mL) against: *S. aureus* NCTC 8325 – 8.6; *Enterococcus faecalis* (strain number not specified) – 7.4; *C. albicans* 5314 – 6.4	Activity against *Trypanosoma brucei* TC221 (MIC > 100 μg/mL)	Shamikh et al., 2020
Micromonospora sp. UA17 + *Nocardia* sp. UA 23 (living cells)	Complex of metabolites, including antibiotic chicamycin B, libramycin-A, alkaloids	MIC (μg/mL) against: *S. aureus* NCTC 8325 – 4.2; *E. faecalis* (strain number not specified) – 3.9; *C. albicans* 5314 – 3.8	Activity against *T. brucei* TC221 (MIC > 100 μg/mL)	
Streptomyces sp. UR23 + *Nocardia* sp. UR27 (living cells)	During growth on ISP2 agar medium: bafilomycins D and A1, aggreceride A, salbostatin During growth in ISP2 liquid medium: lipstatin, trichostatic acid, trichostatin A, terreusinol, platenolide II	–	Activity of metabolites synthesised on agar and in liquid media against *T. brucei* (strain number not specified) (IC_{50} 4.6 and 2.4 μg/mL, respectively)	Gamaleldin et al., 2020
Micromonospora sp. UR17 + *Nocardia* sp. UR27 (living cells)	During growth on ISP2 agar medium: neihumicin, *antascomicins* D and C. During growth in ISP2 liquid medium: geldanamycin, 2-HPAA*, daidzein, GTRI-02	–	Activity of metabolites synthesised on agar and in liquid media against *T. brucei* (IC_{50} 2.7 and 2.5 μg/mL, respectively)	Gamaleldin et al., 2020
Nocardiopsis sp. UR17 + *Nocardia* sp. UR27 (living cells)	During growth on ISP2 agar medium: MPC*, 5-HPA* During growth in ISP2 liquid medium: Forphenicine	–	Activity of metabolites against *T. brucei* (strain number not specified) ($IC_{50} \geq 100$ μg/mL)	Gamaleldin et al., 2020

ISSN: 2409-4951 (Online), 2310-1008(Print)

Producer + inducer	Synthesised metabolites	Antimicrobial activity	Cytotoxic and other activity	Sources
Inducers – other bacteria				
Streptomyces sp. RKND-216 +*Alteromonas* sp. RKMC-009 (living and inactivated cells)	NC-DHBA *	–	Low activity against kidney CCL-81 cells, MCF-7 and HTB26 breast cancer cells, and HCT116 colon cancer cells (IC_{50} ≥ 32 mg/mL)	Liang et al., 2020
Inducers – fungi				
Streptomyces lunalinharesii A54A +*Rhizoctonia solani* (strain number not specified) (living cells)	Complex of new unknown metabolites, including the DFO* siderophores and anisomycin derivatives	Inhibition of growth of *R. solani* (strain number not specified) – 88,43 % (extract concentration 500 mg/µL)	–	Maimone, et al., 2021
Streptomyces sp. CMB-StM0423 + *Aspergillus* sp. CMB-AsM0423 (living cells)	Heronapyrrole B	Diameter of GIZ for *A.* sp. CMB-AsM0423 – not reported	–	Khalil, et al., 2019

Notes: «–» – data not reported; GIZ - growth inhibition zones, **UPG* – undecylprodigiosin; SA-9n - streptoaminal-9n; *RSM – rhodostreptomycin; CBQ – carbazoquinocin;* 5aTHQs - 5-alkyl-1,2,3,4-tetrahydroquinolines; *LCA – longicatenamides;* 2-HPAA - 2-hydroxyphenylacetic acid; MPC - methyl pyrrole-2-carboxylate; 5-HPA – 5-hydroxypicolinic acid; NC-DHBA - N-carbamoyl-2,3-dihydroxybenzamide; DFO – desferrioxamine.

Data from Table 1 also indicate that living cells of other organisms are most commonly employed to induce the synthesis of metabolites not typically observed in monocultures. Liang and co-authors (2020) used living and inactivated cells of *M. smegmatis* ATCC 12051 and *Alteromonas* sp. RKMC-009, and suggested that the presence of inactivated cells in the medium reduces the number of potential secondary metabolites of the inducers that could act as chemical signals on the producer, thereby limiting the induction of new metabolites.

In contrast, when living inducer cells are used, competition for carbon and nitrogen sources in the culture medium occurs, which can act as a trigger for the activation of silent biosynthetic pathways.

Not all authors have described in detail the procedure for introducing the inocula prior to the synthesis of secondary metabolites, which makes it difficult to determine whether the cultivation was carried out with an inducer or with competitive microorganisms. For example, Sugiyama et al. (2015, 2016) do not specify the ratio in which the inocula of *S. nigrescens* HEK616 and *T. pulmonis* TP-B0596 were introduced for the synthesis of the natural lipidic metabolite streptoaminal-9n and 5-alkyl-1,2,3,4-tetrahydroquinoline alkaloids. We consider that in these studies *T. pulmonis* TP-B0596 was used as an inducer, as numerous similar articles report that the inocula of *Tsukamurella* actinobacteria were added in significantly smaller

ISSN: 2409-4951 (Online), 2310-1008(Print)

amounts than that of the producers. In Liang et al. (2020), the inocula of the producer *Streptomyces* sp. RKND-216 and the inducers *M. smegmatis* ATCC 12051 and *Alteromonas* sp. RKMC-009 were introduced into the medium in equal amounts; however, this also constitutes cultivation with inducers, since the producer was introduced 72 hours earlier, resulting in a higher biomass.

Among the possible mechanisms inducing the synthesis of new metabolites, the following can be distinguished: (1) Mycolic acid stimulating biosynthesis pathways in actinobacteria (Shamikh et al., 2020); (2) Mycolic acid triggering biosynthetic routes in producer strains, alongside intercellular interactions with inducers (Hoshino et al., 2018c; Onaka et al., 2011); (3) Specific inducer compounds acting without direct cellular contact (Adnani et al., 2017; Maimone, et al., 2021); (4) Horizontal transfer of plasmid DNA resulting in formation of recombinant strains (Kurosawa et al., 2010); (5) Modification of precursors of target product biosynthesis by an inducer (Hoshino et al., 2017); (6) Inducer-stimulating NO synthesis, which mediates transcriptional activation of silent gene clusters (Khalil, et al., 2019).

Secondary metabolites of actinobacteria synthesised in the presence of inducers are mostly characterised by antimicrobial activity. These include the antibiotics alchivemycin A (Onaka et al., 2011), keyicin (Adnani et al., 2017), rhodostreptomycins A and B (Kurosawa et al., 2008), complexes of antibiotic-containing (Shamikh et al., 2020) and new unknown metabolites (Maimone et al., 2021), gordonic acid (Park et al., 2017), the lipid metabolite streptoaminal-9n (Sugiyama et al., 2016), alkaloids 5-alkyl-1,2,3,4-tetrahydroquinolines (Sugiyama et al., 2015), and longicatenamides A–D (Jiang et al., 2021). All these compounds showed antimicrobial activity against various pathogens, supported by specific data. Such secondary metabolites can be considered as potential antiseptic agents for pharmacological and medical use.

In some studies (Hoshino et al., 2018b; Khalil et al., 2019), the diameters of the growth inhibition zones for test cultures were not reported, but the authors noted that umezawamides A and B and heronapyrrole B also exhibit antimicrobial activity.

New metabolites of actinobacteria obtained in the presence of inducers in the culture media may also exhibit cytotoxic or anti-trypanosomal activity. The antibiotics mirilactams C, D, and E (Hoshino et al., 2018c), chojalactones A, B, and C (Hoshino et al., 2015a), and carbazoquinocin G (Liang et al., 2020) showed no antimicrobial activity, but displayed cytotoxic effects against cancer cells, making them potential antitumour agents.

The use of different nutrient media for inoculum growth and cultivation may complicate process scaling to an industrial level. For example, in Hoshino et al. (2018b, c), the inocula was grown on A-3M medium, while cultivation was carried out on V-22 medium. In contrast, Park et al. (2017) and Liang et al. (2020) used the same medium for both purposes (YM-liquid and ISP2m, respectively) making the process technologically feasible for industrial-scale production.

Overall, the technology of cultivating actinobacteria with biological inducers to produce new metabolites appears promising for practical applications, but further data and optimisation of the production process are required.

Effect on metabolite synthesis

As a result of cultivating actinobacteria together with inducers, the concentration of synthesised secondary metabolites may also increase. Representatives of the genus *Streptomyces* are most frequently used as producers in such studies, but Ma et al. (2020) also report the cultivation of rare actinomycetes *Rhodococcus equi* CGMCC14861 together with a prokaryotic inducer. Biological inducers include living cells (Sharma et al., 2017; Yu et al.,

ISSN: 2409-4951 (Online), 2310-1008(Print)

2015), supernatant (Ma et al., 2020; Shi et al., 2017), and inactivated cells (Song et al., 2020). In Wang et al. (2017), *Penicillium chrysogenum* AS 3.5163 was used as an inducer in a rather original physiological state – the evaporated ethyl acetate extract of the supernatant, which, to our knowledge, has not been reported previously in the available literature. The target products are most often antibiotics, such as natamycin (Shi et al., 2017; Wang et al., 2017), valinomycin (Sharma et al., 2017), and rimocidin (Song et al., 2020). Summary information is provided in Table 2.

Table 2

Cultivation of actinobacteria in the presence of inducers: effects on metabolite synthesis

Producer + inducer	Synthesised metabolites	Concentration		Sources
		With inducer	Without inducer	
Inducers - other actinobacteria				
S. lividans TK23 + *T. pulmonis* TP-B0596 (living cells)	Red pigment actinorhodin	1.9×10^2 μM	0.2 μM	Onaka et al., 2011
Streptomyces sp. NZ-6 + *T. pulmonis* TP-B0596 (living cells)	Niizalactam C (multicyclic macrolactam)	1.3 mg/10 L	in 5 times lower	Hoshino et al., 2015b
Inducers – other bacteria				
R. equi CGMCC14861 + *Staphylococcus* sp. MC7 (living cells, supernatant)	Chitin deacetylase	2,974.05± 208.3 U/mL (living cells); 3,153.90 ± 161.49 U/mL (supernatant)	157.61 U/mL	Ma et al., 2020
S. sp. CGMCC4.7185 + *B. mycoides* GMCC1.197 (living cells)	*N-Ac-Trp, bacillamides A and B	14.9 mg/L, 3 mg/L, 13.7 mg/L, respectively	much lower without inducer	Yu et al., 2015
Inducers – fungi				
S. natalensis HW-2 + *P. chrysogenum* AS 3.5163 (evaporated ethyl acetate extract of supernatant)	Antibiotic natamycin	2.49 g/L	1.33 g/L	Wang et al., 2017
S. natalensis HW-2 + *A. niger* AS 3.6472 (living cells, supernatant)	Antibiotic natamycin	0.799 g/L (living cells), 1.62 g/L (supernatant)	0.639 g/L	Wang et al., 2013
S. natalensis HW-2 + *P. chrysogenum* AS 3.5163 (living cells, supernatant)	Antibiotic natamycin	0.975 g/L (living cells), 1.84 g/L (supernatant)	0.639 g/L	Wang et al., 2013
S. natalensis HW-2 + *Aspergillus oryzae* AS 3.2068 (living cells, supernatant)	Antibiotic natamycin	No effect (living cells), inhibition of synthesis (supernatant)	0.639 g/L	Wang et al., 2013
Streptomyces natalus N5 + *A. niger* (strain number not specified, supernatant)	Antibiotic natamycin	1.44 g/L	67% lower	Shi et al., 2017

ISSN: 2409-4951 (Online), 2310-1008(Print)

Producer + inducer	Synthesised metabolites	Concentration		Sources
		With inducer	Without inducer	
S. natalus N5 + *P. chrysogenum,* supernatant	Antibiotic natamycin	1.42 g/L	66% lower	Shi et al., 2017
S. lavendulae ACR-DA1+ *T. velutinum* (living cells)	Antibiotic valinomycin	26.3 g/L	50 mg/L	Sharma et al., 2017
S. noursei ATCC 11455 + *P. rubens* ATCC 28089 (living cells)	DFO-E, DHXC * and argvalin	Increase in concentration	-	Boruta et al., 2023
Inducers – yeasts				
S. natalensis HW-2 + *S. cerevisiae* AS 2.2081 (living cells, supernatant)	Antibiotic natamycin	No effect	0.639 g/L	Wang et al., 2013
S. natalus N5 + *S. cerevisiae* (strain number not specified, supernatant)	Antibiotic natamycin	Increase in concentration	-	Shi et al., 2017
S. lavendulae ACR-DA1 + *S. cerevisiae* (living cells)	Antibiotic valinomycin	67 mg/L	50 mg/L	Sharma et al., 2017
Streptomyces rimosus M527 + *S. cerevisiae* A3 (supernatant, living and inactivated cells)	Antibiotic rimocidin	0.37 g/L (supernatant), 0.3 g/L (living cells), slight increase (inactivated cells)	0.21 g/L	Song et al., 2020

Notes: «–» – data not reported; *N-Ac-Trp - N-acetyltryptamine; DFO-E - desferrioxamine E; DHXC – deshydroxynocardamine

The article (Ma et al., 2020) describes an atypical case of successful cultivation of actinobacteria with an inducer, as living cells and the corresponding supernatant of *Staphylococcus* sp. MC7 were added to the culture medium at higher concentrations than the inoculum of the producer *R. equi* CGMCC14861 (4:1 and 7:5, respectively), resulting in the synthesis of chitin deacetylase at higher concentrations than when the inocula were added in other ratios. In a study by Boruta et al. (2023), although the inocula of *Streptomyces noursei* ATCC 11455 and *Penicillium rubens* ATCC 28089 were added simultaneously, actinomycetes predominated in the total biomass; therefore, in our opinion, this also constitutes cultivation with an inducer.

The presence of the same inducer in the media can lead to multiple effects simultaneously. For example, Onaka et al. (2011) reported that the cultivation of *S. lividans* TK23 together with living cells of *T. pulmonis* TP- B0596 was accompanied by an increase in the concentration of the red pigment actinorhodin and the synthesis of a new pigment, undecylprodigiosin. A similar situation was described by Hoshino et al. (2015b), where cultivation of *Streptomyces* sp. NZ-6 in a medium containing *T. pulmonis* TP-B0596 resulted in an increase in the concentration of niizalactam C and the synthesis of niizalactams A and B, which are not observed in monoculture.

The effect of biological inducers on the synthesis of secondary metabolites by actinobacteria is not always positive. For instance, the presence of living cells of *Aspergillus oryzae* AS 3.2068 and *S. cerevisiae* AS 2.2081, as well as their corresponding supernatants, in the culture medium of *Streptomyces natalensis* HW-2 did not affect the concentration of natamycin (Wang et al.,

ISSN: 2409-4951 (Online), 2310-1008(Print)

2013). Similarly, the cultivation of *Streptomyces lavendulae* ACR-DA1 with living cells of *Trichoderma velutinum* (strain number not specified) was accompanied by a decrease in valinomycin concentration by 23.7 g/L.

Among the possible mechanisms of induction, the authors highlight the influence of mycolic acid on the induction of biosynthetic pathways in producers, as well as the intercellular interaction of actinobacteria with inducers (Onaka et al., 2011), and the action of extracellular signalling substances produced by an inducer (Ma et al., 2020).

Yu and co-authors (2015) abstractly refer to induction as an "inter-species crosstalk strategy," whereas Wang and co-authors (2017) suggest that the increase in natamycin concentration in *S. natalensis* may represent a protective response to the presence of fungi in the culture medium, mediated by changes in the permeability of the producer's membrane and the influx of extracellular calcium as an activator of enzymes involved in antibiotic biosynthesis.

Not all authors have investigated changes in the antimicrobial and cytotoxic activities of synthesised metabolites in the presence of inducers, which raises questions about the cost-effectiveness of the technology of cultivation with inducers for the industrial production of bioproducts. Hoshino and colleagues (Hoshino et al., 2015b) examined the biological activity of niizalactam C; however, this metabolite exhibited neither antimicrobial activity against *C. albicans, B. subtilis*, and *S. cereviciae* (strain numbers not specified), nor cytotoxic activity against P388 mouse leukaemia cells.

Regarding culture media, not all authors described the experimental preparation procedures in detail. For instance, Yu et al. (2015) do not specify the medium used for cultivating *Streptomyces* sp. CGMCC4.7185 with *Bacillus mycoides* CGMCC1.197, and Sharma et al. (2017) do not indicate the medium used for preparing inocula.

Wang and co-authors (2017) employed different nutrient media for the preparation of the inocula of *S. natalensis* HW-2 and *P. chrysogenum* AS 3.5163, which could potentially complicate the scaling-up of the technology to an industrial level.

On the other hand, in the study by Boruta et al. (2023), the cultivation of *S. noursei* ATCC 11455 with an inducer was performed in a laboratory bioreactor rather than in shaking flasks, which may facilitate the scaling-up to an industrial production level.

Therefore, the technology of cultivating actinobacteria with inducers to obtain target products in higher concentrations is both interesting and promising, but requires further in-depth investigation.

Effect on the synthesis and activity of metabolites

The cultivation of actinobacteria in the presence of inducers can simultaneously produce multiple effects on the same metabolites, such as increased concentration and enhanced antimicrobial activity, which is commercially attractive. We identified two such studies (Patin et al., 2018; Sung et al., 2017). The summarised data are shown in Table 3.

The study of *Streptomyces* sp. PTY087I2 cultivation with different bacteria as inducers (Sung et al., 2017) illustrates that each combination of microorganisms must be investigated separately. Thus, in the presence of living cells of *B. subtilis* ATCC 6051, methicillin-resistant *S. aureus* ATCC BAA-1717, and *P. aeruginosa* ATCC 15442 in the culture medium, antibiotics with enhanced antimicrobial activity were synthesised. By contrast, in the presence of methicillin-sensitive *S. aureus* ATCC BAA-1718, no changes in the biological activity of the synthesised metabolites were observed compared with antibiotics produced in monoculture.

From a practical perspective, it is difficult to estimate the concentrations of synthesised secondary metabolites, as Sung and colleagues (Sung et al., 2017) reported the areas under the peaks obtained by liquid chromatography-mass spectrometry, and Patin and his team (Patin et al., 2018) presented graphs showing the variation of peak areas over time. Moreover, the latter study

ISSN: 2409-4951 (Online), 2310-1008(Print)

does not provide specific values for the growth inhibition zones of test cultures on agar-based medium, nor is the cause of their inhibition clarified.

In the article by Sung et al. (2017), the authors suggest that a possible mechanism for the increased concentration and antimicrobial activity of the antibiotic complex is an ecological stressor, i.e., competition between microorganisms for substrate and space. However, Patin et al. (2018) describe the ecological relevance of induction as "often speculative," since most producers and inducers were isolated from different environments and are unlikely to interact in nature.

Table 3

Cultivation of actinobacteria in the presence of inducers: effects on metabolite synthesis and activity

Producer + inducer	Synthesised metabolites	Effects on concentration and biological activity	Sources
Inducers – other bacteria			
Streptomyces sp. PTY087I2 + *B. subtilis* ATCC 6051 (living cells)	Antibiotics granaticin, granatomycin D, dihydrogranaticin B	Increase in concentration by 10.9–13.8-fold. Reduction in MIC (μg/mL) by 4-fold against *B. subtilis* ATCC 6051, 2-fold against methicillin-sensitive *S. aureus* ATCC BAA-1718 and methicillin-resistant *S. aureus* ATCC BAA-1717, with no change against *P. aeruginosa* ATCC 15442	Sung et al., 2017
Streptomyces sp. PTY087I2 + *S. aureus* sensitive to methicillin ATCC BAA-1718 (living cells)	Antibiotics granaticin, granatomycin D, dihydrogranaticin B	Increase in concentration by 2–73.3-fold. No change in antimicrobial activity against *B. subtilis* ATCC 6051, methicillin-sensitive *S. aureus* ATCC BAA-1718, methicillin-resistant *S. aureus* ATCC BAA-1717, and *P. aeruginosa* ATCC 15442	Sung et al., 2017
Streptomyces sp. PTY087I2 + *S. aureus* resistant to methicillin ATCC BAA-1717 (living cells)	Antibiotics granaticin, granatomycin D, dihydrogranaticin B	Increase in concentration by 15.6–25.9-fold. Reduction in MIC (μg/mL) by 16-fold against *B. subtilis* ATCC 6051, 4-fold against methicillin-sensitive *S. aureus* ATCC BAA-1718, 8-fold against methicillin-resistant *S. aureus* ATCC BAA-1717, with no change against *P. aeruginosa* ATCC 15442	Sung et al., 2017
Streptomyces sp. PTY087I2 + *P. aeruginosa* ATCC 15442 (living cells)	Antibiotics granaticin, granatomycin D, dihydrogranaticin B	Increase in concentration by 3.8–7.3-fold. Reduction in MIC (μg/mL) by 4-fold against *B. subtilis* ATCC 6051, methicillin-sensitive *S. aureus* ATCC BAA-1718, and methicillin-resistant *S. aureus* ATCC BAA-1717, with no change against *P. aeruginosa* ATCC 15442	Sung et al., 2017
Salinispora tropica CNY-681 +*Vibrio* sp. CUA-759, (living cells, supernatant)	Lomaiviticin (glycoside), sioxanthin (carotenoid pigment)	Increase in concentrations. Increase in antimicrobial activity of the metabolite complex (living cells), with a slight increase in antimicrobial activity of the metabolite complex (supernatant) against 12 test cultures.	Patin et al., 2018

ISSN: 2409-4951 (Online), 2310-1008(Print)

The available scientific literature also reports the cultivation of *Streptomyces* sp. 2-85 with *Cladosporium* sp. 3-22 (Liu et al., 2024), which was accompanied by the synthesis of a borrelidin complex and its derivatives, with antimicrobial activity increasing by 36.67 and 42.86% against *B. subtilis* ATCC6633 and *Saprolegnia parasitica* YG438, respectively, compared with the control. In addition, four metabolites not observed in the *Streptomyces* sp. 2-85 monoculture were detected, alongside a 7-30-fold increase in the concentration of other metabolites. This study describes an atypical method of culturing the secondary metabolite producer *Streptomyces* sp. 2-85 with other microorganisms, as the inocula of actinobacteria and fungi were prepared together in equal proportions rather than separately, with *Cladosporium* sp. 3-22 dominating the overall biomass.

Therefore, the cultivation of actinobacteria with biological inducers, which is accompanied by multiple simultaneous effects, is commercially attractive but requires further investigation and clarification.

Effect on metabolite activity

The effect of eukaryotic and prokaryotic inducers in the culture media of *Rhodococcus erythropolis* IMV Ac-5017 and *Nocardia vaccinii* IMV B-7405 on the biological activity of surfactants synthesised under these conditions was studied in detail at the Department of Biotechnology and Microbiology, National University of Food Technologies (Table 4).

Table 4

Cultivation of actinobacteria in the presence of inducers: effect on surfactant activity

Producer + inducer	Effect on antimicrobial activity	Effect on antibiofilm activity	Sources
R. erythropolis IMV Ac-5017 + *S. cerevisiae* BTM-1 (living cells)	Increase in antimicrobial activity by 7.5–30 times against bacteria (*E. coli* IEM-1, *Pseudomonas* sp. MI-2, *S. aureus* BMS-1, *B. subtilis* BT-2) and by 60–240 times against yeasts (*C. albicans* D-6, *C. utilis* BVS-65, *S. cerevisiae* BTM-1)	Increase in antibiofilm activity by 9.1–45.4% against bacteria (*E. coli* IEM-1, *Pseudomonas* sp. MI-2, *S. aureus* BMS-1, *B. subtilis* BT-2) and by 27.1–58.9% against yeasts (*C. albicans* D-6, *C. utilis* BVS-65, *S. cerevisiae* BTM-1), as well as by 3–26 and 6–29% against dual-species bacterial and bacterial–yeast biofilms, respectively	Okhmakevych et al., 2025
R. erythropolis IMV Ac-5017 + *S. cerevisiae* BTM-1 (inactivated cells)	Increase in antimicrobial activity by 1.8-3.5 times against bacteria (*E. coli* IEM-1, *Pseudomonas* sp. MI-2, *S. aureus* BMS-1, *B. subtilis* BT-2) and by 7.1-14.1 times against yeasts (*C. albicans* D-6, *C. utilis* BVS-65, *S. cerevisiae* BTM-1)	Increase in antibiofilm activity by 1.2-23.8% against bacteria (*E. coli* IEM-1, *Pseudomonas* sp. MI-2, *S. aureus* BMS-1, *B. subtilis* BT-2) and by 12.1-45.4% against yeasts (*C. albicans* D-6, *C. utilis* BVS-65, *S. cerevisiae* BTM-1), as well as by 1-14 and 2-15% against dual-species bacterial and bacterial–yeast biofilms, respectively	Okhmakevych et al., 2025

ISSN: 2409-4951 (Online), 2310-1008(Print)

Producer + inducer	Effect on antimicrobial activity	Effect on antibiofilm activity	Sources
R. erythropolis IMV Ac-5017 + *S. cerevisiae* BTM-1 (supernatant)	Increase in antimicrobial activity by 3.6-7.3 times against bacteria (*E. coli* IEM-1, *Pseudomonas* sp. MI-2, *S. aureus* BMS-1, *B. subtilis* BT-2) and by 29.1-14.5 times against yeasts (*C. albicans* D-6, *C.utilis* BVS-65, *S. cerevisiae* BTM-1)	Increase in antibiofilm activity by 13.3-38.4% against bacteria (*E. coli* IEM-1, *Pseudomonas* sp. MI-2, *S. aureus* BMS-1, *B. subtilis* BT-2) and by 26.7-51% against yeasts (*C. albicans* D-6, *C. utilis* BVS-65, *S. cerevisiae* BTM-1), as well as by 1-22 and 7-26% against dual-species bacterial and bacterial–yeast biofilms, respectively	Okhmakevych et al., 2025
R. erythropolis IMV Ac-5017 + *E. coli* IEM-1 (living cells)	Increase in antimicrobial activity by 4-16 times against *E. coli* IEM-1, *S. aureus* BMS-1, *B. subtilis* BT-2	Increase in antibiofilm activity by 3.8-16.6% against *B. subtilis* BT-2	Pirog et al., 2020a
R. erythropolis IMV Ac-5017 +*B.subtilis* BT-2 (living cells)	Increase in antimicrobial activity by 8 times against *E. coli* IEM-1, *S. aureus* BMS-1, *B. subtilis* BT-2	Increase in antibiofilm activity by 15.3-23.7% against *B. subtilis* BT-2; by 2.6-20.8% against *C. utilis* BVS-65	Pirog et al., 2020a
N.vaccinii IMV B-7405 + *E. coli* IEM-1 (living cells)	Increase in antimicrobial activity by 4-16, 3.3-6.25, and 2.9-5.8 times for surfactants, synthesised on biodiesel production waste, refined sunflower oil, and fried sunflower oil, respectively, against *E. coli* IEM-1, *B. subtilis* BT-2, *S. aureus* BMS-1, *P. vulgaris* PA-12, *Pseudomonas* sp. MI-2, *E. cloaceae* C-8	Increase in antibiofilm activity by 11-23% against *E. coli* IEM-1; by 19-31% against *B. subtilis* BT-2; by 10-28% against *Pseudomonas* sp. MI-2; and by 8-22% against *S. aureus* BMS-1	Pirog et al., 2020b
N. vaccinii IMV B-7405 + *E. coli* IEM-1 (inactivated cells)	Increase in antimicrobial activity by 3.3-13.3, 5-10, and 3.5-7 times for surfactants, synthesised on biodiesel production waste, refined sunflower oil, and fried sunflower oil, respectively, against *E. coli* IEM-1, *B. subtilis* BT-2, *S. aureus* BMS-1, *P. vulgaris* PA-12, *Pseudomonas* sp. MI-2, *E. cloaceae* C-8	Increase in antibiofilm activity by 10-24% against *E. coli* IEM-1; by 17-29% against *B. subtilis* BT-2; by 11-30% against *Pseudomonas* sp. MI-2; by 14-24% against *S. aureus* BMS-1	Pirog et al., 2020b

ISSN: 2409-4951 (Online), 2310-1008(Print)

Producer + inducer	Effect on antimicrobial activity	Effect on antibiofilm activity	Sources
N. vaccinii IMV B-7405 + *B. subtilis* BT-2 (living cells)	Increase in antimicrobial activity by 2.9-5.7, 3.3-6.7, and 4-8 times for surfactants, synthesised on biodiesel production waste, refined sunflower oil, and fried sunflower oil, respectively, against *E. coli* IEM-1, *B. subtilis* BT-2, *S. aureus* BMS-1, *P. vulgaris* PA-12, *Pseudomonas* sp. MI-2, *E. cloaceae* C-8	Increase in antibiofilm activity by 18-25% against *E. coli* IEM-1; by 23-34% against *B. subtilis* BT-2; by 14-33% against *Pseudomonas* sp. MI-2; and by 20-26% against *S. aureus* BMS-1	Pirog et al., 2020b
N. vaccinii IMV B-7405 + *B. subtilis* BT-2 (inactivated cells)	Increase in antimicrobial activity by 2.5-5, 2.9-5.7, and 2-8 times for surfactants, synthesised on biodiesel production waste, refined sunflower oil, and fried sunflower oil, respectively, against *E. coli* IEM-1, *B. subtilis* BT-2, *S. aureus* BMS-1, *P. vulgaris* PA-12, *Pseudomonas* sp. MI-2, *E. cloaceae* C-8	Increase in antibiofilm activity by 16-21% against *E. coli* IEM-1; by 20-33% against *B. subtilis* BT-2; by 17-35% against *Pseudomonas* sp. MI-2; and by 17-28% against *S. aureus* BMS-1	Pirog et al., 2020b

Thus, it was reported that the surfactants of *R. erythropolis* IMV Ac-5017, synthesised in the presence of living *Saccharomyces* yeast cells, exhibited higher antimicrobial and antibiofilm activity against single- and dual-species biofilms compared with surfactants synthesised in the presence of inactivated *Saccharomyces* cells or the corresponding supernatant (Okhmakevych et al., 2025). It is suggested that both intercellular and biochemical interactions between the surfactant-producing strain and the inducer are important for induction. Furthermore, in comparison with data reported by Pirog et al. (2020a), it is suggested that changes in the inducer also affect the specificity of the activity of the synthesised antimicrobial compounds.

Okhmakevych et al. (2025) and Pirog et al. (2020a) focused on surfactant synthesis exclusively in ethanol-containing media; therefore, further research on alternative substrates, such as technical glycerol or waste sunflower oil, is required. In Pirog et al. (2020a), inoculum preparation of *E. coli* IEM-1 and *B. subtilis* BT-2 was performed on agar medium, which may complicate scaling up the laboratory technology to an industrial level.

Pirog et al. (2020b) investigated the cultivation of *N. vaccinii* IMV B-7405 in the presence of prokaryotic inducers, resulting in the synthesis of surfactants with higher biological activity against bacterial test cultures compared with those obtained without inducers. However, the effects of eukaryotic inducers on surfactant activity and their impact on yeast test cultures were not evaluated, which warrants further investigation.

Therefore, the technology of cultivating actinomycetes with prokaryotic and eukaryotic inducers to enhance the antimicrobial and antibiofilm activity of the synthesised secondary metabolites is potentially attractive for application in the pharmaceutical industry and medicine, but further research is still required.

ISSN: 2409-4951 (Online), 2310-1008(Print)

Actinobacteria as inducers

Actinobacteria can act not only as producers of secondary metabolites but also as inducers, for example, stimulating the synthesis of metabolites that are not characteristic of fungal monocultures. Stroe et al. (2020) showed that cultivation of *Aspergillus fumigatus* ATCC 46645 with living *Streptomyces rapamycinicus* cells (strain number not specified) or with the corresponding supernatant was accompanied by fumigermin synthesis. Wakefield et al. (2017) demonstrated that cultivation of *A. fumigatus* MR2012 in a medium containing living *Streptomyces leeuwenhoekii* C34 cells resulted in the formation of luteoride D, pseurotin G, terezine D, and 11-O-methylpseurotin A, none of which are typical of fungal monocultures.

Selegato et al. (2023) distinguished two types of induction: single-culture activation and multispecies induction. Whereas the former is widely reported in the scientific literature, the latter remains relatively rare. Wakefield et al. (2017) described bilateral microbial crosstalk occurring within the same cultivation flask, as the concentrations of chaxapeptin and nocardiamin produced by *S. leeuwenhoekii* C34 increased during interaction with the fungus. However, the biological activity of the metabolites formed was not investigated, which raises questions regarding their potential practical applications. Stroe et al. (2020) prepared the fungal inoculum in minimal AMM medium and the actinobacterial inoculum in M79 medium, an approach that may complicate process scaling to the production level.

Therefore, the use of actinobacteria as inducers also requires further investigation and optimisation.

Conclusions

Technologies for cultivating actinobacteria with biological inducers to obtain metabolites that are not characteristic of monocultures, or metabolites with higher concentrations and/or enhanced biological activity, are highly promising. However, the mechanisms by which inducers influence the biosynthesis of secondary metabolites remain insufficiently studied and require further investigation. Additional research is also needed to evaluate the antimicrobial, antibiofilm, cytotoxic, and antitrypanosomal activities of secondary metabolites synthesised in the presence of inducers, as these properties largely determine the feasibility of their industrial production and practical applications. Furthermore, optimisation of nutrient media for both inoculum preparation and metabolite biosynthesis is necessary, since the use of a single medium is more practical and economically advantageous for industrial-scale production. Finally, approaches in which an inducer promotes the synthesis of a complex of metabolites rather than a single product appear especially promising, as they may facilitate the development of integrated industrial technologies for the production of actinobacterial secondary metabolites.

References

Adnani N., Vazquez-Rivera E., Adibhatla S.N., Ellis G.A., Braun D.R., Bugni T.S. (2015), Investigation of interspecies interactions within marine *Micromonosporaceae* using an improved co-culture approach, *Marine Drugs*, 13(10), pp. 6082–6098. https://doi.org/10.3390/md13106082

Adnani N., Chevrette M.G., Adibhatla S.N., Zhang F., Yu Q., Braun D.R., Nelson J., Simpkins S.W., McDonald B.R., Myers C.L., Piotrowski J.S., Thompson C.J., Currie C.R., Li L.,

ISSN: 2409-4951 (Online), 2310-1008(Print)

Rajski S.R., Bugni, T.S. (2017), Coculture of marine invertebrate-associated bacteria and interdisciplinary technologies enable biosynthesis and discovery of a new antibiotic, keyicin, *ACS Chemical Biology*, 12(12), pp. 3093–3102. https://doi.org/10.1021/acschembio.7b00688

Alam A.A., Goda D.A., Soliman N.A., Abdel-Meguid D.I., El-Sharouny E.E., Sabry S.A. (2022), Production and statistical optimization of cholesterol-oxidase generated by *Streptomyces* sp. AN strain, *Journal, Genetic Engineering & Biotechnology*, 20(1), 156. https://doi.org/10.1186/s43141-022-00433-1

Alhadrami H.A., Thissera B., Hassan M.H.A., Behery F.A., Ngwa C.J., Hassan H.M., Pradel G., Abdelmohsen U.R., Rateb, M.E. (2021), Bio-guided isolation of antimalarial metabolites from the coculture of two red sea sponge-derived *Actinokineospora* and *Rhodococcus* spp., *Marine Drugs*, 19(2), 109. https://doi.org/10.3390/md19020109

Boruta T., Ścigaczewska A. (2021), Enhanced oxytetracycline production by *Streptomyces rimosus* in submerged co-cultures with *Streptomyces noursei*, *Molecules (Basel, Switzerland)*, 26(19), 6036. https://doi.org/10.3390/molecules26196036

Boruta T., Ścigaczewska A., Bizukojć M. (2023), Investigating the stirred tank bioreactor co-cultures of the secondary metabolite producers *Streptomyces noursei* and *Penicillium rubens*, *Biomolecules*, 13(12), 1748. https://doi.org/10.3390/biom13121748

Gamaleldin N.M., Bakeer W., Sayed A.M., Shamikh Y.I., El-Gendy A.O., Hassan H.M., Horn H., Abdelmohsen U.R., Hozzein W.N. (2020), Exploration of chemical diversity and antitrypanosomal activity of some Red sea-derived actinomycetes using the OSMAC approach supported by LC-MS-based metabolomics and molecular modelling, *Antibiotics (Basel, Switzerland)*, 9(9), 629. https://doi.org/10.3390/antibiotics9090629

Hoshino S., Wakimoto T., Onaka H., Abe I. (2015a), Chojalactones A-C, cytotoxic butanolides isolated from *Streptomyces* sp. cultivated with mycolic acid containing bacterium, *Organic Letters*, 17(6), pp. 1501–1504. https://doi.org/10.1021/acs.orglett.5b00385

Hoshino S., Okada M., Wakimoto T., Zhang H., Hayashi F., Onaka H., Abe I. (2015b), Niizalactams A-C, multicyclic macrolactams isolated from combined culture of *Streptomyces* with mycolic acid-containing bacterium, *Journal of Natural Products*, 78(12), pp. 3011–3017. https://doi.org/10.1021/acs.jnatprod.5b00804

Hoshino S., Zhang L., Awakawa T., Wakimoto T., Onaka H., Abe I. (2015c), Arcyriaflavin E, a new cytotoxic indolocarbazole alkaloid isolated by combined-culture of mycolic acid-containing bacteria and *Streptomyces cinnamoneus* NBRC 13823, *The Journal of Antibiotics*, 68(5), pp. 342–344. https://doi.org/10.1038/ja.2014.147

Hoshino S., Okada M., Onaka H., Abe I. (2016), Effective production of aromatic polyketides in *Streptomyces* using a combined-culture method, *Natural Product Communications*, 11(7), pp. 979–981.

Hoshino S., Okada M., Awakawa T., Asamizu S., Onaka H., Abe I. (2017), Mycolic acid containing bacterium stimulates tandem cyclization of polyene macrolactam in a lake sediment derived rare actinomycete, *Organic Letters*, 19(18), pp. 4992–4995. https://doi.org/10.1021/acs.orglett.7b02508

Hoshino S., Ozeki M., Awakawa T., Morita H., Onaka H., Abe I. (2018a), Catenulobactins A and B, heterocyclic peptides from culturing *Catenuloplanes* sp. with a mycolic acid-containing bacterium, *Journal of Natural Products*, 81(9), pp. 2106–2110. https://doi.org/10.1021/acs.jnatprod.8b00261

Hoshino S., Wong C.P., Ozeki M., Zhang H., Hayashi F., Awakawa T., Asamizu S., Onaka H., Abe I. (2018b), Umezawamides, new bioactive polycyclic tetramate macrolactams isolated from a combined-culture of *Umezawaea* sp. and mycolic acid-containing bacterium, *The Journal of Antibiotics*, 71(7), pp. 653–657. https://doi.org/10.1038/s41429-018-0040-4

Hoshino S., Ozeki M., Wong C.P., Zhang H., Hayashi F., Awakawa T., Morita H., Onaka H., Abe I. (2018c), Mirilactams C-E, novel polycyclic macrolactams isolated from combined-culture of *Actinosynnema mirum* NBRC 14064 and mycolic acid-containing bacterium, *Chemical*

ISSN: 2409-4951 (Online), 2310-1008(Print)

& Pharmaceutical Bulletin, 66(6), pp. 660–667. https://doi.org/10.1248/cpb.c18-00143

Jiang Y., Matsumoto T., Kuranaga T., Lu S., Wang W., Onaka H., Kakeya H. (2021), Longicatenamides A-D, two diastereomeric pairs of cyclic hexapeptides produced by combined-culture of *Streptomyces* sp. KUSC F05 and *Tsukamurella pulmonis* TP-B0596, *The Journal of Antibiotics*, 74(5), pp. 307–316. https://doi.org/10.1038/s41429-020-00400-3

Khalil Z.G., Cruz-Morales P., Licona-Cassani C., Marcellin E., Capon R.J. (2019), Inter-kingdom beach warfare: microbial chemical communication activates natural chemical defences, *The ISME Journal*, 13(1), pp. 147–158. https://doi.org/10.1038/s41396-018-0265-z

Khedkar M., Bedade D., Singhal R.S., Bankar S.B. (2025), Mixed culture cultivation in microbial bioprocesses, *Advances in Biochemical Engineering/Biotechnology*, 189, pp. 9–69. https://doi.org/10.1007/10_2023_248

Kurosawa K., Ghiviriga I., Sambandan T.G., Lessard P.A., Barbara J.E., Rha C., Sinskey A.J. (2008), Rhodostreptomycins, antibiotics biosynthesized following horizontal gene transfer from *Streptomyces padanus* to *Rhodococcus fascians*, *Journal of the American Chemical Society*, 130(4), pp. 1126–1127. https://doi.org/10.1021/ja077821p

Kurosawa K., Maceachran D.P., Sinskey A.J. (2010), Antibiotic biosynthesis following horizontal gene transfer: new milestone for novel natural product discovery?, *Expert Opinion on Drug Discovery*, 5(9), pp. 819–825. https://doi.org/10.1517/17460441.2010.505599

Liang L., Wang G., Haltli B., Marchbank D.H., Stryhn H., Correa H., Kerr R.G. (2020), Metabolomic comparison and assessment of co-cultivation and a heat-killed inducer strategy in activation of cryptic biosynthetic pathways, *Journal of Natural Products*, 83(9), pp. 2696–2705. https://doi.org/10.1021/acs.jnatprod.0c00621

Liu T., Gui X., Zhang G., Luo L., Zhao J. (2024), *Streptomyces*-fungus co-culture enhances the production of borrelidin and analogs: a genomic and metabolomic approach, *Marine Drugs*, 22(7), 302. https://doi.org/10.3390/md22070302

Ma Q., Gao X., Tu L., Han Q., Zhang X., Guo Y., Yan W., Shen Y., Wang M. (2020), Enhanced chitin deacetylase production ability of *Rhodococcus equi* CGMCC14861 by co-culture fermentation with *Staphylococcus* sp. MC7, *Frontiers in Microbiology*, 11, 592477. https://doi.org/10.3389/fmicb.2020.592477

Maglangit F., Fang Q., Kyeremeh K., Sternberg J.M., Ebel R., Deng, H. (2020), A co-culturing approach enables discovery and biosynthesis of a bioactive indole alkaloid metabolite, *Molecules (Basel, Switzerland)*, 25(2), 256. https://doi.org/10.3390/molecules25020256

Maimone N.M., de Oliveira L.F.P., Santos S.N., de Lira S.P. (2021), Elicitation of *Streptomyces lunalinharesii* secondary metabolism through co-cultivation with *Rhizoctonia solani*, *Microbiological Research*, 251, 126836. https://doi.org/10.1016/j.micres.2021.126836

Okhmakevych A., Pirog T., Kliuchka L. (2025), Dependence of biological activity of surfactants synthesized by *Rhodococcus erythropolis* IMV Ac-5017 on physiological state of yeast inducer, *Ukrainian Food Journal*, 14(1), pp. 111-126. http://doi.org/10.24263/2304-974X-2025-14-1-11

Onaka H., Mori Y., Igarashi Y., Furumai T. (2011), Mycolic acid-containing bacteria induce natural-product biosynthesis in *Streptomyces species*, *Applied and Environmental Microbiology*, 77(2), pp. 400–406. https://doi.org/10.1128/AEM.01337-10

Park H.B., Park J.S., Lee S.I., Shin B., Oh D.C., Kwon H.C. (2017), Gordonic acid, a polyketide glycoside derived from bacterial coculture of *Streptomyces* and *Gordonia* species, *Journal of Natural Products*, 80(9), pp. 2542–2546. https://doi.org/10.1021/acs.jnatprod.7b00293

Patin N.V., Floros D.J., Hughes C.C., Dorrestein P.C., Jensen P.R. (2018), The role of inter-species interactions in *Salinispora* specialized metabolism, *Microbiology (Reading, England)*, 164(7), pp. 946–955. https://doi.org/10.1099/mic.0.000679

Pirog T.P., Skrotska O.I., Shevchuk T.A. (2020a), Influence of biological inducers on

ISSN: 2409-4951 (Online), 2310-1008(Print)

antimicrobial, antiadhesive activity and biofilm destruction by *Nocardia vaccinii* IMV B-7405 surfactants, *Microbiological Journal*, 82(3), pp. 35-44. https://doi.org/10.15407/microbiolj82.03.035

Pirog T., Kluchka L., Skrotska O., Stabnikov V. (2020b), The effect of co-cultivation of *Rhodococcus erythropolis* with other bacterial strains on biological activity of synthesized surface-active substances, *Enzyme and Microbial Technology*, 142, 109677. https://doi.org/10.1016/j.enzmictec.2020.109677

Pirog T.P., Okhmakevych A.M. (2025), Co-cultivation as a factor regulating the secondary metabolism of actinobacteria, *Scientific Works of NUFT*, 31(3), pp. 74-87. https://doi.org/10.24263/2225-2924-2025-31-3-7

Pirog T.P., Parfeniuk M.A., (2023), Influence of competitive eukaryotic microorganisms on the synthesis and properties of secondary metabolites. Part 1. Micromycetes as regulators of the synthesis and biological activity of secondary metabolites, *Scientific Works of NUFT*, 29(3), pp. 33-49. https://doi.org/10.24263/2225-2924-2023-29-3-5

Selegato D.M., Castro-Gamboa I. (2023), Enhancing chemical and biological diversity by co-cultivation, *Frontiers in Microbiology*, 14, 1117559. https://doi.org/10.3389/fmicb.2023.1117559

Shamikh Y.I., El Shamy A.A., Gaber Y., Abdelmohsen U.R., Madkour H.A., Horn H., Hassan H.M., Elmaidomy A.H., Alkhalifah D.H.M., Hozzein W.N. (2020), Actinomycetes from the Red sea sponge *Coscinoderma mathewsi*: isolation, diversity, and potential for bioactive compounds discovery, *Microorganisms*, 8(5), 783. https://doi.org/10.3390/microorganisms8050783

Sharma R., Jamwal V., Singh V.P., Wazir P., Awasthi P., Singh D., Vishwakarma R. A., Gandhi S. G., Chaubey A. (2017), Revelation and cloning of valinomycin synthetase genes in *Streptomyces lavendulae* ACR-DA1 and their expression analysis under different fermentation and elicitation conditions, *Journal of Biotechnology*, 253, pp. 40–47. https://doi.org/10.1016/j.jbiotec.2017.05.008

Shi S., Tao Y., Liu W. (2017), Effects of fungi fermentation broth on natamycin production of *Streptomyces*, *Progress Applied Microbiology*, 1(1), pp. 15-22.

Singh B., Kumar A., Saini A.K., Saini R.V., Thakur R., Mohammed S.A., Tuli H. S., Gupta V.K., Areeshi M.Y., Faidah H., Jalal N.A., Haque S. (2023), Strengthening microbial cell factories for efficient production of bioactive molecules, *Biotechnology & Genetic Engineering Reviews*, 39(2), pp. 1345–1378. https://doi.org/10.1080/02648725.2023.2177039

Song Z., Ma Z., Bechthold A., Yu X. (2020), Effects of addition of elicitors on rimocidin biosynthesis in *Streptomyces rimosus* M527, *Applied Microbiology and Biotechnology*, 104(10), pp. 4445–4455. https://doi.org/10.1007/s00253-020-10565-4

Stroe M.C., Netzker T., Scherlach K., Krüger T., Hertweck C., Valiante V., Brakhage A.A. (2020), Targeted induction of a silent fungal gene cluster encoding the bacteria-specific germination inhibitor fumigermin, *eLife*, 9, e52541. https://doi.org/10.7554/eLife.52541

Sugiyama R., Nishimura S., Ozaki T., Asamizu S., Onaka H., Kakeya H. (2015), 5-Alkyl-1,2,3,4-tetrahydroquinolines, new membrane-interacting lipophilic metabolites produced by combined culture of *Streptomyces nigrescens* and *Tsukamurella pulmonis*, *Organic Letters*, 17(8), pp. 1918–1921. https://doi.org/10.1021/acs.orglett.5b00607

Sugiyama R., Nishimura S., Ozaki T., Asamizu S., Onaka H., Kakeya H. (2016), Discovery and total synthesis of streptoaminals: antimicrobial [5,5]-spirohemiaminals from the combined-culture of *Streptomyces nigrescens* and *Tsukamurella pulmonis*, *Angewandte Chemie (International ed. in English)*, 55(35), pp. 10278–10282. https://doi.org/10.1002/anie.201604126

Sung A.A., Gromek S.M., Balunas M.J. (2017), Upregulation and identification of antibiotic activity of a marine-derived *Streptomyces* sp. via co-cultures with human pathogens, *Marine Drugs*, 15(8), 250. https://doi.org/10.3390/md15080250

Wakefield J., Hassan H.M., Jaspars M., Ebel R., Rateb M.E. (2017), Dual Induction of new

ISSN: 2409-4951 (Online), 2310-1008(Print)

microbial secondary metabolites by fungal bacterial co-cultivation, *Frontiers in Microbiology*, 8, 1284. https://doi.org/10.3389/fmicb.2017.01284

Wang D., Yuan J., Gu S., Shi Q. (2013), Influence of fungal elicitors on biosynthesis of natamycin by *Streptomyces natalensis* HW-2, *Applied Microbiology and Biotechnology*, 97(12), pp. 5527–5534. https://doi.org/10.1007/s00253-013-4786-0

Wang Y., Wang L., Zhuang Y., Kong F., Zhang C., Zhu W. (2014), Phenolic polyketides from the co-cultivation of marine-derived *Penicillium* sp. WC-29-5 and *Streptomyces fradiae* 007, *Marine Drugs*, 12(4), pp. 2079–2088. https://doi.org/10.3390/md12042079

Wang D., Wei L., Zhang Y., Zhang M., Gu S. (2017), Physicochemical and microbial responses of *Streptomyces natalensis* HW-2 to fungal elicitor, *Applied Microbiology and Biotechnology*, 101(17), pp. 6705–6712. https://doi.org/10.1007/s00253-017-8440-0

Wang K., Liu N., Shang F., Huang J., Yan B., Liu M., Huang Y. (2021), Activation of secondary metabolism in red soil-derived *Streptomycetes* via co-culture with mycolic acid-containing bacteria, *Microorganisms*, 9(11), 2187. https://doi.org/10.3390/microorganisms9112187

Yu L., Hu Z., Ma Z. (2015), Production of bioactive tryptamine derivatives by co-culture of marine *Streptomyces* with *Bacillus mycoides*, *Natural Product Research*, 29(22), pp. 2087–2091. https://doi.org/10.1080/14786419.2015.1005619

Author identifiers ORCID

Anastasiia Okhmakevych 0009-0004-3849-1543

Tetiana Pirog 0000-0002-3873-2253

Cite:

Ukr J Food Sci Style

Okhmakevych A., Pirog T. (2025), Biological inducers as regulators of secondary metabolite biosynthesis in actinobacteria, *Ukrainian Journal of Food Science*, 13(2), pp. 254–273, https://doi.org/10.24263/2310-1008-2025-13-2-11

APA Style

Okhmakevych, A., & Pirog, T. (2025). Biological inducers as regulators of secondary metabolite biosynthesis in actinobacteria. *Ukrainian Journal of Food Science, 13*(2), 254–273. https://doi.org/10.24263/2310-1008-2025-13-2-11

ISSN: 2409-4951 (Online), 2310-1008(Print)

Optical grain sorting machines: review of principles of operation and classification

Dmytro Galka, Andrii Sharan

National University of Food Technologies, Kyiv, Ukraine

Keywords:

Grain
Sorting machine
Optical
Impurities
Classification

Article history:

Received 18.05.2025
Received in revised form 23.10.2025
Accepted 31.12.2025

Corresponding author:

Dmytro Galka
E-mail: dima.halka@gmail.com

DOI:
10.24263/2310-1008-2025-13-2-12

Abstract

Introduction. This review summarizes the operating principles and current engineering solutions of Optical Grain Sorting Machines and synthesizes a practical classification to support equipment selection and process tuning for specific crops and quality and safety targets.

Materials and methods. A staged literature search and screening workflow was applied in Web of Science, Scopus, and Google Scholar using Ukrainian and English keyword combinations and predefined relevance criteria, with a primary focus on 2010-2025 publications. The selected evidence was then extracted and systematized to synthesize a generalized classification of Optical Grain Sorting Machines.

Results and discussion. Optical Grain Sorting Machines can be described as a set of functional subsystems: feeding/stream formation, optical acquisition, decision making, rejection and routing, cleaning/diagnostics, and control/integration. Sorting grain targets fall into distinct groups, separating defective kernels from plant, mineral, technogenic, and biological contaminants. Optical Grain Sorting Machines can be compared within a single multidimensional classification defined by six axes: sorting type, structural design and flow handling, automation/intelligent-control level, application focus, crop specificity, and optical-system characteristics. Sorting cues are summarized in a feature taxonomy that links each target group to practical indicators. It covers color/spectral, shape/size (morphometric), texture/surface-defect, and internal/chemical signatures, and also accounts for how cues are observed (surface vs. volumetric; static vs. dynamic) and how they are used in decisions (primary, auxiliary, indicator). This framework makes commercial solutions easier to compare and helps justify sensor and spectral-channel selection for a given crop and impurity profile.

Conclusion. Optical Grain Sorting Machines are a strategically important final-stage technology for quality and safety assurance in grain processing, and the proposed multidimensional classification provides a practical basis for selecting sensor modalities, machine design, and control settings according to the crop, defect types, and target performance indicators.

Introduction

The problem of grain cleaning

During harvesting, transportation, and primary processing, grain lots inevitably contain impurities and a fraction of defective kernels that enter the stream together with the base crop. Even after preliminary cleaning, some problematic material remains because it is physically similar to sound grain or because defects are not visible in bulk handling (Pascale et al., 2022).

This is critical because residual impurities and defective kernels reduce commercial quality, increase wear and maintenance of processing equipment, and, most importantly, can compromise safety when fungal infection and mycotoxin contamination are present even at low levels. As a result, the risk is not limited to downgraded product grade but may extend to exceeding regulatory limits for hazardous compounds (Femenias et al., 2022; Freitag et al., 2022; Kos et al., 2023; McMullin et al., 2015).

Conventional mechanical cleaning is highly effective for removing impurities that differ markedly in size, density, or aerodynamic properties, yet it cannot reliably separate kernels and inclusions that closely match the base crop in mass and geometry, nor can it assess internal or early-stage defects (Abdullayev and Huseynzade, 2025). Therefore, more selective approaches based on optical features (color, texture, fluorescence, and spectral response) are required to detect and remove subtle defects and hazardous contaminants that remain beyond the resolution of purely mechanical separation (Ageh et al., 2025).

Advantages of optical sorting methods

Optical sorting belongs to a group of methods that operate not on the integral mass-geometric characteristics of kernels, but on their optical and morphological features (Abdullayev and Huseynzade, 2025; Yang et al., 2025). Unlike conventional mechanical cleaning-where the decision to remove a particle is based on its size, density, or aerodynamic properties-optical sorters analyze color, brightness, spectral reflectance, surface texture, and grain shape in real time (Abdullayev and Huseynzade, 2025; Feng et al., 2019; Zhu et al., 2021). This enables the detection and removal of problematic kernels that are virtually indistinguishable from sound grain in terms of mass and geometric parameters, yet exhibit characteristic visual or spectral differences (discoloration, darkening, localized spots, signs of micromycete infection) (Femenias et al., 2022; Feng et al., 2019; Kecskes-Nagy et al., 2016).

A key advantage of optical methods is their high selectivity toward specific groups of impurities and defective kernels (Abdullayev and Huseynzade, 2025; Yang et al., 2025). Depending on the configuration of illumination sources and sensors, the machine can respond to changes in the visible range, the near-infrared (NIR) region (Abdullayev and Huseynzade, 2024), the ultraviolet region, as well as to fluorescence and other specific optical effects, including polarization-dependent reflectance, differences in angular scattering, the specular component (gloss), and effects associated with translucency and surface microstructure (Feng et al., 2019; Masilamani et al., 2020). This enables the targeted removal of kernels with an elevated risk of mycotoxicosis, sprouted kernels, kernels with a darkened germ, as well as specific types of plant, mineral, or artificial contaminants that differ in color or spectral signature but are not always detectable at the mechanical cleaning stage (Carmack et al., 2019; Femenias et al., 2022; Graves et al., 1998; Jia et al., 2020; Kecskes-Nagy et al., 2016; Pearson et al., 2009).

Another important advantage is the inherent “kernel-by-kernel” decision-making paradigm. Each kernel or particle within the optical system’s field of view is analyzed individually, and the rejection decision is made based on a selected set of features and predefined thresholds (Feng et

ISSN: 2409-4951 (Online), 2310-1008(Print)

al., 2019; Yang et al., 2025; Zhu et al., 2021). In practice, this not only reduces the proportion of undesirable components in the target product, but also enables more precise control of sound-grain losses by adjusting the trade-off between cleaning intensity and acceptable losses (Carmack et al., 2019; Kecskes-Nagy et al., 2016). Optical sorters often support multiple sorting modes (e.g., "main product - reject - rework"), enabling flexible redistribution of streams according to the requirements of a given process (Abdullayev and Huseynzade, 2025; Yang et al., 2025).

A major advantage of modern optical systems is their programmability and adaptability (Abdullayev and Huseynzade, 2025; Maier et al., 2024). Changing the crop, target product, or end-quality requirements typically does not require equipment replacement, but rather adjustment of software settings, such as color- or spectrum-based sensitivity regions, trigger thresholds, and masks for analyzing specific kernel areas. This significantly reduces line changeover time when switching between crops (e.g., wheat-barley-maize-rice) and allows the same hardware platform to be used across a wide range of processing tasks (Abdullayev and Huseynzade, 2025; Zareiforoush et al., 2015).

From a resource-efficiency perspective, optical sorting provides additional opportunities to improve the efficiency of raw material utilization (Maier et al., 2024). First, it enables reductions in losses of sound grain by more precisely removing impurities and defective kernels that were previously separated together with a portion of the good fraction by coarse mechanical methods (Cujbescu et al., 2023; Kautzman et al., 2015). Second, reducing the content of problematic kernels in a batch at early stages of the process chain helps avoid unproductive costs associated with further processing of off-spec raw material and decreases the load on cleaning facilities and finished-product quality control systems (Delwiche et al., 2005; Dowell et al., 2002). Third, the ability to selectively separate specific fractions (e.g., severely infected or discolored kernels) creates potential for their dedicated utilization or disposal in the safest manner (Abdullayev and Huseynzade, 2025; Carmack et al., 2019; Yang et al., 2025).

Finally, modern optical sorters integrate naturally into the concept of digitalization in food technologies. Most industrial machines are equipped with tools for recording sorting statistics, transmitting data to supervisory control systems, and enabling remote monitoring and configuration (Abdullayev and Huseynzade, 2025; Rakipov et al., 2025). This transforms optical sorting not only into a tool for the physical cleaning of grain, but also into a real-time source of information on raw material quality, which should be taken into account when developing integrated resource-saving grain-processing technologies (Abdullayev and Huseynzade, 2025; Rakipov et al., 2025).

The aim of this review is to synthesize the physical principles and contemporary technical solutions of optical grain sorting and to develop generalized classifications of Optical Grain Sorting Machines and the optical features used to discriminate kernels from impurities. The study integrates scientific literature with evidence from industrial equipment and proposes an original multidimensional framework derived from the analysis of commercial sorter models.

Materials and methods

Approach to structuring the literature review

The review was conducted in a staged manner and included: searching for scientific sources, initial screening against formal criteria, in-depth content assessment, systematization and synthesis of the retrieved data, and the development of a classification of optical grain sorting machines. The search and selection strategy was designed in accordance with recommendations for scoping and systematic reviews reported by M. D. J. Peters and A. Carrera-Rivera (Carrera-

ISSN: 2409-4951 (Online), 2310-1008(Print)

Rivera et al., 2022; Peters et al., 2021), with adaptation to the applied engineering specificity of optical grain sorting.

The literature search was performed using keywords and their combinations in Ukrainian and English across bibliographic and full-text databases, including Web of Science, Scopus, Google Scholar, as well as other available electronic resources. Search queries were structured to cover the key directions of the review: (1) the design, architecture, and operating principles of optical grain sorters (including the feeding unit, inspection zone, and rejection system); (2) sensing and illumination systems and optical/spectral inspection approaches; (3) optical features of impurities and kernel defects; and (4) algorithmic data-analysis methods - image processing, spectral analysis, machine learning, and deep learning - for automated recognition of objects in grain streams.

The formal criteria for the initial screening included the publication type (original research articles and reviews), thematic relevance to sorting in grain streams, absence of duplicates, and availability of the full text (open access or via institutional resources). During the in-depth assessment, priority was given to studies that concurrently reported experimental results (sorting performance/quality metrics), described the equipment design and operating principle, and detailed the features and methods used to discriminate grain kernels, impurities, and defective components.

The primary body of sources was limited to the period 2010-2025, which captures the current state of development of optical systems and data-analysis algorithms for sorting tasks. Publications published before 2010 were included when they were foundational to specific aspects of the topic (in particular, historical background and the evolution of optical sorters) and lacked fully comparable, more recent counterparts. To broaden the set of relevant sources, the reference lists of the selected publications were also screened, which enabled the identification of additional studies and reduced the risk of missing important work.

Approach to developing a generalized classification of machines

The development of a generalized classification of optical grain sorting machines and optical features was conducted as a separate stage of the study, grounded in the compiled body of literature. The underlying assumption was that no single criterion (e.g., spectral range alone or conveying system type alone) can fully capture the diversity of design and functional solutions; therefore, the classification was designed to be multidimensional. For each machine model, a combination of attributes was analyzed, including sorting type (color-based; color-and-shape; color-and-spectral properties), the feeding method and grain-stream formation, the level of automation, the intended application, the operating spectral range and sensor type, and the target crops. The key grouping criteria and the concept of the generalized classification were previously presented and discussed in conference papers (Galka and Sharan, 2025a, 2025b).

In the first stage, models were grouped according to similar design and operational characteristics, identifying "prototype" machine configurations (chute-fed, belt-based, and hybrid; mono- and multispectral; laboratory and industrial, etc.). In the second stage, a "cross-cutting" analysis was performed to determine how consistently the same models were assigned to the same groups under different criteria and to identify the attributes that proved most informative for characterizing differences between equipment classes. As a result, several complementary dimensions of the classification were established: sorting type; design features and stream-handling approach; level of automation; application focus; optical-system characteristics; and orientation toward specific cereal crops.

A similar approach was applied to the classification of optical features. Based on descriptions in scientific publications and technical documentation, the features used to discriminate grain

ISSN: 2409-4951 (Online), 2310-1008(Print)

kernels and impurities were first grouped into broad categories according to their physical nature (color-spectral, morphometric, textural, surface-defect features, and internal/chemical features). The classification was then refined by considering the observation modality (surface vs. volumetric; static vs. motion-dependent) and the role of each feature in decision-making (primary, auxiliary, or indicative). The final classifications of machines and features represent an authorial proposal that synthesizes the available evidence and provides a structured framework for further research and for practical selection of optical sorters.

Results and discussion

Historical aspects of the development of optical grain sorting machines

Before the advent of mechanized cleaning systems, impurities and defective kernels were removed predominantly by manual picking, which was associated with high labor intensity and subjective quality assessment (Xu et al., 2024; Yang et al., 2025). The earliest attempts to mechanize the conditioning of grain mass relied exclusively on mechanical and pneumatic principles (Olkhovskyi and Dudarev, 2021). In industrial practice, fan-based and screen (sieve) separators gradually became established, combining the effects of gravity, air flows, and geometric separation on sieves (Aliev, 2020; Olkhovskyi and Dudarev, 2021). Subsequently, these devices evolved into multi-stage grain-cleaning units incorporating vibrating sieves, adjustable aspiration, and gravity tables (Kharchenko et al., 2024). However, even advanced mechanical process schemes retained a fundamental limitation: they could not reliably remove impurities and defective kernels similar in size and mass to the main fraction, which motivated a shift toward alternative physical sorting principles, including optical methods (Abdullayev and Huseynzade, 2025; Carmack et al., 2019; Kozłowski et al., 2024; Maier et al., 2024; Pascale et al., 2022; Yang et al., 2025).

Early attempts to exploit optical properties of materials in food technologies involved simple photoelectric devices capable of distinguishing only the presence or absence of an object or coarse color differences (He et al., n.d.; Inamdar and Suresh, 2014). In the 1930s-1940s, industrial machines emerged that employed selective color-based recognition for sorting seeds, peas, and legumes; during this period, the first photoelectric sorters with vacuum-tube components and rudimentary threshold-trigger circuits were described in Europe and North America (Yang et al., 2025). Such solutions include early photoelectric sorters developed in the 1930s, in which individual particles sequentially passed through the inspection zone of a photoelectric sensor and the resulting signal actuated a reject mechanism, as well as early UK serial machines developed by Gunson's SORTEX (founded in 1947), such as the G1 electronic separator used for sorting peas and beans, which laid the groundwork for later grain-sorting machines (Abdullayev and Huseynzade, 2025). Although their throughput and reliability were limited, these developments laid the groundwork for the subsequent advancement of machine "vision" in post-harvest grain processing (Abdullayev and Huseynzade, 2025; Maier et al., 2024).

Further technological progress in the 1950s-1960s was associated with the emergence of more sensitive photoelectric sensors, improvements in illumination systems, and a transition from purely laboratory setups to industrial continuous-operation separators (Pasikatan and Dowell, 2001; Yang et al., 2025). Manufacturers began the mass production of color sorters for rice, coffee, and legumes, and subsequently for cereal grains (Abdullayev and Huseynzade, 2025). This period was characterized by the use of narrow-band optical filters and multiple photoelectric sensors tuned to monitor specific spectral bands, enabling, for example, the separation of darkened or discolored kernels from the bulk grain stream (Pasikatan and Dowell, 2001). Nevertheless, the

ISSN: 2409-4951 (Online), 2310-1008(Print)

systems remained single-channel or dual-channel, and the analysis was limited to an integral signal from a small area of the kernel surface (Pasikatan and Dowell, 2001; Yang et al., 2025).

Already at the early stages of optical sorting technology development, specific tasks were formulated specifically for cereal grains (Maier et al., 2024; Pasikatan and Dowell, 2001). A classic example is the removal of ergot from rye seed, where conventional mechanical methods proved inefficient due to the similar size and mass of kernels and sclerotia, whereas differences in coloration enabled reliable separation of these components based on optical features (Pasikatan and Dowell, 2001). Another important direction was the sorting of seed by germination capacity and the degree of disease infestation, while in breeding practice, color traits (e.g., red- and green-kernel forms of wheat and other crops) were used for automated selection of desirable genotypes (Carmack et al., 2019; Cujbescu et al., 2023).

A defining stage in the development of modern optical grain sorting systems was the 1980s-1990s, when advances in microelectronics, the introduction of digital array cameras, and the widespread adoption of digital image-processing methods enabled the creation of high-throughput and reliable machines with automated grain quality assessment (Abdullayev and Huseynzade, 2025; Yang et al., 2025). It became possible to analyze not only the mean brightness level, but also the spatial distribution of color, as well as the shape and orientation of kernels (Pearson, 2010; Pearson et al., 2012; Xie et al., 2004). During this period, a specialized class of machines emerged for sorting wheat, maize, barley, rice, and oilseed crops (Abdullayev and Huseynzade, 2025; Yang et al., 2025). Multichannel systems combining the visible and near-infrared ranges were introduced, enabling assessment of surface condition and, to some extent, the internal structure of kernels (Haff et al., 2013; Pearson et al., 2013a; Peiris and Dowell, 2010).

At the beginning of the 21st century, optical sorting technology gained new momentum due to advances in high-speed processors, LED illumination sources, and digital image-processing algorithms (Ageh et al., 2025; Maier et al., 2024). Commercially available multi- and hyperspectral systems emerged, capable of recording the reflectance or transmittance spectrum of each particle across numerous narrow wavelength bands (Ageh et al., 2025; Femenias et al., 2022; Haff et al., 2013; Li et al., 2022). This substantially expanded the ability to sort based on latent defects, signs of microbiological infection, changes in chemical composition, and related factors, particularly when combined with machine-learning and deep-learning methods (Femenias et al., 2022; Min and Cho, 2015). During the same period, "intelligent" grain sorters entered the market, integrating multiple sensor modalities (RGB, NIR, UV, fluorescence) and supporting adaptive tuning of rejection criteria tailored to specific crops and processing objectives (Armstrong et al., 2016; Maier et al., 2024).

The accumulation of these technical solutions has led to the emergence of modern approaches to classifying optical grain sorting machines by sensor type, the number and spectral range of channels, and the image-analysis algorithms implemented. Thus, the historical development of optical grain sorting machines can be viewed as a transition from simple photoelectric devices to complex multichannel machine-vision systems. Each stage of this evolution was accompanied by broader spectral capabilities, higher spatial resolution, and increasingly sophisticated image-analysis algorithms, which gradually transformed optical sorting into a key tool within resource-efficient technologies for grain cleaning and preparation for processing.

Typical design and operating principle of optical grain sorting machines

The operating principle of optical grain sorting machines can be described as implementing a "kernel-by-kernel" strategy: each particle passing through the inspection zone is captured by optical sensors, the acquired image or spectral response is analyzed in real time, and the control

ISSN: 2409-4951 (Online), 2310-1008(Print)

system then compares the measured feature set against predefined quality criteria to issue a reject or accept command (Dowell et al., 2007; Pearson, 2009, 2010; Pearson et al., 2013a).

A typical optical grain sorter comprises a set of functional subsystems that ensure the successive stages of the process. In general, the machine includes: (1) a feeding system for forming a stable monolayer or controlled grain stream (Kleinhans et al., 2022; Nordell, 1997); (2) an optical module (illumination and acquisition sensors) (Bühler AG, 2016a; Maier et al., 2024); (3) an image-processing and decision-making unit (feature extraction, classification, and synchronization) (Abdullayev and Huseynzade, 2025; Maier et al., 2024); (4) a rejection system and the routing of trajectories/channels for fraction discharge (predominantly pneumatic) (Bühler AG, 2016a, n.d.; Satake Corporation, n.d.); (5) systems for cleaning the optics and working assemblies, diagnostics, and maintenance (Bühler AG, 2016a, 2016d; Satake Corporation, n.d.); (6) a control system and operator interface for setting operating modes, monitoring parameters, and integrating the machine into the processing line (Bühler AG, 2016a; Folgado et al., 2024; TOMRA Sorting, n.d.).

Table 1 summarizes these subsystems, their primary functions, key parameters that govern sorting performance, and typical operational issues. Importantly, overall efficiency is determined not only by the optical module and classification algorithm, but also by the stability of grain-stream formation and the timing accuracy of the rejection actuation, which jointly define the achievable selectivity and product loss.

Table 1

Optical grain sorting machines subsystems

Subsystem	Main function	Adjustable parameters
Feeding	Forms a stable monolayer grain stream with minimal overlap and predictable motion	Feed rate; vibration frequency & amplitude; chute angle; belt speed; stream thickness and uniformity across width
Optical	Illumination and optical information capture	Wavelength (RGB/NIR/UV); illumination intensity/stability; camera resolution; exposure; optics alignment; background/contrast
Image-processing and decision making	Extracts features, classifies accept/reject, and synchronizes decision with actuation	Feature set; decision thresholds; model type (rules/ML/DL); processing latency; trigger alignment; sampling rate
Rejection system and fraction routing	Removes detected objects and directs fractions into separate channels	Air pressure; valve opening time; nozzle pitch; activation window; geometry of chutes/hoppers; number of fractions
Maintenance	Keeps optics and assemblies functional; supports self-checks and planned maintenance	Observed parameters; wiper cycles; cleaning schedule; diagnostics coverage; event logs; logs throttling
Control and Operator Interface	Coordinates subsystems, sets modes/recipes, monitors parameters, and integrates into the processing line	Operating modes/recipes; interlocks; communications with upstream/downstream equipment; logging & traceability; remote diagnostics (if available)

Each subsystem is described in detail below.

ISSN: 2409-4951 (Online), 2310-1008(Print)

Feeding and grain-stream formation system. The feeding system is responsible for conveying grain from the receiving hopper to the optical inspection zone and for establishing a particle-motion regime in which each kernel is maximally accessible for sensor observation (Abdullayev and Huseynzade, 2025; Nordell, 1997). A typical feed path includes a loading hopper, a metering device (gate, feeder, or screw), one or more vibratory or belt feeders, distribution chutes, and a working surface (a chute or belt conveyor) (Nordell, 1997). The primary function of this assembly is to transform a chaotic granular flow into an ordered monolayer or quasi-monolayer with minimal particle overlap (Nordell, 1997).

In chute-fed (gravity) machines, grain leaving the vibratory feeder moves along an inclined surface, where the combined action of vibration and gravity forms a thin, spatially extended stream (Pearson, 2010). Chute geometry, inclination angle, and vibration frequency and amplitude are selected to ensure a uniform stream density and to reduce the likelihood of kernels agglomerating into clusters (Nordell, 1997; Tan et al., 2020). A generalized schematic diagram of the chute-type grain sorting machine is shown in Figure 1.

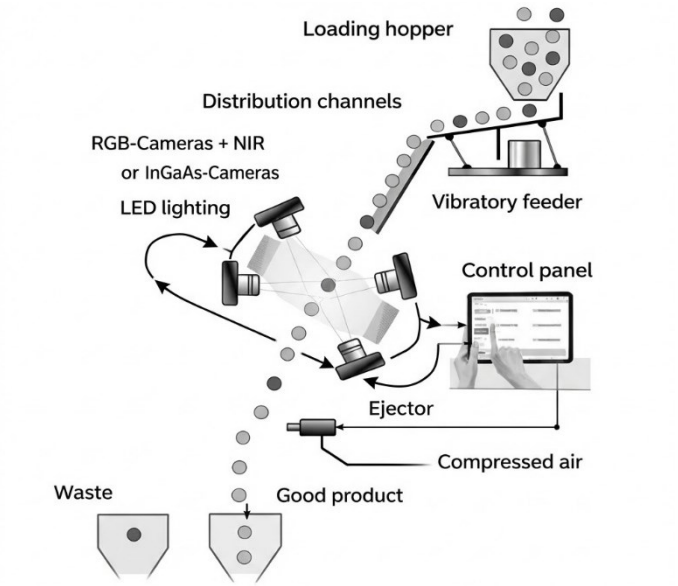

Figure 1. Generalized schematic diagram of the chute-type grain sorting machine

In belt-type machines, the flow is formed on a moving conveyor belt: kernels are arranged into a single layer on a horizontal or slightly inclined surface and then, together with the belt, enter the optical inspection zone (Wallace, 1984). This approach improves the positional stability of particles; however, it requires a more complex mechanical assembly and additional maintenance of the conveyor system (Wallace, 1984). A generalized schematic diagram of the belt-type grain sorting machine is shown in Figure 2.

The key parameters characterizing the performance of the feed system are the uniformity of grain distribution across the flow cross-section, the layer thickness, the particle velocity, and the temporal stability of these indicators (Nordell, 1997; Tan et al., 2020). An excessive layer thickness causes kernels to overlap and leads to loss of information from the lower layers, whereas an overly low flow density reduces the machine's throughput (Dowell et al., 2006; Pearson, 2010; Pearson et al., 2012). Therefore, manufacturers typically provide feed adjustment options by changing the position of gates in the hopper, tuning the vibration

ISSN: 2409-4951 (Online), 2310-1008(Print)

frequency of the feeders, adjusting the chute inclination angle, or varying the belt speed (Nordell, 1997; Tan et al., 2020). In some modern machines, automatic load-control systems are used: based on sensor signals, they regulate the material feed, maintaining an optimal layer thickness for the selected sorting mode (Abdullayev and Huseynzade, 2025; Maier et al., 2024; Pearson et al., 2012).

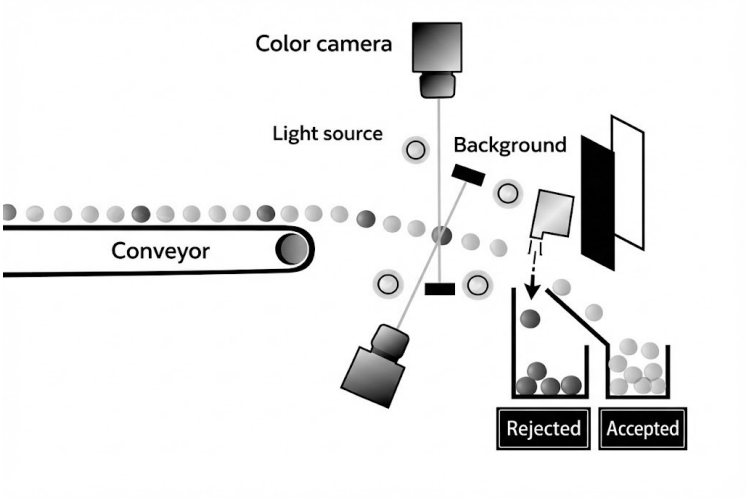

Figure 2. Generalized schematic diagram of the belt-type grain sorting machine

The performance of the feed system directly affects sorting results: a non-uniform flow, local accumulations, or variations in particle velocity complicate optical analysis, increase positioning errors of individual kernels, and reduce the triggering accuracy of reject air nozzles (Tan et al., 2020).

Optical module: illumination and detectors. The optical module of an optical sorter consists of an illumination system and one or more radiation receivers (cameras or other optical sensors) that generate an image or a spectral response for each individual kernel (Abdullayev and Huseynzade, 2025; Ageh et al., 2025). The main task of this subsystem is to ensure stable, reproducible observation conditions under which optical features (color, brightness, spectral reflectance, and surface texture) are maximally contrasted against the background illumination and minimally distorted by external factors (Delwiche, 2008; Haff et al., 2013). The design of the optical module determines the wavelength ranges used for analysis, the spatial resolution at which images are acquired, and how reliably the system can distinguish small defects and subtle differences between kernels (Pearson, 2009; Pearson et al., 2012).

Illumination systems in industrial sorters are predominantly based on light-emitting diode (LED) sources, which provide high intensity stability, low heat generation, and the ability to produce both broadband and narrowband radiation in the visible, near-infrared (NIR), and ultraviolet (UV) ranges (D'Souza et al., 2015; Finardi et al., 2021; Pearson et al., 2013a). In early designs, halogen or xenon lamps with optical filters were used; however, they are gradually being replaced by LED systems due to their longer service life, better spectral controllability, and easier integration with control electronics (Ageh et al., 2025; Delwiche, 2008). The illumination geometry (top, bottom, or angled lighting; combinations of diffuse and

ISSN: 2409-4951 (Online), 2310-1008(Print)

directional light) is selected to reduce specular reflections from smooth surfaces, enhance the contrast of hull defects, and, when required, enable a transillumination mode to assess the internal condition of kernels (Cataltepe et al., 2004b; Wang et al., 2005). To stabilize illumination characteristics, diffusing screens, polarization filters, and optical elements that homogenize the illumination field are often used (Ageh et al., 2025).

Signal acquisition is performed using line-scan or area-scan cameras, sometimes in combination with other sensor types (e.g., NIR detectors or UV receivers) (Ageh et al., 2025; Pearson et al., 2013a; Yao et al., 2023). Line-scan cameras are typically oriented across the flow, and the image is formed by sequentially capturing individual lines as the grain moves; this approach is well suited to chute-type machines with high flow velocities (Ageh et al., 2025; Pearson, 2010). Area-scan cameras are more commonly used in belt sorters, where the motion trajectory is more predictable and each kernel remains in the field of view for a longer time (Ageh et al., 2025; Wallace, 1984). The spatial resolution of the cameras must be sufficient to reliably detect small surface defects and analyze kernel shape, while accounting for the trade-off between detail level and the data volume that must be processed in real time (Ageh et al., 2025; Maier et al., 2024).

In terms of spectral characteristics, optical modules may be single-channel (monochrome) systems with a set of filters, three-channel RGB systems, or multichannel multispectral and hyperspectral cameras (Ageh et al., 2025; Haff et al., 2013; Nansen et al., 2008). RGB systems enable color analysis in three basic channels, which is sufficient for most sorting tasks based on discoloration, darkening, varietal differences, or the degree of surface cleanliness of the grain (Ageh et al., 2025; Pearson et al., 2012). Adding an NIR channel extends the capability to detect internal defects, hidden damage, and differences in chemical composition, since near-infrared reflectance spectra are sensitive to moisture, protein, and fat content, as well as to certain components of cell walls (Dowell et al., 2006; Haff et al., 2013; Jiang, 2020; Siesler et al., 2002). UV and fluorescence channels are used to detect kernels affected by certain micromycete species or foreign impurities that exhibit characteristic fluorescent properties (Ageh et al., 2025; Graves et al., 1998; Min and Cho, 2015; Pearson et al., 2009). Hyperspectral systems, which record dozens to hundreds of narrow spectral bands, are still found mainly in research settings (Nansen et al., 2008; Vejarano et al., 2017; Zhou et al., 2021).

To reduce the impact of random factors (illumination instability, changes in optical contamination, and aging of light sources), optical modules are typically equipped with calibration means: the use of “white” and “black” reference standards, correction of field-of-view non-uniformity, and regular verification of sensor sensitivity (Ageh et al., 2025; Li et al., 2022). Many machines include automated calibration procedures that are initiated when the crop type is changed or after maintenance (Ageh et al., 2025). An important design feature is also whether inspection is performed from one or both sides of the flow: in some sorters, kernels are captured only from the exposed side, whereas other models use dual-side inspection with two rows of cameras, reducing the likelihood of missing defects localized on the opposite surface (Kozłowski et al., 2024; Pearson et al., 2008).

The coordinated operation of the illumination system and sensors determines the quality of the primary data on which all subsequent image-processing algorithms are based. Therefore, developers of optical sorters pay particular attention to selecting spectral ranges, illumination geometry, camera type, and resolution, thereby building into the optical module the potential to implement more advanced analysis and classification methods in downstream system blocks (Abdullayev and Huseynzade, 2025; Yang et al., 2025).

Image-processing and decision-making unit. The image-processing and decision-making unit is the “digital core” of an optical sorter: here, raw data from cameras or other

ISSN: 2409-4951 (Online), 2310-1008(Print)

sensors are transformed into a set of features suitable for classification, and based on these features, a decision is made to reject or accept each individual kernel (Ageh et al., 2025; Maier et al., 2024; Yang et al., 2025). In a typical system architecture, the processing pipeline includes: primary signal processing (normalization, noise filtering, correction for field-of-view non-uniformity), segmentation (separating objects from the background), extraction of informative features (color, spectral, morphometric, textural, and defect-related features), object classification, and generation of control signals for the rejection system (Ageh et al., 2025; Min and Cho, 2015).

At the primary image-processing stage, the main tasks are to compensate for illumination variations, suppress sensor dark noise, and correct non-uniformities in the optical system (Ageh et al., 2025; Feng et al., 2019). For this purpose, various brightness normalization methods are used, including "white" and "black" reference corrections and high-frequency noise filtering (Feng et al., 2019; Gonzalez and Woods, 2017). At the segmentation stage, kernels are separated from the background (e.g., the belt or chute), often using thresholding methods in intensity or color spaces, as well as simple morphological operations to separate touching objects (Gonzalez and Woods, 2017; Pearson et al., 2012). The result is a set of binary masks or contours that define which pixels belong to a specific particle, enabling the transition from the "image" level to the level of "individual objects" (Abbasgholipour et al., 2010; Gonzalez and Woods, 2017).

Feature extraction involves computing, for each kernel, a set of parameters that describe its condition and its deviation from the "reference" product (Haff et al., 2013; Pearson, 2010; Yorulmaz et al., 2011). These parameters include color statistics in different color models (RGB, HSV, etc.), spectral reflectance measures in specific bands, geometric characteristics (area, length, width, aspect ratio, roundness), texture indices (homogeneity, contrast, entropy), as well as local features related to the presence of spots, cracks, darkened regions, and similar defects (Armstrong et al., 2015; Cataltepe et al., 2004b; Pearson, 2010; Pearson et al., 2013a). In many industrial machines, users are given the ability to configure "sensitivity zones"-specific regions of the image for which features are computed (e.g., the germ area or the central part of the endosperm), allowing the system to be finely adapted to the characteristics of a particular crop (Femenias et al., 2022; Haff et al., 2013; Yorulmaz et al., 2011).

Kernel classification is typically implemented by comparing the extracted feature set with predefined thresholds or models corresponding to the classes "acceptable grain," "reject," and sometimes "reprocess" (material requiring additional processing) (Pasikatan and Dowell, 2003; Pearson et al., 2012). In the simplest cases, threshold-based algorithms and rule-based approaches are applied: if the value of a certain indicator (e.g., relative brightness in the "green" channel or fluorescence intensity) falls outside the permissible range, the kernel is assigned to the reject fraction (Yao et al., 2023). More advanced systems use multidimensional threshold regions constructed in feature space or classical machine-learning methods (linear/logistic regression, decision trees, support vector machines, simple neural networks), which better account for interrelationships among different features (Kozłowski et al., 2024; Majumdar and Jayas, 2000a; Santiago et al., 2024).

Modern high-throughput sorters increasingly integrate deep-learning elements for grain image analysis, particularly convolutional neural networks (CNNs) that operate directly on the image or its patches and automatically learn internal feature representations (Hidayat et al., 2023; Santiago et al., 2024). In this case, the image-processing unit includes not only standard preprocessing and segmentation stages but also inference modules of a trained neural network that outputs the probabilities of a kernel belonging to a given class (Fezzai et al., 2023; Zhu et al., 2021). Based on these probabilities, the control system makes the final decision, often with

ISSN: 2409-4951 (Online), 2310-1008(Print)

the option to fine-tune decision thresholds to balance cleaning performance against losses of marketable product (Yang et al., 2025; Yellanki, 2025).

From a technical standpoint, the image-processing and decision-making unit is implemented using embedded industrial controllers, single-board computers, or specialized FPGA/ASIC-based modules, enabling real-time processing of large data streams (Gyaneshwar and Nidamanuri, 2020; Pearson, 2009; VSB Engineering College, India et al., 2020). Strict latency requirements arise because only a very short time elapses between image acquisition and the moment a kernel reaches the actuation zone of the reject nozzle. Therefore, the computational algorithms must be not only sufficiently accurate but also strictly time-deterministic in execution (Pearson, 2009, 2010). To coordinate operation with the actuators, the control system generates a sequence of pulses synchronized with the positions of kernels in the flow, as discussed in more detail in the next subsection.

Rejection system. The rejection system provides the physical separation of the grain stream into the target product and rejects in accordance with the decisions generated by the image-processing unit (Haff et al., 2013; Pearson, 2010; Pearson et al., 2012). In most modern optical grain sorters, pneumatic rejection systems based on compressed-air nozzles are used; short air pulses deflect undesirable particles from the main trajectory (Pearson, 2010; Pearson et al., 2012; Tan et al., 2020). The nozzle arrangement geometry, their number, spacing, and valve opening time are selected with regard to grain velocity and the distance from the optical inspection zone to the rejection zone, in order to maximize jet accuracy on the target kernel and minimize the impact on neighboring particles (Pearson, 2010; Tan et al., 2020).

In chute-type sorters, after passing through the optical analysis zone, the grain follows a ballistic trajectory, and the nozzles are positioned in the lower part of the path so that a compressed-air pulse alters the trajectory of an unwanted particle, diverting it into a separate collection channel (Haff et al., 2013; Pearson, 2010). A key parameter in this case is the delay time between image acquisition and nozzle actuation: it must precisely match the time required for a kernel to travel from the “inspection line” to the “rejection line” (Pearson, 2009, 2010; Tan et al., 2020). To achieve this, the control system uses calibrated flow-velocity values and, in some cases, additional position sensors or synchronization with the camera frame rate (Ageh et al., 2025; Nordell, 1997). Mismatch in these parameters leads to misses (unwanted kernels not being rejected) or excessive removal of good product (Pearson et al., 2012; Tan et al., 2020).

In belt sorters, the rejection zone is typically located near the end of the conveyor belt, where the kernels separate from the belt and enter free flight (Wallace, 1984). The nozzles are oriented to deflect unwanted particles in the vertical or horizontal plane, creating separate trajectories for the main product, rejects, and, if required, an intermediate fraction (reprocess) (Haff et al., 2013; Pearson, 2010). The belt configuration enables better control over the initial motion conditions of particles (speed and direction), which improves rejection accuracy; however, it requires coordinating the pneumatic system with conveyor kinematics and implementing more complex solutions to protect the nozzles from dust and product contamination (Nordell, 1997; Tan et al., 2020; Wallace, 1984).

The operation of the rejection system involves a number of operational trade-offs. Increasing air pressure and pulse duration improves the likelihood of removing unwanted kernels, but it also raises the risk of entraining neighboring, potentially marketable kernels and increases energy consumption (Delwiche et al., 2005; Inamdar and Suresh, 2014; Tan et al., 2020). Conversely, overly short or weak pulses reduce the cleaning efficiency. Therefore, manufacturers provide the ability to adjust pressure, valve opening time, and the nozzle activation “window” depending on the crop, sorting mode, and the desired balance between cleaning performance and losses of the main product (Abdullayev and Huseynzade, 2025;

ISSN: 2409-4951 (Online), 2310-1008(Print)

Pearson, 2010; Tan et al., 2020). In some models, adaptive modes are implemented, where rejection parameters are adjusted based on actuation statistics or feedback from quality-control systems (Kleinhans et al., 2022).

Product trajectories downstream of the rejection zone are arranged using receiving hoppers, chutes, and diverter valves that ensure separate collection of the main product, rejects, and, where applicable, reprocess material (Haff et al., 2013; Nordell, 1997; Wallace, 1984). The receiving channels are designed to minimize cross-contamination of fractions due to ricochets, re-mixing, and secondary dust generation (Nordell, 1997). The quality of flow separation at this stage is no less important than nozzle actuation accuracy, since poor channel geometry can partially negate the advantages of high-precision optical and pneumatic sorting (Nordell, 1997). Overall, the rejection system, together with properly organized product trajectories, determines the final purity of the fractions, the losses of marketable grain, and the energy intensity of the process (Delwiche et al., 2005; Pearson et al., 2012).

Maintenance system. Cleaning systems in optical sorters combine passive and active measures: seals, protective enclosures, and optimized aerodynamics reduce dust deposition on optical components, while compressed-air blow-off, brush/wiper mechanisms, and in some cases washing with drying provide regular cleaning (Bühler AG, 2016a, 2016d); The cleaning modes may be fixed or set by the operator depending on operating conditions and the dust content of the product (Bühler AG, 2016a). In parallel, built-in diagnostics monitor illumination intensity, temperature/humidity, air pressure, nozzle operation, and the state of the electronics, generate warnings for deviations, and often perform self-tests of key modules during startup (Bühler AG, 2016a, 2016d, 2016b).

Service maintenance is supported through the operator interface, which displays event logs, sorting statistics, nozzle actuation counts, operating hours, and other indicators important for planning scheduled maintenance (Bühler AG, 2016a, 2016d). Some manufacturers provide the option of remote access to the machine for diagnostics, software updates, and optimization of settings for specific operating conditions (Bühler AG, 2016b).

Control system and operator interface. The control system coordinates the operation of all units of the optical sorter-from grain feeding and the optical module to the pneumatic rejection system and service subsystems-and synchronizes them with the rest of the processing line equipment (Bühler AG, 2016a; Pearson et al., 2012). Typically, it includes an industrial controller or embedded computer, input/output modules for sensors and actuators, an operator interface (panel/touchscreen or remote access), and communication means for external systems (SCADA, MES) (Bühler AG, 2016a, 2016b; Folgado et al., 2024). Through the control system, operating modes, sorting parameters, acceptance thresholds for optical features, and the logic of interaction with the processing line are configured (e.g., stopping the feed when the allowable reject level is exceeded) (Bühler AG, 2016a; Satake Corporation, n.d.). The operator interface is typically implemented as a graphical menu with “recipes” for different crops and products, specifying color/spectral-response ranges, defect sensitivity, the trade-off between cleaning efficiency and losses of marketable grain, nozzle parameters, and more; the operator can adjust thresholds, enable/disable features, and perform calibration using reference samples (Bühler AG, 2016a). In advanced systems, additional guidance and visualizations are provided-examples of classified kernels and statistical distributions of key features-which simplifies tuning without requiring in-depth knowledge of optical metrology (Bühler AG, 2016a; Satake Corporation, n.d.).

In an integrated processing line, the optical sorter operates as a node within automated production control: it receives signals on the status of upstream and downstream equipment

ISSN: 2409-4951 (Online), 2310-1008(Print)

(hoppers, screw conveyors, bucket elevators, mills, mixers) and transmits data on its own status, throughput, reject fraction, and alarm/warning events (Bühler AG, 2016a; Satake Corporation, n.d.). Via industrial protocols (Modbus, Profibus, Profinet, EtherNet/IP, etc.), its control system is connected to the plant network, enabling scenarios such as automatic feed reduction or shutdown, flow diversion, starting backup lines in the event of a failure, and collecting historical data for analysis (Bühler AG, 2016b; Rakipov et al., 2025). A separate, important aspect is the informational potential: in real time, the machine "sees" grain quality and can serve as a source of operational data on batch-to-batch variability, temporal changes, the appearance of atypical impurities, or signs of contamination (Bühler AG, 2016a; Wang et al., 2013). Integrating these data into monitoring systems enables more flexible management of raw-material flows (e.g., diverting high-risk batches to separate processing or blending) and rapid response to deviations related to suppliers, storage, or weather factors, transforming the sorter from a "local cleaning device" into an active element of the digital infrastructure that supports resource efficiency and stable finished-product quality (Rakipov et al., 2025).

Objects of optical sorting and types of impurities in grain streams.

Objects and impurity classes targeted by optical sorters. Optical sorters do not operate on a "continuous" grain mass but on individual objects passing through the inspection zone: kernels of the base crop, foreign particles, and defective elements of various origins (Maier et al., 2024; Pearson, 2010). For grain processing, it is important not only to reduce the overall impurity content, but also to selectively remove those components that most strongly affect safety, technological properties, and the market quality of the product (Kecskes-Nagy et al., 2016), therefore, it is advisable to use a detailed classification rather than a simple division into "grain" and "impurities". Optical methods make it possible to detect kernels and impurities that are difficult or impossible to reliably separate by mechanical means due to their similarity to the main fraction in size, mass, or density (Aviara et al., 2022; Maier et al., 2024), but that differ in optical, spectral, or morphological characteristics.. In practice, the following groups of objects for optical sorting are typically distinguished: defective and damaged kernels of the base crop; plant impurities (weed seeds, kernels of other crops, and plant residues); mineral impurities; artificial (technogenic) impurities; and biological impurities and manifestations of microbiological contamination - this grouping is then used as a basis for describing optical features and configuring sorting algorithms. (Graves et al., 1998; Jia et al., 2020; Pasikatan and Dowell, 2001).

Defective and damaged kernels of the base crop. Defective and damaged kernels include grains that belong to the base crop (wheat, maize/corn, rice, etc.) but exhibit deviations from the normal morphological or physiological state (Kozłowski et al., 2024; Majumdar and Jayas, 2000a). These may include kernels with hull cracks, shriveled and underdeveloped kernels, as well as heavily broken or mechanically damaged grains incurred during harvesting, transportation, or drying (Kozłowski et al., 2024; Khaeim et al., 2019; Pascale et al., 2022). A separate group comprises sprouted kernels, as well as kernels with visible signs of mold infection (changes in hull color, localized spots, mycelial growth) (Carmack et al., 2019; Guerra and Cuevas, 2024; Jia et al., 2020; Pearson et al., 2013b; Yorulmaz et al., 2011) or discoloration and darkening of the germ (Armstrong et al., 2015; Pearson et al., 2009).

The presence of such kernels impairs the technological properties of the raw material (flour yield and quality, vitreousness, and the stability of baking properties) (Baasandorj et al., 2015; Cha et al., 2025), and, in cases of mycological infection, may compromise safety due to the risk of mycotoxins (Pascale et al., 2022; Pearson et al., 2004). Because defective kernels often differ

ISSN: 2409-4951 (Online), 2310-1008(Print)

only slightly from sound kernels in mass and size, mechanical cleaning is relatively ineffective; in contrast, optical sorters identify them based on changes in color/texture and local defects, and in some cases by spectral or fluorescent signatures (Caporaso et al., 2018; Kecskes-Nagy et al., 2016).

Plant impurities. Plant impurities include foreign inclusions of plant origin that are not part of the target crop: weed seeds, kernels of other crops (e.g., rye in wheat or sorghum in corn), fragments of stems and leaves, glumes/husk scales, parts of corn husks, straw fragments, and similar materials (Aliev, 2020); Some of these impurities differ substantially from grain in size and density and can be removed by mechanical separators, whereas impurities with similar mass-geometric parameters often remain after conventional cleaning. They reduce raw-material uniformity, complicate cleaning/drying/milling operations, and may increase crude fiber content and introduce undesirable flavor and aroma components into the final product (Aliev, 2020; Inamdar and Suresh, 2014). From the perspective of optical inspection, such impurities often exhibit characteristic differences in shape (elongated, flattened, with specific "awns" or needle-like structures), color, and surface gloss. This enables selective removal of weed seeds and kernels of other crops based on color/spectral and morphometric features, especially when a high level of varietal purity is required (Abdullayev and Huseynzade, 2025; Kozłowski et al., 2024; Majumdar and Jayas, 2000a, 2000b).

Mineral impurities. Mineral impurities are inorganic solid particles that enter the grain mass during harvesting, transportation, and storage (stones, soil clods, sand, fragments of glass or slag, ferromagnetic inclusions, etc.); a substantial portion of them is removed by destoners, gravity tables, and magnetic separators (Graves et al., 1998; Reddy, 2010), however, small or atypically shaped particles may remain in the stream and pose a risk to both equipment and consumers (Kecskes-Nagy et al., 2016; Reddy, 2010). For optical systems, these impurities typically differ from kernels in shape, surface texture, and optical properties (hue, matte/glossy appearance, and a different reflection/absorption behavior in the visible and NIR ranges). Therefore, optical sorting can complement mechanical cleaning stages by removing residual stones and soil clods (Abdullayev and Huseynzade, 2025; Feng et al., 2019; Liu et al., 2022), which is particularly important for high-quality food products with strictly regulated levels of hard inclusions.

Artificial (technogenic) impurities. Artificial (technogenic) impurities are foreign objects of industrial or household origin that enter grain streams during harvesting, transportation, or storage (fragments of plastic parts and packaging materials, rubber, textiles, paper, small metal elements, cables, as well as fine polymer particles that are increasingly regarded as microplastics) (Chen et al., 2025); due to sizes comparable to kernels or a "favorable" shape, they can pass through sieve and pneumatic systems and are not always reliably removed by mechanical methods (Graves et al., 1998). At the same time, their optical properties typically differ substantially from those of grain (color, gloss, reflectance behavior in the visible and NIR ranges, and texture), so optical sorters can effectively detect and remove such objects (Abdullayev and Huseynzade, 2025); This is especially true for polymers which, despite their wide range of colors, exhibit characteristic spectral "fingerprints" in the infrared region, making the use of combined visible and NIR channels advantageous for their detection (Masilamani et al., 2020; Stuart, 2004).

Biological impurities and microbiological contamination. Biological impurities include both macroscopic objects (whole insects, larvae, pupae, body fragments, and excreta) and

ISSN: 2409-4951 (Online), 2310-1008(Print)

manifestations of microbiological contamination associated with the growth of molds and bacteria on the grain surface. Some of these occur as separate impurities (insect bodies, mycelial clumps), while others manifest through changes in kernel appearance (darkening, spots, deposits, shifts in hull hue), effectively moving them into the group of defective kernels but with a different etiology (Somiahnadar, 2003; Stathas et al., 2023; Vejarano et al., 2017). Microbiological contamination is particularly hazardous due to the risk of mycotoxin accumulation, which often shows no pronounced visual signs at early stages. However, studies indicate that infected kernels may exhibit specific changes in color-spectral characteristics and fluorescence response, making the use of optical systems in the UV and NIR ranges promising (Jia et al., 2020; Min and Cho, 2015); some industrial solutions already claim a reduction in the proportion of potentially contaminated kernels by combining visible, NIR, and fluorescence channels (Pearson et al., 2009; Yao et al., 2023).

Optical features. From a computer-science perspective, an optical grain sorter can be regarded as a system that solves a multiclass classification problem for objects in a stream (e.g., marketable grain, impurities, defective kernels, etc.) based on visual/spectral observation data (Aznan et al., 2021; Yang et al., 2025). Several methodological approaches are used to implement such classification: (a) algorithmic computer-vision and image-processing methods with explicit extraction of semantically meaningful structures (segmentation, morphological analysis, decision rules) (Aviara et al., 2022; Majumdar and Jayas, 2000a); (b) classical machine learning using relatively simple models (linear classifiers, decision trees, ensembles, etc.) that operate on precomputed features (Cataltepe et al., 2004a); (c) deep-learning methods in which feature representations and the classification rule are largely learned jointly from data (in particular, convolutional neural networks and their variants) (Fezzai et al., 2023; Hidayat et al., 2023; Zhu et al., 2021).

Unlike deep learning, the first two approaches typically require a feature-engineering stage-that is, an explicit definition of an informative feature vector describing the object, on the basis of which the class assignment decision is made (Majumdar and Jayas, 2000a, b; Yorulmaz et al., 2011). It is therefore advisable to present a provisional classification of such features, since it may be practically useful for readers when configuring optical sorting parameters. In this subsection, optical features are conventionally divided into several groups: color-spectral, morphometric, textural, surface-defect features, as well as internal and chemical features

Color-spectral features. Color-spectral features are fundamental for most optical sorters (Ageh et al., 2025; Li et al., 2022). They describe the intensity of reflected or transmitted light in one or more wavelength ranges (visible, near-infrared, ultraviolet), as well as the relationships among these ranges (Caporaso et al., 2018; Li et al., 2022). In the simplest case, these are brightness values in the three RGB channels or coordinates in another color space (e.g., HSV, Lab) that characterize the hue, saturation, and lightness of the grain surface (Ageh et al., 2025; Carmack et al., 2020; Pearson et al., 2012). These features allow the detection of discolored, darkened, yellow, chalky, or locally stained kernels, characteristic in particular of rice, wheat, and corn (Cha et al., 2025; Sairi and Mustaffha, 2020).

In more advanced systems, not only three-color analysis is used, but also measurements of intensity in specific portions of the visible and near-infrared spectrum (Caporaso et al., 2018; Cha et al., 2025; Dowell et al., 2006). The set of such measurements forms a spectral “fingerprint” of a kernel, which may be characteristic of a particular variety, degree of maturity, moisture or protein content, as well as mold infection (Dowell et al., 2006; Femenias et al., 2022; Jia et al., 2020; Wesley et al., 2008). In multispectral and hyperspectral systems, spectral features include dozens to hundreds of channels, enabling more fine-grained recognition

ISSN: 2409-4951 (Online), 2310-1008(Print)

models but requiring more sophisticated analysis algorithms and dimensionality-reduction techniques (Caporaso et al., 2018; Cataltepe et al., 2007; Feng et al., 2019; Gyaneshwar and Nidamanuri, 2020).

For certain tasks, relative spectral measures are important: ratios of intensities across different channels and indices analogous to well-known "vegetation indices" in remote sensing, but adapted to grain and impurities (Li et al., 2022; Pasikatan and Dowell, 2004; Pearson et al., 2004; Zhou et al., 2021). Such indices are less sensitive to changes in absolute illumination brightness and allow the specifics of surface microstructure to be accounted for more effectively (Caporaso et al., 2018).

Morphometric features (shape, size, and proportions). Morphometric features describe the geometric properties of kernels and impurities derived from their projection in the image plane (Aviara et al., 2022; Majumdar and Jayas, 2000a, b). Typical parameters include object area, the length and width of the minimum bounding rectangle, the ratio of maximum to minimum dimensions, degree of roundness or elongation, compactness, eccentricity, and similar measures. More complex shape descriptors may also be used, for example those based on contours or elliptical approximations (Aviara et al., 2022; Majumdar and Jayas, 2000b).

These features are particularly important for separating kernels of the base crop from plant impurities (weed seeds, kernels of other crops), as well as for identifying fractions that are unacceptable in terms of shape or size, such as chipped, fragmented, or excessively small kernels (Maier et al., 2024; Majumdar and Jayas, 2000a). For example, the seeds of many weeds have a more elongated shape, characteristic "spines" (awns), or asymmetric contours, which can be effectively captured by aspect-ratio measures and compactness indicators (Majumdar and Jayas, 2000a, b). In seed production, morphometric features help improve varietal purity by separating characteristically shaped kernels from atypical ones (Abdullayev and Huseynzade, 2025; Maier et al., 2024).

Some morphometric indicators are related to mass-geometric characteristics traditionally used in mechanical systems; however, in optical sorting they are obtained directly from images and can be combined with color-spectral and textural features, improving the overall discriminative power of the system (Ageh et al., 2025; Feng et al., 2019; Majumdar and Jayas, 2000a, b).

Surface texture features. Texture features describe the spatial non-uniformity of brightness or color on the kernel surface-that is, the character of "graininess," roughness, the presence of small inclusions, striping, or other regular or random structures (Carmack et al., 2020; Majumdar and Jayas, 2000b). In practice, they are assessed using statistical measures (variance, entropy, coefficient of variation), features computed from the gray-level co-occurrence matrix (GLCM), local binary patterns, and other texture-analysis methods adapted to the hardware constraints of an industrial system (Cataltepe et al., 2004a; Majumdar and Jayas, 2000b).

Texture features are particularly useful for detecting surface damage that is not always accompanied by a sharp change in average color but alters the hull microrelief-for example, corrosion-like spots, mold foci, erosive damage, or traces of insect pest activity (Jia et al., 2020; Majumdar and Jayas, 2000b; Min and Cho, 2015). In rice, for example, texture characteristics can be used to distinguish chalky kernels from more translucent ones (Majumdar and Jayas, 2000b; Sairi and Mustaffha, 2020), in wheat, they can be used to identify kernels with a disrupted endosperm structure (Cha et al., 2025; Majumdar and Jayas, 2000b).

ISSN: 2409-4951 (Online), 2310-1008(Print)

In combined algorithms, texture features are often used as auxiliary cues that refine decisions made based on color and shape: if the color matches the reference but the texture differs substantially, the kernel may be classified as defective or problematic for a specific product type (Ageh et al., 2025; Aviara et al., 2022; Majumdar and Jayas, 2000b).

Surface defects and damage features. Surface-defect features focus on local changes in the hull appearance: cracks, chips, dents, spots, localized darkening or discoloration, and areas with altered gloss (Chengqian et al., 2025; Kozłowski et al., 2024; Pearson et al., 2012). Unlike global color or texture measures, these features are tied to specific surface regions and require segmentation of the defective areas (Aviara et al., 2022; Chengqian et al., 2025; Guerra Ibarra and Cuevas, 2024). To extract them, local thresholding methods, edge operators, morphological operations, as well as analysis of brightness and texture gradients within small windows are used (Aviara et al., 2022; Guerra Ibarra and Cuevas, 2024; Majumdar and Jayas, 2000b).

These features are critical for tasks where the presence or absence of specific defects matters more than the overall kernel color-for example, hull or endosperm cracks, insect nibbling marks, pinpoint mold lesions, or localized scorching/darkening due to overheating (Cataltepe et al., 2004b, 2004a; Chengqian et al., 2025). In some cases, local defects determine the technological suitability of grain (e.g., in groats production or seed material preparation), so sorting algorithms are designed to detect such regions even when average color indicators remain within normal limits (Liu et al., 2022; Rahman and Cho, 2016).

Modern systems that use deep-learning methods can automatically learn features of surface defects from image analysis without explicit defect-region segmentation; however, from the standpoint of interpretability and fine tuning, it is often useful for the operator to be able to visualize and control these local parameters (Fezzai et al., 2023; Zhu et al., 2021).

Internal and chemical features (NIR spectra, translucency, fluorescence). Internal and chemical features are associated with kernel characteristics that cannot be fully described by surface color or texture but manifest through spectral response in the NIR region, changes in translucency, transmittance indicators, or fluorescent properties (Caporaso et al., 2018; Femenias et al., 2022; Min and Cho, 2015). In the near-infrared range, reflectance and transmittance spectra are sensitive to moisture, protein, fat, starch content, and certain secondary metabolites, enabling indirect assessment of maturity, damage, and microbiological infection of grain (Caporaso et al., 2018; Dowell et al., 2006; Femenias et al., 2022; Masilamani et al., 2020).

Fluorescence features arise when grain is irradiated with ultraviolet light and the resulting secondary emission is recorded in a different wavelength range (Min and Cho, 2015; Yao et al., 2023). Certain mycotoxins and metabolites of molds exhibit characteristic fluorescence bands, which were used in laboratory practice even before industrial sorters became widespread (Min and Cho, 2015). Integrating UV and fluorescence channels into industrial machines enables selective removal of kernels with an elevated risk of mycotoxicosis, although the precise relationship between visible fluorescence and toxin levels remains a complex scientific problem (Femenias et al., 2022; Min and Cho, 2015; Pearson et al., 2009).

These features are particularly promising for applications where safety and functional-technological properties are more critical than visual appearance (e.g., production of infant foods, dietetic products, and specialized feeds) (Femenias et al., 2022). At the same time, their use requires calibration and validation for specific crops and under particular growing and storage conditions, making such systems more complex to implement (Caporaso et al., 2018; Masilamani et al., 2020; Min and Cho, 2015).

ISSN: 2409-4951 (Online), 2310-1008(Print)

Summary and implications

A generalized classification scheme for optical grain sorting machines. Optical grain sorting has progressed from early photoelectric separators to multichannel machine-vision systems that combine several spectral ranges, high-speed imaging, and specialized decision algorithms. The historical perspective indicates that each development stage -from vacuum-tube circuitry to digital systems and deep learning was driven not only by hardware advances but also by evolving views on which objects and discriminative cues should be detected in the grain stream.

Based on an analysis of industrial models of optical grain sorters described in the literature and in manufacturers' technical documentation, a generalized classification of optical grain sorting machines was developed. The baseline version of this generalized classification scheme was presented for expert discussion in the conference paper "Classification of Optical Grain Separators" (Galka and Sharan, 2025a, 2025b). Unlike traditional approaches that focus primarily on a single criterion (e.g., spectral range or the type of conveying system), the proposed classification considers machines simultaneously in terms of sorting purpose, design features, automation level, application focus, crop specificity, and optical-system characteristics. This approach better captures the real diversity of commercially available solutions and provides a convenient framework for comparing and selecting equipment for specific processing tasks.

Suggested Optical Grain Sorter Machines classification is depicted in the Figure 3.

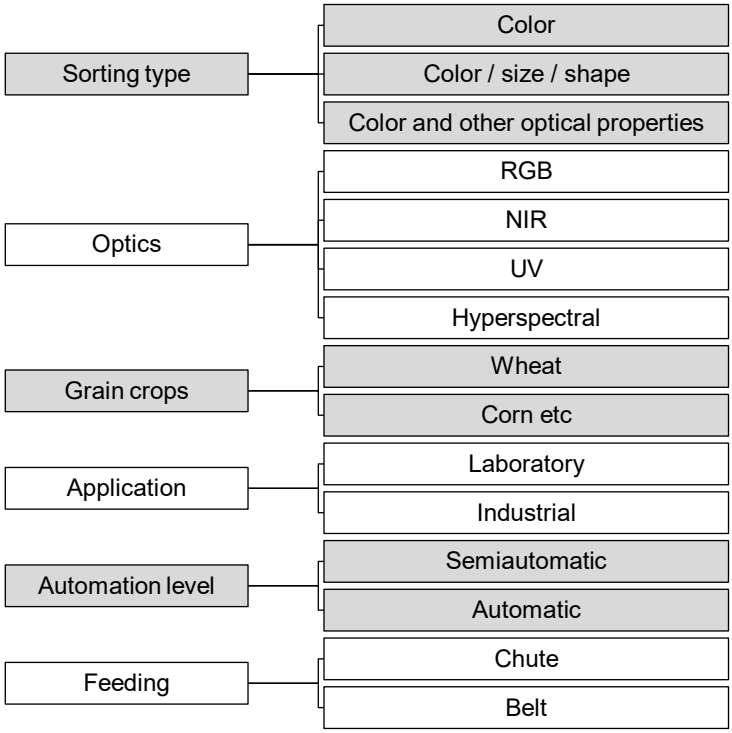

Figure 3. Optical grain sorting machines classification

ISSN: 2409-4951 (Online), 2310-1008(Print)

Following subsections discuss the main dimensions of this classification. The aim is not to "rigidly" assign each machine to a single class: most industrial sorters belong to several groups simultaneously (for example, an industrial belt-based NIR sorter for rice incorporating elements of deep learning). Rather, the classification is proposed as a generalized coordinate system in which a specific model can be positioned, alternative solutions compared, and the development of processing schemes incorporating optical sorting can be planned.

Classification by sorting type. Sorting type is the most intuitive dimension for users and reflects the features used for rejection decisions. Based on technical documentation, three groups are distinguished: (1) color sorters; (2) color + shape/size sorters; (3) color + other optical properties sorters.

(1) Color sorters operate primarily on color–spectral cues and detect discolored, darkened, or spotted kernels, impurities of contrasting color, and foreign particles whose hue differs from the base material. They are typical entry-level solutions for wheat, corn, and barley, aimed at improving appearance and partially removing defective kernels.

(2) Color + shape/size sorters complement color analysis with morphometric control (length, width, aspect ratio, roundness), improving selectivity for weed seeds, kernels of other crops, and fractions atypical in size or shape. They are common where varietal purity or narrow size fractions are required (e.g., seed production).

(3) Color + other optical properties sorters additionally use cues such as NIR reflectance, translucency, gloss, and fluorescence, enabling detection of internal defects, early mycological infection, changes in chemical composition, and specific artificial contaminants. These machines are most relevant for applications with elevated safety requirements and for maintaining stable functional and technological properties of grain raw materials.

Classification by feeding type. This dimension captures how grain is fed and conveyed through the inspection zone. Four groups are distinguished: chute (gravity) sorters, belt sorters, pneumatic-transport machines, and hybrid systems.

Chute sorters form a thin stream on inclined vibrating chutes; grain moves by gravity through the inspection zone. They are structurally simple and high-throughput for basic cleaning, but kernel positional stability is limited, placing higher demands on optical and ejector timing.

Belt sorters spread grain in a single layer on a horizontal or slightly inclined conveyor before optical analysis. This improves control of trajectories and orientation and supports more advanced shape/texture analysis, at the cost of higher mechanical complexity and conveyor maintenance.

Pneumatic and hybrid systems convey grain in airflow channels or combine multiple feeding principles along the pathway. They enable adaptation for fragile, heat-sensitive, or heavily contaminated products.

Classification by automation and intelligent control. Three provisional groups are distinguished: semi-automatic, automatic, and intelligent (smart) optical sorters.

Semi-automatic machines rely on operator-driven setup and monitoring: crop changes, thresholds, and modes are adjusted manually, and visualization tools are limited. They are typical for small enterprises, laboratories, or earlier equipment generations.

Automatic sorters maintain preset parameters, offer crop-specific "recipe" interfaces, and support automated calibration. The operator sets overall targets (e.g., reject fraction or cleaning level), while the system controls feeding, rejection, and basic diagnostics.

ISSN: 2409-4951 (Online), 2310-1008(Print)

Intelligent (smart) sorters add self-tuning and adaptive thresholds, ML/DL-based image analysis, and expanded data logging/communication. They can adapt to raw-material variability, recommend settings, and in some cases refine models from accumulated data, aligning optical sorting with plant digital infrastructure.

Classification by application. By application focus, optical sorters can be divided into laboratory and industrial systems.

Laboratory machines have low throughput and simplified feeding, but typically offer flexible access to raw outputs (images, spectra). They support research, algorithm development, calibration of industrial settings, and detailed inspection of specific batches; in some cases, they serve as prototypes for industrial designs.

Industrial sorters are built for continuous, high-throughput operation within processing lines and include advanced diagnostics and service features. They prioritize reliability, energy efficiency, and operator-oriented interfaces, and in production they function not only as cleaning equipment but also as real-time "quality sensors."

Classification by grain crops (sorting objects). Product catalogs indicate that many optical sorters are offered as crop- or product-specific (e.g., wheat, corn, rice, seeds, groats, compound feed), alongside universal machines that cover diverse bulk foods through flexible software "recipes."

For wheat and other bread cereals, settings typically target defective or infected kernels, weed seeds, and plant/mineral impurities that reduce flour quality and safety. For corn, emphasis is often placed on detecting kernels potentially affected by toxigenic fungi and removing husk/cob fragments and damaged ear pieces.

For rice, key targets depend on husked vs. unhusked material and include yellow, chalky, discolored, and chipped kernels that strongly affect grade and appearance. Seed sorters prioritize varietal purity, kernel integrity, and absence of mechanical damage, usually applying stricter thresholds.

Universal sorters can process multiple crops and even other bulk products (nuts, legumes, dried fruits), but require careful recipe reconfiguration and sometimes mechanical adjustments (e.g., chutes/feeding). In practice, sorting-object classification helps match machine capabilities to the specific needs of an enterprise.

Classification by optical system. This technically central dimension reflects the spectral range and sensor type. Five groups are distinguished: RGB, NIR, UV/fluorescence, multispectral, and hyperspectral systems.

RGB sorters operate in the visible range (three channels) and primarily evaluate surface color and brightness, enabling rejection of discolored or clearly defective kernels and impurities that differ in color.

NIR systems extend sensing beyond the visible range and add information linked to internal structure and chemical composition, supporting detection of subtler differences associated with moisture, infection, and maturity.

UV/fluorescence systems target materials with characteristic fluorescence, including certain molds and organic contaminants.

Multispectral and hyperspectral systems capture responses in dozens to hundreds of narrow bands, enabling more precise recognition of grain condition and impurities, but they are more common in research or highly specialized industrial use due to cost and data-processing complexity.

ISSN: 2409-4951 (Online), 2310-1008(Print)

This classification is also important for ML/DL-based recognition because the selected spectral channels determine which features can be extracted and how effectively hidden defects and hazardous impurities can be detected.

Integration of optical sorting machines into grain processing lines. Optical sorting should be regarded as the final, "fine" stage of grain cleaning, rather than as a universal replacement for traditional mechanical and pneumatic equipment (Kharchenko et al., 2024; Yang et al., 2025). In a typical process flow, optical sorters are installed downstream of the pre-cleaning and main-cleaning equipment train (screen separators, aspirators, destoners, gravity tables, etc.), once most coarse, light, and heavy impurities have already been removed from the stream, along with a substantial portion of plant and mineral inclusions (Kharchenko et al., 2024; Pascale et al., 2022). This is because excessive contamination of the grain mass with nonstandard particles, dust, and fine fractions compromises feed stability, complicates the operation of the optical module, and increases the load on the rejection system (Bühler AG, 2016a; Kleinhans et al., 2022).

Optical sorters are typically selected for a specific raw material and its characteristic impurity profile: wheat, rice, corn, seed material, or groats each require different machine configurations, illumination modes, sets of optical features, and software "recipes" (Ageh et al., 2025; Yang et al., 2025). In practice, this means that when designing a processing line, the equipment manufacturer and the customer agree not only on throughput, but also on the target tasks (which specific defective kernels and foreign materials should be removed, to what extent, and according to which visual criteria) (Ageh et al., 2025). A substantial proportion of machines are delivered with factory presets for common crops, but for industrial operation additional parameter tuning to specific grain lots and the plant's requirements is almost always carried out (Bühler AG, 2016a, 2016b; Yang et al., 2025). In this sense, an optical sorter is not a "standard separator," but a tool that is configured to the customer's needs (Ageh et al., 2025; Bühler AG, 2016a).

From the standpoint of plant layout, optical sorters are demanding in terms of operating conditions. Most industrial models are designed for installation in enclosed facilities with controlled ranges of temperature, relative humidity, and airborne dust levels (Bühler AG, 2016a, 2016b). Excessive dust, condensation, abrupt temperature fluctuations, or drafts can contaminate optical surfaces, destabilize illumination, increase the rate of false triggers, and raise maintenance demands (Bühler AG, 2016a, 2016d). Therefore, when integrating a sorter, a local aspiration hood, isolation from external influences, and accessible process space for scheduled cleaning and service are often provided (Bühler AG, 2016d, 2016c). Installing machines outdoors-without protection from weather conditions and vibration-is generally unacceptable (Bühler AG, 2016b, 2016c).

A separate practical requirement is the sensitivity of optical sorters to vibrations and impact loads (Bühler AG, 2016b, 2016c). Any loss of stability in the positioning of cameras, illumination sources, and feed-system components directly affects image quality, kernel positioning accuracy, and synchronization with the rejection system (Pearson, 2009; Pearson et al., 2012). Therefore, when integrating the machine into the production environment, it is necessary to account for existing vibration sources (bucket elevators, crushers, large fans) and, where needed, use vibration-isolating mounts, damping elements, and a rational equipment layout (Bühler AG, 2016b, 2016c). Improper placement of the sorter relative to vibrating machines can negate the benefits of even a well-tuned optical system (Bühler AG, 2016b).

In summary, integrating optical sorters into grain-cleaning schemes requires: (1) ensuring a sufficient level of preliminary mechanical cleaning; (2) selecting and configuring

ISSN: 2409-4951 (Online), 2310-1008(Print)

the machine for the specific crop and impurity spectrum; (3) providing appropriate indoor operating conditions; and (4) accounting for the sensitivity of the optical and mechanical modules to vibration. Only when these prerequisites are met can optical sorting realize its potential as a "precision" stage for selectively removing problematic kernels and foreign materials at the end of the process chain.

Conclusions

The review demonstrates that optical grain sorting technology has evolved from simple photoelectric devices to advanced machine-vision systems integrating multiple spectral ranges, high-speed cameras, and specialized image-processing algorithms. Each stage of development from vacuum-tube circuits to digital platforms and deep learning has been driven not only by advances in hardware, but also by changing concepts of target objects and relevant features in the grain stream. Based on a systematic analysis of industrial equipment, a multidimensional classification of optical grain sorters is proposed, accounting for sorting mode, design features, automation level, application focus, crop specificity, and optical-system characteristics, enabling consistent comparison of machines and clearer requirements for process-line design. In addition, optical sorting features are structured by physical nature, observation modality, and decision-making role, linking sorter types to impurity classes and recognition strategies. Practical analysis shows that optical sorters function most effectively as a final, fine-cleaning stage following mechanical and pneumatic separation, provided that adequate upstream cleaning, proper machine selection, and stable operating conditions are ensured. Future developments are expected to focus on wider adoption of multi- and hyperspectral systems, deep learning, and deeper integration of sorters into digital production infrastructures, while further research should assess their technological and resource efficiency and promote standardization of feature sets and testing protocols.

References

Abbasgholipour M., Omid M., Keyhani A., Mohtasebi S. (2010), Sorting raisins by machine vision system, *Modern Applied Science*, 4(2), pp. 49–60, https://doi.org/10.5539/mas.v4n2p49

Abdullayev H., Huseynzade E. (2024), Infrared imaging analysis as non-destructive maintenance of food processing equipment, *Journal of Materials and Engineering*, 2(4), pp. 315–322, https://doi.org/10.61552/JME.2024.04.009

Abdullayev H., Huseynzade E. (2025), Automated optical sorting machines for food industry, *Journal of Engineering, Management and Information Technology*, 3(2), pp. 135–140, https://doi.org/10.61552/JEMIT.2025.02.007

Ageh O.M., Hashim N., Shamsudin R., Che Man H., Mohd Ali M., Onwude D.I., Dasore A. (2025), Optical imaging for food grain quality evaluation – recent advances and future perspectives, *International Journal of Agricultural Sustainability*, 23(1), 2569166, https://doi.org/10.1080/14735903.2025.2569166

Aliev E.B. (2020), *Mechanical and technological foundations of precision separation of seeds of agricultural crops, Doctor of Sciences Thesis*, Dnipro State Agrarian and Economic University, Dnipro, Ukraine.

ISSN: 2409-4951 (Online), 2310-1008(Print)

Armstrong P.R., Maghirang E.B., Pearson T.C. (2015), Detecting and segregating black tip-damaged wheat kernels using visible and near-infrared spectroscopy, *Cereal Chemistry*, 92(4), pp. 358–363, https://doi.org/10.1094/CCHEM-09-14-0201-R

Armstrong R.P., Maghirang B.E., Yaptenco F.K., Pearson C.T. (2016), Visible and near-infrared instruments for detection and quantification of individual sprouted wheat kernels, *Transactions of the ASABE*, 59(6), pp. 1517–1527, https://doi.org/10.13031/trans.59.11566

Aviara N.A., Adesanya A.A., Iyilade I.J., Olorunsola E.O., Oyeniyi S.K. (2022), Application of image analysis in food grain quality inspection and evaluation during bulk storage, *Arid Zone Journal of Engineering, Technology and Environment*, 18(4), pp. 693–706, Available at: https://azojete.com.ng/index.php/azojete/article/view/681

Aznan A., Gonzalez Viejo C., Pang A., Fuentes S. (2021), Computer vision and machine learning analysis of commercial rice grains: a potential digital approach for consumer perception studies, *Sensors*, 21(19), 6354, https://doi.org/10.3390/s21196354

Baasandorj T., Ohm J., Simsek S. (2015), Effect of dark, hard, and vitreous kernel content on protein molecular weight distribution and on milling and breadmaking quality characteristics for hard spring wheat samples from diverse growing regions, *Cereal Chemistry*, 92(6), pp. 570–577, https://doi.org/10.1094/CCHEM-12-14-0249-R

Bühler AG (2016a), *SORTEX A ColorVision/MultiVision: Operator's Manual*, Internal technical documentation (PDF), Bühler AG, Uzwil, Switzerland.

Bühler AG (2016b), *SORTEX A ColorVision/MultiVision: Preinstallation Checklist*, Internal technical documentation (PDF), Bühler AG, Uzwil, Switzerland.

Bühler AG (2016c), *SORTEX A ColorVision/MultiVision: Preparation of the Machine*, Internal technical documentation (PDF), Bühler AG, Uzwil, Switzerland.

Bühler AG (2016d), *SORTEX A ColorVision/MultiVision: Supervisor & Maintenance*, Internal technical documentation (PDF), Bühler AG, Uzwil, Switzerland.

Caporaso N., Whitworth M.B., Fisk I.D. (2018), Near-infrared spectroscopy and hyperspectral imaging for non-destructive quality assessment of cereal grains, *Applied Spectroscopy Reviews*, 53(8), pp. 667–687, https://doi.org/10.1080/05704928.2018.1425214

Carmack W.J., Clark A., Dong Y., Brown-Guedira G., Van Sanford D. (2020), Optical sorter-based selection effectively identifies soft red winter wheat breeding lines with Fhb1 and enhances FHB resistance in lines with and without Fhb1, *Frontiers in Plant Science*, 11, 1318, https://doi.org/10.3389/fpls.2020.01318

Carmack W.J., Clark A.J., Dong Y., Van Sanford D.A. (2019), Mass selection for reduced deoxynivalenol concentration using an optical sorter in SRW wheat, *Agronomy*, 9(12), 816, https://doi.org/10.3390/agronomy9120816

Carrera-Rivera A., Ochoa W., Larrinaga F., Lasa G. (2022), How to conduct a systematic literature review: a quick guide for computer science research, *MethodsX*, 9, Article 101895, https://doi.org/10.1016/j.mex.2022.101895

Cataltepe Z., Cetin E., Pearson T. (2004a), Identification of insect-damaged wheat kernels using transmittance images, *2004 International Conference on Image Processing (ICIP 2004)*, IEEE, Singapore, pp. 2917–2920, https://doi.org/10.1109/ICIP.2004.1421724.

Cataltepe Z., Genc H., Pearson T. (2007), A PCA/ICA-based feature selection method and its application for corn fungi detection, *Proceedings of EUSIPCO 2007 (European*

ISSN: 2409-4951 (Online), 2310-1008(Print)

Signal Processing Conference), IEEE Document ID: 7098948, Available at: https://hdl.handle.net/11527/49346

Cataltepe Z., Pearson T., Cetin E. (2004b), Fast insect damage detection in wheat kernels using transmittance images, *2004 IEEE International Joint Conference on Neural Networks (IJCNN 2004)*, IEEE, Budapest, Hungary, pp. 1343–1346, https://doi.org/10.1109/IJCNN.2004.1380142.

Cha J.K., Park H., Kwon Y., Lee S.M. (2025), Enhancing wheat quality through color sorting: a novel approach for classifying kernels based on vitreousness, *Frontiers in Plant Science*, 16, 1534621, https://doi.org/10.3389/fpls.2025.1534621

Chen Z., Carter L.J., Banwart S.A., Kay P. (2025), Environmental levels of microplastics disrupt growth and stress pathways in edible crops via species-specific mechanisms, *Frontiers in Plant Science*, 16, 1670247, https://doi.org/10.3389/fpls.2025.1670247

Chengqian J., Gong C., Zhichang C., Man C., TengXiang Y., Yinyan S., Xiaobin G. (2025), Detection method of broken grains and impurities in harvested soybeans using feature wavelength selection and MobileNetV4-Unet-SGCPNet hybrid network, *Smart Agricultural Technology*, 101749, https://doi.org/10.1016/j.atech.2025.101749

Cujbescu D., Nenciu F., Persu C., Găgeanu I., Gabriel G., Vlăduț N.V., Matache M., Voicea I., Pruteanu A., Bularda M., et al. (2023), Evaluation of an optical sorter effectiveness in separating maize seeds intended for sowing, *Applied Sciences*, 13(15), 8892, https://doi.org/10.3390/app13158892

Delwiche S.R. (2008), High-speed bichromatic inspection of wheat kernels for mold and color class using high-power pulsed LEDs, *Sensing and Instrumentation for Food Quality and Safety*, 2(2), pp. 103–110, https://doi.org/10.1007/s11694-008-9037-1

Delwiche S.R., Pearson T.C., Brabec D.L. (2005), High-speed optical sorting of soft wheat for reduction of deoxynivalenol, *Plant Disease*, 89(11), pp. 1214–1219, https://doi.org/10.1094/PD-89-1214

Dowell F.E., Baenziger P.S., Maghirang E.B. (2007), Automated single kernel sorting for enhancing grain quality in breeding lines, *2007 ASABE Annual International Meeting*, Minneapolis, Minnesota, USA, 17–20 June 2007, Paper No. 073059, American Society of Agricultural and Biological Engineers (ASABE), https://doi.org/10.13031/2013.23179

Dowell F.E., Boratynski T.N., Ykema R.E., Dowdy A.K., Staten R.T. (2002), Use of optical sorting to detect wheat kernels infected with *Tilletia indica*, *Plant Disease*, 86(9), pp. 1011–1013, https://doi.org/10.1094/PDIS.2002.86.9.1011

Dowell F.E., Maghirang E.B., Graybosch R.A., Baenziger P.S., Baltensperger D.D., Hansen L.E. (2006), An automated near-infrared system for selecting individual kernels based on specific quality characteristics, *Cereal Chemistry*, 83(5), pp. 537–543, https://doi.org/10.1094/CC-83-0537

D'Souza C., Yuk H., Khoo G., Zhou W. (2015), Application of light-emitting diodes in food production, postharvest preservation, and microbiological food safety, *Comprehensive Reviews in Food Science and Food Safety*, 14(6), pp. 719–740, https://doi.org/10.1111/1541-4337.12155

Femenias A., Gatius F., Ramos A.J., Teixido-Orries I., Marín S. (2022), Hyperspectral imaging for the classification of individual cereal kernels according to fungal and mycotoxins contamination: a review, *Food Research International*, 155, 111102, https://doi.org/10.1016/j.foodres.2022.111102

ISSN: 2409-4951 (Online), 2310-1008(Print)

Feng L., Zhu S., Liu F., He Y., Bao Y., Zhang C. (2019), Hyperspectral imaging for seed quality and safety inspection: a review, *Plant Methods*, 15(1), Article 91, https://doi.org/10.1186/s13007-019-0476-y

Fezzai O., Taibeche A., Karima R. (2023), Deep learning for product quality inspection: state of the art, *2023 IEEE 17th International Conference on Applied Computational Intelligence and Informatics (SACI)*, IEEE Record: 10156475, https://doi.org/10.1109/SACI57756.2023.10156475

Finardi S., Hoffmann T.G., Schmitz F.R.W., Bertoli S.L., Khayrullin M., Neverova O., Ponomarev E., Goncharov A., Kulmakova N., Dotsenko E., et al. (2021), Comprehensive study of light-emitting diodes (LEDs) and ultraviolet-LED lights application in food quality and safety, *Journal of Pure and Applied Microbiology*, 15(3), pp. 1125–1135, https://doi.org/10.22207/JPAM.15.3.54

Folgado F.J., Calderón D., González I., Calderón A.J. (2024), Review of Industry 4.0 from the perspective of automation and supervision systems: definitions, architectures and recent trends, *Electronics*, 13(4), 782, https://doi.org/10.3390/electronics13040782

Freitag S., Sulyok M., Logan N., Elliott C.T., Krska R. (2022), The potential and applicability of infrared spectroscopic methods for the rapid screening and routine analysis of mycotoxins in food crops, *Comprehensive Reviews in Food Science and Food Safety*, 21(6), pp. 5199–5224, https://doi.org/10.1111/1541-4337.13054

Galka D.V., Sharan A.V. (2025a), Classification of optical grain separators, *Trends in lean manufacturing and food packaging: Proceedings of the 14th International Specialized Scientific and Practical Conference, National University of Food Technologies, Kyiv,* pp. 179–180

Galka D.V., Sharan A.V. (2025b), Classification of optical grain separators, *Proceedings of the 91st International Scientific Conference of Young Scientists and Students "Youth Scientific Achievements to the 21st Century Nutrition Problem Solution"*, National University of Food Technologies, Kyiv, pp. 115–116.

Gonzalez R.C., Woods R.E. (2018), *Digital Image Processing*, 4th ed. (Global Edition), Pearson, New York, NY, USA.

Graves M., Smith A., Batchelor B. (1998), Approaches to foreign body detection in foods, *Trends in Food Science & Technology*, 9(1), pp. 21–27, https://doi.org/10.1016/S0924-2244(97)00003-4

Guerra J.P., Cuevas F.J. (2024), Application of digital image processing techniques for agriculture: a review, In: *Digital Image Processing – Latest Advances and Applications*, IntechOpen, https://doi.org/10.5772/intechopen.1004767

Gyaneshwar D., Nidamanuri R. (2020), A real-time FPGA accelerated stream processing for hyperspectral image classification, *Geocarto International*, 37, pp. 1–18, https://doi.org/10.1080/10106049.2020.1713231.

Haff R.P., Pearson T.C., Maghirang E. (2013), A multispectral sorting device for isolating single wheat kernels with high protein content, *Journal of Food Measurement and Characterization*, 7(4), pp. 149–157, https://doi.org/10.1007/s11694-013-9150-7.

He L., Niu Z., Chen D. (2011), Research on development of color sorter using TRIZ, in: *IFIP Advances in Information and Communication Technology*, Vol. 370, Springer, Berlin, Heidelberg, pp. 271–279, https://doi.org/10.1007/978-3-642-27281-3_32

Hidayat S.S., Rahmawati D., Prabowo M.C.A., Triyono L., Putri F.T. (2023), Determining the rice seeds quality using convolutional neural network, *JOIV: International Journal on Informatics Visualization*, 7(2), p. 527, https://doi.org/10.30630/joiv.7.2.1175

ISSN: 2409-4951 (Online), 2310-1008(Print)

Inamdar A.A., Suresh D.S. (2014), Application of color sorter in wheat milling, *International Food Research Journal*, 21(6), pp. 2083–2089, Available at: http://www.ifrj.upm.edu.my/21%20(06)%202014/3%20IFRJ%2021%20(06)%202014%20Suresh%20621.pdf

Jia B., Wang W., Ni X.Z., Chu X., Yoon S.C., Lawrence K.C. (2020), Detection of mycotoxins and toxigenic fungi in cereal grains using vibrational spectroscopic techniques: a review, *World Mycotoxin Journal*, 13(2), pp. 163–178, https://doi.org/10.3920/WMJ2019.2510

Jiang G.L. (2020), Comparison and application of non-destructive NIR evaluations of seed protein and oil content in soybean breeding, *Agronomy*, 10(1), Article 77, https://doi.org/10.3390/agronomy10010077

Kautzman M.E., Wickstrom M.L., Scott T.A. (2015), The use of near infrared transmittance kernel sorting technology to salvage high quality grain from grain downgraded due to Fusarium damage, *Animal Nutrition*, 1(1), pp. 41–46, https://doi.org/10.1016/j.aninu.2015.02.007

Kecskes-Nagy E., Korzenszky P., Sembery P. (2016), The role of color sorting machine in reducing food safety risks, *Potravinarstvo Slovak Journal of Food Sciences*, 10(1), pp. 354–358, https://doi.org/10.5219/511

Kleinhans K., Küppers B., Hernández Parrodi J.C., Ragaert K., Dewulf J., De Meester S. (2022), Increase throughput and sorting quality with flowcontrol, *9th Sensor-Based Sorting & Control 2022 (SBSC 2022)*, Shaker Verlag, Aachen, Germany, pp. 85–98, https://doi.org/10.2370/9783844085464-85, ISBN: 978-3-8440-8546-4.

Kharchenko Ye.I., Sharan A.V., Yaniuk T.I., Suprun-Krestova O.Yu. (2024), *Innovatsii v zernovykh tekhnolohiiakh* [Innovations in grain technologies], Oldi+, Odesa.

Kos J., Anić M., Radić B., Zadravec M., Janić Hajnal E., Pleadin J. (2023), Climate change – a global threat resulting in increasing mycotoxin occurrence, *Foods*, 12(14), 2704, https://doi.org/10.3390/foods12142704

Kozłowski M., Szczypiński P.M., Reiner J., Lampa P., Mrzygłód M., Szturo K., Zapotoczny P. (2024), Identifying defects and varieties of malting barley kernels, *Scientific Reports*, 14(1), 22143, https://doi.org/10.1038/s41598-024-73683-3

Li L., Chen S., Deng M., Gao Z. (2022), Optical techniques in non-destructive detection of wheat quality: a review, *Grain & Oil Science and Technology*, 5(1), pp. 44–57, https://doi.org/10.1016/j.gaost.2021.12.001

Liu Y., Zhang J., Yuan H., Song M., Zhu Y., Cao W., Jiang X., Ni J. (2022), Non-destructive quality-detection techniques for cereal grains: a systematic review, *Agronomy*, 12(12), Article 3187, https://doi.org/10.3390/agronomy12123187

Khaeim H.M., Clark A., Pearson T., Van Sanford D. (2019), Methods of assessing Fusarium damage to wheat kernels, *Al-Qadisiyah Journal for Agriculture Sciences (QJAS)*, 9(2), pp. 297–308, https://doi.org/10.33794/qjas.Vol9.Iss2.91

Maier G., Gruna R., Längle T., Beyerer J. (2024), A survey of the state of the art in sensor-based sorting technology and research, *IEEE Access*, 12, pp. 6473–6493, https://doi.org/10.1109/ACCESS.2024.3350987

Majumdar S., Jayas D. (2000a), Classification of cereal grains using machine vision: I. Morphology models, *Transactions of the ASAE*, 43, pp. 1669–1675, https://doi.org/10.13031/2013.3107

Majumdar S., Jayas D. (2000b), Classification of cereal grains using machine vision: III. Texture models, *Transactions of the ASAE*, 43(6), pp. 1681–1687, https://doi.org/10.13031/2013.3068

ISSN: 2409-4951 (Online), 2310-1008(Print)

Masilamani P., Venkatesan S., Janaki P., Eevera T., Sundareswaran S., Rajkumar P. (2020), Role of near-infrared spectroscopy in seed quality evaluation: a review, *Agricultural Reviews*, Article R-1960, https://doi.org/10.18805/ag.R-1960

McMullin D., Mizaikoff B., Krska R. (2015), Advancements in IR spectroscopic approaches for the determination of fungal derived contaminations in food crops, *Analytical and Bioanalytical Chemistry*, 407(3), pp. 653–660, https://doi.org/10.1007/s00216-014-8145-5

Min H., Cho B.K. (2015), Spectroscopic techniques for nondestructive detection of fungi and mycotoxins in agricultural materials: a review, *Journal of Biosystems Engineering*, 40(1), pp. 67–77, https://doi.org/10.5307/JBE.2015.40.1.067

Nansen C., Kolomiets M., Gao X. (2008), Considerations regarding the use of hyperspectral imaging data in classifications of food products, exemplified by analysis of maize kernels, *Journal of Agricultural and Food Chemistry*, 56(9), pp. 2933–2938, https://doi.org/10.1021/jf073237o

Nordell L.K. (1997), Particle flow modeling: transfer chutes & other applications, *15th International Materials Handling Conference (BELTCON 9)*, Johannesburg, South Africa, 22–23 October 1997, Available at: https://cvdyn.com/wp-content/uploads/2020/01/Particle-Flow-Modeling.pdf

Olkhovskyi V., Dudarev I. (2021), Separation methods and separators of grain mass, *Agricultural Machines*, 47, pp. 102–112, https://doi.org/10.36910/acm.vi47.655

Pascale M., Logrieco A.F., Lippolis V., De Girolamo A., Cervellieri S. (2022), Industrial-scale cleaning solutions for the reduction of Fusarium toxins in maize, *Toxins*, 14(11), 728, https://doi.org/10.3390/toxins14110728

Pasikatan M., Dowell F. (2001), Sorting systems based on optical methods for detecting and removing seeds infested internally by insects or fungi: a review, *Applied Spectroscopy Reviews*, 36(4), pp. 399–416, https://doi.org/10.1081/ASR-100107719

Pasikatan M., Dowell F. (2003), Evaluation of a high-speed color sorter for segregation of red and white wheat, *Applied Engineering in Agriculture*, 19, pp. 71–76, https://doi.org/10.13031/2013.12725

Pasikatan M., Dowell F.E. (2004), High-speed NIR segregation of high- and low-protein single wheat seeds, *Cereal Chemistry*, 81(1), pp. 145–150, https://doi.org/10.1094/CCHEM.2004.81.1.145

Pearson T. (2009), Hardware-based image processing for high-speed inspection of grains, *Computers and Electronics in Agriculture*, 69(1), pp. 12–18, https://doi.org/10.1016/j.compag.2009.06.007

Pearson T. (2010), High-speed sorting of grains by color and surface texture, *Applied Engineering in Agriculture*, 26(3), pp. 499–505, https://doi.org/10.13031/2013.29948

Pearson T., Brabec D., Haley S. (2008), Color image based sorter for separating red and white wheat, *Sensing and Instrumentation for Food Quality and Safety*, 2(4), pp. 280–288, https://doi.org/10.1007/s11694-008-9062-0

Pearson T., Maghirang E., Dowell F. (2013a), A multispectral sorting device for wheat kernels, *American Journal of Agricultural Science and Technology*, 2, pp. 45–60, https://doi.org/10.7726/ajast.2013.1004

Pearson T., Moore D., Pearson J. (2012), A machine vision system for high speed sorting of small spots on grains, *Journal of Food Measurement and Characterization*, 6(1–4), pp. 27–34, https://doi.org/10.1007/s11694-012-9130-3

ISSN: 2409-4951 (Online), 2310-1008(Print)

Pearson T., Wicklow D., Bean S., Brabec D. (2013b), Sorting of fungal-damaged white sorghum, *American Journal of Agricultural Science and Technology*, 1(3), pp. 93–103, https://doi.org/10.7726/ajast.2013.1009

Pearson T.C., Wicklow D.T., Brabec D.L. (2009), Technical Note: Characteristics and Sorting of White Food Corn Contaminated with Mycotoxins, *Applied Engineering in Agriculture*, 26(1), pp. 109–113, https://doi.org/10.13031/2013.29463

Pearson T.C., Wicklow D.T., Pasikatan M.C. (2004), Reduction of aflatoxin and fumonisin contamination in yellow corn by high-speed dual-wavelength sorting, *Cereal Chemistry*, 81(4), pp. 490–498, https://doi.org/10.1094/CCHEM.2004.81.4.490

Peiris K.H.S., Dowell F.E. (2010), Single kernel NIR sorting to enhance quality of wheat breeding lines, *CST-SA–ICC International Grains Symposium: Quality and Safety of Grain Crops and Foods*, Gauteng, South Africa, 3–5 February 2010, University of Pretoria Conference Centre, University of Pretoria, *Proceedings of Papers*, pp. 16–21.

Peters M., Marnie C., Tricco A., Pollock D., Alexander L., Mcinerney P., Godfrey C., Khalil H. (2021), Updated methodological guidance for the conduct of scoping reviews, *JBI Evidence Implementation*, 19(1), pp. 3–10, https://doi.org/10.1097/XEB.0000000000000277

Rahman A., Cho B.K. (2016), Assessment of seed quality using non-destructive measurement techniques: a review, *Seed Science Research*, 26(4), pp. 285–305, https://doi.org/10.1017/S0960258516000234

Rakipov V., Gulyaev R., Yunusov R., Sultonov A., Rafikov D. (2025), Optical sorting methods and information technologies in the integrated system for improving the quality and traceability of bare sown cotton seeds, *Proceedings of SPIE – Optical and Computational Technologies for Measurements and Industrial Applications (OptiComp 2025)*, 13803, Article 1380302, Bukhara, Uzbekistan, https://doi.org/10.1117/12.3075464

Reddy R.N. (Ed.) (2010), *Agricultural process engineering*, Gene-Tech Books, New Delhi, India, ISBN: 978-8181921734 (ISBN-10: 8181921731).

Sairi S.A.M., Mustaffha S. (2020), Comparative study of three rice brands' quality through measuring broken rice percentage using Sortex A ColorVision (Buhler) optical sorters, *IOP Conference Series: Earth and Environmental Science*, 515, Article 012017, https://doi.org/10.1088/1755-1315/515/1/012017

Santiago P., Pascual R., Cumbe M., Macaso J., Villanueva F., Dioses I.A. (2024), Classification of rice grain varieties based on morphological features using image processing and machine learning techniques, *Proceedings of ICSGRC 2024*, https://doi.org/10.1109/ICSGRC62081.2024.10691272

Satake Corporation (n.d.), *Instruction Manual: Optical Sorter Satake SSM3001/SSM5001 (AMS/BM/DMS/AIS/BI/DIS)*, Internal technical documentation (PDF), Satake Corporation.

Siesler H.W., Ozaki Y., Kawata S., Heise H.M. (Eds.) (2002), *Near-Infrared Spectroscopy: Principles, Instruments, Applications*, Wiley-VCH Verlag GmbH, Weinheim.

Stathas I.G., Sakellaridis A.C., Papadelli M., Kapolos J., Papadimitriou K., Stathas G.J. (2023), The Effects of Insect Infestation on Stored Agricultural Products and the Quality of Food, *Foods*, 12(10), Article 2046, https://doi.org/10.3390/foods12102046

Stuart B.H. (2004), *Infrared Spectroscopy: Fundamentals and Applications*, John Wiley & Sons, Ltd.

ISSN: 2409-4951 (Online), 2310-1008(Print)

Tan Y.N., Thanh Son L., Quang Tuyen T., Huy Bich N., Truong Thinh N. (2020), Study of Design and Manufacture for One-Line Rice Color Sorting Machine, *Science & Technology Development Journal – Engineering and Technology*, 3(SI1), pp. SI71–SI79, https://doi.org/10.32508/stdjet.v3iSI1.724

Sujitha S., Augustia N. (2020), FPGA implementation of CALIB_IO, wave and clock generation modules for grain sorting machine, *ICTACT Journal on Microelectronics*, 5(4), pp. 854–860, https://doi.org/10.21917/ijme.2020.0147

TOMRA Sorting GmbH. (2016), AUTOSORT & FINDER: common user interface – user manual (UM-KO-0020-REV2.1-en, Rev. 2.1), TOMRA Sorting GmbH, Mülheim-Kärlich, Germany.

Vejarano R., Siche R., Tesfaye W. (2017), Evaluation of biological contaminants in foods by hyperspectral imaging: a review, *International Journal of Food Properties*, 20(Suppl 2), pp. 1264–1297, https://doi.org/10.1080/10942912.2017.1338729

Wallace B.W.H. (1984), Seed conveyors - comparison & contrasts, *Proceedings of the Short Course for Seedsmen*, Mississippi Agricultural and Forestry Experiment Station (MAFES), Mississippi State University, pp. 89–102, available at: https://scholarsjunction.msstate.edu/seedsmen-short-course/418

Wang F., Xi Z., Yang J., Yang X. (2013), Research progress of grain quality nondestructive testing methods, In: Li D., Chen Y. (Eds.), *Computer and Computing Technologies in Agriculture VI* (IFIP Advances in Information and Communication Technology, Vol. 393), Springer, Berlin, Heidelberg, pp. 255–262, https://doi.org/10.1007/978-3-642-36137-1_31

Wang N., Zhang N., Dowell F.E., Pearson T. (2005), Determining vitreousness of durum wheat using transmitted and reflected images, *Transactions of the ASAE*, 48(1), pp. 219–222, https://doi.org/10.13031/2013.17920

Wesley I.J., Osborne B.G., Larroque O., Bekes F. (2008), Measurement of the protein composition of single wheat kernels using near infrared spectroscopy, *Journal of Near Infrared Spectroscopy*, 16(6), pp. 505–516, https://doi.org/10.1255/jnirs.820

Xie F., Pearson T., Dowell F.E., Zhang N. (2004), Detecting vitreous wheat kernels using reflectance and transmittance image analysis, *Cereal Chemistry*, 81(5), pp. 594–597, https://doi.org/10.1094/CCHEM.2004.81.5.594

Xu S., Wang H., Liang X., Lu H. (2024), Research progress on methods for improving the stability of non-destructive testing of agricultural product quality, *Foods*, 13(23), 3917, https://doi.org/10.3390/foods13233917

Yang M., Shi Y., Song Q., Wei Z., Dun X., Wang Z., Wang Z., Qiu C.W., Zhang H., Cheng X. (2025), Optical sorting: past, present and future, *Light: Science & Applications*, 14(1), 103, https://doi.org/10.1038/s41377-024-01734-5

Yao H., Zhu F., Kincaid R., Hruska Z., Rajasekaran K. (2023), A low-cost, portable device for detecting and sorting aflatoxin-contaminated maize kernels, *Toxins*, 15(3), 197, https://doi.org/10.3390/toxins15030197

Yellanki V.S., Kavuri S., Anitha K., Lydia M.S., Srilakshmi N., Das M.N., Tripathy J. (2025), Grain quality testing using neural networks, *International Journal of Environmental Sciences*, 11(8), pp. 893–900, https://doi.org/10.64252/awrwt611

Yorulmaz O., Pearson T.C., Çetin A.E. (2011), Cepstrum based feature extraction method for fungus detection, In: Kim M.S., Tu S.-I. and Chao K. (Eds.), *Sensing for Agriculture and Food Quality and Safety III*, Proceedings of SPIE, 8027, 80270E, https://doi.org/10.1117/12.882406

ISSN: 2409-4951 (Online), 2310-1008(Print)

Zareiforoush H., Minaei S., Alizadeh M.R., Banakar A. (2015), Potential applications of computer vision in quality inspection of rice: a review, *Food Engineering Reviews*, 7, pp. 321–345, https://doi.org/10.1007/s12393-014-9101-z

Zhou Q., Huang W., Liang D., Tian X. (2021), Classification of aflatoxin B1 concentration of single maize kernel based on near-infrared hyperspectral imaging and feature selection, *Sensors*, 21(13), Article 4257, https://doi.org/10.3390/s21134257

Zhu L., Spachos P., Pensini E., Plataniotis K.N. (2021), Deep learning and machine vision for food processing: a survey, *Current Research in Food Science*, 4, pp. 233–249, https://doi.org/10.1016/j.crfs.2021.03.009

Author identifiers ORCID
Dmytro Galka 0009-0009-8877-1136
Andrii Sharan 0009-0000-7140-5038

Cite:

Ukr J Food Sci Style

Galka D., Sharan A. (2025), Optical grain sorting machines: review of principles of operation and classification, *Ukrainian Journal of Food Science*, 13(2), pp. 274–304, https://doi.org/10.24263/2310-1008-2025-13-2-12

APA Style

Galka, D., & Sharan, A. (2025). Optical grain sorting machines: review of principles of operation and classification. *Ukrainian Journal of Food Science, 13*(2), 274–304. https://doi.org/10.24263/2310-1008-2025-13-2-12

Effect of tablet density and punch kinematics on tablet quality

Oleksandr Zomenko, Oleksii Gubenia

National University of Food Technologies, Kyiv, Ukraine

Keywords:

Tablet
Compression
Kinematics
Punch
Density
Strength
Friability

Article history:

Received 21.09.2025
Received in revised form 30.11.2025
Accepted 31.12.2025

Corresponding author:

Oleksandr Zomenko
E-mail: zemenkoaleksandr@gmail.com

DOI:
10.24263/2310-1008-2025-13-2-13

Abstract

Introduction. The aim of the research was to determine the effect of tablet density and punch movement kinematics on tablet quality indicators, namely strength, friability, and density distribution.

Materials and methods. Tablet strength was determined by destructive stress during diametric compression, while friability was evaluated based on mass loss after processing in a rotating drum. The volumetric density distribution under different punch kinematics was analysed using the Finite Element Method method implemented in COMSOL Multiphysics software.

Results and discussion. At a density below 0.45 g/cm³, tablets exhibited low strength and were unsuitable for subsequent technological operations. Three zones of strength variation were identified: (I) tablet strength increased proportionally with density; (II) strength increased at a higher rate, following a parabolic relationship, with the transition from zone I to zone II occurring at approximately 0.7–0.8 g/cm³; (III) the rate of strength increase slowed, and beyond a certain density, strength decreased. The maximum tablet strength observed was 4.6 MPa, while the recommended working range was 1.5–3 MPa. At density above 1.5 g/cm³, lamination defects were observed. These results indicate the existence of an optimal density range that ensures adequate mechanical integrity without inducing structural defects. Deviations from this range may negatively affect both tablet performance and manufacturability.

Tablet friability decreased with increasing density following a parabolic trend and fell below 1% at densities of 1.04–1.06 g/cm³, meeting pharmacopoeial requirements. However, at densities exceeding 1.3–1.4 g/cm³, friability increased and can exceed acceptable limits.

During one-sided compression, stress and density near the die-contact edges differed from those in the tablet core. The core density did not exceed the average by more than 7%, and this heterogeneity had a negligible effect on strength and friability.

Under two-sided compression, higher-density zones appeared near the tablet edges, while the core density differed from the average by no more than 5%. These findings did not support the hypothesis that punch kinematics significantly affect density distribution.

Conclusions. Tablet density significantly affects strength and friability, whereas punch kinematics have a negligible influence on density distribution within the tablet volume.

ISSN: 2409-4951 (Online), 2310-1008(Print)

Introduction

Direct compression of non-metallic granular materials is a primary technological process in the production of solid medicinal forms, such as tablets (Gubenia et al., 2025). The aim of this process is to transform a loose, porous system of granules and excipients into a solid tablet with defined shape, size, and mechanical properties. During compression, the system transitions from a free-flowing to a compressed state, resulting in spatial inhomogeneity due to contact friction along the die surface, tool geometry (Qiu et al., 2017), and various compaction gradients (Swarbrick, 2007).

Deviations in tablet strength and friability can occur during compression, potentially affecting manufacturability (Sinka et al., 2007; Swarbrick, 2007) and the tablet's integrity during subsequent processes such as coating, packaging, transportation, and storage (Akande et al., 1998; Natoli et al., 2017).

Tablet strength is not regulated by external standards and is determined by the manufacturer of the medicinal product (CDER, 2015). For example, strength may range from 1.5 to 2.5 MPa (Gubenia et al., 2025), with deviations from the target value not exceeding 5%. Friability, according to the Harmonized European Pharmacopoeia (2024), should not exceed 1%, however, some researchers recommend a stricter limit of 0.3–0.5% (Podczeck, 2012).

The main factor affecting the strength and fragility of a tablet is its density. During compression, granule density can range from about 0.35 g/cm³ (typical for round granules) to 1–1.5 g/cm³ (Akande et al., 1998; Natoli et al., 2017). Literature provides limited data on how tablet density affects strength and friability, highlighting the need for further research. Some studies suggest that punch kinematics (one-sided or two-sided compression) can significantly influence density distribution within the tablet and, consequently, property heterogeneity along its height (Brewin et al., 2008). However, quantitative data on such distributions are scarce, and this aspect remains largely theoretical.

Empirical methods such as Heckel analysis (Heckel, 1961) and general approaches to compression evaluation (Leuenberger and Rohera, 1986) are commonly used to describe the compressibility of powders, granules, and tablets. These methods rely on average properties and often do not account for factors such as die geometry, friction, or punch movement sequences, which affect density and stress distribution. Moreover, their ability to model stages like decompression and ejection is limited, even though these stages are critical for understanding residual stresses and tablet failure risks. Therefore, modelling the spatial heterogeneity of the compression process is essential for analyzing potential defects (Partheniadis et al., 2022).

Advanced simulation methods are required to predict and analyze tablet density distribution during compression, allowing the spatial behavior of the tablet to be reproduced throughout all stages of the compression process (Partheniadis et al., 2022; Wu et al., 2008).

The finite element method (FEM), combined with constitutive compression models, allows the transition from general parameters to detailed distributions of stress, strain, and relative density within a tablet. The most commonly used model is the density-dependent Drucker-Prager Cap (DPC), which integrates shear strength with volumetric compression under hydrostatic pressure and permits parameter calibration based on relative density (Baroutaji et al., 2017; Han et al., 2008). Employing density-dependent (or solid-fraction-dependent) DPC parameters improves agreement with experimental compression and unloading curves, as well as predictions of tool displacements (Sinha et al., 2010a). For greater accuracy, viscoelastic or plastic models are sometimes applied, providing better reproduction of experimental curves during unloading (Diarra et al., 2013).

ISSN: 2409-4951 (Online), 2310-1008(Print)

The aim of this study was to investigate the influence of tablet density on key quality parameters including hardness and friability, and to assess the influence of compression method on density distribution within the tablet.

Materials and methods

Experimental studies

Materials. The strength of two well-known medicinal tablet products was examined. Sample 1 contained excipients including citric acid monohydrate, potato starch, povidone, cocoa, and calcium stearate, along with active pharmaceutical ingredients (APIs) acetylsalicylic acid, paracetamol, and caffeine. Sample 2 contained excipients such as potato starch, talc, and calcium stearate, with the API sodium metamizole.

Experimental equipment. In this study, a field experiment was performed. The tablets were made under production conditions using a Korsch XL 400 tablet press. This press operates with a pre-compression force of 20 kN and a main compression force of 100 kN, with a maximum output of 338,000 tablets per hour at a maximum drum rotation speed of 120 rpm.

Determination of tablet strength. The strength, or breaking point, of tablets (European Pharmacopoeia, 2024) was determined using a standard pharmaceutical method: the tablet was subjected to diametric compression, and the force PPP at which it fractured was measured, with this breaking force representing the tablet's breaking point:

$$\sigma = \frac{P}{d \cdot h} \text{ Pa}, \quad (1)$$

where P is the breaking force (N), d is the tablet diameter (m), and h is the tablet height (m). Tablet breaking force and strength were measured using the PTB-M 300 N Pharma Test device, whose working element consists of two jaws facing each other and moving horizontally to compress the tablet across its diameter. The device has a precision of 1 N, and each measurement was performed 10 times.

Determination of tablet friability. The friability of tablets was tested using the "ERWEKA TAR II" device, which features a rotating wheel with a single paddle (European Pharmacopoeia, 2024). Ten tablets were initially dusted off, weighed, and placed into a drum, which was then closed with a lid. The device was operated for 4 minutes, and afterward, the tablets were weighed again. The friability index P, %, is calculated using the formula:

$$P = 100 - \frac{m_b - m_f}{m_b} \cdot 100 , \quad (2)$$

where m_b and m_f are the mass of tablets before and after processing, respectivelly.

Determination of tablet density heterogeneity

The distribution of tablet density within the volume was analysed using simulation modeling in COMSOL Multiphysics® based on the finite element method (FEM). The mechanical behavior of the powder during compression was represented by an elastic-plastic model for powder compression, specifically the Drucker-Prager Cap (DPC) model (Frenning,

ISSN: 2409-4951 (Online), 2310-1008(Print)

2023), which defines key material parameters as functions of relative density or porosity. This approach allows the prediction of stress, strain, and local density fields throughout the entire tablet volume during compression, as well as the assessment of density heterogeneity, including variations or gradients between the core and outer zones, near the punches, and along the die wall (Sinha et al., 2010b). The model also accounts for the material properties and initial state of the powder, simulating powder compression within the die to form the tablet under quasi-static loading conditions. The initial powder state is characterized by the true density ρ_{true} and the bulk density ρ_{bulk}. For calibration purposes, the following values were used: ρ_{true} = 1.59 g/cm³ (1590 kg/m³); ρ_{bulk} = 0.36 g/cm³ (360 kg/m³).

Accordingly, the initial relative density (solid fraction) is $\rho_{rel(0)} = \rho_{bulk}/\rho_{true} = 0.22642$. The density distribution within the powder volume is considered uniform, and the material is assumed to be isotropic at the start of the simulation.

Geometry of the tool, volume parameterization, and assumptions. The model is built in a 2D axisymmetric system, which is a common approach for round tablets and ensures accurate consideration of the contact interaction between the powder and the tool (Cunningham et al., 2004; Sinka et al., 2003). The initial geometry of the powder column is defined by the die radius R_0 and the filling height H_0:

$$R_0 = 5 \text{ mm}, H_0 = 12.5 \text{ mm}$$

The cross-sectional area of the powder A_0 is calculated as

$$A_0 = \pi R_0^2,$$

and the initial volume

$$V_0 = A_0 \cdot H_0.$$

For the given values

$$A_0 = 7.854 \times 10\ m^2,$$

$$V_0 = 9.8175 \times 10\ m^3.$$

The mass of the powder m in the die remains constant:

$$m = \rho_{fill} \cdot V_0 = 3.5343 \times 10^4\ kg.$$

The target height of the powder H_f after compression is determined based on mass conservation and the actual density (excluding material losses):

$$H_f = (m/A_0)/\rho_{actual} = 0.0028302m\,(2.8302\ mm).$$

The tool (die and punches) in this model is treated as rigid (rigid tooling), meaning tool deformation is not accounted for, and the focus is on the stress-strain state of the powder body and the effects of contact and friction (COMSOL AB, 2022).

Input and derived parameters for process simulation are shown in Tables 1 and 2.

Constitutive model of powder (Drucker-Prager Cap). The mechanical behaviour of the powder is described using a continuous elastoplastic model of porous plasticity based on the Capped Drucker-Prager (DPC) model, which is used for compression processes with pressure-dependent flow and “cap' densification (Baroutaji et al., 2017; Partheniadis et al., 2022). The evolution of the material state is determined by the relative density ρ_rel, which changes due to irreversible plastic deformation and influences the mechanical properties during compression. Hardening was regulated according to the implementation of DPC in the COMSOL model (COMSOL AB, 2022).

ISSN: 2409-4951 (Online), 2310-1008(Print)

Table 1

Input parameters of the model

Symbol	Value	Description
R_0	5 mm	Initial radius of the powder column (die radius)
H_0	12.5 mm	Initial height of powder filling
ρ_{true} (R_{hof})	1.59 g/cm^3	True powder density
ρ_{bulk} (R_{hobulk})	0.36 g/cm^3	Loose bulk density of the powder

Table 2

Derived parameters

Symbol	Expression	Value (SI)	Description
A_0	$\pi \cdot R_0^2$	$7.854 \cdot 10^{-5}$	Cross-sectional area
V_0	$A_0 \cdot H_0$	$9.8175 \cdot 10^{-7}$	Initial powder volume
m	$\rho_{bulk} \cdot V_0$	$3.5343 \cdot 10^{-4}$	Mass of powder in the die
$\rho_{rel(0)}$	ρ_{bulk}/ρ_{true}	0.22642	Initial relative density
H_f	$(m/A_0)/\rho_{true}$	0.0028302	Final height of the powder after compression

Density-dependent material functions (COMSOL parameters). Material parameters depend on the relative density $x = \rho_{rel}$. All formulas are used with the same units as in the COMSOL model (Young's modulus and yield strength in MPa; parameter a_1 is dimensionless). Young's modulus is defined as:

$$E(x) = 90 \cdot \exp^{4.395 \cdot x}, \text{ MPa}$$

Yield strength:

$$\sigma_y(x) = 0.2955 \cdot (4.5642 \cdot x)\ 4.395 \cdot x$$

Yield function parameter:

$$a_1(x) = \mathrm{tg}(12.628 \cdot x + 56.194)^\circ.$$

The Poisson's ratio remained constant at $\nu = 0.16$. This approach, which involves the dependence of E and flow parameters on ρ_{rel} at a fixed ν, is commonly used in modeling tablet compression because it captures how stiffness and strength change with increasing density, simplifying the process of determining ν (COMSOL AB, 2022; Cunningham et al., 2004; Partheniadis et al., 2022).

Contact interaction and friction. Contact between granules and the press tool was modelled as a Coulomb Friction Problem. The coefficient of friction between the powder and the wall of the die or the surface of the punch is set based on the model scenario; for demonstration purposes, a typical value is around 0.1. It is advised to measure or estimate this during sensitivity analysis, as friction affects density gradients and stress distributions (COMSOL AB, 2022; Cunningham et al., 2004).

Loading program: compression and decompression. The pressing process occurs through controlled movement of the upper punch (displacement-controlled), which ensures a consistent deformation path and stability of the numerical solution for the non-linear contact-plastic problem. The load trajectory includes a compression stage until the final height H_f is reached and a decompression stage.

ISSN: 2409-4951 (Online), 2310-1008(Print)

Output quantities and post-processing details. The analysis was performed using the following indicators: Fields of relative density $\rho_{rel}(r,z)$ at the end of compression and after decompression; Components of stresses σ_z, σ_r, σ_θ, and the equivalent stresses or plastic deformations. The heterogeneity of compression was also examined through the difference $\rho_{rel(max)} - \rho_{rel(min)}$ and the identification of potential risk zones for defects linked to tensile and shear stresses during the unloading phase (Partheniadis et al., 2022; Wu et al., 2008).

Results and discussion

Influence of density on tablet strength

The graphical relationship between tablet strength and its density is shown in Figure 1.

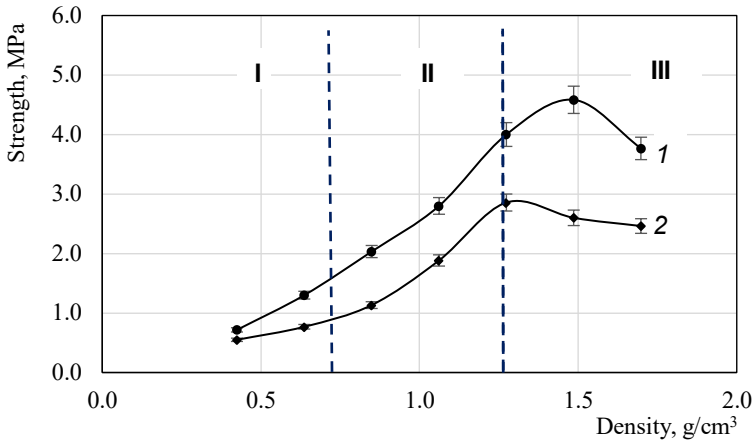

Figure 1. The influence of tablet density on its strength:
1 – sample 1; 2 – sample 2

In general, three zones can be identified in the relationship between tablet strength and density. In Zone I, strength increases nearly proportionally with density. In Zone II, strength rises more rapidly following a parabolic trend, with the transition occurring at around 0.7–0.8 g/cm³. In Zone III, the rate of strength increase slows, and beyond a certain density, strength decreases, with tablet quality deteriorating due to delamination and particle chipping.

Zones I and II are not always distinguished, and they are sometimes considered as a single zone of increasing tablet strength with rising density or compression pressure. Since the increase in strength is explained by granule particle fragmentation (Yadav et al., 2018) and the formation of additional bonds between granules (Siiriä et al., 2011), these zones should be treated separately.

As the force and pressing pressure increase, particles begin to deform and break into smaller fragments during the initial stage, creating new bonding zones between them (Garekani et al., 2001). The granulate mass becomes more compact as smaller fragments fill the voids between larger ones. Beyond a certain pressure, it can be assumed that the maximum number of bonds has formed, the material no longer consists of separate granules but becomes continuous, and its porosity approaches minimal values (Manufacturingchemist, 2020).

ISSN: 2409-4951 (Online), 2310-1008(Print)

Influence of tablet density on their friability

The relationship between tablet friability and density is shown in Figure 2.

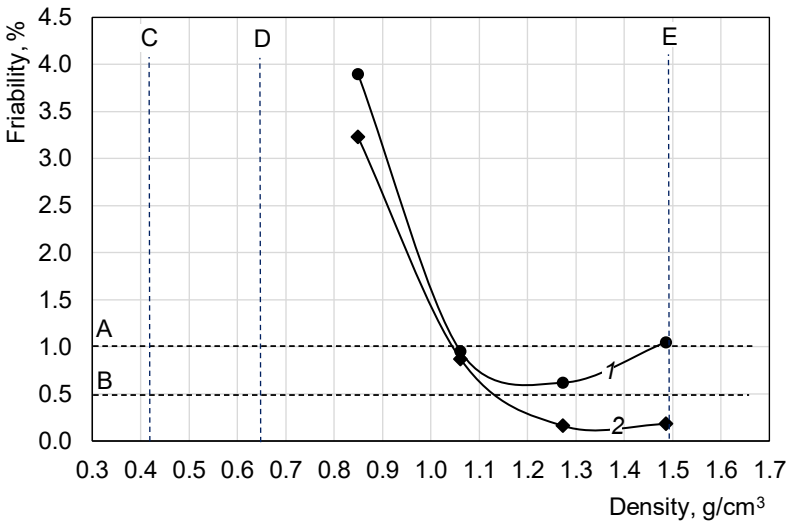

Figure 2. Influence of tablet density on friability:
1 – Sample 1; 2 – Sample 2.
A – friability limit according to regulatory standards;
B – recommended friability limit according to researchers;
C – tablet density at which tablets disintegrate in hands;
D – tablet density at which tablets disintegrate in the drum of the friability tester;
E – tablet density at which delamination occurs in the drum of the friability tester.
* Note – points (experimental values) are connected by a smooth curve for clarity and better visual perception. Such a connection should not be considered as a mathematical dependence.

Initially, when tablets reach the minimum density at which they do not disintegrate in hands or in the drum of the friability tester, friability decreases following a parabolic trend. At a density of 0.8 g/cm³, friability ranges from 3.2 to 3.8%, significantly exceeding the pharmacopoeial limits (European Pharmacopoeia, 2024) and even stricter values reported in the literature (Podczeck, 2007).

At densities of 1.04–1.06 g/cm³, friability falls below 1%, meeting pharmacopoeial requirements. For sample 2, friability drops further to less than 0.5% at around 1.13 g/cm³, in line with recommendations from other researchers. Sample 1, however, did not reach this value, remaining above 0.6% within the studied conditions. This indicates that further reduction of friability for sample 2 would require adjustment of technological parameters such as formulation, granulation method, and processing regimes.

With densities above 1.2–1.3 g/cm³, friability begins to increase again following a parabolic trend. At 1.5 g/cm³, friability of sample 1 exceeds regulated limits, while sample 2 remains below 0.5%.

ISSN: 2409-4951 (Online), 2310-1008(Print)

Influence of punch kinematics on stress and density distribution during compression

Case 1. One-sided compression is a method in which the lower punch remains stationary while the upper punch compacts the granulate within the die. The terms "upper" and "lower" are used conditionally for clarity.

The results of numerical simulations of granule compression in a die were analyzed using the elastoplastic Drucker-Prager Cap (DPC) model. The analysis considers the main punch positions (Figure 3):

- Position 0 – initial punch position, no load applied, with uniform material density;
- Position 1 – final lower position of the punch, end of compression, with maximum load;
- Position 2 – punch position at the final stage of decompression (unloading).

As punch displacement increases during compression, axial pressure rises following a parabolic trend, with a more pronounced increase near the end of the compressing process (Figure 4).

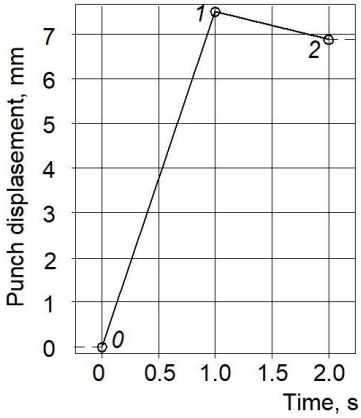

Figure 3. Puncture position

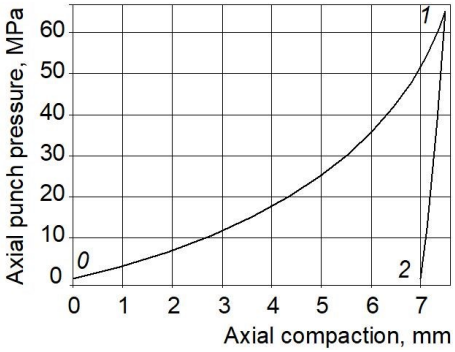

Figure 4. Change in compressing pressure during punch movement

Punch position: 0 – initial position; 1 – final lower position; 2 – final stage of decompression

During the axial displacement of the punch ΔH from position 0 to position 1, approximately 7–7.6 mm, the maximum compressive pressure P_{max} is about 67 MPa. Such behaviour is characteristic of powder compression with density-dependent stiffness and strengthening in the DPC model: as the relative density ρ_{rel} increases, the strength parameters (including Young's modulus) also increase, which enhances the nonlinearity of the axial pressure dependence on the degree of compression (COMSOL AB, 2024; Partheniadis et al., 2022).

It is analysed the fields of equivalent stresses σ_{eq} according to von Mises for position 1. High stress values are observed within the volume of the compressed tablet, with localisation in the contact zone with the surface of the die at the upper and lower edges of the tablet (Figure 5). The maximum value $\sigma_{eq(max)}$ is approximately 65 MPa. This is explained by stress localisation due to the combined effect of contact constraints and friction, which creates a complex stress-strain state with an increased shear component (Sinka et al., 2003; Cunningham et al., 2004).

ISSN: 2409-4951 (Online), 2310-1008(Print)

After decompression (Position 2), a significant reduction in stresses is observed compared to position 1, but the relative densities ρ_{rel} remain uneven.

Data on the change in stresses within the tablet during compression are important from a quality control perspective: potential defects (capping/lamination) depend on the compression force, as well as on the nature of residual stresses and tensile zones that may form during unloading or ejection (Partheniadis et al., 2022; Wu et al., 2008).

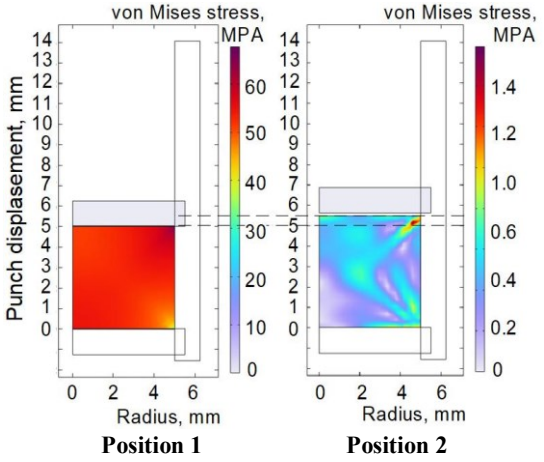

Figure 5. Equivalent stress σ_{eq} according to von Mises, (MPa) (for position 1 and position 2).

It should be noted that this part of the research uses the concept of relative density, which is optimal for powder compaction models. Relative density reflects the degree of volume filled with solid material and directly characterizes it. This parameter is important because, during compression, only the spatial arrangement and porosity change, while the true density remains constant. As a universal indicator, relative density is useful for describing compaction, performing simulation modeling, scaling and comparing materials, ensuring calculation stability, and supporting modifications of tablet strength models. Its use is fully justified and consistent with modern theories (Cunningham et al., 2004).

Spatial heterogeneity in the relative density ρ_{rel} is observed (Figures 6 and 7), it varies from 0.45 to 0.57. The maximum values are concentrated near the upper edge of the tablet in the contact zone with the wall of the mould, while the minimum values are observed near the lower edge. Such behaviour is typical for axisymmetric compression problems with wall friction: friction limits radial sliding, enhances shear deformation, and creates compression gradients (Cunningham et al., 2004; Sinka et al., 2003). A comparison of the data for position 1 and position 2 shows that after decompression, the field of relative density ρrel changes insignificantly. This is explained by the fact that the relative density is primarily determined by irreversible plastic deformation, and during unloading, a reduction in stresses occurs (COMSOL AB, 2024).

At the end of the compression process, a difference of about 7% is observed between the values of the relative density in the core (centre) of the tablet and its average relative density of the entire tablet (Figure 8).

ISSN: 2409-4951 (Online), 2310-1008(Print)

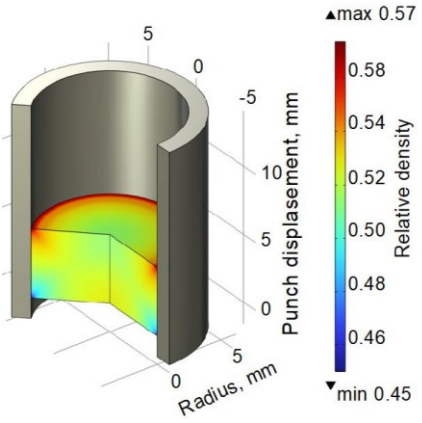

Figure 6. 3D visualisation of the distribution of relative tablet density during compression

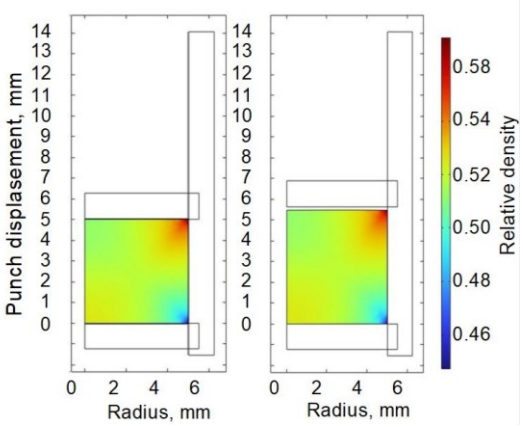

Figure 7. Change in tablet density during compression for position 1 (end of compression) and position 2 (after decompression)

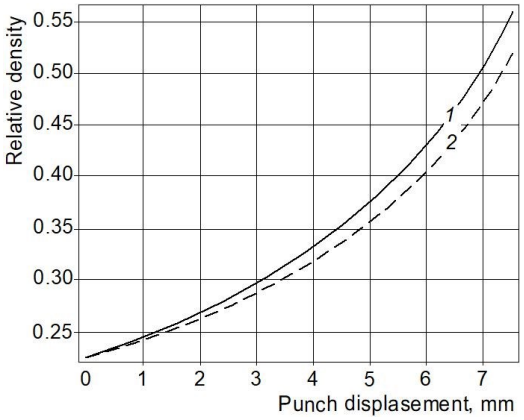

Figure 8. Change in relative densities during complete displacement of punch: 1 – relative density at the core (centre) of the tablet; 2 – average relative density of the tablet

Case 2. Double-sided compression is a method in which the granulate in the die is compacted simultaneously from both sides by the punches. Similar to one-sided compression, the stress and density fields (Figure 9) and the final tablet densities (Figure 10) were analyzed. The main difference is that higher-density zones appear on both sides at the points of contact with the die surfaces, while a lower-density zone forms in the middle near the die surface. The position of this lower-density zone can shift vertically depending on the relative speeds of the punches.

At the end of the compression process, there is a difference of about 4% between the relative density values in the core (center) of the tablet and its average relative density of the entire tablet (Figure 10). This is less compared to the case of one-sided compression.

ISSN: 2409-4951 (Online), 2310-1008(Print)

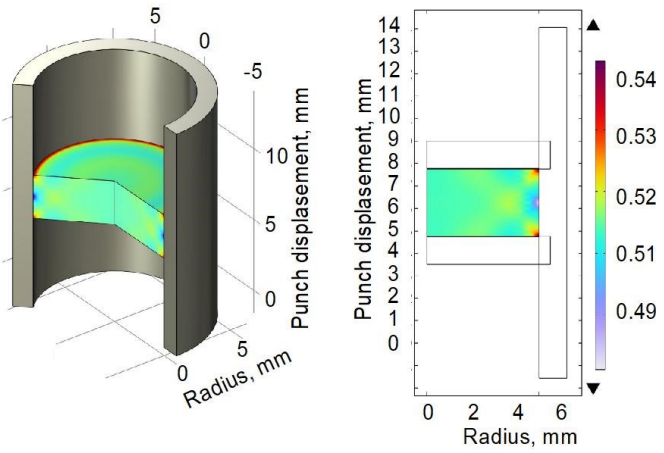

Figure 9. Relative density distribution of a tablet produced by double-sided compression

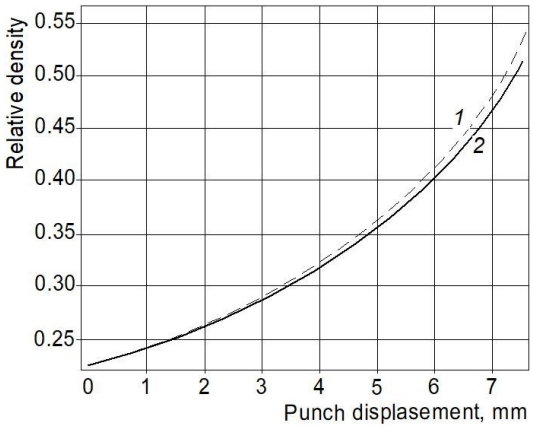

Figure 10. Change in relative densities of a tablet produced by double-sided compression: 1 – relative density at the core (centre) of the tablet; 2 – average relative density of the tablet

Therefore, punch kinematics, whether one sided or two sided compression, has a negligible effect on the density distribution within the tablet. It should be noted that the common assumption in textbooks that two sided compression provides a more uniform density and strength distribution (Sydorov et al., 2009) is not statistically confirmed for tablets in which the height is much smaller than the diameter.

Conclusions

Tablet strength shows a complex dependence on density. At densities below 0.45 g/cm³, tablets have low strength, crumble in the hands, and are unsuitable for subsequent coating, packaging, or transportation. Three zones can be distinguished: in Zone I, strength increases

ISSN: 2409-4951 (Online), 2310-1008(Print)

roughly proportionally with density; in Zone II, strength rises more rapidly following a parabolic trend, with the transition from Zone I occurring at about 1 g/cm³; in Zone III, the rate of strength increase slows and eventually decreases. The maximum strength observed was 4.6 MPa, while the recommended working range is 1.5–3 MPa, and at densities above 1.5g/cm³ delamination may occur. Friability decreases with increasing density in a parabolic manner, falling below 1% at 1.04–1.06 g/cm³, which meets pharmacopoeial standards. At densities above 1.2–1.3 g/cm³, friability begins to rise again, exceeding regulated limits.

During one-sided compression, zones of higher and lower stress and density appear near the die surfaces, while the core density does not exceed the average by more than 7%, slightly affecting strength and friability but potentially causing chipping. Double-sided compression produces higher-density zones at the tablet edges, with core density differences also within 7%, lower than in one-sided compressing, showing that the compressing method has minimal effect on density and strength distribution. Strength data and compressing forces are critical for selecting compression methods and modes, designing the press cycle, and calculating the compressing units and drive system.

References

Akande O.F., Ford J.L., Rowe P.H., Rubinstein M.H. (1998), The effects of lag-time and dwell-time on the compaction properties of 1:1 paracetamol–microcrystalline cellulose tablets prepared by pre-compression and main compression, *Journal of Pharmacy and Pharmacology*, 50(1), pp. 19–28, https://doi.org/10.1111/j.2042-7158.1998.tb03300.x

Baroutaji A., Lenihan S., Bryan K. (2017), Combination of finite element method and Drucker-Prager Cap material model for simulation of pharmaceutical tableting process, *Materialwissenschaft und Werkstofftechnik*, 48(11), pp. 1133–1145, https://doi.org/10.1002/mawe.201700048

Brewin P.R., Coube O., Doremus P., Tweed J.H. (Eds.), (2008), *Modelling of Powder Die Compaction*, Springer, London, https://doi.org/10.1007/978-1-84628-099-3

Center for Drug Evaluation and Research (CDER). (2015), Size, Shape, and Other Physical Attributes of Generic Tablets and Capsules: Guidance for Industry. *U.S. Food and Drug Administration*, Available at: https://www.fda.gov/media/87344/download

COMSOL AB (2022), Simulating the pharmaceutical tableting process (Pharmaceutical Tableting Process model: pharmaceutical_tableting_process), *COMSOL Blog / COMSOL Multiphysics® Application Library*, Available at: https://www.comsol.com/blogs/simulating-the-pharmaceutical-tableting-process

Cunningham J.C., Sinka I.C., Zavaliangos A. (2004), Analysis of tablet compaction. I. Characterization of mechanical behavior of powder and powder/tooling friction, *Journal of Pharmaceutical Sciences*, 93(8), pp. 2022–2039, https://doi.org/10.1002/jps.20110

Diarra H., Mazel V., Busignies V., Tchoreloff P. (2013), FEM simulation of the die compaction of pharmaceutical products: Influence of visco-elastic phenomena and comparison with experiments, *International Journal of Pharmaceutics*, 453(2), pp. 389–394, https://doi.org/10.1016/j.ijpharm.2013.05.038

European Pharmacopoeia (2024), *General chapters and monographs related to tablet friability and resistance to crushing (Ph. Eur., 11th Edition, Supplement 11.4)*, European Directorate for the Quality of Medicines & HealthCare (EDQM), Council of Europe, Available at: https://pheur.edqm.eu

ISSN: 2409-4951 (Online), 2310-1008(Print)

Frenning G. (2023), On the thermodynamic consistency of the Drucker–Prager Cap model: Modification of the plastic potential and analysis of unloading, *Powder Technology*, 423, 118503, https://doi.org/10.1016/j.powtec.2023.118503

Gubenia O., Zomenko O., Samarchuk S., Mnerie D. (2025), On the strength and friability of series products manufactured by direct compression of non-metallic granules, *Nonconventional Technologies Review*, 29(3), pp. 15–21, Available at: https://www.revtn.ro/index.php/revtn/article/view/532

Han L.H., Elliott J.A., Bentham A.C., Mills A., Amidon G.E., Hancock B.C. (2008), A modified Drucker–Prager Cap model for die compaction simulation of pharmaceutical powders, *International Journal of Solids and Structures*, 45(10), pp. 3088–3106, https://doi.org/10.1016/j.ijsolstr.2008.01.024

Heckel R.W. (1961), Density–pressure relationships in powder compaction, *Transactions of the Metallurgical Society of AIME*, 221, pp. 671–675.

Leuenberger H., Rohera B.D. (1986), Fundamentals of powder compression. I. The compactibility and compressibility of pharmaceutical powders, *Pharmaceutical Research*, 3(1), pp. 12–22, https://doi.org/10.1023/A:1016364613722

Natoli D., Levin M., Tsygan L., Liu L. (2017), Development, optimization, and scale-up of process parameters: tablet compression. In: Y. Qiu, Y. Chen, G.G.Z. Zhang, L. Yu, R.V. Mantri (Eds.), *Developing Solid Oral Dosage Forms: Pharmaceutical Theory and Practice* (2nd ed.), pp. 917–951, Academic Press, https://doi.org/10.1016/B978-0-12-802447-8.00033-9

Partheniadis I., Samiotakis A., Bouzid A. (2022), Finite element analysis and modeling in pharmaceutical tableting, *Pharmaceutics*, 14(3), 673, https://doi.org/10.3390/pharmaceutics14030673

Podczeck F. (2012), Methods for the practical determination of the mechanical strength of tablets – from empiricism to science, *International Journal of Pharmaceutics*, 436, pp. 214–232, https://doi.org/10.1016/j.ijpharm.2012.06.059

Qiu Y., Chen Y., Zhang G.G.Z., Yu L., Mantri R.V. (Eds.), (2017), *Developing Solid Oral Dosage Forms: Pharmaceutical Theory and Practice* (2nd ed.), Academic Press.

Sinha T., Bharadwaj R., Curtis J.S., Hancock B.C., Wassgren C. (2010a), A study on the sensitivity of Drucker–Prager Cap model parameters during the decompression phase of powder compaction simulations, *Powder Technology*, 198(3), pp. 315–324, https://doi.org/10.1016/j.powtec.2009.10.025

Sinha T., Bharadwaj R., Curtis J.S., Hancock B.C., Wassgren C. (2010b), Finite element analysis of pharmaceutical tablet compaction using a density dependent material plasticity model, *Powder Technology*, 202(1–3), pp. 46–54, https://doi.org/10.1016/j.powtec.2010.04.001

Sinka I.C., Cunningham J.C., Zavaliangos A. (2003), The effect of wall friction in the compaction of pharmaceutical tablets with curved faces: a validation study of the finite element method, *Powder Technology*, 130(1–3), pp. 238–251, https://doi.org/10.1016/S0032-5910(03)00094-9

Sinka I.C., Pitt K.G., Cocks A.C.F. (2007), The strength of pharmaceutical tablets. In: *Handbook of Powder Technology*, 12, pp. 941–970, https://doi.org/10.1016/S0167-3785(07)12025-X

Swarbrick J. (Ed.), (2007), *Encyclopedia of Pharmaceutical Technology* (3rd ed., Vol. 6), Informa Healthcare / Taylor & Francis, https://doi.org/10.1201/b19309

Sydorov Yu.I., Chuieshov V.I., Novikov V.P. (2009), *Processes and Apparatus of Chemical-Pharmaceutical Industry*, Nova Knyga, Vinnytsia.

ISSN: 2409-4951 (Online), 2310-1008(Print)

Wu C.Y., Hancock B.C., Mills A., Bentham A.C., Best S.M., Elliott J.A. (2008), Numerical and experimental investigation of capping mechanisms during pharmaceutical tablet compaction, *Powder Technology*, 181, pp. 121–129, https://doi.org/10.1016/j.powtec.2006.12.017

Author identifiers ORCID
Oleksandr Zomenko 0009-0002-7370-8870
Oleksii Gubenia 0000-0003-2773-4373

Cite:

Ukr J Food Sci Style

Zomenko O., Gubenia O. (2025), Effect of tablet density and punch kinematics on tablet quality, *Ukrainian Journal of Food Science*, 13(2), pp. 305–318, https://doi.org/10.24263/2310-1008-2025-13-2-13

APA Style

Zomenko, O., & Gubenia, O. (2025). Effect of tablet density and punch kinematics on tablet quality. *Ukrainian Journal of Food Science, 13*(2), 305–318. https://doi.org/10.24263/2310-1008-2025-13-2-13

Instructions for Authors

Dear colleagues!

The Editorial Board of scientific periodical «**Ukrainian Journal of Food Science**» invites you to publish of your scientific research.

A manuscript should describe the research work that has not been published before and is not under consideration for publication anywhere else. Submission of the manuscript implies that its publication has been approved by all co-authors as well as by the responsible authorities at the institute where the work has been carried out.

It is mandatory to include a covering letter to the editor which includes short information about the subject of the research, its novelty and significance; state that all the authors agree to submit this paper to Ukrainian Journal of Food Science; that it is the original work of the authors.

Manuscript requirements

Authors must prepare the manuscript according to the instructions for authors. Editors reserve the right to adjust the style to certain standards of uniformity.

Title page, references, tables and figures should be included in the manuscript body.

Language – English

Manuscripts should be submitted in as a Word document.

Use 1.0 spacing and 2 cm margins.

Use a normal font 14-point Times New Roman for text, tables, and captions for figures.

Provide tables and figures in the text of the manuscript.

Consult a recent issue of the journal for a style check.

Number all pages consecutively.

Abbreviations should be defined on first appearance in text and used consistently thereafter. No abbreviation should be used in title and section headings.

Please submit math equations as editable text and not as images (It is recommended to use MathType or Microsoft Equation Editor software).

Minimal size of the research article (without Abstract and References) is 10 pages; for the review article minimal size is 25 pages (without Abstract and References).

Manuscript should include:

Title (should be concise and informative). Avoid abbreviations in it.

Authors' information: the name(s) of the author(s); the affiliation(s) of the author(s), city, country. One author has been designated as the corresponding author with e-mail address. If available, the 16-digit ORCID of the author(s).

Declaration of interest

Author contributions

ISSN: 2409-4951 (Online), 2310-1008(Print)

Abstract. The **abstract** should contain the following mandatory parts:

Introduction provides an aim for the study (2-3 lines).

Materials and methods briefly describe the materials and methods used in the study (3-5 lines).

Results and discussion describe the main findings (23-26 lines).

Conclusion provides the main conclusions (2-3 lines).

The abstract should not contain any undefined abbreviations or references to the article.

Keywords. Immediately after the abstract provide 4 to 6 keywords.

Text of manuscript
References

Manuscripts should be divided into the following sections:

- **Introduction**
- **Materials and methods**
- **Results and Discussion**
- **Conclusions**
- **References**

Introduction. Provide background information without an extensive literature review, and clearly state the aim of the present research. Identify knowledge gaps and justify the relevance of the topic. The length should not exceed 1.5 pages.

Materials and methods. Provide sufficient detail to enable an independent researcher to replicate the study. For methods that are already published, cite the original references and provide only a brief summary. Full descriptions are required only for new techniques. Clearly describe any modifications made to existing methods.

Results and discussion. Results should be presented clearly and concisely, using tables and/or figures where appropriate. The significance of the findings should be discussed, including comparisons with existing literature.

Conclusions. The main conclusions should be drawn from results and be presented in a short Conclusions section.

Acknowledgments(if necessary). Acknowledgments of individuals, grants, or funding sources should be placed in a separate section. List the names of all persons who contributed to the research. Funding organizations should be named in full.

Divide your article into sections and into subsections if necessary. Any subsection should have a brief heading.

References

Please, check references carefully.

The list of references should include works that are cited in the text and that have been published or accepted for publication.

All references mentioned in the reference list are cited in the text, and vice versa.

Cite references in the text by name and year in parentheses. Some examples:

(Drobot, 2008); (Qi and Zhou, 2012); (Bolarinwa et al., 2019; Rabie et al., 2020; Sengev et al., 2013).

Reference list should be alphabetized by the last names of the first author of each work: for one author, by name of author, then chronologically; for two authors, by name of author,

ISSN: 2409-4951 (Online), 2310-1008(Print)

then name of coauthor, then chronologically; for more than two authors, by name of first author, then chronologically.

If available, please include full DOI links in your reference list (e.g. “https://doi.org/abc”).

Reference style

Journal article

Please follow this style and order: author's surname, initial(s), year of publication (in brackets), paper title, *journal title (in italic)*, volume number (issue), first and last page numbers, e.g.:

Ivanov V., Shevchenko O., Marynin A., Stabnikov V., Gubenia O., Stabnikova O., Shevchenko A., Gavva O., Saliuk A. (2021), Trends and expected benefits of the breaking edge food technologies in 2021–2030, *Ukrainian Food Journal*, 10(1), pp. 7–36, https://doi.org/10.24263/2304-974X-2021-10-1-3

The names of all authors should be provided. Journal names should not be abbreviated.

Book

Deegan C. (2000), *Financial Accounting Theory*, McGraw-Hill Book Company, Sydney.

Book chapter in an edited book

Kochubei-Lytvynenko O., Bilyk O., Bondarenko Y., Stabnikov V. (2022), Whey proteins in bakery products, In: O. Paredes-López, O. Shevchenko, V. Stabnikov, V. Ivanov (Eds.), *Bioenhancement and Fortification of Foods for a Healthy Diet*, pp. 67-88, CRC Press, Boca Raton, https://doi.org/10.1201/9781003225287-5

Online document

Mendeley, J.A., Thomson, M., Coyne, R.P. (2017), *How and When to Reference*, Available at: https://www.howandwhentoreference.com

Conference paper

Arych M. (2018), Insurance's impact on food safety and food security, *Resource and Energy Saving Technologies of Production and Packing of Food Products as the Main Fundamentals of Their Competitiveness: Proceedings of the 7th International Specialized Scientific and Practical Conference, September 13, 2018,* NUFT, Kyiv, pp. 52–57.

Figures

All figures should be made in graphic editor using a font Arial.

The font size on the figures and the text of the article should be the same.

Black and white graphic with no shading should be used.

The figure elements (lines, grid, and text) should be presented in black (not gray) colour.

Figure parts should be denoted by lowercase letters (a, b, etc.).

All figures are to be numbered using Arabic numerals.

Figures should be cited in text in consecutive numerical order.

Place figure after its first mentioned in the text.

Figure captions begin with the term Figure in bold type, followed by the figure number, also in bold type.

Each figure should have a caption describing what the figure depicts in bold type.

ISSN: 2409-4951 (Online), 2310-1008(Print)

Supply all figures and EXCEL format files with graphs additionally as separate files.

Photos are not advisable to be used.

If you include figures that have already been published elsewhere, you must obtain permission from the copyright owner(s).

Tables

Number tables consecutively in accordance with their appearance in the text.

Place footnotes to tables below the table body and indicate them with superscript lowercase letters.

Place table after its first mentioned in the text.

Ensure that the data presented in tables do not duplicate results described elsewhere in the article.

Suggesting / excluding reviewers

Authors are welcome to suggest reviewers and/or request the exclusion of certain individuals when they submit their manuscripts.

When suggesting reviewers, authors should make sure they are totally independent and not connected to the work in any way. When suggesting reviewers, the Corresponding Author must provide an institutional email address for each suggested reviewer. Please note that the Journal may not use the suggestions, but suggestions are appreciated and may help facilitate the peer review process.

Submission

Email for all submissions and other inquiries:

ukrfoodscience@meta.ua

ISSN: 2409-4951 (Online), 2310-1008(Print)

Ukrainian Journal of Food Science

Ukrainian Journal of Food Science публікує оригінальні наукові статті, короткі повідомлення, оглядові статті, новини та огляди літератури.

Тематика публікацій в **Ukrainian Journal of Food Science:**

Харчова інженерія
Харчова хімія
Мікробіологія
Властивості харчових продуктів
Якість та безпека харчових продуктів
Нанотехнології
Процеси та обладнання
Економіка і управління
Автоматизація процесів
Упаковка для харчових продуктів
Здоров'я

Періодичність журналу 2 номери на рік (червень, грудень).

Результати досліджень, представлені в журналі, повинні бути новими, мати зв'язок з харчовою наукою і представляти інтерес для міжнародного наукового співтовариства.

Ukrainian Journal of Food Science індексується наукометричними базами**:**

EBSCO (2013)
Google Scholar (2013)
Index Copernicus (2014)
Directory of Open Access scholarly Resources (ROAD) (2014)
CAS Source Index (CASSI) (2016)
FSTA (Food Science and Technology Abstracts) (2018)

Ukrainian Journal of Food Science включено у перелік наукових фахових видань України за галузями науки: економічні (28.12.2019) технічні (17.03.2020)

Спеціальності: 51 (28.12.2019), 73 (28.12.2019), 75 (28.12.2019), 141 (28.12.2019), 144 (28.12.2019), 162 (28.12.2019), 181 (28.12.2019), 133 (17.03.2020).

Рецензія рукопису статті. Наукові статті, представлені для публікації в «**Ukrainian Journal of Food Science**» проходять «подвійне сліпе рецензування» (рецензент не знає, чию статтю рецензує, і, відповідно, автор не знає рецензента) двома вченими, призначеними редакційною колегією: один є членом редколегії, інший – незалежний учений.

Веб-сайт журналу:
https://ukrfoodscience.nuft.edu.ua

ISSN: 2409-4951 (Online), 2310-1008(Print)

Редакційна колегія

ISSN: 2409-4951 (Online), 2310-1008(Print)

Шановні колеги!

Редакційна колегія наукового періодичного видання
«**Ukrainian Journal of Food Science**»
запрошує Вас до публікації результатів наукових досліджень.

Вимоги до оформлення статей

Мова статей – англійська.

Мінімальний обсяг статті – **10 сторінок** формату А4 (без врахування анотацій і списку літератури)**.**

Для всіх елементів статті шрифт – **Times New Roman**, кегль – **14**, інтервал – 1.

Всі поля сторінки – по 2 см.

Структура статті:

1. **Назва статті.**
2. Автори статті (ім'я та прізвище повністю, приклад: Денис Озерянко).
3. *Установа, в якій виконана робота*.
4. Анотація. **Обов'язкова** структура анотації:
   - Вступ (2–3 рядки).
   - Матеріали та методи (до 5 рядків)
   - Результати та обговорення (пів сторінки).
   - Висновки (2–3 рядки).
5. Ключові слова (3–5 слів, але не словосполучень).

Пункти 2–6 виконати англійською і українською мовами.

6. Основний текст статті. Має включати такі обов'язкові розділи:
   - Вступ
   - Матеріали та методи
   - Результати та обговорення
   - Висновки
   - Література.

За необхідності можна додавати інші розділи та розбивати їх на підрозділи.

7. Авторська довідка (Прізвище, ім'я та по батькові, вчений ступінь та звання, місце роботи, електронна адреса або телефон).
8. Контактні дані автора, до якого за необхідності буде звертатись редакція журналу.

Рисунки виконуються якісно. Скановані рисунки не приймаються. Розмір тексту на рисунках повинен бути **співрозмірним** (!) тексту статті. **Фотографії можна використовувати лише за їх значної наукової цінності.**

Фон графіків, діаграм – лише білий. Колір елементів рисунку (лінії, сітка, текст) – чорний (не сірий).

Рисунки та графіки EXCEL з графіками додатково подаються в окремих файлах.

Скорочені назви фізичних величин в тексті та на графіках позначаються латинськими літерами відповідно до системи СІ.

У списку літератури повинні переважати англомовні статті та монографії, які опубліковані після 2010 року.

ISSN: 2409-4951 (Online), 2310-1008(Print)

Оформлення цитат у тексті статті:

Кількість авторів статті	Приклад цитування у тексті
1 автор	(Arych, 2019)
2 і більше авторів	(Bazopol et al., 2021)

Приклад тексту із цитуванням: It is known (Bazopol et al., 2006; Kuievda, 2020), the product yield depends on temperature, but, there are some exceptions (Arych, 2019).

У цитуваннях необхідно вказувати одне джерело, звідки взято інформацію.
Список літератури сортується за алфавітом, літературні джерела не нумеруються.

Правила оформлення списку літератури

В **Ukrainian Journal of Food Science** взято за основу загальноприйняте спрощене оформлення списку літератури згідно стандарту Garvard. Всі елементи посилання розділяються **лише комами**.

1. Посилання на статтю:

Автори А.А. (рік видання), Назва статті, *Назва журналу (курсивом)*, Том (номер), сторінки, DOI.

Ініціали пишуться після прізвища.

Всі елементи посилання розділяються комами.

1. Приклад:
   Ivanov V., Shevchenko O., Marynin A., Stabnikov V., Gubenia O., Stabnikova O., Shevchenko A., Gavva O., Saliuk A. (2021), Trends and expected benefits of the breaking edge food technologies in 2021–2030, *Ukrainian Food Journal*, 10(1), pp. 7–36, https://doi.org/10.24263/2304-974X-2021-10-1-3

2. Посилання на книгу:

Автори (рік), *Назва книги (курсивом)*, Видавництво, Місто.

Ініціали пишуться після прізвища.

Всі елементи посилання розділяються комами.

Приклад:

2. Wen-Ching Yang (2003), *Handbook of fluidization and fluid-particle systems*, Marcel Dekker, New York.

Посилання на електронний ресурс:

Виконується аналогічно посиланню на книгу або статтю. Після оформлення даних про публікацію пишуться слова **Available at:** та вказується електронна адреса.

Приклади:

(2013), *Svitovi naukovometrychni bazy*, Available at: http://www.nas.gov.ua/publications/q_a /Pages/scopus.aspx

Cheung T. (2011), *World's 50 most delicious drinks*, Available at: http://travel.cnn.com/explorations/drink/worlds–50-most-delicious-drinks–883542

Список літератури оформлюється лише латиницею. Елементи списку українською та російською мовою потрібно транслітерувати. Для транслітерації з українською мови використовується паспортний стандарт.

Зручний сайт для транслітерації з української мови: http://translit.kh.ua/#lat/passport

ISSN: 2409-4951 (Online), 2310-1008(Print)

Детальні інструкції для авторів розміщені на сайті:

http://ukrfoodscience.nuft.edu.ua

Стаття надсилається за електронною адресою:

ukrfoodscience@meta.ua

ISSN: 2409-4951 (Online), 2310-1008(Print)

Наукове видання

Ukrainian Journal of Food Science

Volume 13, Issue 2
2025

Том 13, № 2
2025

Адреса редакції:

Національний університет
харчових технологій
Вул. Володимирська, 68
Київ
01601
Україна

E-mail:

Ukrfoodscience@meta.ua

Підп. до друку 31.12.2025 р. Формат 70x100/16.
Обл.-вид. арк. 2.05. Ум. друк. арк. 2.09.
Гарнітура Times New Roman. Друк офсетний.
Наклад 100 прим. Вид. № 31н/25.

НУХТ 01601 Київ–33, вул. Володимирська, 68

Ідентифікатор у реєстрі суб'єктів у сфері медіа:
R30-02091